Infrared thermography for the assessment of lumbar sympathetic blocks in patients with Complex Regional Pain Syndrome

PhD in Technologies for Health and Well-being

Submitted by:

Mar Cañada Soriano
València, January 2022

Supervised by:

Prof. Dr. David Moratal Pérez
Center for Biomaterials and Tissue Engineering
Universitat Politècnica de València

Dr. José Ignacio Priego Quesada
Department of Physical Education and Sports
Universitat de València

UNIVERSITAT POLITÈCNICA DE VALÈNCIA

To everyone who supported me.

Nothing in life is to be feared; it is only to be understood.

Marie Curie

ACKNOWLEDGEMENTS

A mis directores de tesis David y José. No puc estar més agraïda d'haver-vos trobat en el camí. A José por sus consejos, ayuda estadística y su disponibilidad de cerrajero 24-7. A David per confiar en mi des del primer moment, pel seu pragmatisme combinat sempre amb toc d'humor. Gràcies a la seua eficàcia, tracte i ànims, este procés ha sigut molt gratificant.

A Rosa y a Rosario por ofrecerme este trabajo, además de su amabilidad y disposición. Al grupo de investigación en Biomecánica Deportiva de la Universitat de València (GIBD) por los materiales que han puesto a mi disposición sin los que no hubiera sido posible realizar esta tesis. A Carles y a Maite, así como a su equipo del Hospital Intermutual por haberme abierto las puertas y darme la posibilidad de estar presente en los procedimientos, con los que tanto he aprendido. A los participantes de este estudio porqué sin ellos no hubiera sido posible llevar a cabo esta tesis. Al Grupo de Pesquisa em Neuromecánica Aplicada (GNAP), y en especial al profesor Felipe Carpes, por acogerme desde la distancia y virtualmente con los brazos abiertos.

A Rafa por confiar siempre en mí, darme mi primera oportunidad y, sobre todo, introducirme en el apasionante mundo de la termografía. A Salvador, por contar siempre conmigo y animarme a iniciar esta carrera. Al resto de compañeros y compañeras por su apoyo incondicional. A Ana, perquè amb ella començà tot este camí. Per la seua efectivitat, disposició i per donar-me a conèixer el món gim que tan bé m'ha vingut! A Joseca por sus consejos acertados siempre desde la calma, a Guillermo por su entusiasmo infinito y a David por su motivación de equipo, vamos, que sois un grupo fenomenal.

A mi familia y a todos mis amigos y amigas que me han animado y apoyado. En especial a les Marus: Aina, Anna B., Anna C., Mireia, Neus, Pau, Rosa, Tono, Vicki i Víctor per estar en els millors, i molt especialment, en els pitjors moments i demostra-me així la definició d'amistat, vos estime.

A mi padre y a mi madre. Gracias a su educación, amor y confianza he podido llegar hasta aquí. No hay día que no eche mano de lo que almacené y así seguiré haciéndolo para el resto del camino.

ABSTRACT

Complex regional pain syndrome (CRPS) is a debilitating chronic pain condition that usually affects one limb, and it is characterized by its misunderstood underlying pathophysiology, resulting in both challenging diagnosis and treatment. To avoid the patients' impairment quality of life, the achievement of both an early diagnosis and treatment marks a turning point. Among the different treatment approaches, lumbar sympathetic blocks (LSBs) are addressed to alleviate the pain and reduce some sympathetic signs of the condition. This interventional procedure is performed by injecting local anaesthetic around the sympathetic ganglia and, until now, it has been performed under different imaging techniques, including the ultrasound or the fluoroscopy approaches. Since infrared thermography (IRT) has proven to be a powerful tool to evaluate skin temperatures and taking into account the vasodilatory effects of the local anaesthetics injected in the LSB, the use of IRT has been considered for the LSBs assessment.

Therefore, the purpose of this thesis is to evaluate the capability of IRT as a complementary assessment technique for the LSBs procedures performance. To fulfil this aim, three studies have been conducted implementing the IRT in patients diagnosed with lower limbs CRPS undergoing LSBs.

The first study focuses on the feasibility of IRT as a complementary assessment tool for LSBs performance, that is, for the confirmation of the proper needle position. When LSBs are performed, the correct needle placement is critical to carry out the procedure technically correct and, consequently, to achieve the desired clinical outcomes. To verify the needle placement position, imaging techniques have traditionally been used, however, LSBs under radioscopic guidance do not always ensure an exact performance. For this reason, the thermal alterations induced by the local anaesthetics (i.e., lidocaine), have been exploited and assessed by means of IRT. Thus, the LSB procedure was considered successfully performed when thermal changes within the affected plantar foot were observed in the infrared images after the lidocaine injection.

The second study deals with the quantitative analysis of the thermal data collected in the clinical setting through the evaluation of different temperature-based parameters extracted from both feet. According to the results, the proper LSB success prediction could be achieved in the first four minutes after the block through the evaluation of the feet skin temperatures.

Therefore, the implementation of IRT in the clinical setting might be of great help in assessing the LSBs performance by evaluating the plantar feet temperatures in real time.

Finally, the third study addresses the quantitative analysis by implementing machine learning (ML) tools to assess their capability to automatically classify LSBs. Machine learning has experienced a fast growth in recent years resulting in an effective tool for a wide range of applications in computer science and beyond but, especially in medical applications. In this study, a set of thermal features retrieved from the infrared images have been used to evaluate four ML algorithms (ANN: Artificial Neuronal Network, KNN: K-Nearest Neighbours, RF: Random Forest, and SVM: Support Vector Machine) for three different moments after the baseline time (lidocaine injection). The results indicate that all four models evaluated present good performance metrics to automatically classify LSBs into successful and failed. Therefore, combining infrared features with ML classification models shows to be effective for the LSBs procedures automatic classification.

In conclusion, the use of IRT as a complementary technique in daily clinical practice for LSBs assessment has been evidenced entirely effective. Since IRT is an objective method and it is not very demanding to perform, it is of great help for pain physicians to identify failed procedures, and consequently, it allow them to reverse this situation.

Keywords: chronic pain, thermal imaging, interventional treatment, image guidance, artificial intelligence, thermal alterations, machine learning.

RESUMEN

El síndrome de dolor regional complejo (SDRC) es un trastorno de dolor crónico debilitante que suele afectar a una extremidad, y se caracteriza por su compleja e incomprendida fisiopatología subyacente, lo que supone un reto para su diagnóstico y tratamiento. Para evitar el deterioro de la calidad de vida de los pacientes, la consecución de un diagnóstico y tratamiento tempranos marca un punto de inflexión. Entre los diferentes tratamientos que se suelen considerar, los bloqueos simpáticos lumbares (BSLs) tienen como objetivo aliviar el dolor y reducir algunos signos simpáticos de la afección. Este procedimiento intervencionista se lleva a cabo inyectando anestesia local alrededor de los ganglios simpáticos y, hasta ahora, se realiza frecuentemente bajo el control de diferentes técnicas de imagen, como los ultrasonidos o la fluoroscopia. Dado que la termografía infrarroja (TIR) ha demostrado ser una herramienta eficaz para evaluar la temperatura de la piel, y teniendo en cuenta el efecto vasodilatador que presentan los anestésicos locales inyectados en los BSLs, se ha considerado el uso de la IRT para la evaluación de los BSLs.

El objetivo de esta tesis es, por tanto, estudiar la capacidad de la TIR como una técnica complementaria para la evaluación de la eficacia en la ejecución de los BSLs. Para cumplir este objetivo, se han realizado tres estudios implementando la TIR en pacientes diagnosticados de SDRC de miembros inferiores sometidos a BSLs.

El primer estudio se centra en la viabilidad de la TIR como herramienta complementaria para la evaluación de la eficacia ejecución de los BSLs, es decir, para la confirmación de la posición adecuada de la aguja. Cuando se realizan los BSLs, la colocación correcta de la aguja es crítica para llevar a cabo el procedimiento técnicamente correcto y, en consecuencia, para lograr los resultados clínicos deseados. Para verificar la posición de la aguja, tradicionalmente se han utilizado técnicas de imagen, sin embargo, los BSLs bajo control fluoroscópico no siempre aseguran su exacta ejecución. Por este motivo, se han aprovechado las alteraciones térmicas inducidas por los anestésicos locales (como la lidocaína) y se han evaluado mediante la TIR. Así, cuando en las imágenes infrarrojas se observaron cambios térmicos en la planta del pie afectado tras la inyección de lidocaína, se consideró que el BSL se había realizado con éxito.

El segundo estudio trata del análisis cuantitativo de los datos térmicos recogidos en el entorno clínico a través de la evaluación de diferentes parámetros basados en las temperaturas extraídas de ambos pies. Según los resultados, para predecir adecuadamente la ejecución exitosa de un BSL, se deberían analizar las temperaturas de las plantas de los pies durante los primeros cuatro minutos tras la inyección del anestésico local. Así, la aplicación de la TIR en el entorno clínico podría ser de gran ayuda para evaluar la eficacia de ejecución de los BSLs mediante la evaluación de las temperaturas de los pies en tiempo real.

Por último, el tercer estudio aborda el análisis cuantitativo mediante la implementación de herramientas de aprendizaje automático o machine learning (ML) para evaluar su capacidad de clasificar automáticamente los BSLs. El aprendizaje automático ha experimentado un rápido crecimiento en los últimos años, lo que ha dado lugar a una herramienta eficaz para una amplia gama de aplicaciones en ciencias de la computación y en muchos otros campos, pero, especialmente en aplicaciones médicas. En este estudio se han utilizado una serie de características térmicas extraídas de las imágenes infrarrojas para evaluar cuatro algoritmos de ML (ANN: Artificial Neuronal Network (Red Neuronal Artificial), KNN: K-Nearest Neighbours (Vecinos más cercanos), RF: Random Forest (Bosque aleatorio), y SVM: Support Vector Machine (Máquinas de vectores de soporte)) para tres momentos diferentes después del instante de referencia (inyección de lidocaína). Los resultados indican que los cuatro modelos evaluados presentan buenos rendimientos para clasificar automáticamente los BSLs en exitosos y fallidos. Por lo tanto, la combinación de parámetros térmicos junto con modelos de clasificación ML muestra ser eficaz para la clasificación automática de los procedimientos de BSLs.

En conclusión, el uso de la TIR como técnica complementaria en la práctica clínica diaria para la evaluación de los BSLs ha demostrado ser totalmente eficaz. Dado que la TIR es un método objetivo y relativamente sencillo de implementar, resulta de gran ayuda para que los médicos especialistas en dolor identifiquen los bloqueos realizados fallidos y, en consecuencia, puedan revertir esta situación

Palabras clave: dolor crónico, imágenes térmicas, tratamiento intervencionista, orientación por imagen, inteligencia artificial, alteraciones térmicas, aprendizaje automático.

RESUM

La síndrome de dolor regional complex (SDRC) és un trastorn de dolor crònic debilitant que sol afectar una extremitat, i es caracteritza per la seua complexa i incompresa fisiopatologia subjacent, la qual cosa suposa un repte per al seu diagnòstic i tractament. Per a evitar la deterioració de la qualitat de vida dels pacients, la consecució d'un diagnòstic i tractament primerencs marca un punt d'inflexió. Entre els diferents tractaments que se solen considerar, els bloquejos simpàtics lumbars (BSLs) tenen com a objectiu alleujar el dolor i reduir alguns signes simpàtics de l'afecció. Aquest procediment intervencionista es duu a terme injectant anestèsia local al voltant dels ganglis simpàtics i, fins ara, es realitza freqüentment sota el control de diferents tècniques d'imatge, com els ultrasons o la fluoroscopia. Atés que la termografia infraroja (TIR) ha demostrat ser una eina eficaç per a avaluar la temperatura de la pell, i tenint en compte l'efecte vasodilatador que presenten els anestèsics locals injectats en els BSLs, s'ha considerat l'ús de la TIR per a l'avaluació dels BSLs.

L'objectiu d'aquesta tesi és, per tant, estudiar la capacitat de la TIR com una tècnica complementària per a l'avaluació de l'eficàcia en l'execució dels BSLs. Per a complir aquest objectiu, s'han realitzat tres estudis implementant la TIR en pacients diagnosticats de SDRC de membres inferiors sotmesos a BSLs.

El primer estudi se centra en la viabilitat de la TIR com a eina complementària per a l'avaluació de l'eficàcia en l'execució dels BSLs, és a dir, per a la confirmació de la posició adequada de l'agulla. Quan es realitzen els BSLs, la col·locació correcta de l'agulla és crítica per a dur a terme el procediment tècnicament correcte i, en conseqüència, per a aconseguir els resultats clínics desitjats. Per a verificar la posició de l'agulla, tradicionalment s'han utilitzat tècniques d'imatge, no obstant això, els BSLs baix control fluoroscòpic no sempre asseguren la seua exacta execució. Per aquest motiu, s'han aprofitat les alteracions tèrmiques induïdes pels anestèsics locals (com la lidocaïna) i s'han avaluat mitjançant la TIR. Així, quan en les imatges infraroges es van observar canvis tèrmics en la planta del peu afectat després de la injecció de lidocaIna, es va considerar que el BSL s'havia realitzat amb èxit.

El segon estudi tracta de l'anàlisi quantitativa de les dades tèrmiques recollides en l'entorn clínic a través de l'avaluació de diferents paràmetres basats en les temperatures extretes d’ambdós peus. Segons els resultats, per a predir

adequadament l'execució exitosa d'un BSL, s'haurien d'analitzar les temperatures de les plantes dels peus durant els primers quatre minuts després de la injecció de l'anestèsic local. Així, l'implementació de la TIR en l'entorn clínic podria ser de gran ajuda per a avaluar l'eficàcia d'execució dels BSLs mitjançant l'avaluació de les temperatures dels peus en temps real.

Finalment, el tercer estudi aborda l'anàlisi quantitativa mitjançant la implementació d'eines d'aprenentatge automàtic o machine learning (ML) per a avaluar la seua capacitat de classificar automàticament els BSLs. L'aprenentatge automàtic ha experimentat un ràpid creixement en els últims anys, la qual cosa ha donat lloc a una eina eficaç per a una àmplia gamma d'aplicacions en ciències de la computació i en molts altres camps, però, especialment en aplicacions mèdiques. En aquest estudi s'han utilitzat una sèrie de característiques tèrmiques extretes de les imatges infraroges per a avaluar quatre algorismes de ML (ANN: Artificial Neuronal Network (Xarxa Neuronal Artificial), KNN: K-Nearest Neighbours (Veïns més pròxims), RF: Random Forest (Bosc aleatori), i SVM: Support Vector Machine (Màquines de vectors de suport)) per a tres moments diferents després de l'instant de referència (injecció de lidocaïna). Els resultats indiquen que els quatre models avaluats presenten bons rendiments per a classificar automàticament els BSLs en exitosos i fallits. Per tant, la combinació de paràmetres tèrmics juntament amb models de classificació ML mostra ser eficaç per a la classificació automàtica dels procediments de BSLs.

En conclusió, l'ús de la TIR com a tècnica complementària en la pràctica clínica diària per a l'avaluació dels BSLs ha demostrat ser totalment eficaç. Atés que la TIR és un mètode objectiu i relativament senzill d'implementar, resulta de gran ajuda perquè els metges especialistes en dolor identifiquen els bloquejos realitzats fallits i, en conseqüència, puguen revertir aquesta situació.

Paraules clau: dolor crònic, imatges tèrmiques, tractament intervencionista, orientació per imatge, intel·ligència artificial, alteracions tèrmiques, aprenentatge automàtic.

CONTENTS

ABBREVIATIONS

AAT	American Academy of Thermology
ANN	Artificial neural networks
AUC	Area under the curve
AVAs	Arteriovenous anastomoses
Caret	Classification and regression training
CI	Confidence interval
CNS	Central nervous system
CRPS	Complex regional pain syndrome
CSS	CRPS severity score
DT	Decision trees
EAT	European Association of Thermology
ES	Cohen effect size
FL	Fluoroscopic guidance
FN	False negatives
FOV	Field of view
FP	False positives
FPA	Focal plane array
FPR	False positive rate
GUI	Graphic user interface
HFOV	Horizontal field of view
HFPA	Horizontal array size
IACT	International Academy of Clinical Thermology
IASP	International Association for the Study of Pain
ICD	International Classification of Diseases
IEC	International Electrotechnical Commission
IFOV	Spatial resolution
IRT	Infrared thermography
ISO	International Organization of Standardization
KNN	K-nearest neighbours
LPA	Lateral plantar artery
LSB	Lumbar sympathetic block
LWIR	Longwave infrared
MCA	Medial calcaneal artery
MPA	Medial plantar artery
MSX	Multi spectral dynamic imaging
MWIR	Midwave infrared
NETD	Thermal sensitivity
NIR	Near infrared

NP4	Neuropathic pain questionnaire
NRS	Numerical rating scale
NSAIDs	Non-steroidal anti-inflammatory drugs
PNS	Peripheral nervous system
PTA	Posterior tibial artery
QOLs	Quality of life scale
RF	Random forests
RFE	Recursive feature selection
ROC	Receiver operating characteristic
ROI	Region of interest
SD	Standard deviation
SHAP	Shapley additive explanations
SVM	Support vector machines
SWIR	Shortwave infrared
TN	True negatives
TNR	True negative rate
TP	True positives
TPR	True positive rate
US	Ultrasound guidance
VAS	Visual analogue scale
VFPA	Vertical array size
VHOV	Vertical field of view
VRS	Verbal rating scale

FIGURES

TABLES

MOTIVATION
AND OBJECTIVES

01

1 MOTIVATION AND OBJECTIVES

1.1 Motivation

Chronic pain is an important source of suffering since it results in the patient's life impairment and, in developed countries, it constitutes a major healthcare problem. The Complex Regional Pain Syndrome (CRPS) is usually considered as a chronic pain condition which usually develops in one limb after minor injuries such as surgeries or fractures. The myriad of presentations and the underlying pathophysiologic mechanisms make its diagnosis and treatment a difficult task. CRPS symptoms include persistent pain, sensitivity, changes in colour, texture, temperature, stiffness, and weakness of the affected limb. Its causes are unknown although an interplay between peripheral and central mechanisms are suggested. To date, there is no satisfactory cure for this condition and its treatment focus on achieving pain relief and diminishing symptoms. Lumbar sympathetic blocks (LSBs) are performed to treat lower extremity CRPS with disruption of the nerve supply from the sympathetic chains to the lower extremities.

In medicine, temperature is correlated with several pathological conditions. Infrared thermography (IRT) constitutes an interesting technique to assist physicians in the clinical setting due to its innocuousness along with its capability of performing fast analysis of the skin temperature evolution. The body temperature assessment is complex because of its dependence on several agents including individual or environmental factors. There is no gold standard when body temperature must be measured although IRT has shown to be a reliable technique to this purpose. The use and applicability of IRT has been studied in several pathologies such as breast cancer, rheumatoid arthritis, diabetes and so forth. However, the limited use of the IRT in this specific condition motivated the development of this thesis. In this sense, this technique presents the ability to depict temperature data in a non-invasive and visual way for human skin temperature variations.

1.2 Objectives and hypotheses

Currently there is no gold standard for evaluating the success of the lumbar sympathetic block procedures and usually, their assessment is ambiguous. The imaging techniques considered until now to help in these interventional procedures, such as the fluoroscopy, present occasionally limited precision.

Therefore, the main hypothesis of this thesis is that the implementation of IRT in the assessment of the of lumbar sympathetic blocks (LSBs) in real time, would be valuable to improve their performance.

Hence, three specific objectives (O) of this thesis and the corresponding hypotheses (H) are presented:

O1. To study the feasibility of infrared thermography as a complementary technique in the clinical setting for LSBs assessment in real time.

H1. The use of IRT in the clinical setting during the procedures will improve the rates of successful LSBs.

O2. To establish specific indicators of successful LSBs through the statistical analysis performed on the thermal data acquired in the clinical setting.

H2. Cut-off time and temperature values could be obtained to predict successful outcomes which may allow the classification of the interventions in real time.

O3. To evaluate the capability of machine learning methods to automatically classify the performance of LSBs using thermal data.

H3. The implementation of ML methods using the thermal data previously acquired would allow the automatic classification of the LSBs.

1.3 Thesis structure

This thesis is structured in 8 chapters. Chapter 1 is based on the research motivation, and both the hypotheses and objectives addressed in this work are also described. Chapter 2 gives a background on the CRPS starting from its definition and its relationship with chronic pain features. A historical context is provided and general aspects about the diagnosis, underlying mechanisms, epidemiology, and pain assessment of the disease which is the central point are described. The treatment approaches are also explained, specifically LSBs, which is the interventional treatment performed in this work. Likewise, several key aspects of LSBs are detailed, such as the performance steps, and the assessment tools usually employed. Finally, a brief review of the recently published works about this disease is presented. Chapter 3 describes the basis of the heat transfer and its relevance on the human body, but it also describes both contact and non-contact methods for skin temperature assessment. Among the latter, the infrared thermography is described, which is a key part of this work. Hence, the physical principles behind thermal imaging along with the performance parameters of an infrared system are explained. Finally, an overview of general applications in which IRT is implemented and, specifically the ones performed in the biomedical field, are also presented. Chapter 4 provides an overview of data analysis and machine learning (ML) algorithms. Hence, the different ML models used in classification problems, the thermal features selection along with models' performance metrics are explained. Chapter 5 describes the materials used and the methods carried out to perform the three studies. Patients included in this work along with the experimental procedure in the clinical setting are described. Moreover, the classification analysis approaches are detailed. Chapter 6 presents the results regarding the three classification performance approaches performed. First, the outcomes obtained using the medical classification based on real time infrared images. Second, the results obtained with the quantitative classification through statistical analysis and, finally the results regarding the quantitative analysis based on the implementation of machine learning algorithms are presented. Chapter 7 has the goal of providing the discussion of the key findings obtained in the previous chapter. Furthermore, areas for future research are included. Finally, chapter 8 presents the conclusions about the applicability and suitability of the present work.

INTRODUCTION

02

Infrared thermography for the assessment of lumbar sympathetic blocks in patients with Complex Regional Pain Syndrome

2 COMPLEX REGIONAL PAIN SYNDROME

Complex Regional Pain Syndrome (CRPS) is considered as a chronic pain condition that commonly affects one limb [1]. Pain, changes in colour and temperature, or range of motion loss in the affected limb are some of the symptoms. As its name indicates, the nature of this disorder is intricated and for this reason, both its diagnosis and treatment are challenging. Patients suffering from this condition live under constant discomfort and their daily routines can be strongly altered. For this reason, achieving pain relief along with alleviating symptoms is of paramount importance for them.

2.1 Chronic pain

Depending on the duration, different types of pain have been categorized [1]. Acute pain normally extends for less than three days, whereas chronic pain persists beyond the expected healing period for a specific injury or disease, extending more than three months [2,3]. According to a recently proposed definition of pain by the International Association for the Study of Pain (IASP) Council Task Force [4], pain is “an aversive sensory and emotional experience typically caused by, or resembling that caused by, actual or potential tissue injury”. On the other hand, the International Classification of Diseases (ICD-11) considers pain lasting more than three months as primary chronic pain [1]. Primary chronic pain may be regarded as a disease itself and include conditions such as migraine, fibromyalgia, or complex regional pain syndrome, whereas in secondary chronic pain conditions, pain develops as a symptom of a different disease, such as the pain associated with cancer [1]. According to epidemiologic studies, about 19% of European adults suffer from chronic pain of moderate to severe intensity [5].

The concept of pain has changed and shifted from being a moral, religious or punishment phenomenon to a more biological phenomenon [2]. In this sense, the definition of the term chronic pain has evolved over time not without being surrounded by controversy regarding its consideration as a symptom or as a disease itself [6,7]. John Bonica, an American anaesthesiologist, was the first (1953) who took notice of the pain’s duration and physiology. His observation was described in “The Management of Pain”, in which he considered pathologic pain when it was persisting and “intractable” [8]. A distinction between acute pain and chronic pain was considered in later works, in which chronic pain was described as persisting pain which exceeded beyond the normal healing time

[9,10]. It was not until years later, in 1999 and then in 2004, when chronic pain was regarded as a disease entity itself and it was characterized by its own pathology, symptoms, and signs [11,12]. Since that time, the debate over considering chronic pain as a disease itself or not has remained, due to mainly, the lack of its pathologic features determination [13].

Currently, CRPS refers to a primary chronic pain [1] which usually affects one limb, and it is characteristically associated with edema, sweating and vasomotor abnormalities, limited mobility, and bone demineralization [14,15]. The pain, in turn, is usually intense, continuous, and disproportionately persistent in time in relation to the initial injury or trauma.

2.2 History

The earliest descriptions of a syndrome that could be related to the current condition of CRPS were reported by Ambroise Paré in the 16th century, who observed in wounded soldiers, persistent pain following injuries [16]. It was not until 1813 when it was reported a detailed description from a wounded serviceman hit by a missile in the distal humerus and who presented signs and symptoms compatible to CRPS [17]. Silas Weir Mitchell described in his book "Gunshot wounds and other injuries of nerves" (1864), that American civil war veterans suffered from a burning pain which persisted long after the removal of the bullets [18]. He referred it as "causalgia" coined from the Greek terms 'kausis' (fire) and 'algos' (pain), and he associated this pain to nerve injury. Mitchell also reported that the burning sensation experienced by patients became hyperaesthetic in the way that soft touch increased it. Paul Sudeck, a German surgeon, presented at the 29th Congress of the German Surgical Society in Berlin 1900, a work in which examples of bone atrophy triggered by fractures, nerve injuries, or herpes zoster infections were described [19,20]. Besides, he observed that this condition sometimes disappeared as quickly as it appeared, but sometimes persisted. This was a milestone in the condition known today as CRPS, since the terms 'Sudeck's atrophy' and 'post-traumatic osteodystrophy' became popular to describe this condition, especially in Europe [21]. Indeed, a myriad of terminologies have been proposed over the years, such as 'Sudeck's atrophy', Sudeck's dystrophy', 'algodystrophy' or 'algoneurodystrophy' among others. Nevertheless, the most widely used has been the term coined by James Evans "reflex sympathetic dystrophy", who suggested that sympathetic hyperactivity was involved in the abnormal activity at the periphery [22]. Currently, almost 80 names in the English literature can be found, although, the term 'Complex Regional Pain Syndrome' is the one used in the scientific medical literature as a result of the consensus reached in a meeting in Orlando 1994 organized by the IASP [21,23]. In Figure 1, some of the terminologies used over time are depicted.

Figure 1. Different names used over time to describe the complex regional pain syndrome (CRPS).

The most recent definition was presented in 2007 in the "Proposed new diagnostic criteria for CRPS" [24]. This review article states that "CRPS describes an array of painful conditions that are characterized by a continuing (spontaneous and/or evoked) regional plain that is seemingly disproportionate in time or degree to the usual course of pain after trauma or another lesion. The pain is regional and usually has a distal predominance of abnormal sensory, motor, sudomotor, vasomotor edema, and/or trophic findings. The syndrome shows variable progression over time" [24].

2.3 Diagnosis and classification of the disease

In a similar way as what has been abovementioned about the names, CRPS diagnostics along with their criteria have considerably evolved in time [25,26]. In 1994, the IASP published a set of diagnostic criteria and almost at the same time, Veldman et al. published another [23,27]. However, further research suggested that overdiagnosis occurred when these criteria were used [28]. As a consequence, in 2007, "The new Budapest criteria" were proposed [24]. These criteria were again refined and validated three years later [26].

Currently, there is no gold standard concerning CRPS diagnosis, although physicians usually rely on the 'Budapest Criteria' since it is the most accepted diagnostic approach [15]. Regarding 'the Budapest criteria', two different approaches can be distinguished, the clinical, and the research version (Table 1). Thus, depending on either optimizing the diagnostic sensitivity with adequate specificity or equally reaching the optimal equilibrium between sensitivity and specificity, two different approaches of the proposed criteria, the clinical or the research version would be used [24].

Table 1. Proposed diagnostic criteria for CRPS. From [24].

Clinical diagnosis. The following criteria must be met
1. Continuing pain, which is disproportionate to any inciting event
2. Must report at least 1 <u>symptom</u> in 3 of the 4 following categories: **Sensory**: reports of hyperesthesia and/or allodynia. **Vasomotor**: reports of temperature asymmetry and/or skin colour changes and/or skin colour asymmetry. **Sudomotor/ edema**: reports of edema and/or sweating changes and/or sweating asymmetry. **Motor/trophic**: reports of decreased range of motion and/or motor dysfunction (weakness, tremor, dystonia) and/or trophic changes (hair, nail, skin).
3. Must display at least <u>1 sign</u> at time of evaluation in 2 or more of the following categories: **Sensory**: evidence of hyperalgesia (to pinprick) and/or allodynia (to light touch and/or temperature sensation and/or deep somatic pressure and/or joint movement). **Vasomotor**: evidence of temperature asymmetry (> 1ºC) and/or skin colour changes and/or skin colour asymmetry. **Sudomotor/ edema**: evidence of edema and/or sweating changes and/or sweating asymmetry. **Motor/trophic**: evidence of decreased range of motion and/or motor dysfunction (weakness, tremor, dystonia) and/or trophic changes (hair, nail, skin).
4. There is no other diagnosis that better explains the signs and symptoms
Research diagnosis. Differs from the clinical diagnosis in statement 2, in which must report at least <u>1 symptom in each</u> of the 4 categories.

As depicted in Figure 2, distinctions between CRPS type I (old name: reflex sympathetic dystrophy) and CRPS type II (old name: causalgia) subtypes are also described, depending on whether the absence or presence of peripheral nerve injury evidence, respectively [23,24,29]. Despite 'The Budapest criteria', there is still difficulty in diagnosing CRPS due to the heterogeneity of patient's signs and symptoms [30]. In this sense, a third diagnostic subtype named CRPS-NOS (CRPS not otherwise specified) has been recommended in those patients who partially meet the clinical criteria and whose signs and symptoms cannot be better explained by another condition [24].

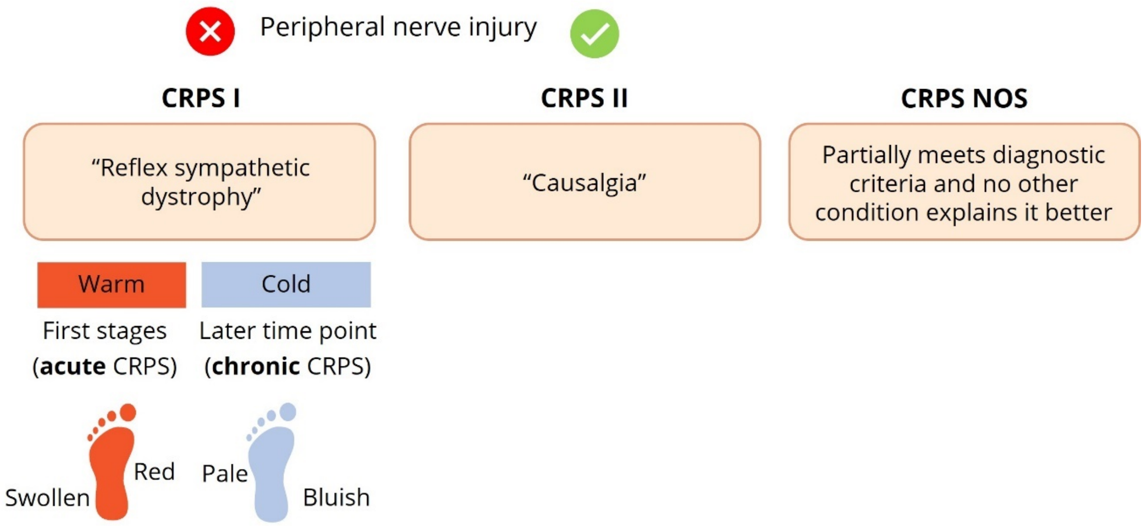

Figure 2. Complex Regional Pain Syndrome (CRPS) distinctions according to the practical diagnostic and treatment guidelines [14,31].

Among CRPS type I patients, the "warm" and "cold" subtypes have been described in which the affected limb is warm, red, and swollen, or cold, pale, and presenting less edema, respectively (Figure 3) [31]. CRPS patients typically belong to the warm subtype at presentation, transforming to the cold subtype later [32,33]. Therefore, the warm subtype is more associated with the first stage of the disease (< 1 year), whereas over time, patients are more likely to present the cold subtype, with atrophic and blue limbs [31].

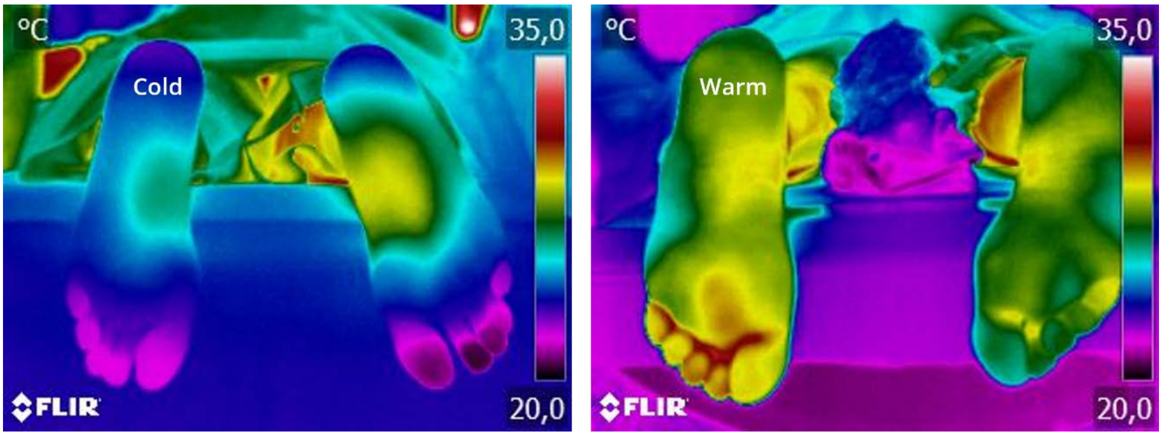

Figure 3. Cold and warm subtypes of Complex Regional Pain Syndrome.

Several techniques are used in the diagnosis of CRPS patients including bone scintigraphy, electromyography, quantitative sensory testing, or infrared thermography [15,33]. Bone scintigraphy evaluates the bone metabolism, and it has been observed that adults with CRPS typically show characteristic scintigraphy findings [34,35]. Electromyography is performed to evaluate possible nerve injury, hence, to distinguish between CRPS type I or II, although its use is not extended because it is considered a painful procedure [14,30,36]. Therefore, quantitative sensor testing is also performed to detect small fibre dysfunction [14,37,38]. Thermography, in turn, is used as a diagnostic tool to detect temperature differences between limbs since the acute phase of the condition is usually associated with higher temperatures on the affected limb [39,40].

On the other hand, in order to characterize the disease's severity, a CRPS Severity Score (CSS) was created [39,41]. In this sense, the CSS includes 17 signs and symptoms derived from 'the Budapest criteria' and each patient's response is graded as present (1 point) or absent (0 point) [39,41]. The symptoms included are allodynia, temperature asymmetry, skin colour changes, edema, sweating asymmetry, trophic/ dystrophic changes, motor changes and decreased dynamic range of motion. On the other hand, signs included are hyperalgesia to pinprick, allodynia, temperature asymmetry, skin colour changes, edema, sweating asymmetry, trophic/ dystrophic changes, motor changes and decreased active range of motion. Hence, the resulting score would be comprised between 0 and 17 [39,41].

2.4 Pathophysiology

Different underlying mechanisms can explain the signs and symptoms in CRPS patients including inflammation, sensitization, cortical reorganization, or autoimmunity among others. For this reason, the CRPS pathophysiology has been suggested to be multifactorial, involving both the peripheral and central nervous system [33,42,43].

Inflammation is often expected in response to trauma or surgery regarding the healing process [44,45], however when it concerns CRPS, this mechanism appears to be excessive [46,47]. Several signs and symptoms shown during the early phase of the CRPS course such as elevated skin temperature, edema, or pain, resemble clinical presentation of peripheral inflammation [48]. However, when pain does not fade out over time, central inflammation seems to be involved suggesting that inflammatory pathways evolve in duration and severity [49-51]. In this sense, when peripheral inflammatory signs dissipate but autonomic symptoms remain, such as cold bluish skin, and/or sweating changes, another mechanism is suggested to be actuating [52].

Hyperalgesia encompasses all conditions of increased pain sensitivity, and allodynia is a special case of hyperalgesia [53]. In Figure 4, the different pain sensations triggered by an injury are depicted, considering allodynia as the pain sensation in response to a non-nociceptive stimulus [53-55]. The release of neuropeptides by the peripheral terminals of sensory nerve fibres in the skin, muscle, and joints, sensitize and increase the activity of local peripheral and secondary central nociceptive neurons resulting in these sensory disturbances [56].

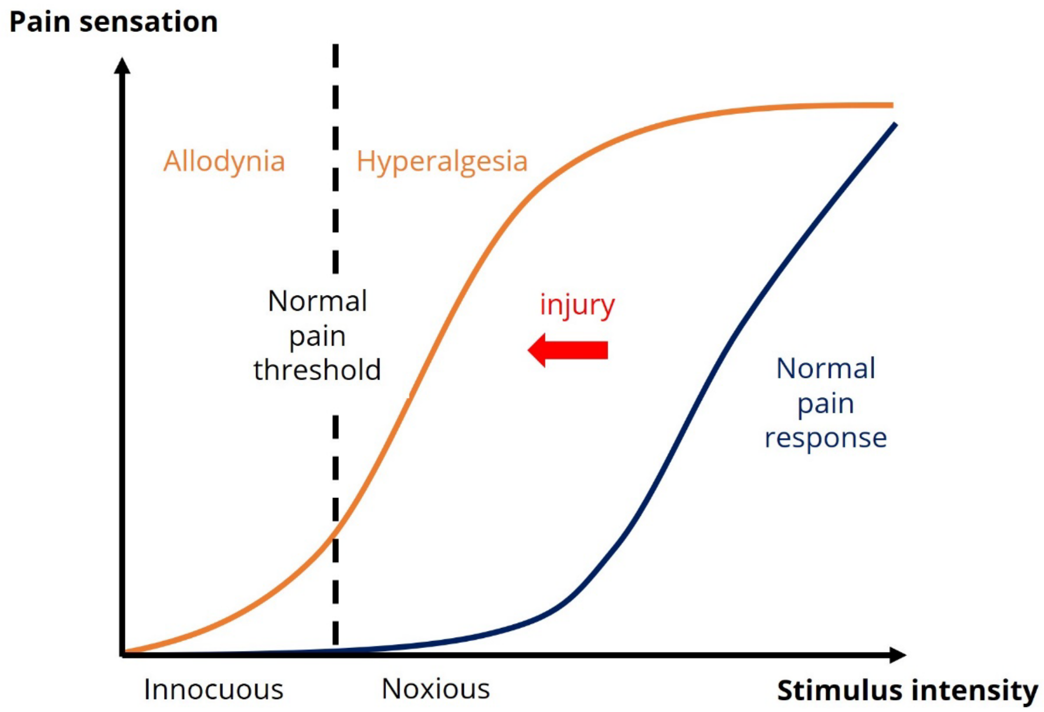

Figure 4. Different pain sensations triggered by injury. Adapted from [55].

Some studies supported the premise that in CRPS patients, reorganisation of the primary somatosensory cortex is presented [57-59], although some others do not support this assumption [60,61]. Patients with CRPS can experience disruption in the cortical map resulting in an altered perception of the size and location in the space of their affected limb [62,63], and/or hostility or disgust feeling toward it [64].

On the other hand, autoimmunity has also been supported as a cause of some CRPS' signs [65,66]. Other studies suggest that genetics contributes to CRPS [67,68] since microRNAs which may be involved in the pain and in the inflammatory process have been identified [69]. For this reason, miRNA expression is being explored as a biomarker of pain [70-72]. Regarding psychological factors, some authors support the theory that there is a higher incidence of CRPS in patients presenting psychological features [73] although many other do not support it [74]. Conversely, it is suggested that CRPS patients are more likely to suffer from depression and anxiety, which may, in turn, lead to a vicious cycle [75,76].

2.5 Epidemiology

Although the incidence of CRPS has not been broadly investigated, some population-based studies have been carried out (Table 2) [77-80].

Table 2. Summary of some epidemiological studies performed [77-80].

Area	Incidence				Nº of cases	Onset age	Extremity	Study
	Type I	Type II	Women	Men				
Europe	88%	12%	71 %	29 %	1043	50.9	Upper	Ott 2018
	13.6*							
Asia	43%	57%	45%[a]	55%[a]	74349	70-79	Lower	Kim 2018
	29*[a]							
Europe	97.1%	2.9%	77%	23%	238	52.7	Upper	De Mos 2007
	26.2*							
US	87%	13%	8.57*	2.16*	85	46	Upper	Sandroni 2003
	6.28*							

NOTE: (*) the incidence is reported per 10000 person-years

(**) population subscribed (51448491) in the national health insurance service from 2011 to 2015 diagnosed with CRPS.

[a] referred to 2015

The most recent ones correspond to a retrospective epidemiological analysis of 1043 patients performed in Germany [77], and a population-based study of 74349 patients in Korea [78]. Ott et al. carried out their study in Germany by using the medical records from patients diagnosed with CRPS between 1993 and 2014, and they obtained an incidence of 13.6 per 100000 people per year for the city of Erlangen [77]. On the other hand, Kim et al. obtained an incidence of 29 per 100000 person-years [78]. Both the incidence and the overall patients analysed are higher than previous studies, probably because this research was conducted among all population in Korea, hence the data analysed was extracted from their National Health Insurance Service from 2011 to 2015 [78]. A previous study conducted by De Mos et al. during 1996-2005 using more than 600000 electronic patients' records throughout Netherlands, an incidence of 26.2 per 100000 population each year was estimated [79]. The smallest incidence rate among the studies is the one reported by Sandroni et al. of 6.28 per 100000 person-years, a study conducted in Minnesota using medical records of patients diagnosed with CRPS in 1989-1999 [80]. According to these studies, women are more likely to be affected by CRPS, and the extremity usually most affected is the upper limb [81-83].

2.6 Pain pathways

The term nociception describes the pain perception, and it involves several areas of the spinal cord, brainstem, and brain [84-86]. The steps of this process include transduction, transmission, modulation, and perception. As it is depicted in Figure 5, when a noxious stimulus occurs, nociceptors are activated and transmitted to the dorsal horn via primary afferent neurons. Among them, Aδ fibres are responsible for transmitting the first pain feeling, C fibres are responsible for the secondary pain feeling, and Aβ fibres carry the non-noxious stimuli or light touch. In the dorsal horn, the primary afferent neurons synapse with secondary afferent neurons resulting in an action potential ascending primarily within the spinothalamic tract. Then, the secondary afferent neurons synapse with tertiary afferent neurons in the thalamus generating an action potential travelling to the somatosensory cortex. There, the nociceptive signal is received (pain perception) and an emotional, autonomic and/or motor response is generated as a result [87,88].

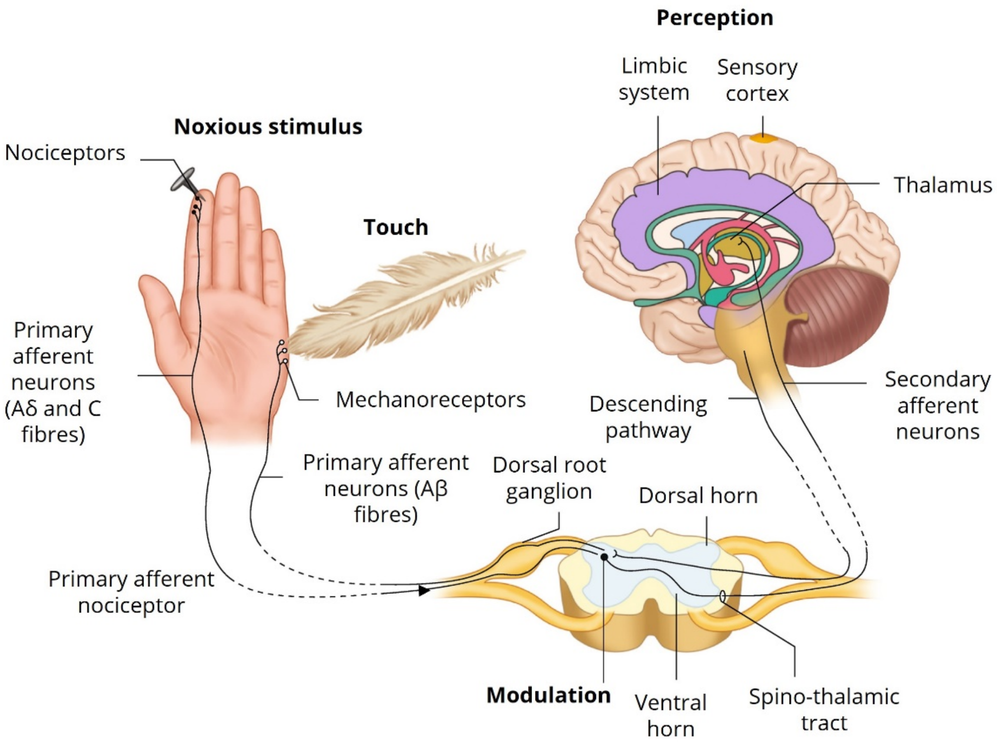

Figure 5. Pain pathways. Adapted from [84].

2.7 Pain assessment scales

Due to the multifactorial features of pain, there is no objective method to measure it [89]. However, several procedures that have proven to be helpful are commonly used in the clinical setting including the visual analogue scale (VAS), the verbal rating scale (VRS) or the numerical rating scale (NRS) [90].

The visual analogue scale (VAS) is a linear model in which a numerical value is plotted on a line along with various pain descriptors, with 0 equating to no pain, and 10 with the worst pain [91]. Patients are asked to mark where on the line their pain intensity lies.

The verbal rating scale (VRS) consists of a list of qualitative descriptors used to define various levels of pain intensity, for instance, describing pain as severe, moderate, mild or no pain. Moreover, each descriptor is associated with a numeric value in an ascending order or intensity, that is, no pain = 0, mild pain = 1, etc, until 15. Patients are asked to select the term which best correlates to their perception.

The numerical rating scale (NRS) is a numerical scale, usually ranging from 0 equating no pain, to 10 as the most severe pain ever. Patients are instructed to pick a number that best reflects their pain intensity [92].

Apart from evaluating the pain as a unique factor, additional aspects, such as the quality of life of a patient, have been assessed using the following questioners:

Quality of life scale (QOLs) is an indicator of the quality of life of a patient [93,94]. In this scale, 10 groups of activities are arranged according to the capability of the patient to develop personal skills, fulfilment, social activities, etc, with 0 equating “a non-functioning life” (staying in bed all day and feeling hopeless and helpless about life), and 10 equating “normality quality of life” (going to work each day, normal daily activities, having a social life outside of work, taking an active part in family life) [93,94].

Neuropathic pain questionnaire (NP4) consists of 4 questions, each one involving several descriptions about pain signs the patient must evaluate as positive (1) or negative (0) [95]. Then the score of each item (10 in total) is summed, and the evaluation is performed out of 10. Scores ≥4 indicate neuropathic pain [95].

Likert scale is a rating scale in which the responses associated with several items are scored along a range [96]. The pain intensity is usually rated using a five- or seven-point scale in which 0 means "no pain", and 5 or 7 means "the worst possible pain".

2.8 Treatment

As a general rule, a multidisciplinary treatment approach is recommended in patients suffering from CRPS, in which medical, physical, occupational, and psychological therapies would be included [76,97]. To achieve this, a dedicated, coordinated, and trained team of professionals should plan this approach.

Although there are no official recommendations for the management of CRPS, several guidelines supporting pharmacological management along with physical and occupational therapies have been developed [14,76,97-99]. Among them, in 2019 the European Pain Federation task force presented 17 standards for the diagnosis and management of CRPS [76]. These standards were developed in different areas of care, that is, 2 standards in diagnosis, 5 in management and referral, 1 in information and education, 4 in pain management, 3 in physical and vocational rehabilitation, and 2 in identifying and treating distress (Figure 6) [76].

Diagnosis

1. "Budapest" diagnostic criteria must be used
2. Diagnostic tests are not required

Management and referral

3. CRPS severity dictates the need of multi-professional care
4. Proper assessment
5 and 6. CRPS severity dictates the referral to (super) specialized care
7. Specialized care facilities must provide advanced treatments

Information and education

8. Adequate information after diagnosis (definition, natural course, signs and symptoms, outcomes, treatment options, etc)

Pain management

9. Patients' access to pharmacological treatments
10. Pain control with tailored rehabilitation plan
11. Medication
12. Re-evaluation depending on the condition development

Physical and vocational rehabilitation

13. Assessment of limb and overall function and activity participation
14. Patients' access to rehabilitation by physiotherapists and/or occupational therapists
15. Physiotherapists and occupational therapists must have access to training in rehabilitation

Identifying and treating distress

16. Patients screened for distress including depression, anxiety, post- traumatic stress, etc.
17. Patients must have access to evidence-based psychological treatment if required

Figure 6. The 17 standards for diagnosis and management of CRPS based on the results of a European Pain Federation task force [76].

On the other hand, the Royal College of Physicians presented in 2018 guidelines for diagnosis, referral, and management of patients with CRPS in a variety of clinical settings (for primary and secondary care, occupational therapists and physiotherapists, emergency departments, surgical practice, neurologists, dermatologists, pain specialists, rehabilitation services or long-term care departments) [97]. Some of them are depicted in Figure 7.

Diagnosis

"Budapest" diagnostic criteria must be used
Clinical examination

Referral

To specialized care center facilities
To specialists

Management

Information and education
Leaflets and additional sources
Treatment plan

Drugs and interventions
Effective drugs for neuropathic pain
Interventional treatments
Treatment re-evaluation when lack of improvement

Physical and vocational intervention
Addressing functional needs
Strategies to support self-management

Figure 7. Some guidelines for pain specialists according to Goebel et al. [97].

Although full recovery is often hard to achieve, the primary aim of the treatment is the reduction of pain and symptoms, but also the motor function restoration [76,97]. Likewise, it is important to provide patients with essential tools to manage their condition and improve their daily life [76,100,101].

Physical and occupational therapies are usually performed in the treatment of mild CRPS, including graded motor imagery [102-104], mirror therapy [105-107], or functional movement techniques [62]. By graded motor imagery, the disparity between motor and sensory feedbacks is intended to be removed. Mirror therapy has been used in stroke patients to treat phantom pain by moving the unimpaired limb [108]. On the other hand, functional movement techniques are recommended to improve the movement of the affected limb and muscle strength, among others [102].

Educational treatment about CRPS is important to explain the condition, its features, available treatments, or the possible outcomes [109-111]. Likewise, psychological interventions may be helpful to treat anxiety and to reduce distress, along with improving daily activities [111].

Pain management can be distinguished between pharmacological options and interventional management (Figure 8) [112,113].

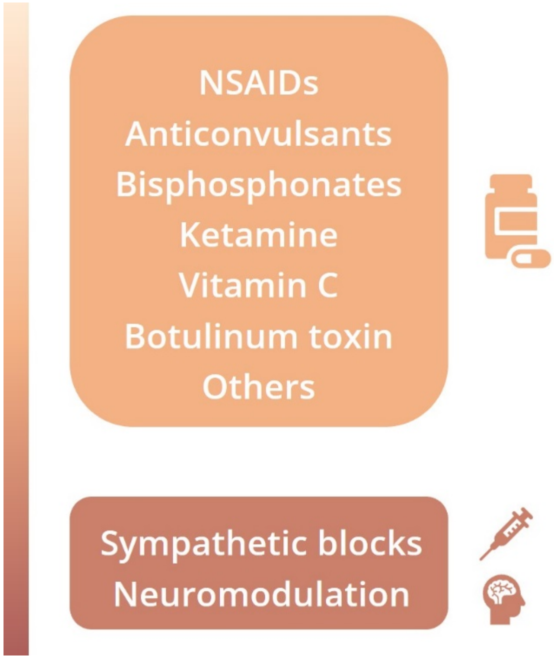

Figure 8. Pharmacological agents and interventional techniques commonly used in pain management of CRPS.

The pharmacological agents are intended mainly to achieve pain relief, and several have been tried for the past years such as anti-inflammatory medications, steroids, anticonvulsants, bisphosphonates, or antioxidants among others [113-115]. Non-steroidal anti-inflammatory drugs (NSAIDs) and corticosteroids are commonly used to reduce inflammation, particularly in the short-term [115-117], although some studies do not support their use due to the lack of demonstrated evidence [118]. Anticonvulsants such as gabapentin, have been shown to be effective in treating neuropathic pain [119,120], and they are also used for the treatment of CRPS since patients undergo pain relief [121,122]. Bisphosphonates have been suggested in the treatment of CRPS to cope with stiffness and pain relief [123,124]. It has been reported that bisphosphonates may have an influence on the inflammatory mediators [123,124], although in 2013, its use evidence was reported to be low and insufficient [125]. Ketamine has been suggested to play a role in central sensitization, and it has been used in the treatment of chronic pain [126] and CRPS [127,128]. Similarly, as reported in other medications, its use is controversial due to the weak evidence found [127,129]. Antioxidants, and specifically vitamin C, has shown as an effective antioxidant to prevent developing CRPS after surgeries [130-132]. On the other hand, some emerging medications have been investigated such as botulinum toxin [133-135], naltrexone [136,137], or plasma exchange [138]. Finally, other pharmacological therapies such as opioids [115], or calcitonin [139], have been studied although results supporting their efficacy are usually controversial.

When patients' condition does not show improvement signs with oral medication, then interventional treatments are carried out [112] including intravenous therapies [140,141], sympathetic nerve blocks [142], and neuromodulation therapies [143,144]. As a general rule, less invasive procedures such nerve blocks are performed in the first place. In case patients do not respond, then more invasive therapies such as neurostimulation are considered. The last option would be amputation of the affected limb in resistant cases of CRPS [145]. Sympathetic blocks can be differentiated between stellate ganglion blocks and thoracic sympathetic blocks for upper extremities [146-148], and lumbar sympathetic blocks (LSBs) for lower extremities [149]. Sympathetic blocks have been used broadly to provide pain relief through the injection of a local anaesthetic around the sympathetic ganglia, intending the interruption of pain signal that sympathetic nerves send to the brain [150]. Although the Cochrane review suggested their lack of high-quality evidence [151], sympathetic blocks are still being used [152]. Neuromodulation therapies involve electrical stimulation of the nervous system [153,154] and include peripheral nerve stimulations [155-157], dorsal root ganglion stimulation [158,159], or spinal cord stimulation [160-162]. Peripheral nerve stimulations consist of the electrical stimulation of nerves, and they are intended to inhibit primary pain afferents. Dorsal root ganglion stimulation was approved for the treatment of lower extremity pain in patients with CRPS [163-165], and in some cases, it is preferred to spinal cord stimulation since it can be applied to more specific areas [166,167]. Spinal cord stimulation is aimed to decrease pain sensation through delivering low voltage electrical stimulation on the dorsal column of the spinal cord [168]. On the other hand, brain stimulation is also applied to improve the patient's condition, although there is a lack of randomized control trials supporting this intervention [169-171]. Only as a last measure, amputation is performed due to the high risk of suffering from phantom limb pain or presenting recurrence of CRPS [145,172,173].

Once the different features of the CRPS has been described, a further research about them has been carried out. Thus, Table 3 shows a summary of published works from 2016 differentiated by aspects such as the condition diagnostic, treatment, or the disease effects.

Table 3. Summary of published works related to CRPS in the last 5 years.

Topic	Subtopic	References
General		[30,114,175,175]
Diagnostic	Guidelines and standards	[41,76,97,176-180]
	Diagnostic tools	[25,34,181-191]
	Miss or late diagnostics	[192-194]
	Signs and symptoms	[77,195-220]
	Risk factors	[82,83,221-251]
	Incidence	[78,82,252-254]
	Pathophysiology and underlying mechanisms	[37,43,60,61,225-343]
Pain assessment		[344-346]
Treatment	Physical, occupational, and psychological interventions	[102,105,347-381]
	Pharmacologic treatment	[116,117,122,127,130-132,135,139,382-422]
	Intravenous therapies	[133,140,141,423-434]
	Neuromodulation	[156,157,160,162,163,165,166,435-485]
	Sympathetic blocks	[142, 149,151,152,486-505]
	Amputation	[506-516]
	Other types of treatment	[517-533]
Disease effects	Pain's perception	[110,354-547]
	Recovery and rehabilitation	[548-557]
Reviews		[558-567]

2.9 Lumbar sympathetic blocks

Sympathetic blocks are interventional procedures which pretend the interruption of the activity of the sympathetic nerves alongside the spine by injecting local anaesthetics [147,151]. Depending on which area of the spine is blocked, different sympathetic blocks can be distinguished. Stellate ganglion blocks are focused on the sympathetic nerves involving the upper part extremities, chest, neck, and head [568]. The celiac plexus blocks involve the nerves in the central spinal segment that reach the abdomen [569,570]. The lumbar sympathetic blocks target the nerves of the lower spine involving the limbs and the sacral, and the ones performed to alleviate pain in patients suffering from lower limbs CRPS [150,571].

Specifically, in lumbar sympathetic blocks (LSBs), a local anaesthetic drug around the sympathetic ganglia is injected between lumbar vertebral levels L2 and L4 [149,572]. By this injection, the pain signal that sympathetic nerves send to the brain is temporarily interrupted, resulting in the disruption of the patient's pain perception, and the abolition of the sympathetic tone [151,504].

The first percutaneous lumbar sympathetic block was described in 1924 by Brunn and Mandl, for which they initially used local anaesthetic [573]. About this time, Kappis also referred to this technique [574]. Then in 1925, Brown and Adson demonstrated the efficacy of LSBs for the Raynaud's disease [575,576]. During World War II, LSBs were performed as an interventional treatment in patients with lower limb neuropathic pain. In 1950, Bonica et al. described them as a treatment of causalgia in wounded soldiers after World War II [8]. Thereafter, LSBs have broadly been employed to treat many pain afflictions in the lower limbs such as CRPS (152,577), hyperhidrosis [578,579], herpes zoster [580], or diabetic neuropathy [581,582].

Although LSBs are described as a minimally invasive procedure, and they are indicated for several pain disorders, neurological, renal, or vascular complications related to the needle placement or resulting from the solution injected can occur [149,151,583]. Renal or ureteric injuries may occur when the entry point is not accurate since the kidneys and ureters are located on the level of L2, L3, and L4 respectively [584,585]. Sexual dysfunction may develop owing to the spread of the neurolytic solution to the genitofemoral nerve. If a neurolytic agent is used and it spreads to the genitofemoral nerve, patients can develop neuralgia. Bleeding can also occur when the needle entry angle is not appropriate because the inferior vena cava and the aorta lie next to the sympathetic ganglia [583,584]. Hence, to prevent or to keep these complications to a minimum, LSBs are performed under several imaging techniques.

2.9.1 The lumbar sympathetic chain and the nervous system

According to the anatomy, the nervous system is divided into the **central nervous system (CNS)**, formed by the brain and the spinal cord, and the **peripheral nervous system (PNS)**, composed mainly by nerves joined to the brain (cranial nerves), and to the spinal cord (spinal nerves) and their ramifications within the body (Figure 9) [586,587]. The PNS constitutes the link between the CNS and the limbs and organs, acting therefore as a transmitter between the brain and the spinal cord, and the rest of the body. According to the function, the nervous system can be divided into the autonomic and the somatic nervous system, and the autonomic may be further subdivided into the sympathetic and the parasympathetic system.

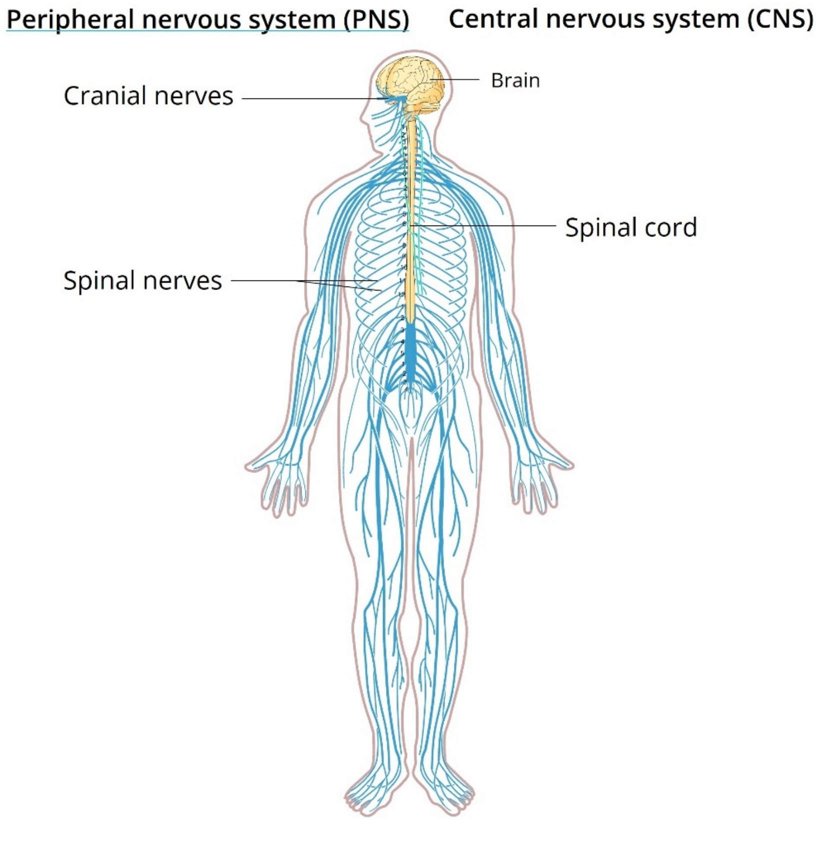

Figure 9. Representation of the nervous system. Adapted from [588].

The **spinal cord** constitutes an extensive network of the nervous tissue since it transmits nerve impulses to 31 pairs of **spinal nerves** attached to the spinal cord. These nerves allow the communication between the brain and peripheral nerves through the afferent and efferent nerve fibres they contain. The afferent (also called sensory) fibres carry information from peripheral receptors to the CNS, whereas the efferent ones, carry impulses away from the CNS (also called motor when they innervate muscle and cause movement).

The spinal cord contains in its centre the grey matter, which is enriched in nerve cell bodies, and in the periphery, the white matter is situated, which mainly contains nerve processes (Figure 10). At each vertebral level, the dorsal and ventral roots arise from the spinal cord [589,590,591]. The dorsal root carries afferent (sensory) nerve fibres, whereas the ventral root carries efferent (motor) nerve fibres. Each dorsal root has a ganglion which contains the cell bodies of the sensory neurons that enter the spinal cord through the dorsal root [586,590]. The dorsal root fibres synapse with neurons in the spinal cord, sending their axons to various parts of the brain.

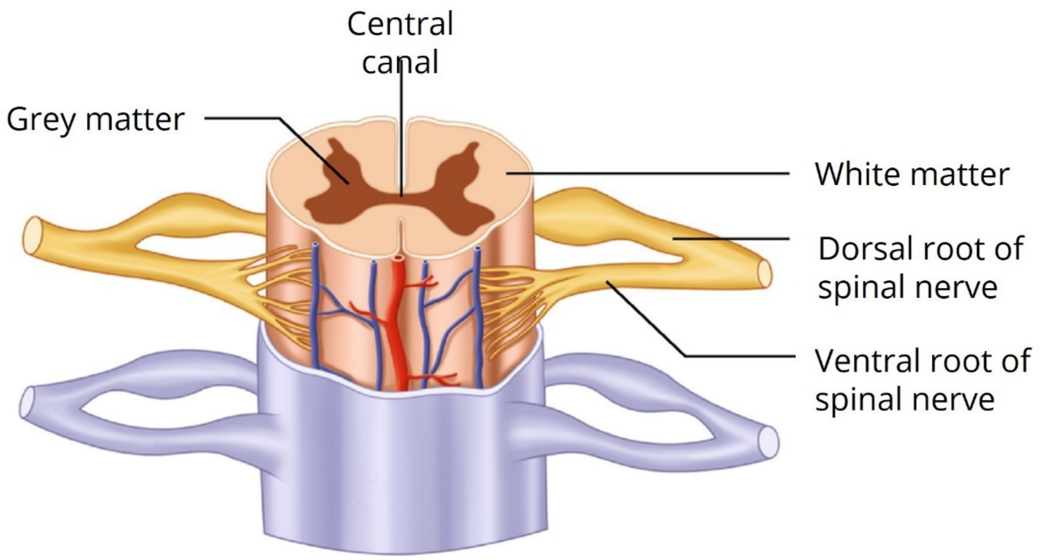

Figure 10. A cross-sectional view of the spinal cord anatomy. Adapted from [591].

The dorsal and ventral root form a spinal nerve which, in turn, divides into ventral (anterior) and dorsal (posterior) ramus, as depicted in Figure 11 [571]. The ventral rami communicate with the sympathetic trunk through the communicating rami and supply the anterior and lateral regions of the trunk and limbs. Conversely, the dorsal rami supply facet joints of the vertebral column, muscles of the back and overlying integument.

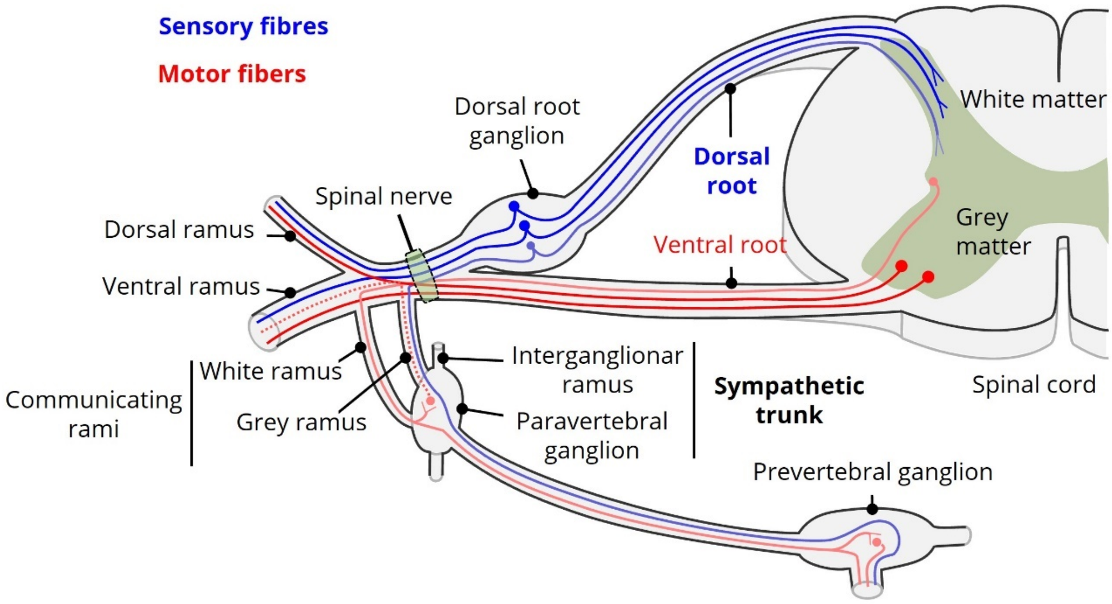

Figure 11. Spinal cord transverse section, showing the attachment of spinal nerve roots and the sympathetic trunk. Adapted from [150,571].

Longitudinally, the spinal cord is divided into 31 segments, one for each pair of spinal nerves: 8 cervical (C1-C8), 12 thoracic (T1-T12), 5 lumbar (L1-L5), 5 sacral (S1-S5) and 1 coccygeal [591]. The combination of the ventral rami of the spinal nerves forms the brachial and lumbar plexus when it is referred to the upper and lower limbs respectively.

Specifically, the lumbar plexus is formed by the ventral rami of L1, L2, L3, and L4 spinal nerves, and provides motor and sensory innervation to the abdominal wall muscles, pelvis, and anterior and medial aspects of the lower extremity. In Figure 12, both the lumbar and sacral nerves are shown.

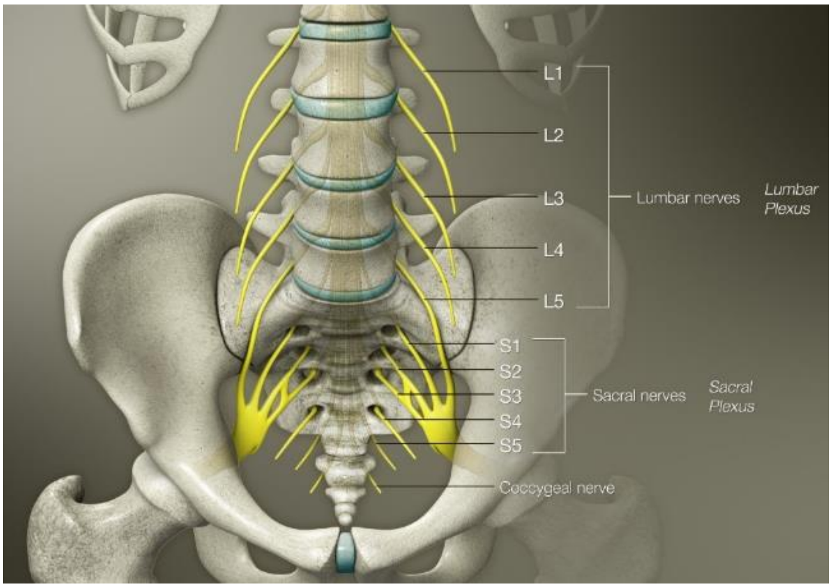

Figure 12. Lumbar and sacral plexus and their associated spinal nerves. From [592].

The sympathetic trunk lies alongside the vertebral column, and it is composed of bilateral sympathetic chain ganglia. There are 3 pairs of ganglia in the cervical region, 11 in the thoracic region, 4 in the lumbar region and 4 to 5 in the sacral region [149]. The lumbar portion of the sympathetic trunk is the **lumbar sympathetic chain**, and it is located on the anterolateral aspect of the lumbar vertebral bodies (Figure 13) [593,594]. Although their exact location, number and size are variable, four ganglia in each trunk are usually encountered [572,593]. The abdominal aorta lies anterior to the chain on the left, and the inferior vena cava is located anterior to the chain on the right [572,594].

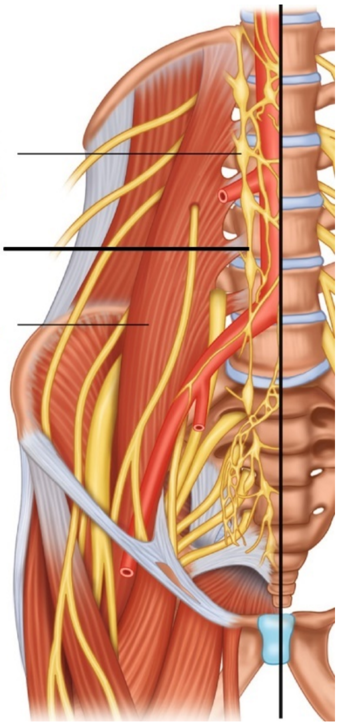

Figure 13. Schematic of the lumbar portion of the sympathetic trunk. Adapted from [149].

2.9.2 Guidance and assessment of lumbar sympathetic blocks

Before imaging techniques were developed, anatomic landmarks were used as guidance in most blocks [8]. However, the small inaccuracies in the needle placement could lead to complications because of the closeness of vital elements. For this reason, and as imaging techniques improved, blocks started to be performed under image guidance resulting in a greater control of the needle placement and, therefore, in a safer technique.

Although currently there is no standard method to perform LSBs, different approaches are employed among pain physicians, such as fluoroscopic guidance [595], ultrasound guidance [424,596], computerized tomography [597], or magnetic resonance [598]. Among them, the fluoroscopic guidance is the most frequently used approach as it provides great accuracy with success rates of 67% [599,600]. When this imaging method is employed, LSBs are often considered correctly performed when there is radioscopically confirmed contrast dye spread [505,595]. However, the variability of contrast spread may be subject to anatomic differences and or secondary redistribution following injection, and LSB under radioscopic guidance does not always ensure an exact performance [601,602].

On the other hand, when the success of a block was assessed in the clinical setting, several methods have been described, including skin conductance response [503], laser Doppler flowmetry [603], plethysmography [604,605], perfusion index [606], skin temperature [607,609], or any combination of them. On the other hand, methods such as the laser Doppler flowmetry, skin temperature, or the perfusion index are performed to assess blood flow alterations [610,611].

From clinical observations, it has been demonstrated that the skin temperature and the blood flow after sympathectomy rise immediately, and they decrease after the intervention [612,613]. In some cases, cutaneous nerve block yields an increase in skin blood flow, indicating the abolition of extant vasoconstrictor nerve activity and resting tone [614].

When fluoroscopy is used, the LSBs can be performed in different manners (Figure 14), however, the prone approach aimed at L4 level under fluoroscopic technique is described since it is the one used in this work.

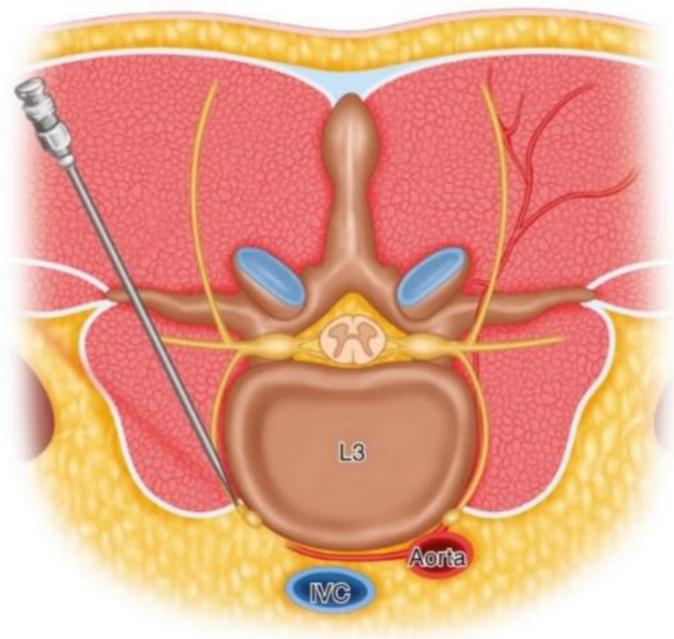

Figure 14. Axial schematic of needle trajectory using paravertebral approach. From [149].

The fluoroscopic guidance is performed using a C-arm which can moves around the patient to obtain the image of interest for the interventionalist (Figure 15). This procedure can be divided mainly in 5 steps, being 1) the preparation of the patients, 2) the visualization of the entry point, 3) the needle introduction, 4) the confirmation of the needle position, and 5) the medication injection.

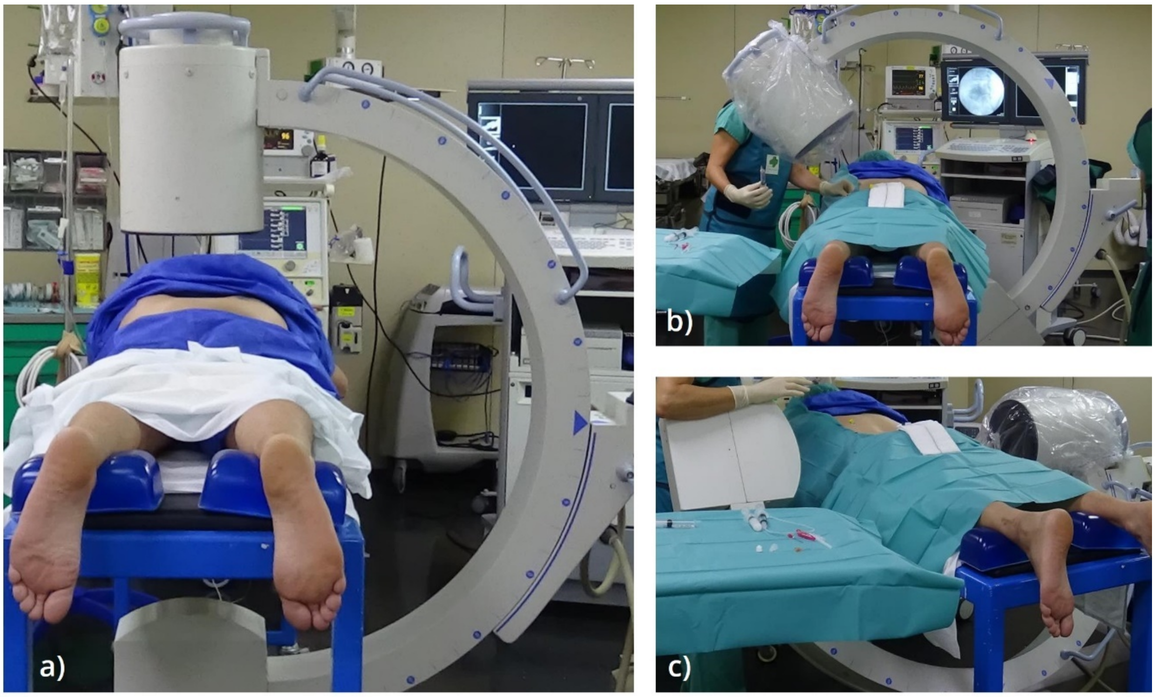

Figure 15. The C-arm in a) posteroanterior, b) oblique, and c) lateral view.

A more detailed description is provided in section 5.2.1, however it is important to note some aspects regarding the confirmation of the needle through the observation of the contrast spread in the fluoroscopic images. An appropriate spread of the contrast should appear in the lateral view as a straight line as possible at the anterior border of the vertebral body (Figure 16a), and in the posteroanterior view, close to the vertebral body (Figure 16b). Otherwise, when the contrast of the spread is not considered appropriate (Figure 17), another attempt of the collocation of the needle should be performed until repeat injection of contrast shows appropriate spread. Once an appropriate contrast spread is observed on the fluoroscopic images, the local anaesthetic is injected.

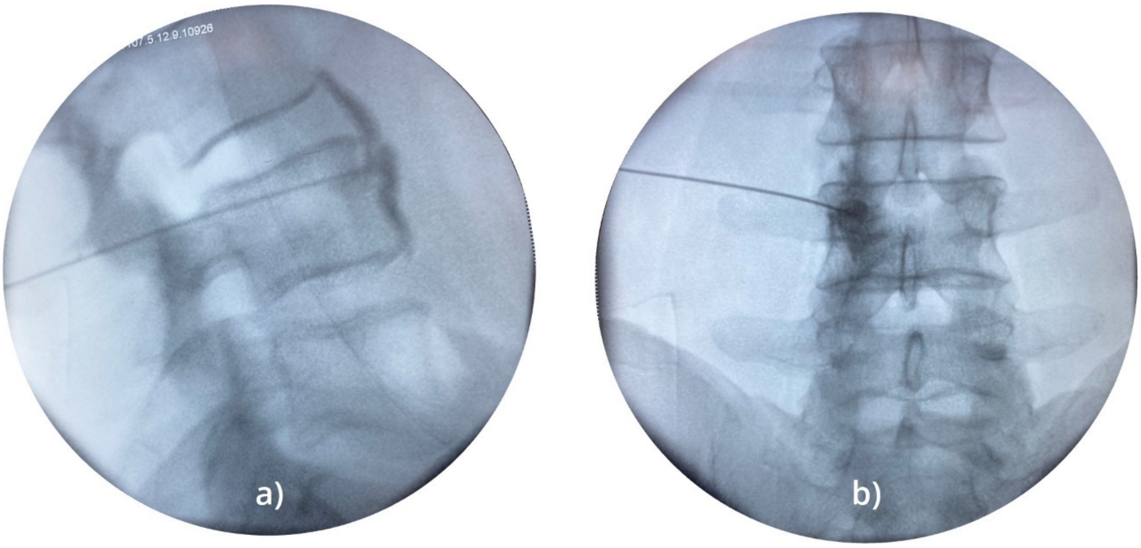

Figure 16. Confirmation of the needle position with proper contrast spread in a) lateral, and b) posteroanterior views.

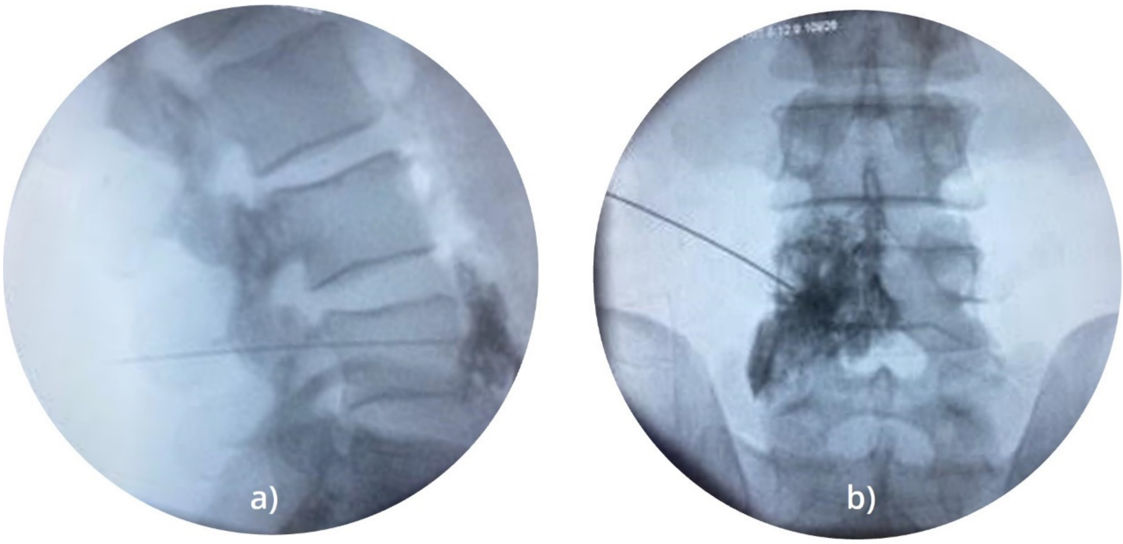

Figure 17. Confirmation of the needle position with not proper contrast spread in a) lateral, and b) posteroanterior views.

TEMPERATURE, HEAT TRANSFER AND INFRARED THERMOGRAPHY

03

Infrared thermography for the assessment of lumbar sympathetic blocks in patients with Complex Regional Pain Syndrome

3 TEMPERATURE, HEAT TRANSFER AND INFRARED THERMOGRAPHY

3.1 Temperature and heat transfer

Temperature measures the average internal molecular kinetic energy of a body, and it is an intensive property, that is, independent of the system mass. When this parameter is measured, several scales can be used, although the most known are Celsius (ºC), Kelvin (K) and Fahrenheit (ºF). The Fahrenheit scale is limited to the Anglo-Saxon field, the Celsius scale is broadly used around the world, whereas Kelvin is the international system scale. To convert a temperature measured in Celsius into Kelvin, 273 must be added, that is, 20ºC corresponds to 293 K.

Heat transfer is the thermal energy in transit due to a temperature difference. The SI unit is the Joule (J), which is expressed as the amount of energy required to raise the temperature of a unit of weight (1 kg) of water from 0ºC to 1ºC. Whenever a temperature difference exists within a medium or between media, heat transfer will occur spontaneously from the body with higher temperature to the one with lower temperature, as it is stated in the Second Law of Thermodynamics. Otherwise, the body would be in thermal equilibrium, that is, at the same and constant temperature. When in a steady state (regardless of time) exists a temperature difference between two bodies or between areas of the same body, heat transfer would occur spontaneously from the hottest elements to the colder ones until the thermal equilibrium is reached. This heat transfer would occur by means of primarily, three different heat transfer modes: conduction, convection, and radiation. Conduction will take place across the medium (inside it) or between two or more solids in contact [615]. The heat flow rate is described by the relationship proposed by Fourier in 1822:

$$q_{\mathrm{conduction}}\,[\mathrm{W}] = -\mathrm{k} \cdot \mathrm{A} \cdot \frac{\Delta \mathrm{T}}{\mathrm{L}} \qquad \text{Equation [1]}$$

Where:

$\mathrm{k}\ [\mathrm{W/mK}]$ is the thermal conductivity of the material. It describes the material's ability to conduct heat (metals present higher values of conductivity whereas insulation materials present the lowest values).

$A\ [m^2]$ is the transverse section of area. That is, the area perpendicular to the heat flow.

$\Delta T\ [^\circ C \text{ or } K]$ is the temperature difference between the solids among the conduction takes place.

$L\ [m]$ is the thickness of the solid the heat flow goes through.

In the human body, conduction occurs within the different body tissues (i.e., between muscles and skin) and between the most superficial layer of the body and clothing.

Heat transfer by convection will occur between the surface of a solid and a fluid in contact with, provided they are at different temperatures [615]. The convection mode is described by Newton's law:

$$q_{convection}\ [W] = h \cdot A \cdot (T_s - T_\infty) \qquad \text{Equation [2]}$$

Where,

$h\ [W/m^2K]$ is the convection coefficient. It depends mainly on the fluid in contact with the surface, and on the fluid movement. Typical values of h when the body is in contact with quiescent air range from 6 W/m^2K to 10 W/m^2K.

$A\ [m^2]$ is the surface in contact with the fluid. That is, the surface through which heat is dissipated.

$T_s\ [^\circ C \text{ or } K]$ is the surface temperature of the body.

$T_\infty\ [^\circ C \text{ or } K]$ is the temperature of the fluid which is in contact with the surface.

Regarding heat dissipation by convection involving humans, it occurs when the skin is in contact with a fluid at a different temperature. In those circumstances, the heat loss will depend on both the temperature and the convection coefficient (which would depend on several factors as the type of fluid). When convection is evaluated in a body at a skin temperature of 35ºC surrounded by quiescent air or by water instead of at 23ºC, in the last situation, since the convection coefficient would be greater, the convective heat loss rate would increase. This is the reason why, a body in contact with water would feel cooler than in air (both at the same temperature). Likewise, when the fluid presents velocity, the convection coefficient increases, resulting in a greater dissipation by means of convection. In this sense, when a patient is to be assessed in a room where air is forced, heat dissipation from the body to the environment would be increased.

Thermal radiation is the other mode of heat transfer which is referred as the energy emitted by surfaces in the form of electromagnetic waves [615]. When the object evaluated can be assumed as a small convex object in a large cavity, the equation describing this mode could be described as:

$$q_{\mathrm{radiation}}\ [\mathrm{W}] = \varepsilon \cdot \sigma \cdot \mathrm{A} \cdot \left(\mathrm{T_s^4} - \mathrm{T_{surroundings}^4}\right) \qquad \text{Equation [3]}$$

Where,

$\varepsilon\ [-]$ is the emissivity. It is the surface's ability to emit infrared radiation.

$\sigma\ [\mathrm{W/m^2K^4}]$: is the Stefan-Boltzmann constant ($\sigma = 5.67 \cdot 10^{-8}\ \mathrm{W/m^2K^4}$)

$\mathrm{A}\ [\mathrm{m^2}]$ is the surface which dissipates the heat.

$\mathrm{T_s}\ [\mathrm{K}]$ is the surface temperature of the body.

$\mathrm{T_{surroundings}}\ [\mathrm{K}]$ is the temperature of the surroundings.

Since human skin resembles a perfect emitter, the amount of heat dissipated by radiation would be strongly related to the skin temperature, which will be explained in the following section. Therefore, radiation constitutes an important heat transfer mode in medicine [616]. When both convection and radiation are evaluated in a body at a skin temperature of about 35ºC embraced by surroundings and quiescent air, both at about 23 ºC, from the total amount of energy dissipated by the human skin, approximately 60% is dissipated in the form of radiation whereas the remaining 40% corresponds to convection (Figure 18).

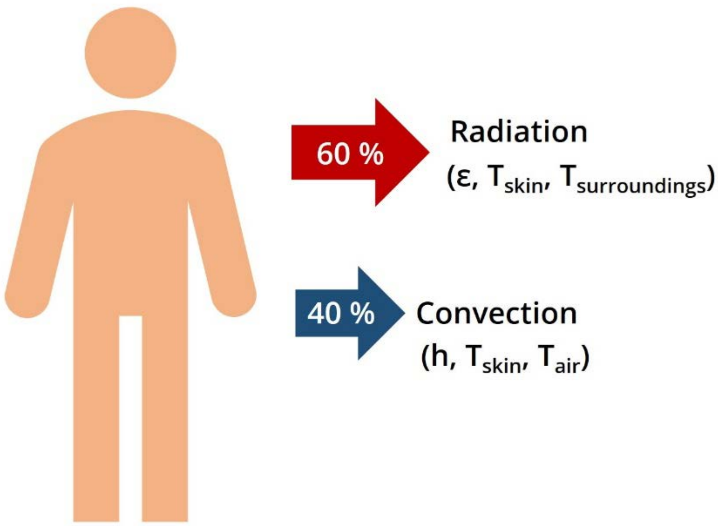

Figure 18. Primary heat transfer dissipating mechanisms of the human body considering skin temperature of 35ºC and surroundings and air both at 23ºC.

The mechanisms used by the human body to transfer heat are, therefore, conduction, convection, radiation. The importance of heat transfer when the human body is assessed lies, for instance, in the heat dissipation from the skin to the environment due to the temperature differences. Additionally, body posture changes the amount proportion of heat transfer by the different mechanisms. For instance, when a person is in supine position, it will exchange heat by conduction through their feet and by convection and radiation from the exposed surface. Besides, natural convective boundary layers would depend also on the posture and flows are generally slower when lying than when standing [617].

Finally, another heat transfer mechanism through which the human body dissipates heat is evaporation, which occurs when individuals sweat. In this sense, the evaporation rate would depend on factors such as relative humidity of the ambient and skin temperature.

3.2 Thermoregulation

Apart from the mechanisms described in the previous section, the human thermoregulation must also be considered, which is defined as the physiological process responsible for keeping constant the human core temperature within about 36.5ºC and 37.5ºC [617]. Hence, thermoregulation aims to maintain the core temperature in a narrow range regardless of both internal and external conditions and to achieve it, a regulation loop is required [618]. In this sense, the human body is composed by the central core, which is mainly the responsible for the heat production and by an outer shell, the skin, which regulates the body heat loss [619,620].

The heat balance equation describes the thermal steady state of a body in which both superficial and core temperatures are constant. That is, the heat loss must be equal to the heat gain.

$$\mathrm{S}\,[\mathrm{W}] = \mathrm{M} - \mathrm{W} - \mathrm{E} - \mathrm{C} - \mathrm{K} - \mathrm{R} \qquad \text{Equation [4]}$$

Where,

S is the storage of body heat. Positive values mean an increase in body heat content.

M is the metabolic rate, which is always positive in living organisms.

W is the work rate, which presents positive values when useful mechanical power is performed.

E is the evaporative heat transfer and has positive values when there is evaporative heat loss.

C is the convective heat transfer, taking positive values when it is transferred to the environment.

R is the radiant heat exchange.

The thermoneutral zone has been described as “the range of ambient temperature within which temperature regulation is achieved by non-evaporative physical processes alone” [621]. In different conditions, the same person usually presents drastically different zones of thermal neutrality. Thus, when temperatures are out of these ranges, changes in heat dissipation through vasodilation and sweating, and heat generation by shivering occur [622].

Above the upper end of the thermoneutral zone, that is, to protect the body against overheating, several autonomic responses such as the increase of the area of heat dissipation, the reduction of blood perfusion due to vasodilation, or the activation of sweat glands to promote cooling by evaporation are triggered. The temperature related responses are activated by the sympathetic nerves, which are the responsible for widening or narrowing the diameter of the blood vessels in the periphery in vasodilation or vasoconstriction processes, respectively [617].

As described before, the core is surrounded by the skin, which is the outside layer of the shell and, in contrast with the central core, it presents significant thermal gradients. The skin, in turn, is the largest sensory organ in our body, and it maintains the internal temperature stabilized by acting as the interface between the central core and the external environment. As depicted in Figure 19, when room temperatures are close to the core temperature (35ºC), shell temperatures show little differences throughout the body. Conversely, when the body is surrounded by lower temperatures (20ºC), regions where vital organs are situated, present temperatures close to the core temperature. However, the areas in the periphery, such as the limbs, temperature differences about 20ºC in comparison to the core temperatures can be observed [617]. Therefore, the gradient extent would depend on the difference between the core and the ambient temperature.

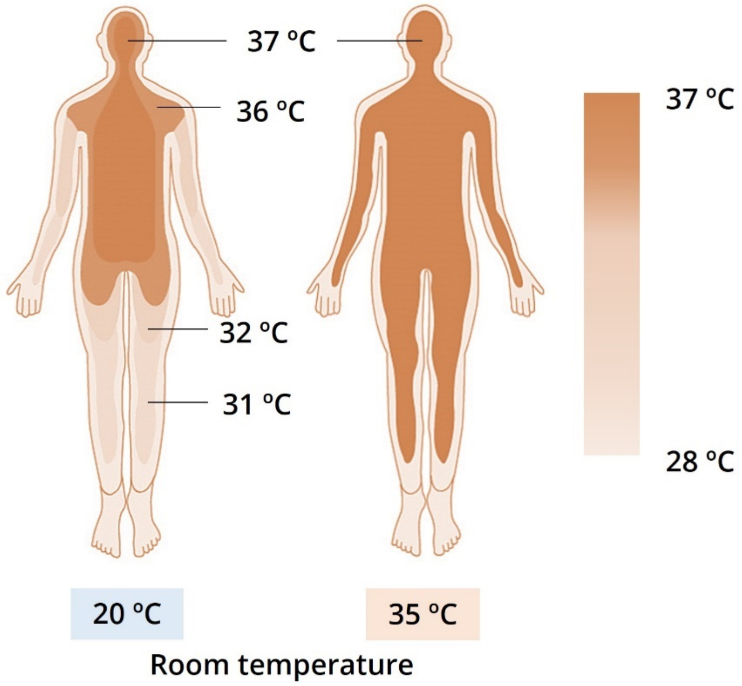

Figure 19. Core and shell temperatures in two different ambient temperatures of 20ºC and 35ºC. Adapted from [623].

Table 4 shows different regional skin temperatures obtained by infrared thermography, both in males and females, in standing position and after 20 minutes of acclimation in a room at 25ºC and 60% relative humidity [624]. From Table 4, it can be observed that the highest mean temperature values are presented in the trunk (chest and upper part of the back), whereas the lowest mean temperature values are found in the distal parts of the body, especially on the lower limbs (shin and calf) [624].

Table 4. Mean surface temperatures in men and women obtained by thermography. From [624].

Region	Mean surface temperature		
	Men	Women	Mean
Chest	33.15	33.47	33.31
Back upper	33.92	33.55	33.73
Front forearm	32.61	32.02	32.31
Back forearm	32.34	31.94	32.14
Front hand	31.89	31.89	31.89
Back hand	31.77	31.77	31.77
Abdomen	32.72	32.23	32.47
Back lower	32.80	32.52	32.66
Thigh front	31.96	31.17	31.56
Thigh back	31.17	30.43	30.80
Shin	31.97	31.16	31.56
Calf	31.41	30.95	31.18

In another study, it was observed that foot temperatures could vary considerably during the day, and they also would differ among individuals [625]. Moreover, asymmetry between the two feet in healthy subjects has been evaluated to be around 0.4ºC [626]. Generally speaking, healthy feet are thermally symmetric, although the mean temperatures in toes are found to be lower than the ones in the plantar surface. Specifically, it has been reported that the second, third, and fourth toes present lower temperatures in relation to the first and fifth toe [627-630].

Heat reaches the skin surface via the subcutaneous tissue through the local skin capillaries. Particularly, in glabrous skin, which is the hairless skin found on palms and soles, a network of vessels, known as arteriovenous anastomoses (AVAs), which form direct connections between small arteries and veins, are usually found [631]. For this reason, the glabrous skin is an indicator of the vasomotor tone, and when vasoconstriction occurs, the skin temperature decreases, whereas when vasodilation takes place, the skin temperature increases [620].

3.3 Feet vasculature

The peripheral microvasculature of the feet plays an important role in thermoregulation mainly due to the existence of the arteriovenous anastomoses (AVAs) which connect the small arteries and veins within the feet [631].

As it has been described in the latter sections, the body's surface temperature is influenced by both the internal processes and the external conditions. Thus, when the body needs to dissipate heat, the blood flow is increased (vasodilation) whereas when the body must be prevented from heat loss, the blood flow decreases (vasoconstriction).

As depicted in Figure 20, the foot blood supply is provided from the posterior tibial and dorsalis pedis arteries [587]. When the posterior tibial artery (PTA) reaches the sole, it branches off into the lateral plantar artery (LPA) and the medial plantar artery (MPA). The MPA, which is the smaller of the two branches, runs alongside the medial aspect of the foot and, as it approaches to the base of the first metatarsal, it divides into a superficial and a deep branch. The LPA, in turn, gives off a branch which supplies the small toe (the lateral plantar digital artery of the 5th toe) and another branch. This last branch (from the LPA) along with the deep plantar artery, which comes from the dorsal pedis artery, form the plantar arch. Thus, the plantar arch runs from the base of the fifth metatarsal to the first interosseous space. Besides, it gives rise to the four plantar metatarsal arteries which supply the medial three toes and each of the plantar metatarsal arteries then bifurcates into two plantar digital arteries [587]. The first plantar metatarsal artery divides into two branches. One branch supplies the medial aspect of the hallux, whereas the other one bifurcates into two plantar digital arteries which supply the second toe and the lateral aspect of the hallux. The branch supplying the medial aspect of the hallux then anastomoses with the superficial branch (dot circle in Figure 20 [632]). Although the arteries described previously are usually found in the normal course, some of them can present variations in their formation, course, and branching patterns [632]. Thus, the variations in plantar metatarsal arteries due to the variation of anatomical variations of the plantar arch have been observed [632-634].

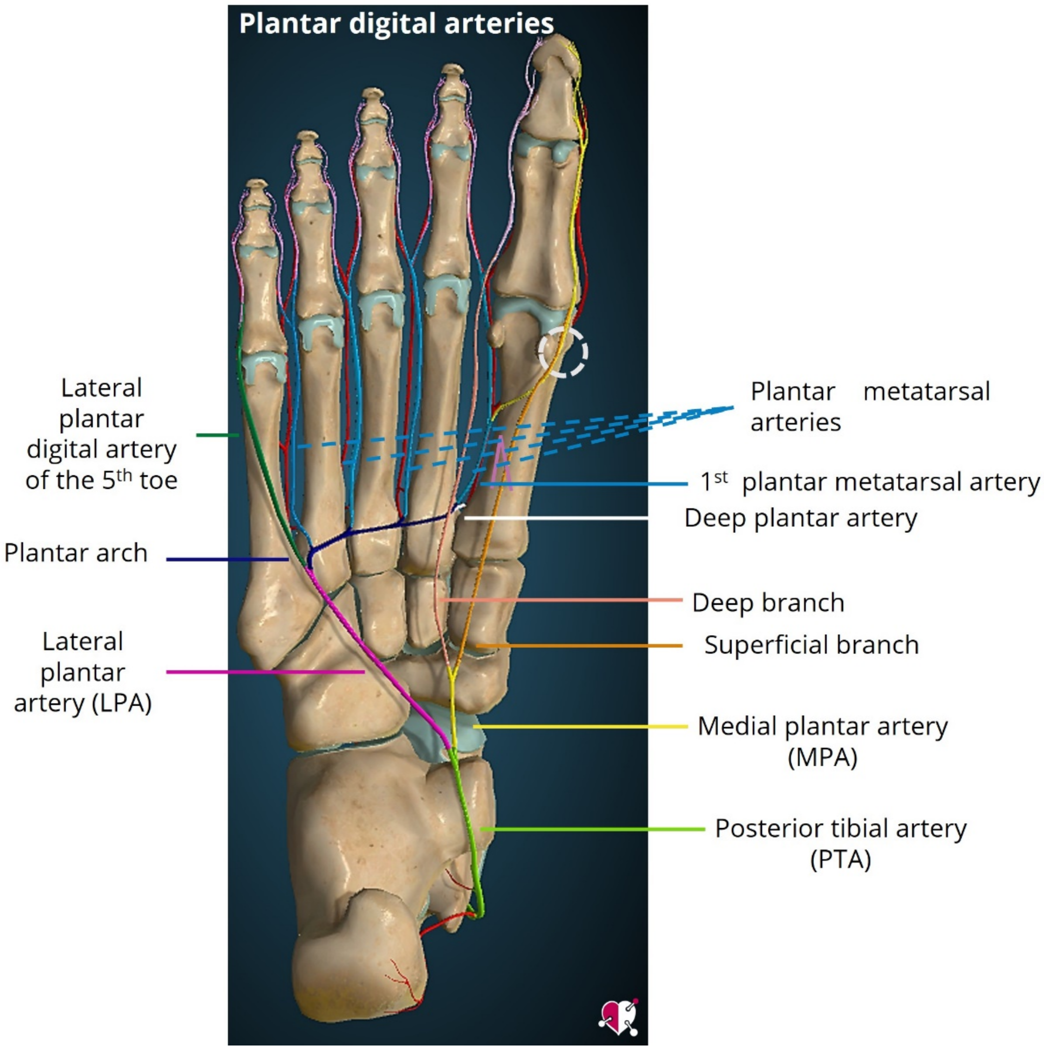

Figure 20. Arteries in the sole of the foot. (Adapted from: www.AnatomyLearning.com).

On the other hand, veins networks are deep (Figure 21a) and superficial (Figure 21b) within the foot. As it happens with the arteries variations, in the veins networks several differences have also been described [635,636]. The deep veins follow the arteries whereas the superficial veins drain into a dorsal venous arch on the dorsal surface of the foot over the metatarsals [587]. It appears that the deep plantar arch mainly drains the metatarsal veins. A consistent connection to the lateral plantar vein would indicate that blood from the metatarsal veins flows primarily through the lateral plantar vein and drains into the posterior tibial veins. However, the presence of dorsal connections in several feet raises the possibility of both plantar and dorsal drainage of the metatarsal veins. Although dorsal drainage is not systematically assessed in all the dissected feet, the contribution of the deep arch to the greater saphenous vein has been noted.

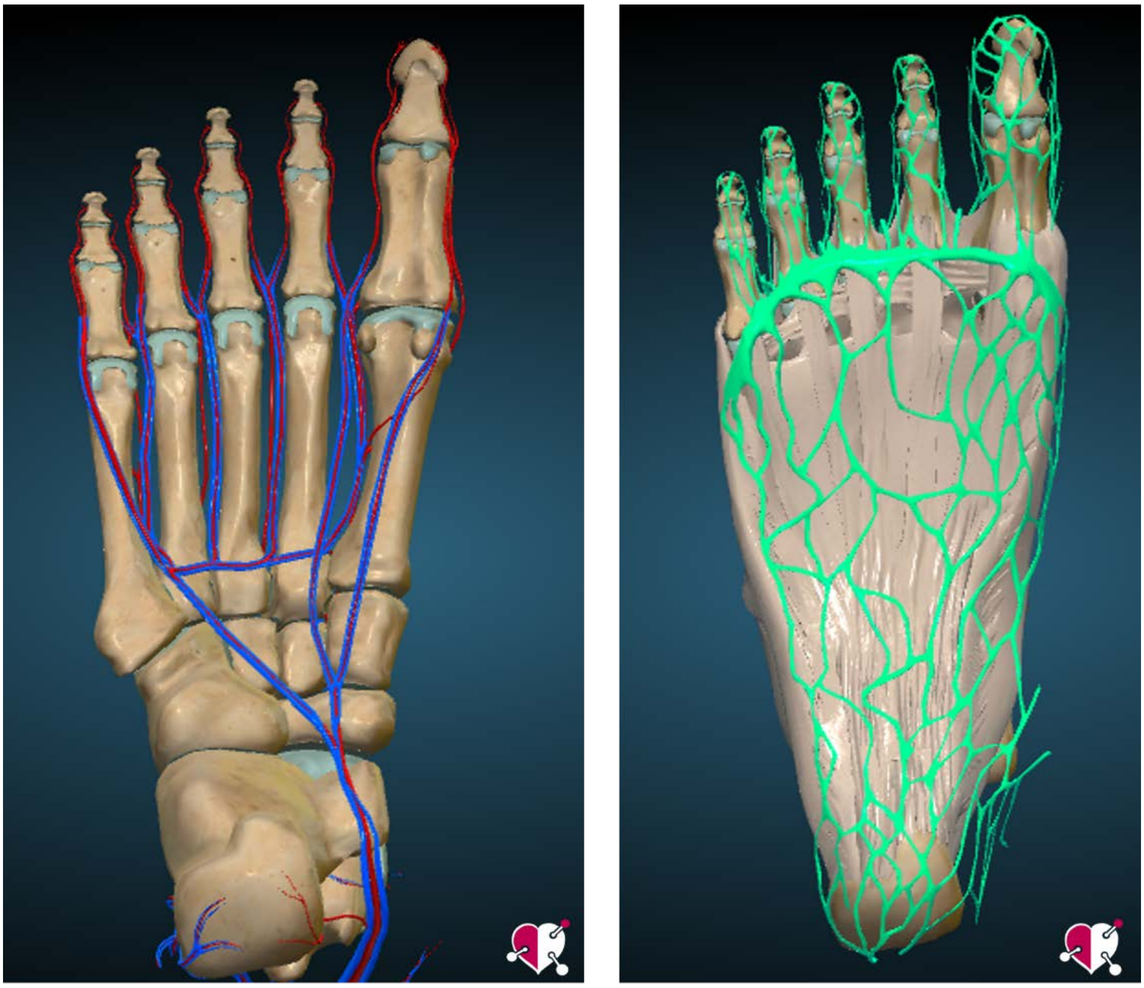

a) b)

Figure 21. Venous plantar network a) deep plantar veins b) cutaneous plantar veins. (Adapted from www.AnatomyLearning.com.)

3.4 Skin temperature assessment using contact methods

Although first skin temperature assessments were based on the palpation of the afflicted area, this “approach” has been almost dismissed due to its low level of reliability. Hence, skin temperature is nowadays measured mainly with thermal contact sensors such as thermocouples or thermistors, or with non-contact devices such as infrared thermometers or infrared cameras [619]. When skin temperature is measured by contact methods, the direct contact between the skin surface and the sensor or device is required since the temperature measurement is obtained by conductive heat transfer between these two elements. Before the widespread use of infrared thermography, these were the most common methods to measure skin temperature due to their relative low cost, sensor size, and potential robustness [637,638]. Among them, and depending on the underlying measurement principles, different devices such as thermocouples, thermistors or thermometers can be found.

Thermocouples work on the basis of the *Seebeck effect*, which occurs when a potential difference (voltage) is created between two different metals (conductor or semiconductor materials) in contact at different temperatures [639,640]. Thermocouples are small, they present relatively fast response (down to 1 ms) and long-term stability. They also provide high accuracy, sensitivity, and reproducibility, and they also present high range of temperature measurements. The accuracy of common thermocouples ranges from 0.25 to 1% [641].

Thermistors are devices in which the temperature changes with electrical resistance or conductance variations, depending upon the semiconductors used [641]. They can be formed in a variety of shapes and sizes, and because of that, they are often manufactured for specific probes to be used on the skin surface (Figure 22).

In both thermocouples and thermistors, the skin sensor and the measuring device or data logger are usually connected through wires, which results in movement limitation and inconvenience. In this sense, wireless temperature systems are also used for skin temperature such as the iButton systems, which have a semiconductor temperature sensor and a computer chip to store information (Figure 22).

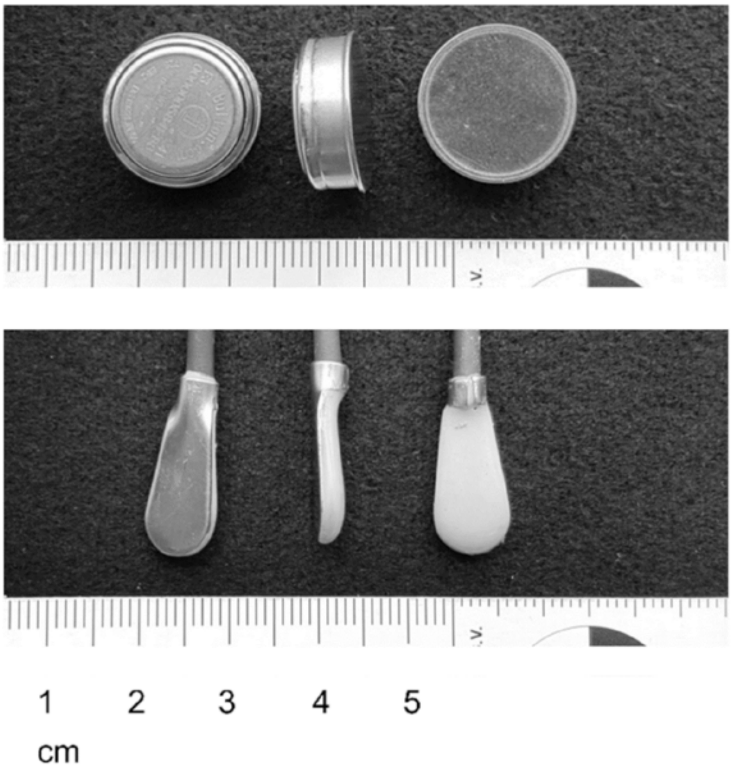

Figure 22. Skin temperature sensors iButtons (on the top) and thermistors (on the bottom). Adapted from [638].

On the other hand, **thermometers** rely upon the expansion of a liquid or solid as the temperature rises, and there are digital thermometers, electronic thermometers, chemical thermometers.

When any of these methods are used, the good thermal contact between the skin and the probe must be ensured. For this purpose, different modes of attachment such as clinical tapes are commonly used, which may result in alterations of the temperature measurements [642-644]. Additionally, since the temperature obtained is the one of the sensor itself, the thermal equilibrium must be achieved. In this sense, the thermal inertia, that is, the response time of the probe, must be minimized through reducing the heat capacity of the probe [645]. Another consideration when these sensors are used to measure skin temperatures is the obstruction of evaporative losses through the skin in the covered area. Moreover, since each sensor or probe can only provide temperatures within small areas, the existence of temperature gradients within the measurement area cannot be properly recorded [638]. Therefore, some of the issues that thermal contact devices present can be overcome using devices based on infrared radiation. These instruments do not require contact with the skin, which is one of the main features that makes this method to be appropriate for evaluating skin temperatures.

3.5 Skin temperature assessment using non-contact methods

The use of devices capable of obtaining skin temperatures at a distance have increased significantly to overcome the most typical problems that contact temperature measurement methods present. These instruments work on the basis of the infrared radiation emitted by objects at a temperature above absolute zero (0K, -273.15ºC). Depending mainly on their performance features, different types of contactless devices can be found such as spot infrared thermometers (pistols, guns, pyrometers) or infrared cameras.

In **infrared thermometers,** the optical element collects the infrared radiation from the area established by a circular measurement spot, and then, it is focused on the detector. In these devices, the optical resolution is defined by the ratio of the distance from the instrument to the object compared to the size of the spot being measured, that is, the distance-to-spot ratio (D:S). In Figure 23 an example of an infrared thermometer operation with two different distance spot ratios of 8:1 and 50:1 is shown. As can be observed, the larger the D:S is, the smaller the spot size that can be measured. That is, at one-meter distance from an object, an infrared thermometer with a D:S of 50:1 would be capable of measuring the temperature of a 2 cm-object, whereas an infrared thermometer with a D:S of 80: 1 would require a spot size of 12.5 cm to do the temperature measurement.

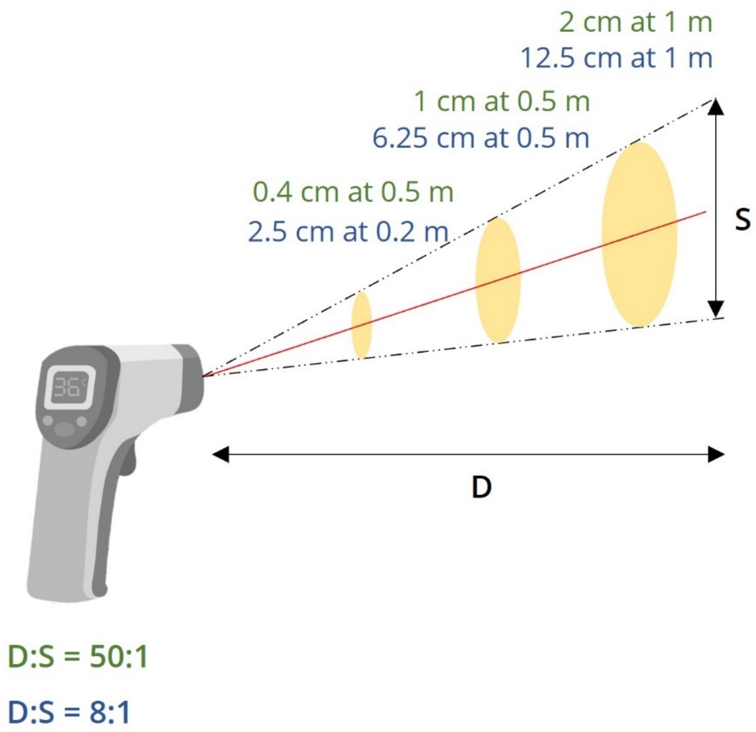

Figure 23. Distance-to-spot size (D:S) ratio of an infrared thermometer.

Among infrared thermal imaging devices, **smartphone-based thermal cameras** have gained popularity in the past few years. They are halfway between thermal cameras and spot infrared thermometers because they provide infrared images within the smartphone screen with a relatively affordable price (Figure 24). On the other hand, they commonly present few thermal detectors compared to infrared cameras, and their battery autonomy is limited.

Figure 24. Examples of smartphone-based cameras. (From flir.es and thermal.com.)

Additionally, low-cost thermal cameras have also spread over the market since both their price and their size make them convenient to use in not very demanding applications (Figure 25).

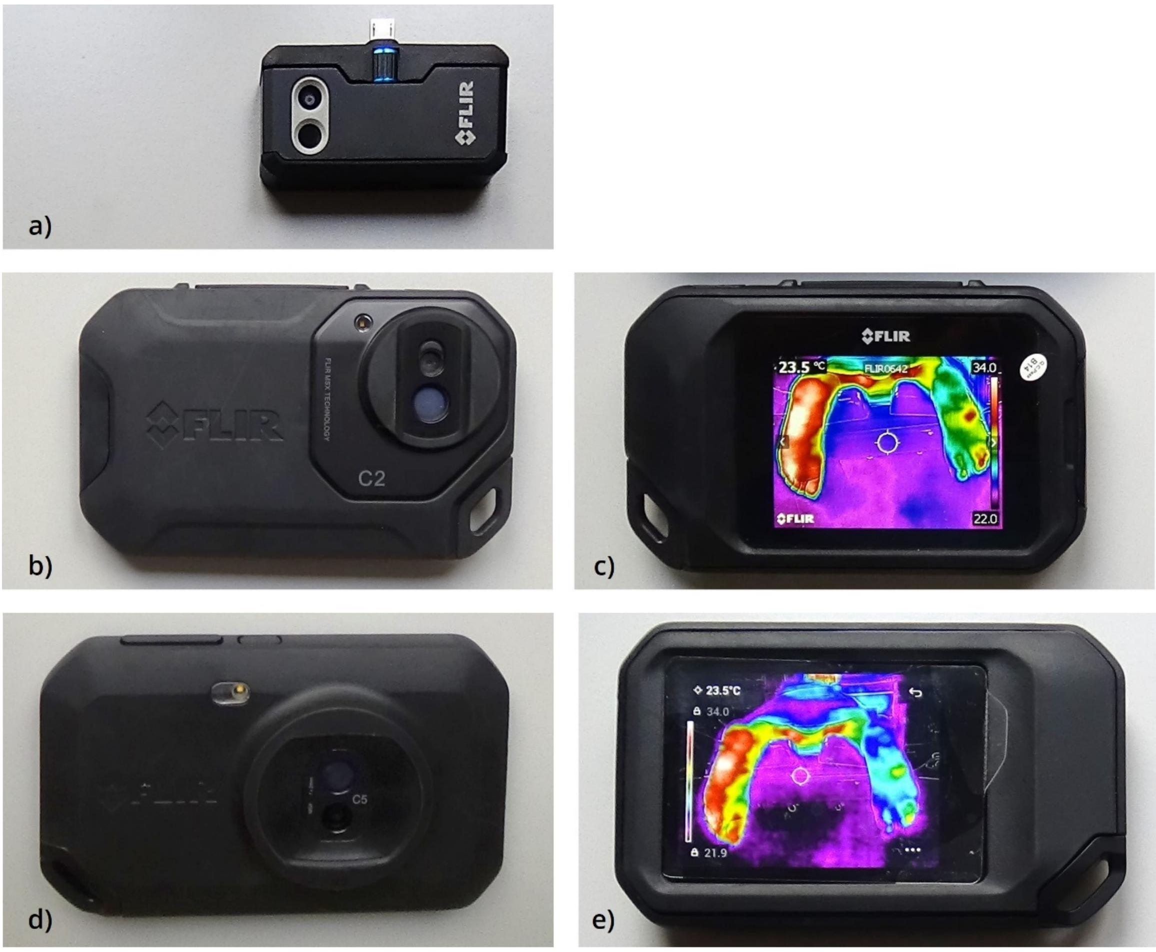

Figure 25. Different low-cost IR camera models a) FLIR ONE b) and c) FLIR C2, d) and e) FLIR C5.

3.6 Infrared thermography

Infrared thermography (IRT) constitutes the basis of this thesis. In the following part, the physics behind this technique along with some image analysis features are explained. Apart from its use in the medical field, IRT has been employed since around the 60's in military, surveillance, electrical, mechanical, factories, building or evaluation of composite materials among a wide range of fields. IRT has his basis on infrared radiation, which in turn, it is based on heat transfer.

3.6.1 Principles of IRT

Infrared radiation was first predicted around 1737 by Emilie du Châtelet, who, in her publication "Dissertation sur la nature et la propagation du feu" suggested that different colours of light carried different heating power [646]. Later, in 1800, Sir Frederick William Herschel experimentally discovered the infrared radiation while he was studying the solar radiation. Using a glass prism, he made solar radiation pass through it decomposing the light into the visible spectrum [647]. Then, he placed mercury thermometers on the different visible colours of the spectrum but also beyond it. As a result, he found that temperature values were different depending on where the thermometers were placed, observing a temperature increase from the violet to the red edge of the visible spectrum. Moreover, beyond the red edge, where no colour could be detected, the highest temperature was obtained.

IRT is a technique that captures the infrared radiation from the bodies surface and at a distance from them. All objects with a temperature above absolute zero (> -273ºC) emit infrared radiation in the form of electromagnetic waves. The electromagnetic spectrum is a representation of the distribution of all the electromagnetic waves in function of their wavelength. These waves differ in length and, according to this, as depicted in Figure 26, it extends from the gamma rays, the waves with highest energy and lowest wavelength, to radio waves, the ones with lowest energy. The infrared band ranges from 0.7 to 1000 µm and it is usually divided into 3 different bands: the near infrared (NIR) which ranges from 0.7 to 1 µm, the shortwave infrared (SWIR), ranging from 1 to 3 µm, the midwave infrared (MWIR), the region from 3 to 5 µm, and the longwave infrared (LWIR), which ranges from 7 to 14 µm. Between 3 to 5 µm, the atmosphere attenuates the radiation, resulting pointless the IR equipment in this range [648].

Although commercial IR cameras are available for NIR, SWIR, MWIR and LWIR, the band mainly used in medical applications is LWIR because most of the radiation emitted by human body lies at these wavelengths (from 7 to 14 µm). This circumstance can be explained by the radiation laws, whose are described for blackbodies.

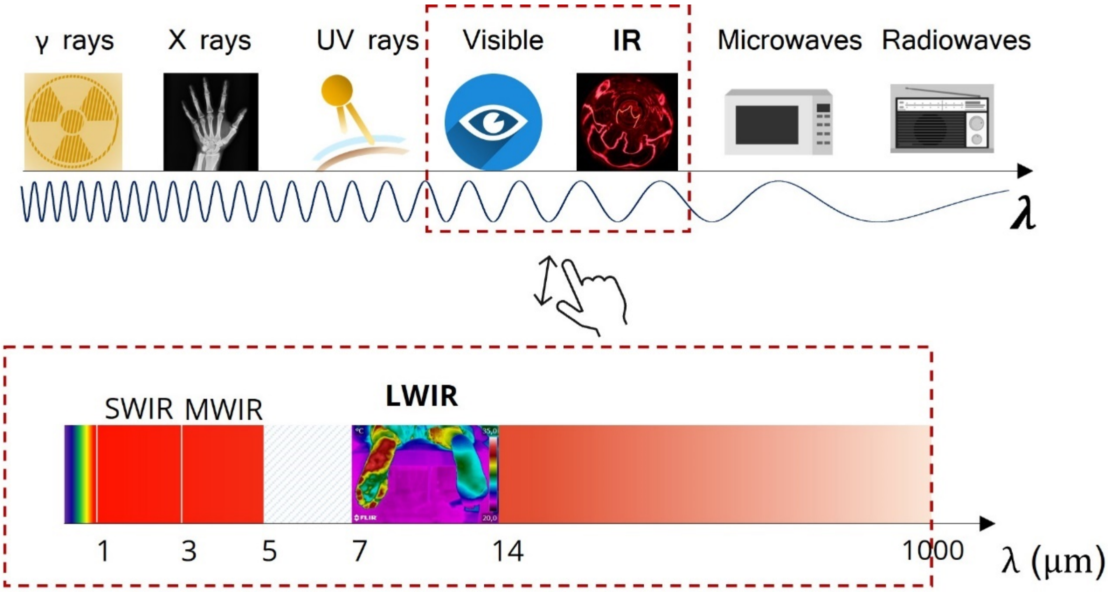

Figure 26. Electromagnetic spectrum.

The concept *black body* was developed by Kirchhoff in 1860 as a theoretical body which absorbs all incident electromagnetic radiation regardless of its wavelength and direction [615]. Moreover, for a given temperature and wavelength, no surface can emit more than a blackbody. Therefore, this theoretical surface behaves as an ideal perfect emitter of infrared radiation. Although these kind of bodies do not exist in nature, they are commonly used as standards in radiometry, and radiation laws are defined according to them.

Planck's law describes the spectral emissive power of a blackbody at temperature T and wavelength λ [615]:

$$E_{b\lambda}(\lambda, T)\left[{}^{W}/_{m^2 \cdot \mu m}\right] = \frac{C_1 \cdot \lambda^{-5}}{e^{C_2/\lambda T} - 1} \qquad \text{Equation [5]}$$

Where,

$C_1 = 3.742 \cdot 10^8 \left[{}^{W \cdot \mu m^4}/_{m^2}\right]$

$C_2 = 1.439 \cdot 10^4\ [\mu m \cdot K]$

Figure 27 depicts different emissive blackbody power distribution for four different temperatures. The lowest temperature spectra could correspond to the skin temperature (35ºC = 308 K) presenting the maximum emission around 9 µm, which is comprised in the LWIR band. On the other hand, bodies at 1000 K (i.e., furnaces tubes), present their maximum emission around 3 µm. Thus, blackbodies at lower temperatures lead to longer wavelengths and vice versa.

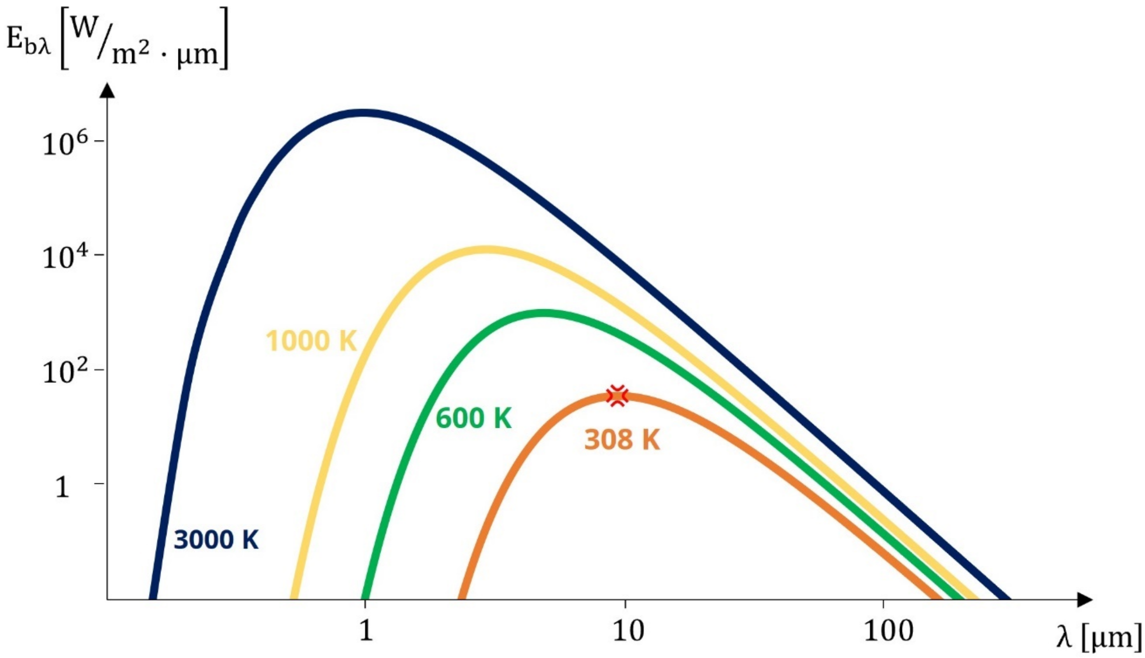

Figure 27. Planck's law distribution for blackbodies at different temperatures.

Wien's displacement law determines the wavelength at which the emissive power of a blackbody is maximum [615].

$$\lambda_{max}\ [\mu m] = \frac{2898}{T\ [K]} \qquad \text{Equation [6]}$$

This law confirms the fact described previously and observed in Figure 26. For blackbodies at 308 K (the skin could resemble a blackbody at 35ºC), the emissive power peak lies at 9.4 µm, that is, the far infrared (LWIR), which constitutes the reason why most common applications use IR cameras working within the LWIR band.

Stefan-Boltzmann's law expresses the total emissive power of a blackbody at temperature T [K] and corresponds to the Planck's law integration from λ=0 to λ=∞ [615]:

$$E_b \left[{}^{W}/_{m^2}\right] = \sigma \cdot T^4 \qquad \text{Equation [7]}$$

Where the Stefan-Boltzmann constant is defined as:

$\sigma = 5.678 \cdot 10^{-8} \left[{}^{W}/_{m^2 \cdot K^4}\right]$

In real conditions, although human skin resembles a blackbody, it is not one, because its surface characteristics are not capable to emit and/or absorb the whole radiation. Blackbodies are idealizations, and real objects always emit less than a blackbody at a given temperature. In order to compute this proportion, the **emissivity (ε),** of an object is used, which can be described as the ratio of the amount of radiation actually emitted from an object to the one emitted by a blackbody at the same temperature [615]:

$$\varepsilon\,(T) = \frac{E\,(T)}{E_b(T)} \qquad \text{Equation [8]}$$

For simplicity, diffuse, grey surfaces are to be considered since they behave independently of direction and wavelength, respectively.

When radiation reaches a body (R) (Figure 28a), it can partially be absorbed, reflected, or transmitted through it, and when the outgoing radiation of a body is evaluated (Figure 28b), it can be reflected and/or transmitted when coming from other sources (R). Finally, the body can also emit radiation.

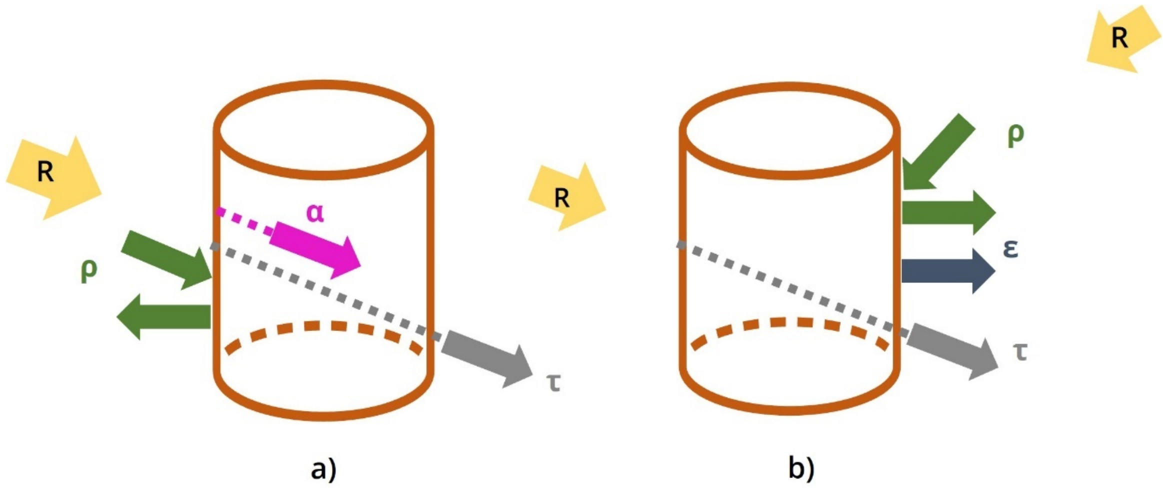

Figure 28. Fractions of radiation when the radiation a) reaches a body and b) abandons the body.

Thus, when radiation reaches a body the proportion of radiation that can be absorbed, reflected and/or transmitted will depend on its intrinsic features described below:

Absorptivity (**α**): the capacity of a body to absorb radiation.

Reflectivity (**ρ**): the capacity of a body to reflect radiation.

Transmissivity (**τ**): the capacity of a body to transmit radiation. When a body is opaque, transmissivity would be 0 because no radiation can pass through it.

According to Kirchhoff's law, the amount of radiation absorbed by an object must be equal to the amount of radiation emitted by this object, which can be expressed:

$$\alpha = \varepsilon \qquad \text{Equation [9]}$$

Moreover, energy conservation states that any radiation reaching a body can be reflected, transmitted through the object, or absorbed within the object. Considering the fraction of the incident radiation:

$$1 = \alpha + \rho + \tau \qquad \text{Equation [10]}$$

When Equations 9 and 10 are combined, the emissivity can be estimated, which in the case of an opaque object ($\tau = 0$), that is an object which does not transmit any radiation:

$$1 = \varepsilon + \rho \qquad \text{Equation [11]}$$

This relationship is of paramount importance in thermography because it states that bodies with lower emissivity would have higher values of reflectivity, which would lead to greater surroundings' influence. In this sense, most bodies are non-transparent to infrared radiation, that is, there are opaque and therefore, only their surface contributes to the emission of the infrared radiation toward the surroundings. This is this reason why, the temperature used in the Stefan-Boltzmann equation corresponds to the body's surface temperature.

In order to describe the emission power of a grey body, the equation 7 is modified adding the emissivity, which is referred to the body's surface.

$$E\left[{}^{W}/_{m^2}\right] = \varepsilon \cdot \sigma \cdot T^4 \qquad \text{Equation [12]}$$

When a body emits radiation, surroundings play a fundamental role. The above equation is referred to the radiative process occurring at a single surface, but common situations involve the exchange between two or more surfaces. For the sake of simplification, it would be assumed that surfaces are separated by a nonparticipating medium, that is, a medium which neither emits, absorbs and therefore, it has no effect on the radiation transfer between surfaces. This exchange between surfaces assessment must take into account geometric factors, resulting in quite complex calculations. However, a simplification can be considered. Hence, it can be assumed the evaluated body as a small convex object in a large cavity so the net radiation exchange between the body and its surroundings can be expressed as:

$$q_{body-surroundings}\,[W] = \varepsilon \cdot \sigma \cdot A \cdot \left(T_{sup}^4 - T_{surroundings}^4\right) \qquad \text{Equation [13]}$$

Where,

ε $[-]$: body's emissivity.

σ $[\mathrm{W/m^2K^4}]$: is the Stefan-Boltzmann constant ($\sigma = 5.67 \cdot 10^{-8}\ \mathrm{W/m^2K^4}$)

A $[\mathrm{m^2}]$: body's surface through which heat is dissipated.

$\mathrm{T_{sup}}$ $[\mathrm{K}]$: surface temperature of the body.

$\mathrm{T_{surroundings}}$ $[\mathrm{K}]$: temperature of the surroundings.

According to equation 13, infrared radiation from objects in the surroundings also affects the heat exchange by radiation. For this reason, direct and reflected radiation that may origin from natural and/or artificial sources such as devices, light bulbs, or people, must be considered when temperature assessments are performed.

The different radiant features described above will have different values according to the body properties and the wavelength at which they are evaluated. For instance, when the infrared band of the spectrum is compared to the visual band, the different behaviour of materials can be discerned [648]. From Figure 29, it can be observed that glass is transparent (a) on the visual band whereas it is opaque (b) on the LWIR. For this reason, lenses employed in thermal cameras are usually made of germanium, which is transparent on LWIR. Another material which behaves in a different way when it is observed with an LWIR camera is polyethylene (Figure 30). In the visual band, it is not possible to see through it (a), whereas the body behind it can be seen when the thermal image is observed (b).

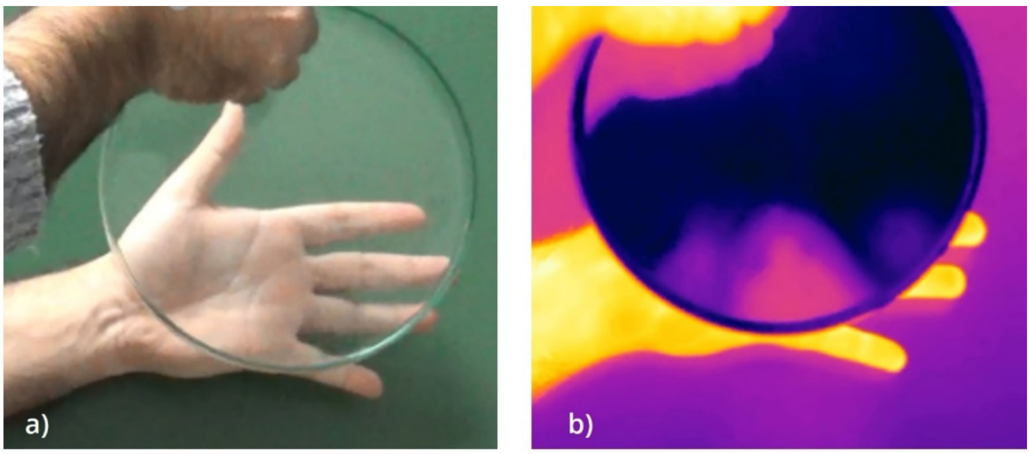

Figure 29. Images showing the different behavior of a glass in the a) visual and b) LWIR band.

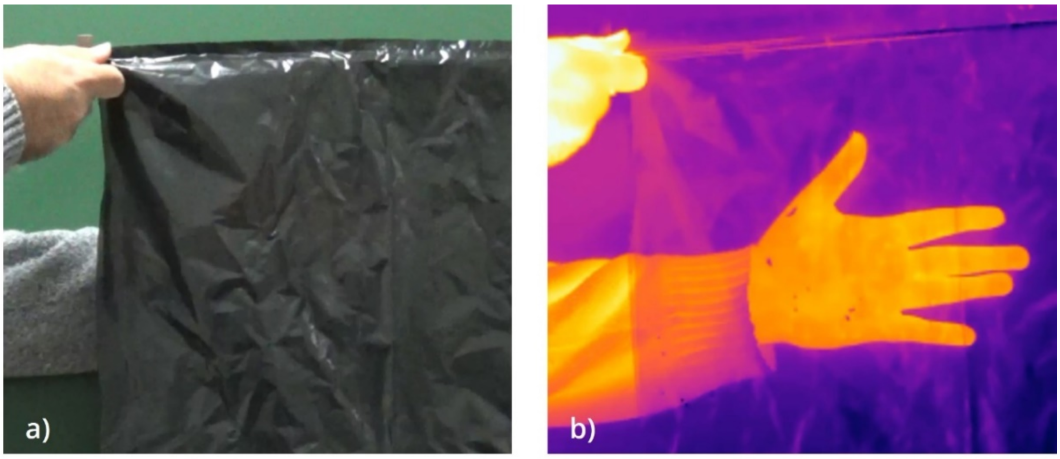

Figure 30. Images showing the different behavior of polyethylene in the a) visual and b) the LWIR band.

3.6.2 Thermal imaging characteristics

The different colours commonly presented in a thermogram represent different radiation intensity values. In fact, each pixel on the image provides an intensity value of radiation, which is, then, transformed into a temperature value. The brightness intensity seen on a thermogram, which is usually directly related to the amount of radiation of a pixel, will depend on the emitted radiation by the object along with the surroundings effects [648]. Since the amount of radiation reaching the detector is affected by these factors, some parameters (compensation parameters) must be considered to accurately measure temperatures.

As it is shown in Figure 31, the body to be assessed, emits an amount of radiation, which is influenced by its temperature and characteristics (mainly its emissivity). When it reaches the detector, the quantity of radiation varies because of the atmosphere's influence. This effect would have less or greater importance depending on the distance between the body and the camera, the ambient temperature, and the relative humidity of the atmosphere. Finally, since the body is not isolated, the surroundings will reflect on the surface of the assessed object, and therefore, an additional amount of radiation related with this reflected radiation will reach the IR camera.

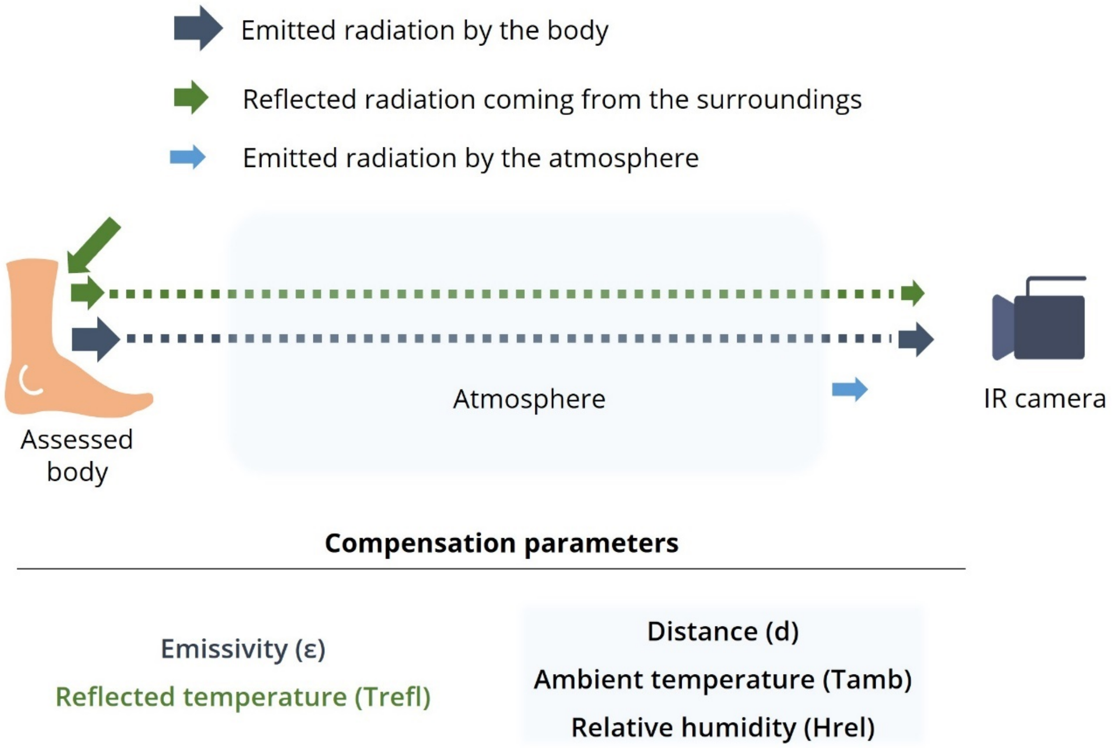

Figure 31. The radiation components leaving the surface and arriving at the infrared camera and the compensation parameters related to them.

In order to obtain accurate temperature readings of the assessed body, these five compensation parameters (Figure 31) must be set correctly either on the camera itself or on the analysis software. In this sense, the higher emissivity value presents the assessed body, the less influence would have the other compensation parameters on the temperature value obtained.

3.6.3 Infrared camera performance characterization

An infrared camera converts the electromagnetic infrared radiation received into a visual image in which the radiation intensity distribution emitted by the objects within the observed scene is represented. Following this, the different radiation values are transformed into temperature readings. To make this happen, as depicted in Figure 32, several components of the IR camera play a role in this process [648].

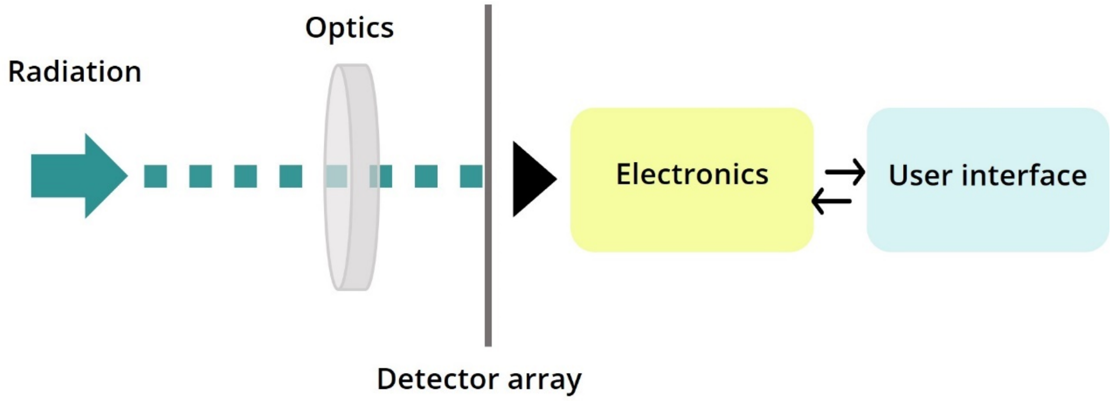

Figure 32. Different components of an infrared camera.

In the first place, the object emits infrared radiation, which passes through the **lens** and reaches the **detector array**, also known as **focal plane array (FPA)**. Then, this radiation is converted into electrical signals, and finally into the resulting image. The greatest amount of radiation is intended to reach the detectors and to achieve this, the transmissivity of the lens must be as highest as possible. For this reason, the most distinctive feature of the lenses is that they are made of germanium, which is transparent to infrared radiation at the wavelengths within the LWIR at some extent. Moreover, the lens would define some performance parameters as the **field of view (FOV)** or the **spatial resolution (IFOV)**, which will be described later.

Depending on the set of elements forming the camera system and their characteristics, several different IR camera systems can be found [648]. Generally, when an IR camera is to be chosen, the appropriate waveband should be selected based on the application to be investigated. In this sense, the waveband most used is the Long Wave Infrared Band (**LWIR**), because at temperatures below around 300 K, the major portion of radiation falls into the LWIR band. As depicted in Figure 33, the objects around 300 K emit nearly no radiation in the short-wave band (SWIR). Indeed, in SWIR the major portion of radiation derive from object at temperatures around 1000 K and for this reason, the IR cameras working in this waveband are commonly used for applications in which high temperature objects are evaluated (i.e., furnaces). Therefore, it would be stated that LWIR cameras would be superior to evaluate temperatures around 300 K although this is not the only consideration. The detector's performance, such as their sensitivity or time response also play a role when specific problems are evaluated [648].

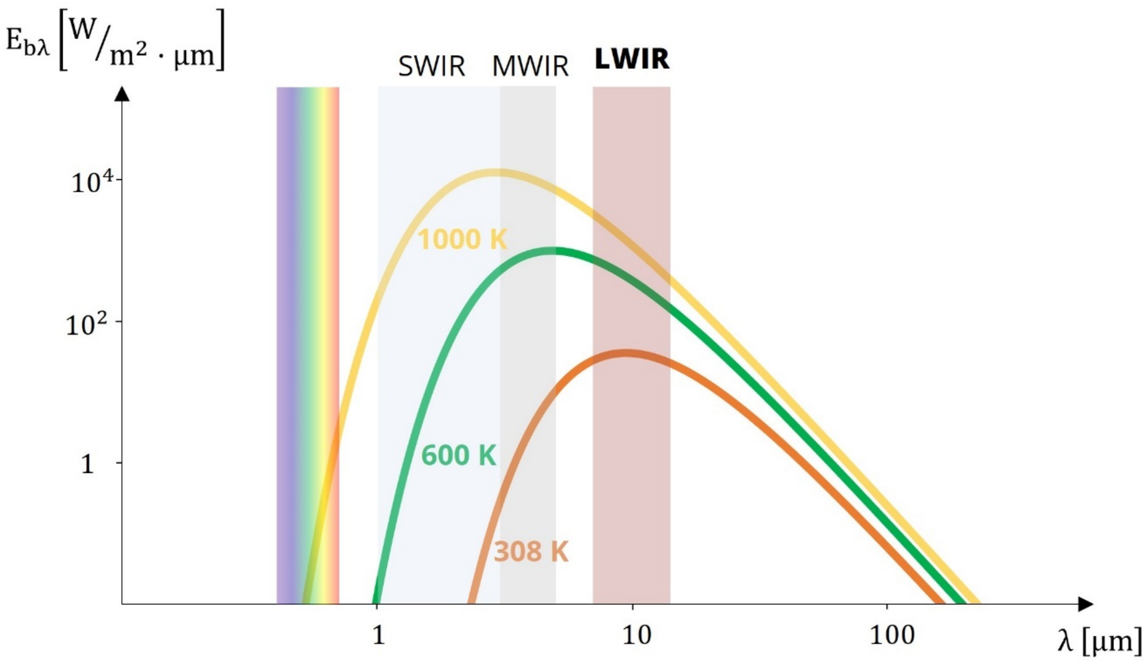

Figure 33. Blackbody power distribution for three different temperatures.

In this sense, detectors are responsible for transforming the incoming radiation into the electrical signal, and two different types can be differentiated: **microbolometers** (usually uncooled) and **photonics** (usually require additional cooling systems). While in photon detectors, the radiation is absorbed within the material by interaction with electrons, microbolometers absorb the incident radiation and because of the temperature variation of the material they are made of, some of their physical properties change, leading to the generation of an electrical output. As it can be observed in Figure 34, where the different operational scheme for both sensors is shown, microbolometer detectors require more steps resulting in an overall greater response time, whereas photon detectors achieve the same process with less time (milliseconds vs. microseconds) [648].

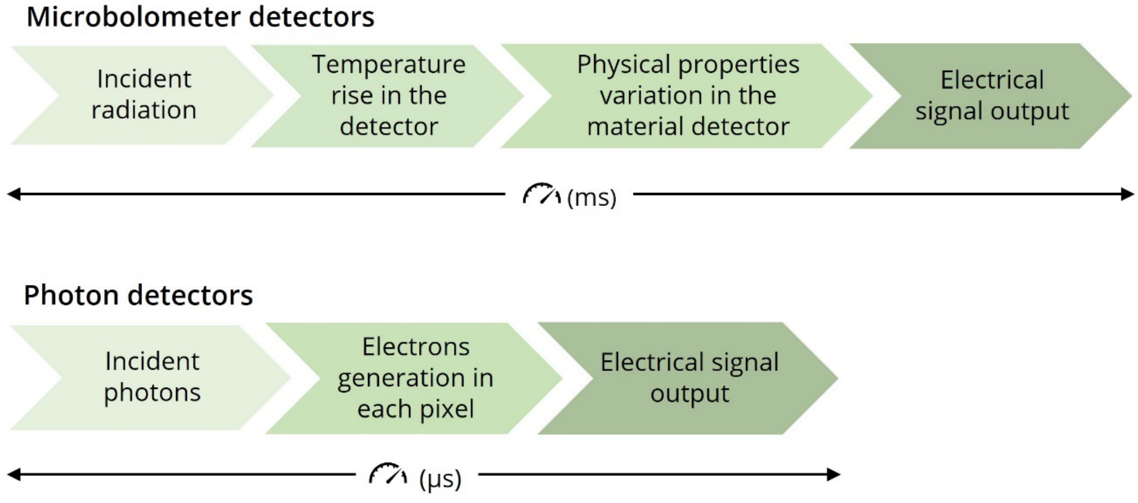

Figure 34. Principle operation of microbolometer and photon detectors.

Photon detectors present better performance when they operate in the MWIR and LWIR band in comparison with microbolometers working in the LWIR band, as it was remarked before. Likewise, photon detectors usually present better sensitivities and faster responses, however, they usually require cooling systems leading to a more bulking, heavy, and expensive systems. On the other hand, although microbolometers present slower responses and inferior thermal sensitivities, their overall performance is usually sufficient for most ordinary applications. Therefore, microbolometer detectors working in the LWIR are the preferred option in most applications (building, mechanical and electrical maintenance or medical among others), since they are more affordable, portable, and user-friendly, camera systems with. Table 5 describes a summary of both photon and microbolometer detectors mainly performance features [648].

Table 5. Performance features of photon and microbolometer detectors.

Features	Microbolometers	Photon
Wavebands	LWIR	MWIR, SWIR
Cooling system	No	Yes
Response time	Slow (ms)	Fast (µs)
Cost	Affordable	Expensive
Size	Portable	Bulky

The **focal plane array (FPA)** comprises a variable number of single detectors, also known as pixels, arranged in a matrix of columns and rows depicting each one a radiation value. The FPAs in IR commercially available cameras range from 80 x 60 pixels in some cameras used on mobile phones, to 1024 x 868 pixels in the most advanced IR cameras. Therefore, the bigger the FPA size is, the greater number of detectors will dispose (Figure 35).

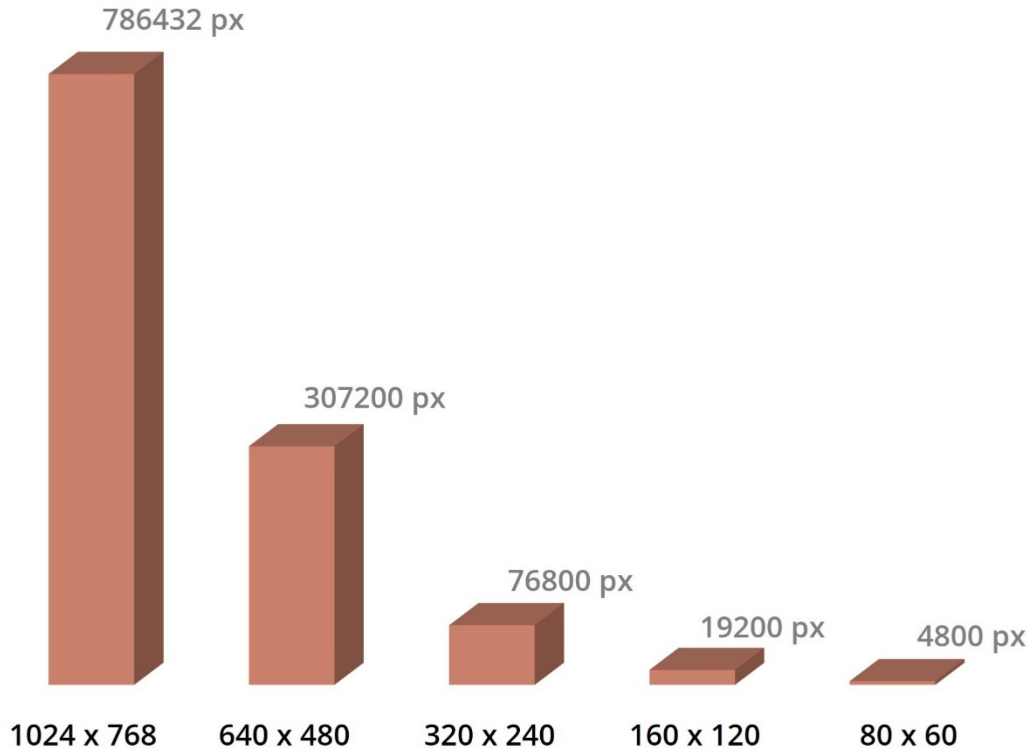

Figure 35. Number of pixels for different focal plane array sizes.

Another example illustrating the array size effect is observed in Figure 36, in which two infrared images from the same scene but using two different cameras are shown. Figure 36a displays the image of the camera with the biggest FPA (1024 x 768 pixels) whereas Figure 36b displays the image taken with the smaller FPA camera (320 x 240). Moreover, the “320 x 240” IR image has also been overlapped on the left bottom corner of the “1024 x 768” IR image, showing in this way how much space would comprise.

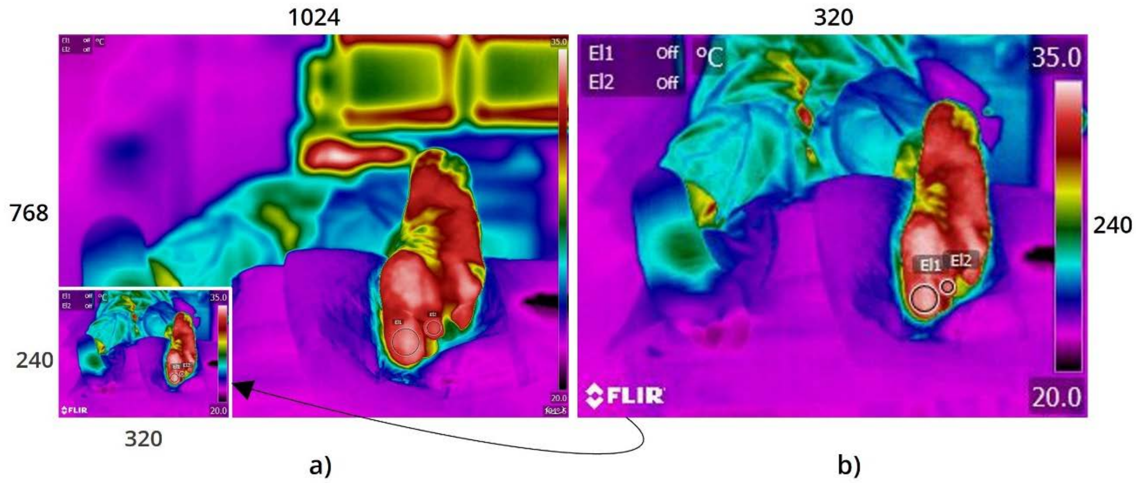

Figure 36. Infrared images of different detector array’s size a) 1024x768 b) 320x240. In the left bottom corner of a) the image b) is place according to its proportion.

The optics, and particularly the camera lens, defines the size of the scene that can be evaluated along with the minimum size of a detectable object within the image.

The **field of view (FOV)** is described as the angular extent of the observable scene, and it is defined by the camera lens and the FPA dimensions. Since the detector array has a rectangular shape, the evaluated scene presents two different fields of view, the horizontal (HFOV) and vertical (VFOV) field of view [648] (Figures 37 and 38).

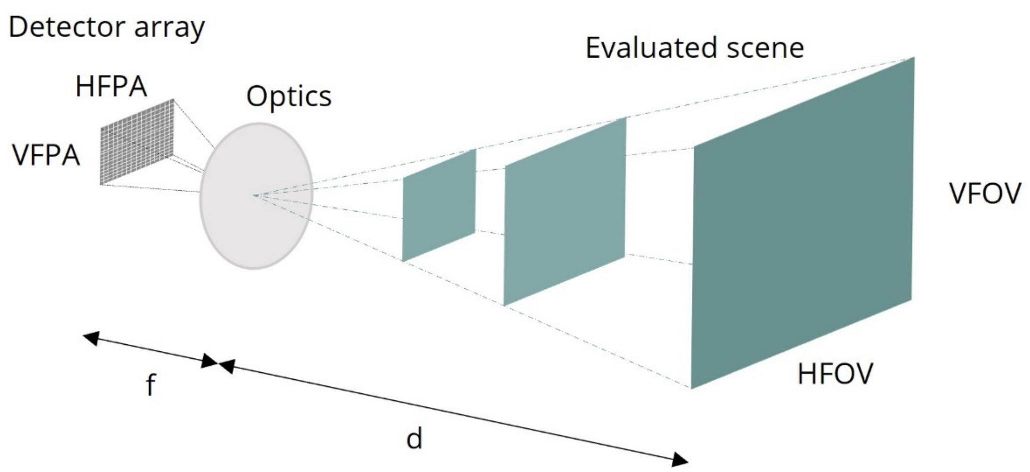

Figure 37. The flied of view for a camera lens with a focal length f and at a given object distance d. Adapted from [648].

To calculate the horizontal and the vertical field of view, Equation 14 and 15 can be used:

$$\mathrm{HFOV(m)} = 2 \cdot \mathrm{d} \cdot \mathrm{tg}\left(\frac{\mathrm{HFOV}(^{\circ})}{2}\right) \qquad \text{Equation [14]}$$

$$\mathrm{VFOV(m)} = 2 \cdot \mathrm{d} \cdot \mathrm{tg}\left(\frac{\mathrm{VFOV}(^{\circ})}{2}\right) \qquad \text{Equation [15]}$$

Where,

d (m) is the distance between the lens and the evaluated scene.

FOV (º) is the lens angle associated with the horizontal (HFOV) and the vertical (VFOV) dimension. Typically, the greater FOV (º) is associated with the horizontal dimension.

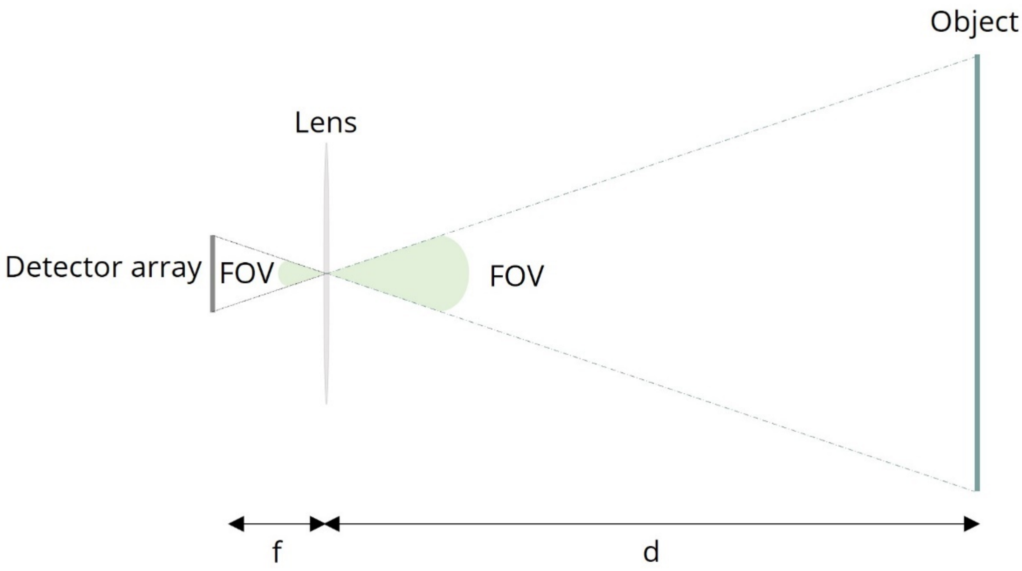

Figure 38. 2D field of view (FOV) representation.

Using the relationship between the focal length and the angular field of view of the camera, the detector array size can be calculated:

$$\mathrm{HFPA(mm)} = 2 \cdot \mathrm{f} \cdot \left(\frac{\mathrm{HFOV}(°)}{2}\right) \qquad \text{Equation [16]}$$

$$\mathrm{VFPA(mm)} = 2 \cdot \mathrm{f} \cdot \left(\frac{\mathrm{VFOV}(°)}{2}\right) \qquad \text{Equation [17]}$$

Where f (mm) is the focal length of the camera lens.

Finally, the pixel size can be obtained from the detector size dimensions and the number of pixels:

$$\mathrm{Pixel\ size(mm)} = \frac{\mathrm{FPA\ (mm)}}{\mathrm{nº\ of\ pixels}} \qquad \text{Equation [18]}$$

In figure 39, a representation of a pixel within the detector array is depicted. For instance, a camera with a FPA of 320 x 240 pixels, using a lens with a FOV of 25º x 19º and a focal length of 18 mm, would have a detector array size of 7.9 mm x 6 mm and a detector size of 24.9 µm.

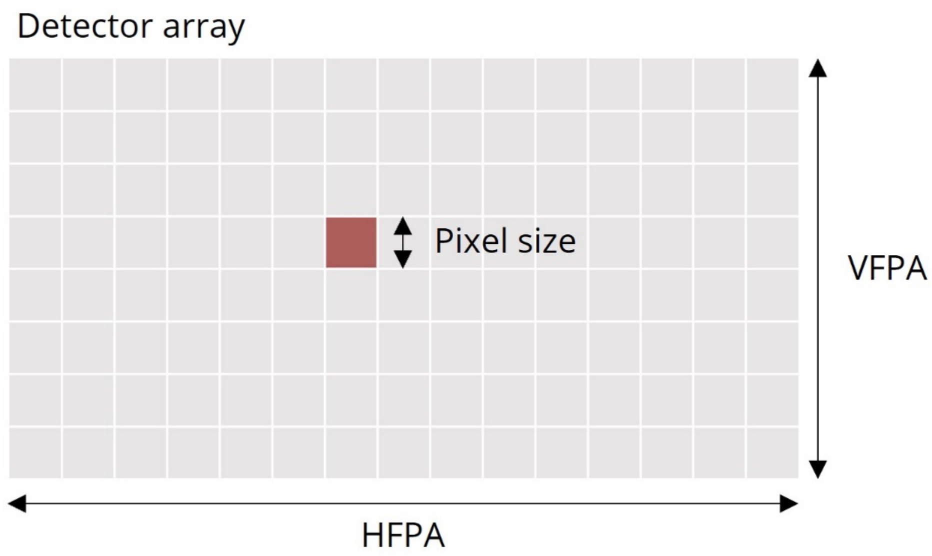

Figure 39. Representation of the pixel size within the detector array.

Therefore, lenses with greater FOV (Figure 40a), would correspond to wide angle lenses (used when getting distance from the object results in a hard matter), whereas lenses with smaller FOV, such as 7º or 12º, would correspond to telescopes lenses (Figure 40b).

Figure 40. Two different lenses a) 45º and b) a telescope lens.

The **instantaneous field of view (IFOV)** or **spatial resolution,** indicates the minimum object size which fits on a single detector element for a given distance (Figure 41). It is a geometric value calculated from the detector array and the optics, and it is expressed in milliradians (mrad) [648]. It can be calculated using the following expression:

$$\text{IFOV (mrad)} = \frac{\text{FOV}(°)}{\text{nº pixels}} \cdot \frac{2000\pi}{360} \qquad \text{Equation [19]}$$

Where the number of pixels correspond to the appropriate FOV (º) dimension.

That is, a camera with a detector array of 320 x 240 and 25ºx19º lens, would present an IFOV of 1.36 mrad. To obtain this result, when the 25º is chosen, 320 pixels must be placed in the denominator. Indeed, in most commercial datasheets, when only one FOV value is provided, it is usually the greater one. To continue this example, an IFOV of 1.36 mrad expresses that the camera would be able to detect a minimum object size of 1,36 mm at a distance of 1 m. However, it should be taken into account that, the system resolution is additionally influenced by the diffraction of the optics, so in order to achieve an accurate temperature measurement, the absolute minimum size of the object should be 2 or 3 times the IFOV. According to this, a minimum object size of about 6 mm may be necessary to obtain an accurate temperature measurement regarding the previous IFOV of 1.36 mrad.

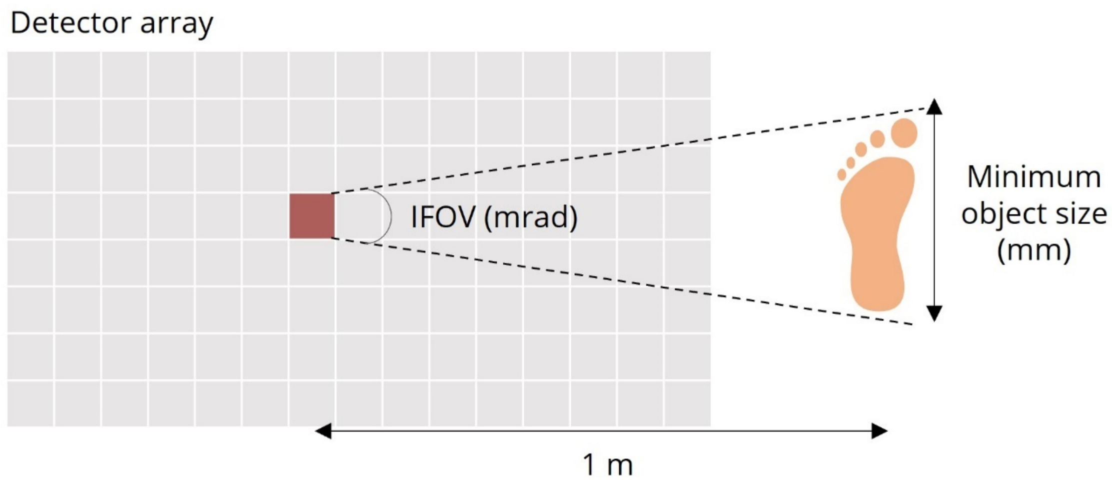

Figure 41. Representation of the instantaneous field of view (IFOV) value associated with the minimum object size which can be detected.

In a visual way, Figure 42, depicts two IR images from the same scene, taken at the same distance with 1024 x 768 (a) and 320 x 240 (b) FPA sizes cameras respectively Moreover, two different regions of interest have been placed, the first one (El1) on the hallux and the second one (El2) on the second toe. When each tool is compared between the two images, it can be observed that the number of pixels comprised within the same tool is much greater in the image with bigger detector array size (almost 3 times). These observations are in line with the IFOV values of each camera, since the IFOV of the "320 x 240 camera" is almost three times the one of the "1024 x 768 camera". Consequently, when the application aims to detect small objects, the greater the size array, the smallest the IFOV and, therefore, the better features.

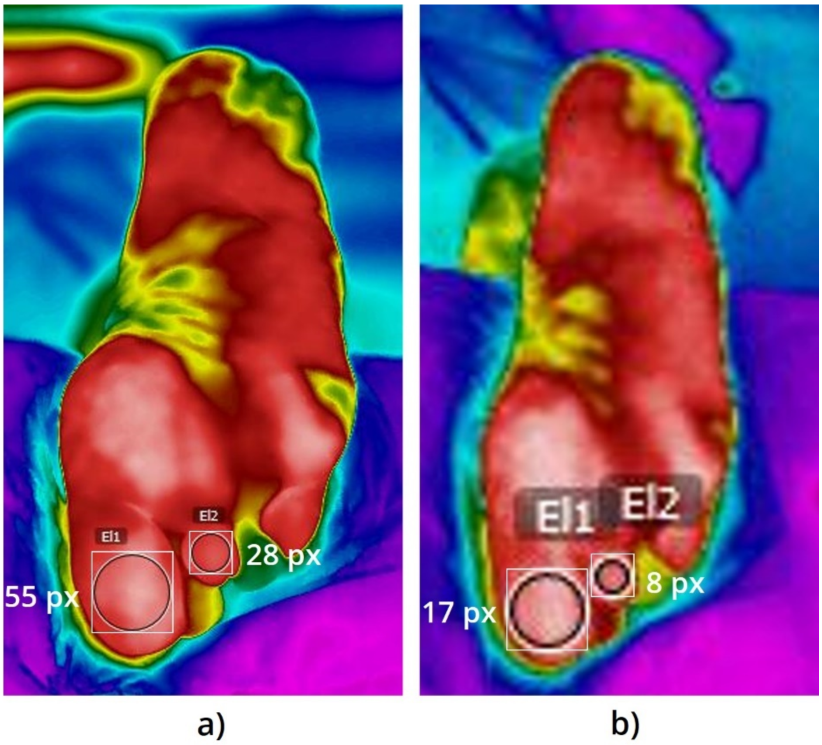

Figure 42. Comparison between two cameras of different focal plane array size of a) 1024 x 768 and b) 320 x 240. Two regions of interest in each image have also been used (El1 and El2).

Another parameter which directly affects the image quality is the **thermal sensitivity (NETD),** which describes the camera's ability to detect small temperature differences within the image [648]. This parameter is also associated with the system's noise since the NETD expresses the amount of energy required to produce a signal of equal or greater size than the noise produced by the camera system. In this sense, the lower the NETD value, the lower noise and the smaller the temperature differences can be detected within the image. It is advisable to remark the object temperature and the NETD value dependence. In fact, the NETD decreases when the object temperature values are higher. For this reason, and to avoid confusion, the NETD must be expressed at a defined temperature (usually 30ºC).

The **temperature accuracy** gives the absolute value of the temperature measurement error for blackbody temperature measurements. It can be expressed as a temperature value or as a percentage of the measured temperature and common values are about ±2ºC or ±2% of the measured temperature.

The **temperature range** defines the minimum and maximum apparent temperatures that detectors can measure. Depending on the camera, the temperature range can be more or less wide, and, in some cameras, several ranges can be selected. It should be noted that, according to the object temperature and the NETD dependence, the narrowest temperature range should be selected to achieve better thermal resolutions. For instance, an object at a temperature about 30ºC is to be evaluated using a camera with two temperature ranges, the first one from -20 to +120ºC and the other one from 0 to 650ºC. Although the temperature of the object to be assessed is comprised in both temperature ranges, the best option would be selecting the narrowest one, that is the -20 to +120ºC range.

The **frame rate** defines the time resolution a camera is able to store. It is usually expressed in Hertz (Hz) so, a camera with a frame rate of 50 Hz would be able to record 50 consecutive thermal images in a minute. Hence, fast transient thermal processes require high frame rates in order to record the maximum possible details going on. However, typical frame rates of 30 Hz are usually enough to capture common transient processes.

A summary of the most remarkable parameters of three different camera systems are presented in Table 6.

Table 6. Performance parameters of different infrared cameras.

Performance parameters	FLIR T1020	FLIR E60	FLIR One PRO
Detector type	Uncooled microbolometer		
Spectral range	7.5 – 14 μm	7.5 – 13 μm	8 – 14 μm
Focal Plane Array (FPA)	1024 x 768	320 x 240	160 x 120
Field of View (FOV)	28º x 21º	25º x 19º	50º x 43º
Instantaneous Field of View (IFOV)	0.47 mrad	1.36 mrad	6.5 mrad
Minimum IR focus distance	0.4 m	0.4 m	0.15 m
Temperature range	-40ºC to +2000ºC	-20ºC to +120ºC	-20ºC to +400ºC
Thermal sensitivity at 30ºC (NETD)	< 20 mK	45 mK	70 mK
Accuracy	± 1ºC*	± 2ºC	± 3ºC
Frame rate	30 Hz**	60 Hz	8.7 Hz

** the accuracy when temperature range is +5ºC to +100ºC. Otherwise, it would be ± 2ºC.*

*** it can reach 120 Hz when a High-Speed Interface is used.*

The performance parameters as the ones described above, must be determined once the camera has been calibrated by manufacturers. The **calibration** process is performed by means of several black bodies sources at different temperatures resulting in the definition of each pixel signal. In this way, a relationship between the camera signal and the black body temperature is established and all single detectors provide accurate temperature values [648].

Thermal drifts on the camera could occur when the camera has not reached the equilibrium following it has switched on, or when a drastic thermal change takes place. In these circumstances, the temperature values provided could be inaccurate [648]. To avoid these effects, a LWIR microbolometer camera should be switched on about 10 minutes before starting the measurements so a temperature accuracy of ± 2ºC can be achieved. On the other hand, when the camera undergoes a drastic thermal change, the accuracy gets worse which can result in wrong temperature readings. In these situations, and depending on the extent of the thermal change, about 20 to 30 minutes should be waited before starting the measurements. In low- cost cameras, this time is critical [649].

3.6.4 Applications of IRT

At the present time, thermography is broadly applied in a wide variety of applications, including industry and surveillance, buildings, veterinary and naturally, medicine.

The first thermal patterns observations go back in time to the Egyptians, who move their hands across the bodies of ill people to detect emitted heat to "diagnose" possible diseases. Ancient Greeks also examined how bodies dried after their immersion in wet mud [650]. However, it was not until 1866 when, what we now know as a thermal image was obtained [651]. As in many other technologic devices, great developments were achieved in the military field, on this occasion, regarding the World War II in 1934, where image intensification systems were first used [652]. These systems were the basis for the early night vision systems (Figure 43a) [653]. Thermal imaging in civilian use emerged in the 60s. The first IR imagers were developed by AGA (now FLIR Systems, USA) which were not portable because they were heavy and bulky (Figure 43b), they had restricted movements since they must be plugged in, and their performance parameters were poor. However, from this point, the development in the infrared technology evolved rapidly and the applications started to expand [654].

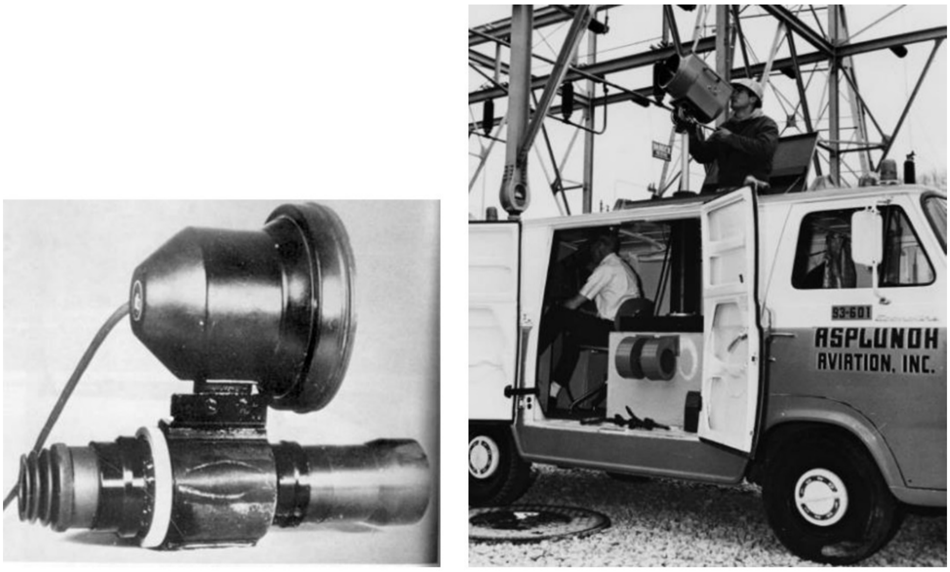

a) b)

Figure 43. a) Zielgerät 1229 “Vampir”, the first night-vision system and b) the inspection of an electrical substation using AGA Thermovision 650 (From [655]).

By now, infrared thermography is being used in a wide variety of fields. For instance, IRT is usually integrated into predictive maintenance programs since heat is often an early warning of damage or malfunction. In this sense, this technology is critical to avoid equipment failures which, in turn, it is directly related with cost saving. Thus, among the inspected equipment are pipes, electrical circuits, engines, pumps, vessels, and so forth. Likewise, the IRT applications in industry are diverse. Regarding electrical applications, the inspection of high-voltage components such as the ones in substations, (Figure 44a) or the inspection of low voltage components or electronic boards are very common. When it comes to mechanical systems, valves, engines (Figure 44b), pumps, pipelines, or industry facilities such as heating, ventilation, and air-conditioning systems are also usually inspected by IRT [656].

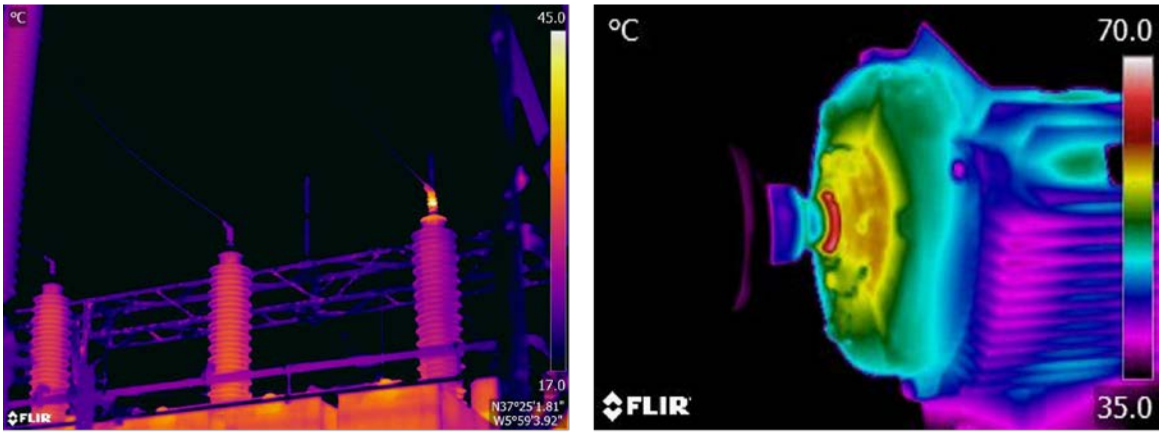

a) b)

Figure 44. Infrared images of a) substation components and b) engine bearings.

Building inspection is one of the most commercial applications in which IRT is employed. Some problems to be detected include the state of buildings diagnosis, the insulation evaluation (Figure 45a), water leaks or water intrusion along with moistures and uncontrolled airflows localization (Figure 45b). Hence, the main purpose regarding IRT in building inspection is to identify problems associated with heat (thermal bridges), water (leaks and intrusions) and airflows through the building envelope [657-659].

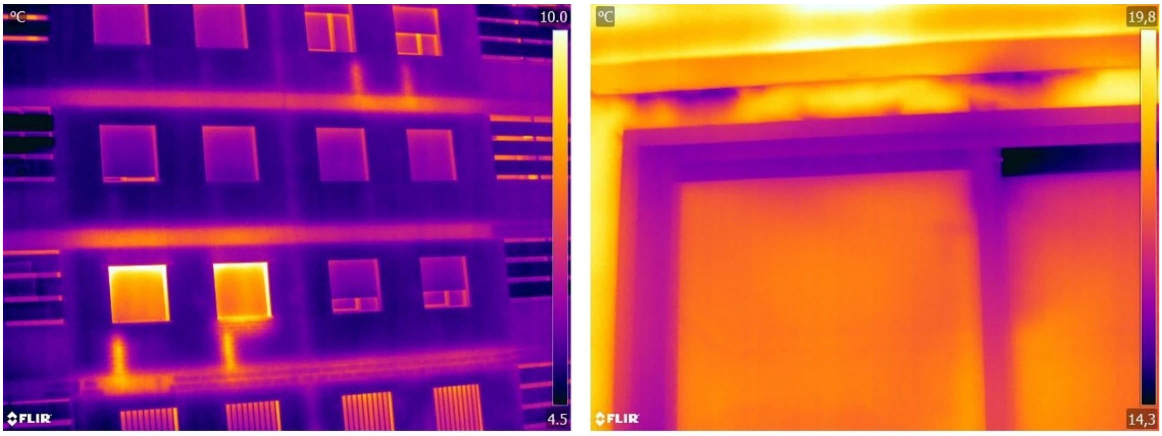

a) b)

Figure 45. Infrared images of a) external façade in winter and b) indoors in winter where the air infiltrations can be observed.

Another field in which the IRT is frequently applied is in renewables energies components such as the evaluation of solar panels (Figure 46a), in which faulty interconnections, cracks in cells, or temporary shadowing can be detected [660,661]. Likewise, the critical components of wind turbines are commonly inspected with IRT, for instance, the evaluation of rotor blades checking for subsurface defects within the rotor blades (Figure 46b) [662-664].

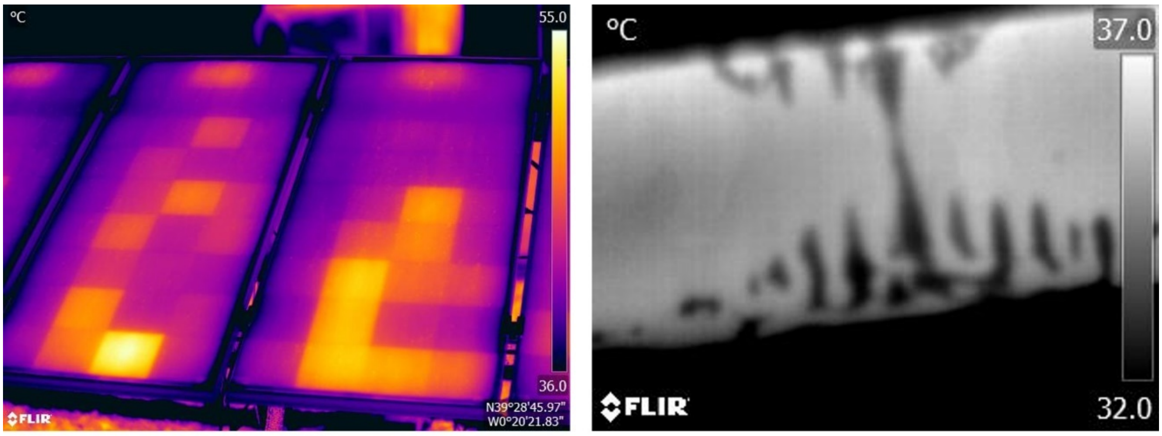

a) b)

Figure 46. Infrared images of a) solar panels and b) a rotor blade with disbanded areas.

IRT has shown to be a reliable technique for non-destructive evaluation of composite materials used in the aerospace field (Figure 47). Thus, the water ingress in some areas of the aircraft or delaminations within the layers of a component are some problems that can be detected [665,666].

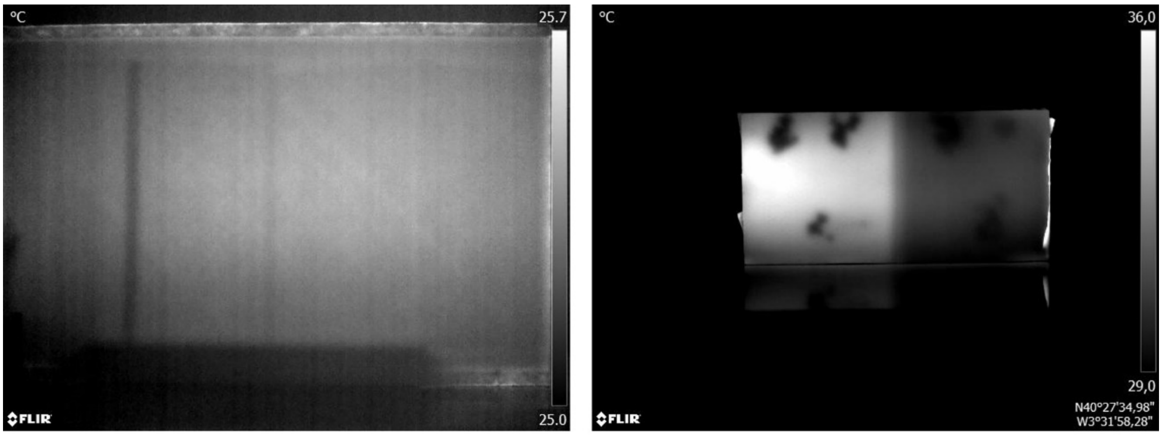

a) b)

Figure 47. Infrared images of a) delaminations and b) water ingress in aerospace composite materials.

The IRT is also employed in the study of cultural heritage and artwork materials since it does not cause any damage on them (Figure 48). Its use has been described for cracks analysis in sculptures, the detection of material detachments or subsurface defects beneath paint layers among others [667,668].

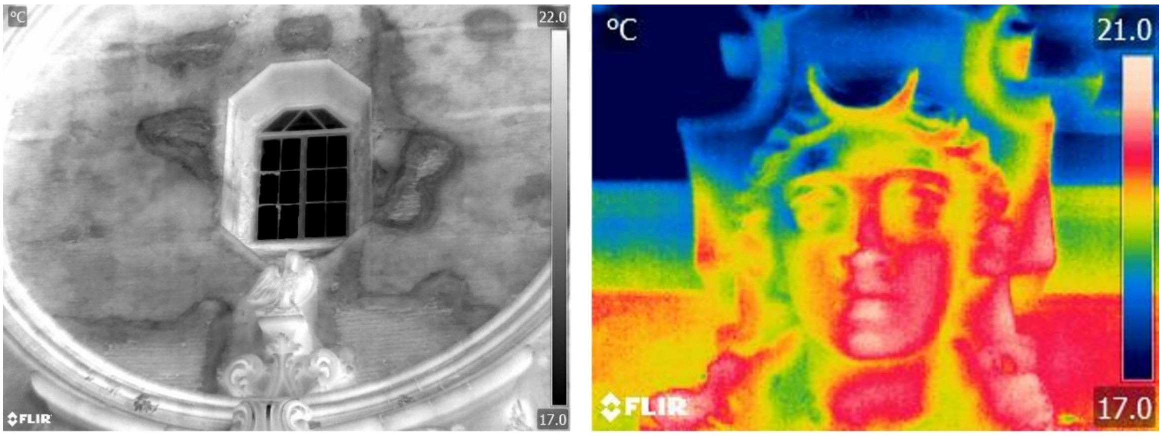

a) b)

Figure 48. Infrared images of cultural heritage a) façade evaluation and b) sculpture analysis.

On the other hand, aerial IR imaging with the use of drones has increased dramatically over the last years. Its scope is considerably broad, but it is mainly focused on the evaluation of areas with difficult access. Some of the applications of aerial thermal imaging include follow-up fire monitoring [669], localization of missing people [670,671], wildlife animals' study [672,673], agriculture evaluation [674], active volcanoes monitoring [675], industrial facilities or buildings inspection [676], archaeological sites assessment [677,678], bridge condition monitoring [679], high-voltage power lines evaluation [680], solar plants [681-683], or wind turbines rotor blades monitoring [684].

3.7 IRT in the biomedical field

Since IRT is an imaging technique performed without physical contact, it is safe and intrinsically harmless. As a result, a temperature distribution of an area of interest within the body can be obtained in form of a 2D false colour image. Thus, through this image, known as thermogram, alterations on skin temperature can be identified, which may indicate the presence of infection or inflammation [685].

During the first decades (1960-1970s), the IRT used in human research was first focused as a diagnostic technique (Figure 49), and it was used mainly on the diagnostic of breast cancer [686-688], and skin malignancies [689]. Apart from these first applications, since then, a vast number of diseases have been included on the IRT evaluation such as diabetes, rheumatic diseases [690,691], Raynaud's phenomenon [692], vascular conditions [693], dermatological applications, or CRPS [191]. Moreover, the use of IRT is also widespread in sports science [694]. In recent years pandemic fever outbreaks, such as COVID-19, has provoked an outburst in the use of IR devices to detect fever [695].

Figure 49. Evaluation of facial infrared images. From [655].

Table 7 presents different applications regarding the medical field published during the last 5 years (2016-2021) in which the topic and the corresponding references can also be found. As can be observed, along with cancer diagnosis, the IRT is very popular for an early-stage detection of diabetic foot disorders since they usually present abnormal plantar temperature.

Table 7. Applications in the medical and sport field using infrared thermography.

Application	References
Breast cancer	[688,696-716]
Other cancers	[717-728]
Vascular disorders	[628,729-760]
Rheumatic disorders	[629,761-786]
Dermatological	[787,801]
Ocular	[802-809]
Dental	[810-814]
Musculoskeletal	[814-825]
Fever screening	[826-837]
Thermoregulation and skin temperature	[838-849]
Sports	[781,850-880]
Others (Brown adipose tissue, cellulite, pregnancy)	[881-891]
CRPS	[189-191,199,220,245,892-894]

At the beginning, the lack of standardized procedures and protocols along with the unfamiliarity with the technique and the poor performance parameters of the IR equipment, resulted in high false positive and negative rates, which led to a distrust of the technique. However, the improvement of the technology along with the research on the field have contributed to promote scientific validity of the thermography. Likewise, several protocols and different proposed procedures have been published over the years (Figure 50). In 2008 "The Glamorgan protocol" was the first publication in which technical factors influencing infrared data acquisition were collected [895]. In this protocol, an "Atlas of Infrared Images of Healthy Subjects "was described in which the definition of different regions interest from different parts of the body could be found. Studies analysing the influence that technical factors could have on the results when using IRT on human's assessment have also been performed [896,897]. In 2012, as a result of their previous publications, Ring E.F.J. and Ammer K., published "Infrared thermal imaging in medicine", in which IRT technology features and the standardization of the protocols for thermal imaging in medicine were described [898]. The book "The thermal human body: a practical guide to thermal imaging", is the most recent guide of the same authors related to this topic. Indeed, a chapter addressed to a protocol based on their broad clinical practice can be found [617]. In 2017, it was developed a 15-items checklist for collecting skin temperatures using IRT in sports and exercise medicine (TISEM) [851]. The checklist included items associated with individual information of the participants, extrinsic factors affecting skin temperature, environmental factors, equipment characteristics, acclimation period, conditions of image recording, or image evaluation [851]. Moreover, different associations, academies and organizations have also published guidelines that include most important methodological aspects concerning the use of IRT on humans' assessment. The International Academy of Clinical Thermology (IACT) has published medical infrared imaging standards and guidelines "issued as a quality assurance guideline for the clinical use" [899]. The International Organization of Standardization (ISO), in turn, published the ISO 9886:2004 [900], which describes methods for measuring and interpreting some physiological parameters along with the IEC 80601-2-59:2017 regarding the technical requirements of screening thermographs for fever assessment [901]. The American Academy of Thermology (AAT) published in 2016 a guideline aimed at neuromuscular thermography [902]. In Europe, The European Association of Thermology (EAT) has published several studies focused on the standardization concerns in medicine thermal imaging [903-905], most of them summarized in the Glamorgan Protocol [895]. In 2015, during the EAT Congress, a "Protocol for thermographic assessment in humans" was published taking into account the most recent updates and results [906].

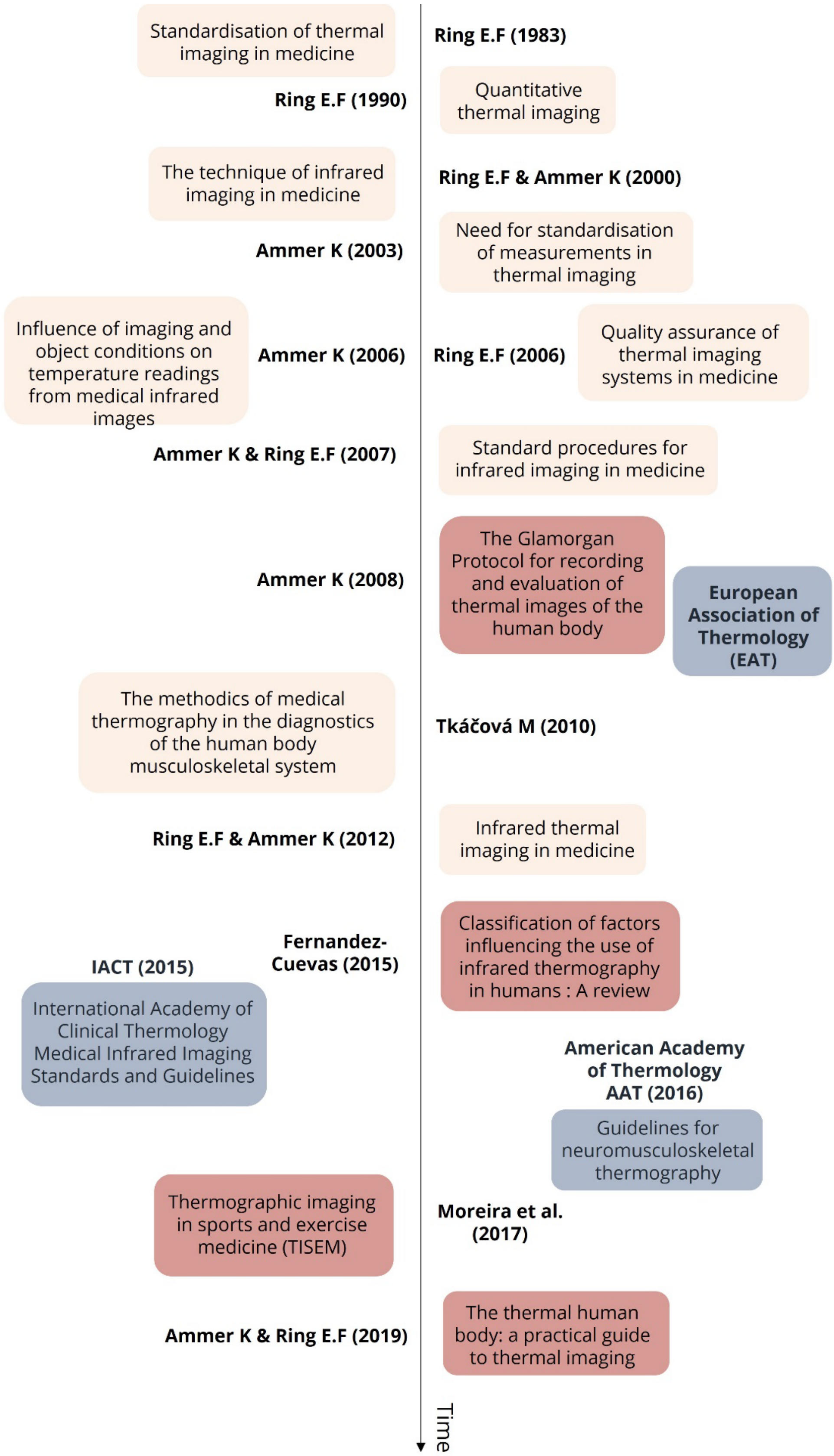

Figure 50. Different guidelines and protocols published over the years.

The emergence of all these standards and protocols have promoted the use of IRT on medicine, which is nowadays acknowledged and promoted by different associations, including The International Thermographic Society, The European Association of Thermology, The Northern Norwegian Centre for Medical Thermography, The German Society of Thermography and Regulation Medicine, The American Academy of Medical Infrared Imaging, or the International Academy of Clinical Thermography. Nevertheless, as pointed out in several publications described previously, there are several factors responsible for influencing the temperature assessment in humans, such as environmental, individual, and technical factors [617,896,907]. In Figure 51, these factors, and their concerning parameters when IRT is performed in human's assessment are presented.

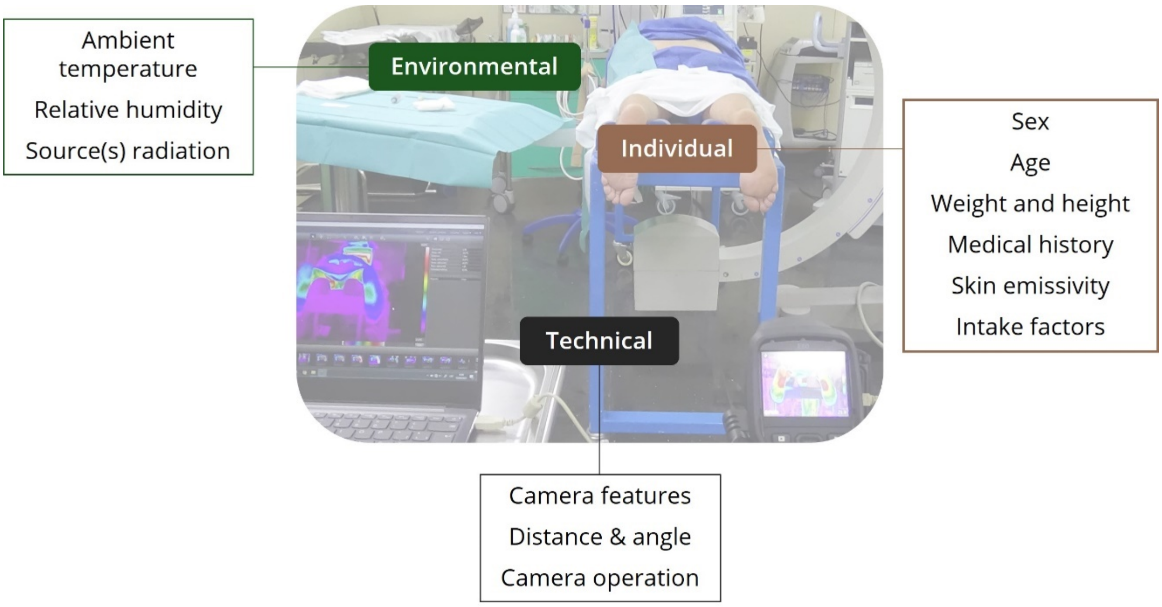

Figure 51. Influencing factors when infrared thermography is performed in humans.

Among the **environmental factors**, the following parameters concerning the room where the assessment is performed should be looked out: the ambient temperature, the relative humidity, and possible sources of radiation. The ambient temperature is suggested to be between 22ºC and 24ºC when extremities are evaluated because the influence of the sympathetic nervous system and the tendency of extremities to have lower skin temperatures [617]. Likewise, it is important to follow an acclimation period that should last from 10 min to 30 min during which the person achieves the thermal equilibrium with the room conditions [896,908]. Although relative humidity does not influence significantly on skin temperature when the ambient temperature is within an acceptable range of thermal comfort, it is usually reported to be between 40% and 70% [896,909,910]. External sources of radiation can be present inside the evaluating room, such as, medical equipment, lighting, airflows or even the presence of people. Generally, since the temperature values of the external sources are lower than the skin temperature values, they would have in the end poor influence on the final skin temperature. Nevertheless, if direct air currents or significant sources of radiation with a direct impact on the person assessed are observed in the room, it would be advisable to remove, avoid or shield them [617,896].

Variables such as sex, age, medical history of the patient, or intake factors constitute **individual factors** which may have influence on the final registered temperature. For instance, the thermal pattern would vary depending on the patient's sex and or age [624,911,912]. On the other hand, the individual anatomy, such as the weight or height, may be related to the heat dissipation in certain body areas [913,914]. The medical history of each patient may also play a role on its own thermal patterns, especially when they have experienced previous injuries, degenerative processes, or vascular alterations [915-917]. Skin emissivity is one of the most important parameters in IRT and regarding several works on the matter, 0.98 is commonly adopted as a standard skin emissivity value [918-920]. Finally, intake factors include not also medication but also alcohol, stimulants, or tobacco, which may temporarily influence on the thermoregulation [921-923]. Likewise, practicing exercise prior the assessment must be avoided since physical activity induces thermoregulatory processes leading to unreliable temperature measurements [852,924]. For this reason, when thermal data is to be collected, some indications should be described to avoid the above-described factors.

Technical factors such as the camera performance parameters or its position in relation with the surface of the body to be evaluated must be considered. In this sense, it is important to place the camera as perpendicular possible to the assessed area because when angles between the camera and the element are greater than 50º, emissivity is altered, and inaccurate temperature values may be obtained [648,897,907]. Likewise, the distance between the assessed area and the IR camera should be the minimum at which the whole area to be analysed is comprised within the image [648,897,907]. Thus, the greater number of pixels included, the greater thermal information [648,925]. In this sense, camera performance parameters such as the FPA size or the lens angle, would determine the camera capability to provide enough thermal information [648]. As described previously (section 3.6.3), since each detector of the FPA (i.e., a single pixel) provides a radiation value, the larger number of pixels the camera accounts for, the more thermal information would provide. Moreover, the smaller the IFOV, the smaller elements would be detected. On the other hand, a stabilization period of the camera after switching it on is recommended to avoid temperature drifts triggered by the electronics. In this sense, uncooled cameras must be switched on about 5 to 10 minutes before starting images acquisition to ensure correct temperature measurements [648].

The non-contact methods are based on radiation basis and diverse devices are embraced, ranging from infrared thermometers to smartphone-based cameras to infrared cameras. Regarding their use to skin temperature measurements, some remarks are hereafter presented. The COVID-19 pandemic has triggered the interest over the skin temperature measurement in a simple, contactless, and fast way to control the access in hospitals, airports, workplaces, etc. [831,926]. This situation has led to the widespread of skin temperature controls, in most cases, by means of infrared thermometers [927,928]. Although complying with the corresponding standards, the use of these devices is under suspicion when discerning and discriminating symptomatology such as fever or temperature asymmetries. In this sense, several studies have investigated the performance and reliability of infrared thermometers for skin temperature measurements [929,930]. Results indicate that parameters such as the working distance along with the angle of inclination of the device, can result in temperature measurements errors [929]. Likewise, the uncertainty of infrared thermometers has been estimated to range between 0.4ºC and 0.62ºC in uncontrolled conditions [930]. Regarding the low-cost infrared cameras, the first models emerged in 2014 and from that moment, they have been implemented in several medical applications since they are financially more viable and considerably more portable over other thermal cameras [931,932]. At first, the issue about these devices suitability for clinical use was raised, and their performance has been evaluated for different applications. Some results showed that smartphone-based infrared imaging devices could assess burns, subclinical inflammations in diabetic feet, or limb perfusions [738,932]. However, a recent study suggests the operational performance of these low-cost infrared devices do not comply with the minimum standards for clinical use [931]. Likewise, an overestimation of temperature readings was observed, and a minimum time to reach measurement stabilization of 15 to 20 minutes was required [931]. Recently, Vila et al. analysed different low-cost and smartphone-compatible thermal cameras and they observed that apart from switching on the device at least 15 minutes before the acquisition, which is in line with previous studies [931], a controlled environment should be required for a reliable performance [649]. To date, low cost or smartphone-based thermal cameras present still limited decisive performance parameters such as inadequate FPA size arrays, thermal sensitivities (NETD) or accuracies, and therefore their use should be primarily intended for assisting in some specific medical applications rather than using them in more demanding procedures such as diagnostics or absolute temperature assessments.

Therefore, when skin temperatures are to be assessed by means of non-contact devices, they must comply with some minimum operational specifications. According to the thermography guidelines of The International Academy of Clinical Thermology (IACT), the minimum specifications depend on the type of IR equipment [899]. Regarding the IR thermometers (with 3 or more spot radiometers), the repeatability and precision must be 0.1ºC of the temperature difference, and the accuracy should be ± 2% or less. However, when it comes to IR cameras, some additional specifications are required, for instance, spatial resolution of 1 sq. mm at 40 cm from the detector, or high-resolution image display for interpretation. Furthermore, it is suggested that infrared sensors are not suitable for some analysis such as breast cancer since they present many data acquisition problems. Nevertheless, if the device is manufactured complying the strict minimum standards regarding quality clinical infrared devices (i.e., accuracy, repeatability, and thermal stability), the information acquired would have diagnostic value [899]. On the other hand, according to the IEC 80601-2-59:2019, minimum performance parameters such as FPA array of at least 160 x 120, along with a NETD of < 50 mK at 30ºC, and a measurement uncertainty of ± 2% of the overall measurements are specified for fever screening devices [901].

3.7.1 IRT in the assessment of feet temperatures

Since the interest of this work lies in the evaluation of feet temperatures by means of infrared thermography, its utilization in previous works for different medical applications has been analysed. On the one hand, Table 8 shows related works on feet temperature measurements using IR cameras from 2016 to date. On the other hand, Table 9 depicts the works in which low-cost and smartphone-based cameras have been used to assess feet temperatures.

Table 8. Infrared camera models used on feet temperature assessment from 2016 to 2021.

Infrared camera	Focal Plane array size	Thermal resolution	Application	Ref.
FLIR SC640	640 x 480	< 30 mK	Rheumatoid foot	[933]
SmartIR 640	640 x 480	< 50 mK	Foot thermoregulation	[934]
Xenics Gobt 640	640 x 480	< 55 mK	Peripheral arterial disease	[691]
FLIR E60	320 x 240	< 50 mK	Diabetic foot	[935-941]
			Rheumatoid arthritis	[942]
			Sports	[873,878,943, 944]
			Temperature asymmetries	[626]
FLIR T430 sc	320 x 240	< 30 mK	Peripheral arterial disease	[945]
FLIR SC7200	320 x 240	20 mK		[946]
FLIR A320, A325, SC300, SC305	320 x 240	< 50 mK	Diabetic foot	[629,947-952]
Fluke Ti32, Ti560	320 x 240	< 50 mK		[953,954]
Flir E6	160 x 120	< 60 mK		[955]
Flir Lepton 3.0	160 x 120	< 50 mK		[956]
Fluke Ti10	160 x 120	< 130 mK	Diabetes mellitus	[957]
Testo 875	160 x 120	< 80 mK	CRPS	[191]

As can be observed in Table 8, the infrared camera models most frequently employed present a FPA array size of 320 x 240 along with thermal sensitivities around 50 mK. Regarding smartphone-based thermal cameras (Table 9), the FLIR One and their subsequent versions (FLIR One Pro LT and FLIR One Pro) have been widely used in different applications such as the localization of potential inflammation regions, evaluating risks of foot ulcers, or assessing peripheral perfusion [958-960].

Table 9. Smartphone and low cost cameras models ued on feet temperature assessment from 2016 to 2021.

IR Camera	FPA array	NETD	Application	Ref.
SEEK Thermal Compact XR	320 x 240	< 70 mK	Limb ischemia	[961]
FLIR One Pro	160 x 120	70 mK	Inflamattion localization	[958]
			Peripheral Arterial Disease	[962]
FLIR Lepton 2.5	80 x 60	< 50 mK	Diabetes	[963]
FLIR One	80 x 60	100 mK	Subclinical inflammation	[932]
			Diabetic foot	[759,959,964-967]
			Peripheral perfusion	[960]
			CRPS	[190]
FLIR One Pro	160 x 120	70 mK	Comparison for thermal applications	[649]
SEEK Thermal Compact PRO	320 x 240	< 70 mK		
TE-Q1 Plus	384 x 288	< 50 mK		
Opgal Therm-App	384 x 288	< 70 mK		
FLIR C2 FLIR One Pro LT	80 x 60	< 100 mK	Evaluator reproducibility	[873]

As it has been mentioned above, infrared devices must comply with some minimum technical requirements when clinical assessment is to be performed. However, although the greater the performance parameters of the device (the combination of the highest FPA array along with the lowest IFOV and NETD), the less these variables would influence on the thermographic assessments [968], additional factors must be considered [969,970]. On the one hand, peripheral circulation in the distal regions of the body is weaker, which may result in both greater variability and less reproducibility of skin temperature measurements within the feet [970]. On the other hand, regarding environmental conditions, the ambient temperature effect on skin temperatures has been evaluated by several authors confirming that as higher the ambient temperature is, the higher skin temperatures are measured [617,628,971].

Therefore, the thermal equipment holding the minimum requirements of the operation parameters for medical applications is already available. Although the recent emergence of low cost and smartphone-based thermal cameras could raise the issue about the performance of the technique in the medical field, these concerns would most likely be overcome in the short run because the IRT technology is growing day by day. However, it is of paramount importance to take into account the limitations of the technique for certain purposes.

DATA ANALYSIS

04

Infrared thermography for the assessment of lumbar sympathetic blocks in patients with Complex Regional Pain Syndrome

4 DATA ANALYSIS

When the aim of a study is focused on the thermal patterns of specific regions of interest and accurate temperature measurement assessment is not intended, a qualitative analysis is usually performed. However, when temperature variables such as the average temperature, the maximum temperature or the standard deviation within an image or a specific area are to be accurately determined, a quantitative approach must be performed. In these cases, the compensation parameters along with the influencing factors must be considered. Additionally, once the variables of interest are retrieved from the thermal data, they can be analysed implementing statistical methods, although currently, the analysis approach is moving toward machine learning.

4.1 Qualitative approach

The image appearance displayed on the camera screen or on the analysis software mainly depends on each manufacturer of the IR equipment. However, the general appearance has lots of similarities and they usually include the same features. Regardless of the colours of the scene, the colour scale containing the maximum and minimum temperatures are often presented. Likewise, tools showing areas of different shapes and presenting maximum, average, or minimum temperature values can be displayed (Figure 52).

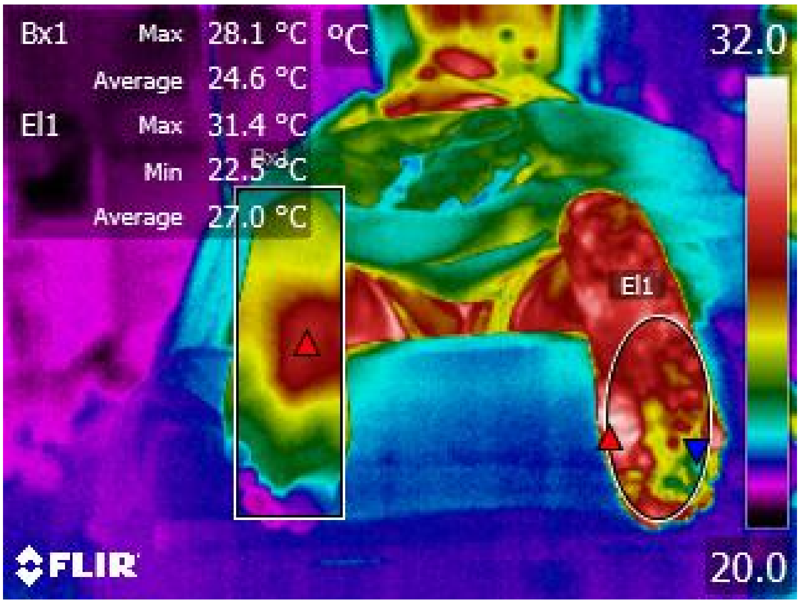

Figure 52. Two geometric areas (a box and an ellipse) provided by an analysis software showing their average, maximum and/or minimum temperatures.

Moreover, the camera display can also be set to show certain compensation parameters within the image, for instance, the emissivity value, the reflected temperature, or the temperature range at which the camera is working with.

Nevertheless, before adjusting some of the features described previously, a distinction between qualitative and quantitative thermography must be made because depending on the aim of the evaluation, the analysis approach would differ. When just thermal patterns are of interest and the temperature evaluation is not intended, the qualitative approach is performed, in which temperatures readings are apparent (the emissivity and distance values would set equal to 1 and 0, respectively). The qualitative approach may be, therefore, performed as a previous step in order to visualize the proper and adjusted thermal patterns within the area under evaluation. Conversely, the quantitative approach intends to determine temperature values accurately. For this reason, when this approach is carried out, all the compensation parameters and influencing factors described must be accurately adjusted to obtain correct temperature measurements.

Although in medical infrared imaging and especially in this work, the quantitative approach is performed, some aspects regarding qualitative IRT should be described. The **temperature scale** defines the minimum and maximum temperatures depicted on the infrared image. When the automatic mode is selected, the maximum and minimum temperatures are automatically adjusted, commonly based on the values comprised within the image. If the difference between the maximum and minimum temperature within the image are big, some thermal details may be overlooked. Moreover, the areas presenting temperatures out of the established limits, would appear without colour contrast (Figure 53a, 54a). Because of this, adjusting the scale manually at one's own interest, thus, narrowing the scale, should be of paramount importance. Thus, the temperature scale should be adjusted in order to comprise the temperature interval of interest so that the background or other radiation sources out of the assessment' scope are discarded. Figures 53 and 54a and 54b, demonstrate this effect. When automatic mode is selected, the temperature scale limits are broader. Conversely, when the temperature scale limits are manually adjusted, the difference between the maximum and minimum temperatures can be reduced (the minimum difference is about 2ºC at most).

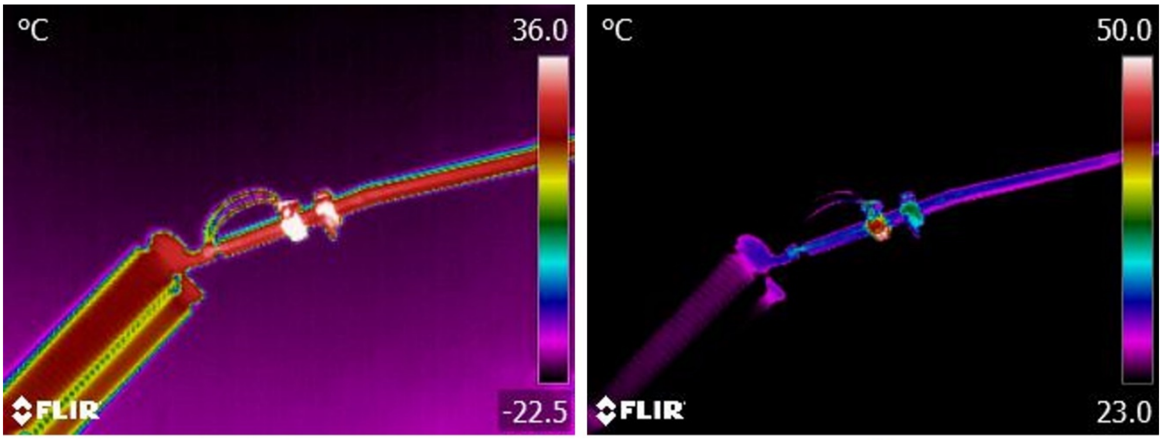

a) b)

Figure 53. The effect of the temperature scale adjustment in an image with a) automatic adjustment b) manual adjustment.

As one would assume, the temperature scale adjustment would play an important role in situations where significant temperature differences between the element under assessment and the background or specific external sources occur. An example of this is depicted in Figure 53, in which an electric component situated in an electric substation is evaluated. Since this element is situated outdoors, the sky temperatures are considerably low and when the temperature scale is automatically adjusted, a significant difference between the temperature limits (about 60ºC) are observed. In this infrared image (Figure 53a), little thermal details within the element can be distinguished. However, if the temperature limits are adjusted, thus, narrowing this temperature difference (Figure 53b), thermal details can be observed.

Color **palettes** are another adjustment feature that would make a difference when interpretation is involved. As can be observed in Figure 54 and considering that, the same baseline image has been used, images in rainbow high contrast palette show greater details as the ones in grey palette. In fact, when the grey palette image is observed in automatic temperature scale (Figure 54c), several details would be overlooked in comparison with Figure 54b (in manual temperature scale).

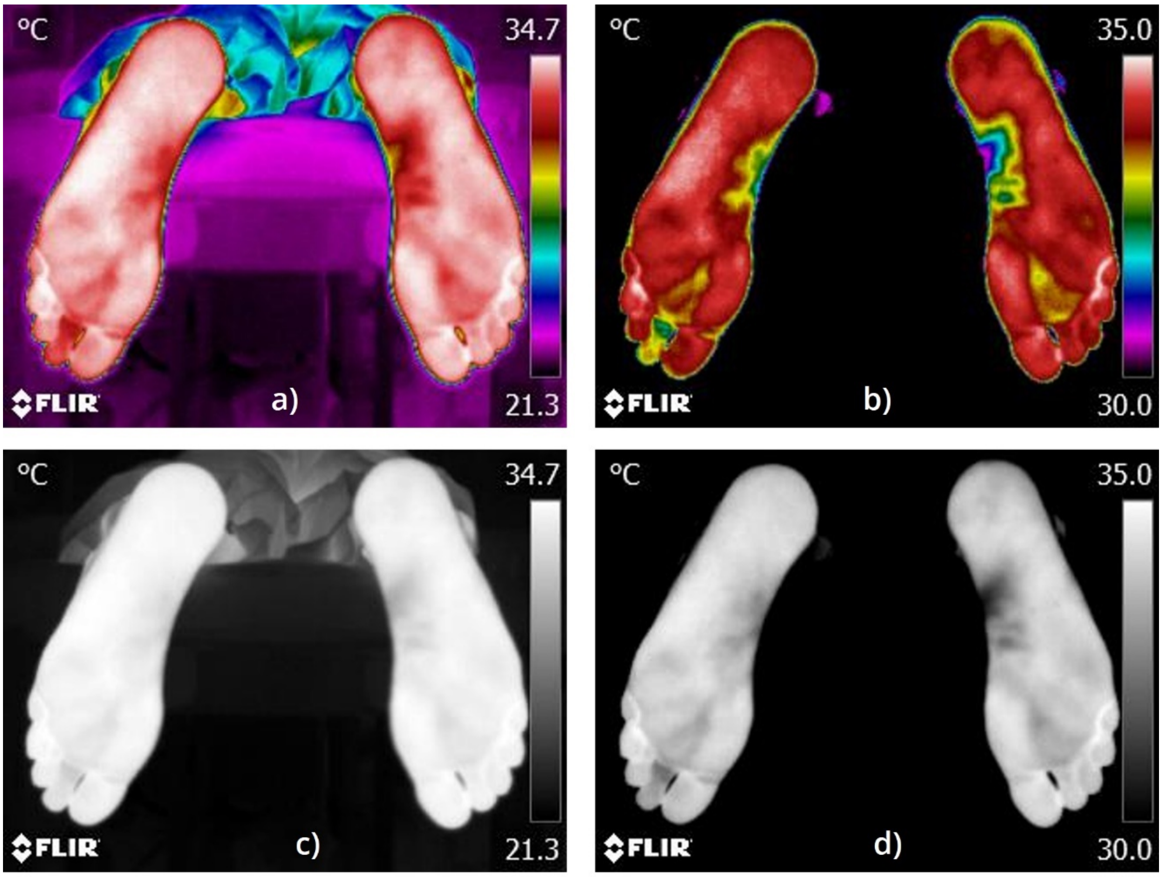

Figure 54. Examples of different temperature image scale adjustments: automatic in a) and c) or manual in b) and d). The differences between grey palette (c and d) and rainbow high contrast (a and b) are also shown. The baseline image is the same in the 4 cases.

To date, recent cameras are also capable to display thermal images in different modes (Figure 55). **Thermal fusion** consists of combining the digital image with the thermal one in the way that, depending on the temperature limits adjusted, some parts of the image are displayed in infrared (Figure 55a and b). When only a specific part of the image is to be highlighted, then an infrared image frame on top of the digital photo is displayed (Figure 55c). Finally, **MSX** (Multi Spectral Dynamic Imaging) depicts the infrared images including the edges of the objects within the scene (Figure 55d).

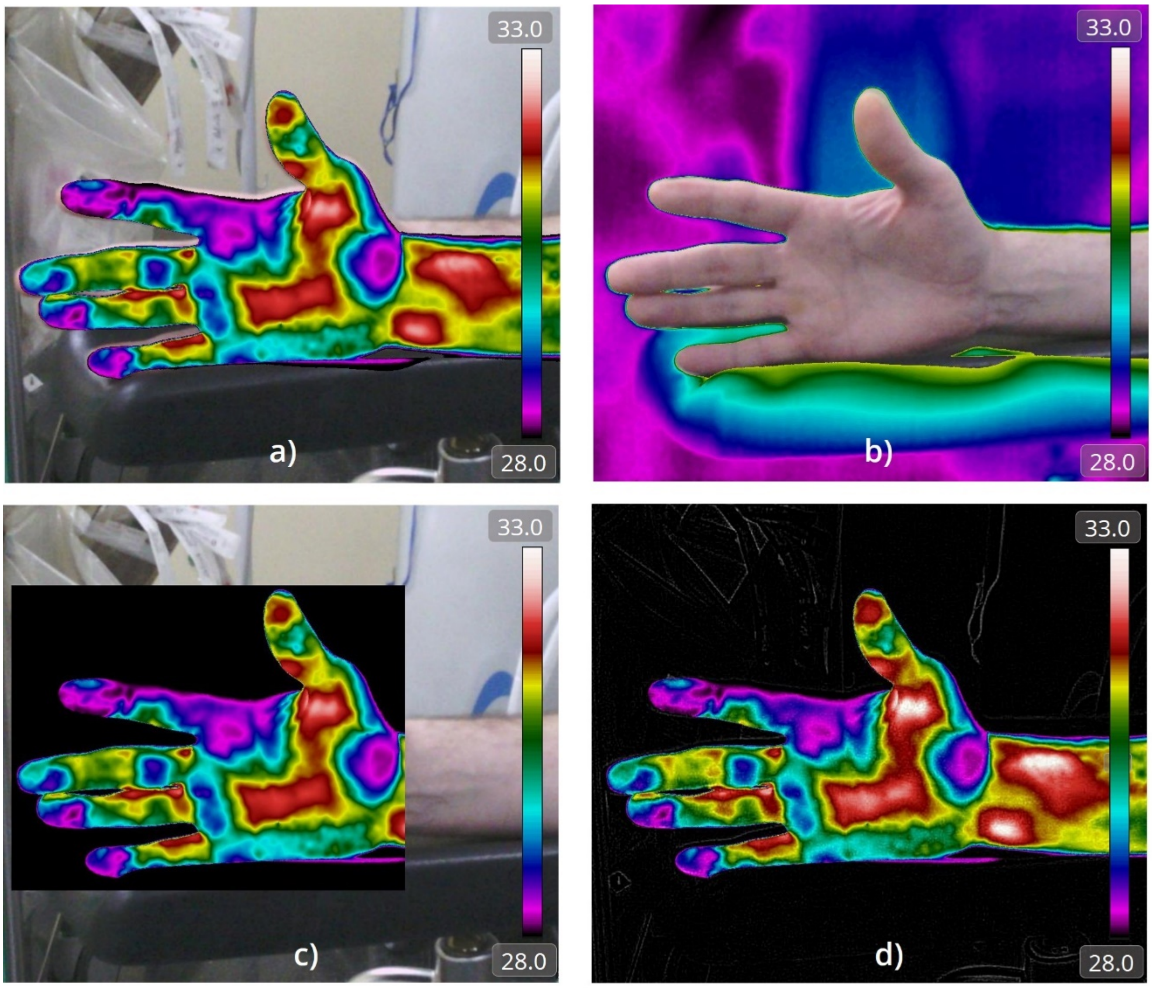

Figure 55. Image modes a) and b) Thermal fusion; c) Picture-in-picture d) Thermal MSX.

When an infrared image is to be evaluated either through the qualitative or the quantitative approach, the **image focusing** is of utmost importance. In this sense, the object under evaluation must be focused because otherwise, temperature values retrieved would be inaccurate. The reason behind this relies on the effect of the surroundings since the temperatures of the unfocused areas would be an average between the area of interest but also the surroundings (Figure 56). Therefore, the temperature of the object under evaluation has higher temperatures than the elements around it, and the result values of the object temperature would be lower than the expected. On the other hand, when elements around are at higher temperatures, measurements on the assessed object would be greater than should be.

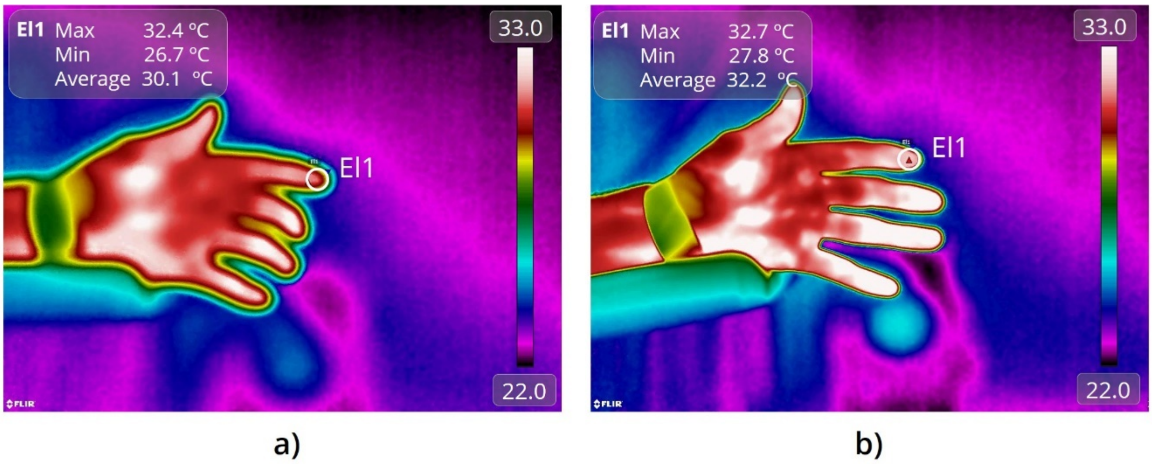

Figure 56. Effect of the image focusing. Example of a) an unfocused and b) a focused image.

4.2 Quantitative approach

4.2.1 Regions of interest definition

In contrast to qualitative approaches, the analysis carried out in the quantitative approach is usually based on **regions of interest (ROIs)** within the infrared image from which different variables would be retrieved (Figure 57). The ROIs definition is a challenging task, and it supposes one of the key steps when analysing and processing thermal data in the biomedical field, since the thermal evaluations would be related to it [974]. Indeed, different approaches can be found in the literature depending on the methods used for the ROIs selection. In general, the ROIs definition is characterized by parameters such as size, shape, and location, and depending on the procedure, it can be performed in a manual, semi-automatic or automatic way.

In “the Glamorgan Protocol”, 90 ROIs defined for different parts of the body are provided [895]. According to this approach, one ROI with a polygonal shape following the outline of the foot is suggested for the plantar feet evaluation [617,895]. Other authors also define their own specific ROIs based on the anatomical landmarks [876,947,972]. The use of markers placed on the body surface to mark the area of interest has also been described [973]. When ROIs are selected manually, the reliability of ICC results (intra-and inter-examiner correlation coefficient) are often suboptimal due to the ability of the observer [970].

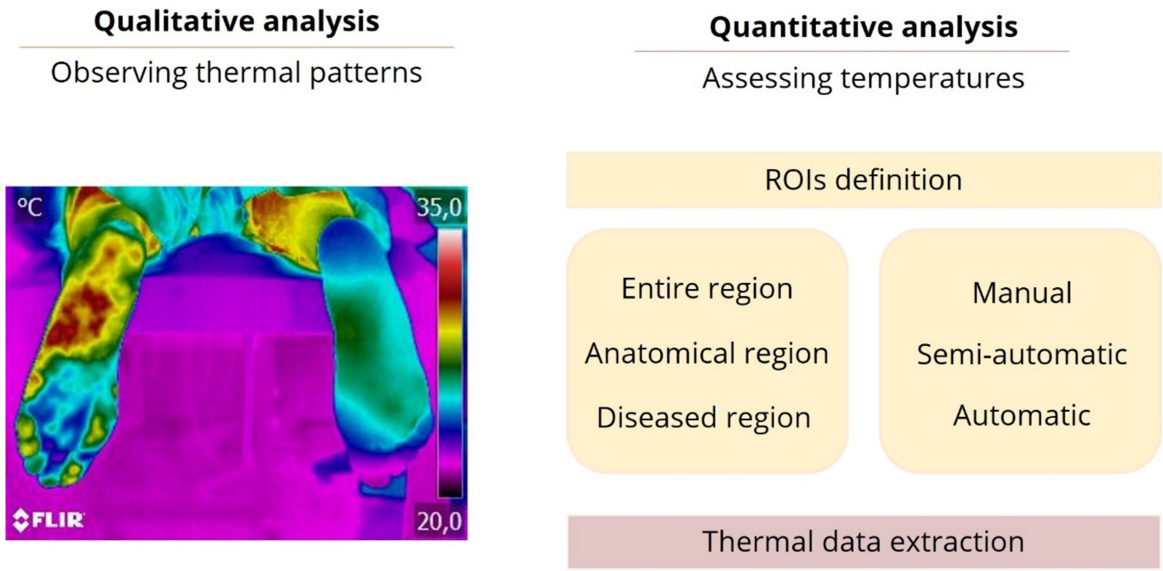

Figure 57. Qualitative and quantitative approaches for infrared analysis.

In the **manual** approach, the decision of the ROIs definition is exclusive of the user, who generally employs pre-defined shapes such as those provided by commercial software (rectangles, circles, etc.) [944,947,975]. However, they usually present limitations since fitting them to complex geometric regions is difficult, and as a result, either the exclusion or inclusion of irrelevant data occur [976,977]. Some computational software may overcome these limitations and in the **semi-automatic** procedures, the user is assisted, for instance in the modification of the ROIs shape [978]. On the other hand, in **the automatic approach**, the ROIs selection process is fully performed by computational algorithms without human intervention [954,979,980]. In this case, procedures are objective, they usually present greater reliability and reproducibility and, depending on the algorithm used, the time expended is reduced. Moreover, the automated approach can also be categorized depending on the selection performed into the entire, the anatomical or the diseased region. When the entire region is selected, techniques such as the edge detection or thresholding are used to extract the region from the background [950,976,981]. The algorithms which segment the ROIs over an anatomical region use specific anatomical regions. On the other hand, when the diseased regions are selected, machine learning algorithms are usually implemented, based on the detection of distinctive temperatures, among them, the definition of the ROIs in function of the warmest or coldest pixels to identify disease areas [949,982,983].

When feet are evaluated at rest, as it was observed in the first images of this study before the lidocaine's vasodilation effect (Figure 58), some areas (mainly toes and heels) are usually mixed up with the background [984]. Likewise, when an area situated within the image present higher temperatures (an external source of radiation, people, another body part), it could be mixed with truly regions of interest [617]. For this reason, in situations like this, the user contribution on the ROIs definition can be valuable.

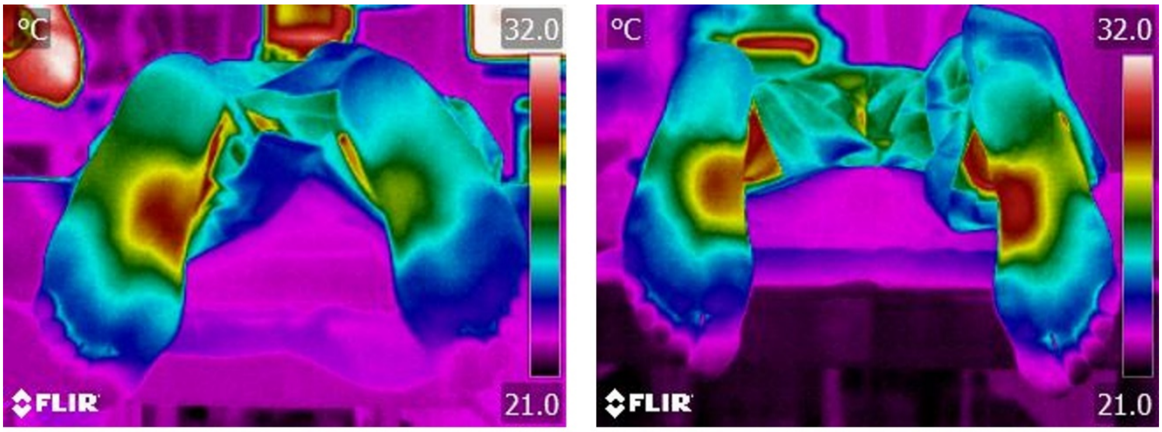

a) b)

Figure 58. Examples of toes presenting similar values to the room temperature and in b) the leg would be mixed up with the medial part of the foot.

According to a recent work, the number of publications involving the definition of ROIs in feet are abundant, and this body part is the second most analysed after the breast [979]. In pathologies such as diabetes mellitus and other vascular disorders, the temperature evaluation within the feet is frequently studied since skin asymmetries between feet may be useful for the identification of dysfunctions. Among the publications focused on feet evaluation, diverse approaches for the ROIs definition have been described, including manual, semi-automatic, and automatic ROIs selection. Regarding the manual approach, the "Glamorgan protocol" proposes, for instance, just a single region per sole consisting of the outline of the foot [895]. However, a greater number of ROIs may be desirable depending on the purpose of the work. In this sense, most studies concerning disorders in diabetic feet, opt for dividing the sole of the foot into several ROIs based on anatomical landmarks, usually associated with common foot ulceration sites as depicted in Figure 59.

The hallux, lesser toes, metatarsus (can be separate or together), and the heel are commonly considered [940,947,985]. In other cases, divisions in the arch and the lateral zone of the midfoot are also selected [627,754,936].

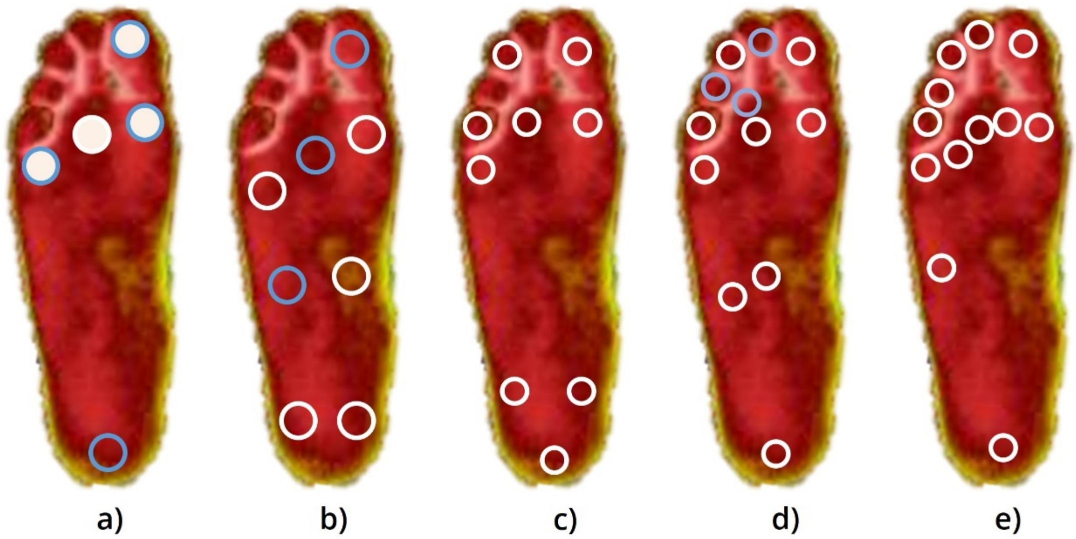

Figure 59. Regions of interest (ROIs) selection according to different works related to diabetes disorders: a) 4 ROIs according to [985] (filled) and with blue contour [941] b) 5 ROIs [947] and adding 3 additional ROIs in blue [939], c) 9 ROIs [940], d) 9 ROIs [754] and adding 3 additional ROIs in blue [936], e) 12 ROIs [627].

Concerning the evaluation of diabetic feet, some authors opt to divide the sole into 4 zones in accordance with the plantar angiosomes [986,987], defined as a 3D area supplied by specific arteries and drained by specific veins. Hence, the foot is often divided into the angiosomes of the medial plantar artery (MPA), the angiosomes of the lateral plantar artery (LPA), the angiosomes of the medial calcaneal artery (MCA) and the angiosomes of the lateral calcaneal artery (LCA) (Figure 60) [938,988,989].

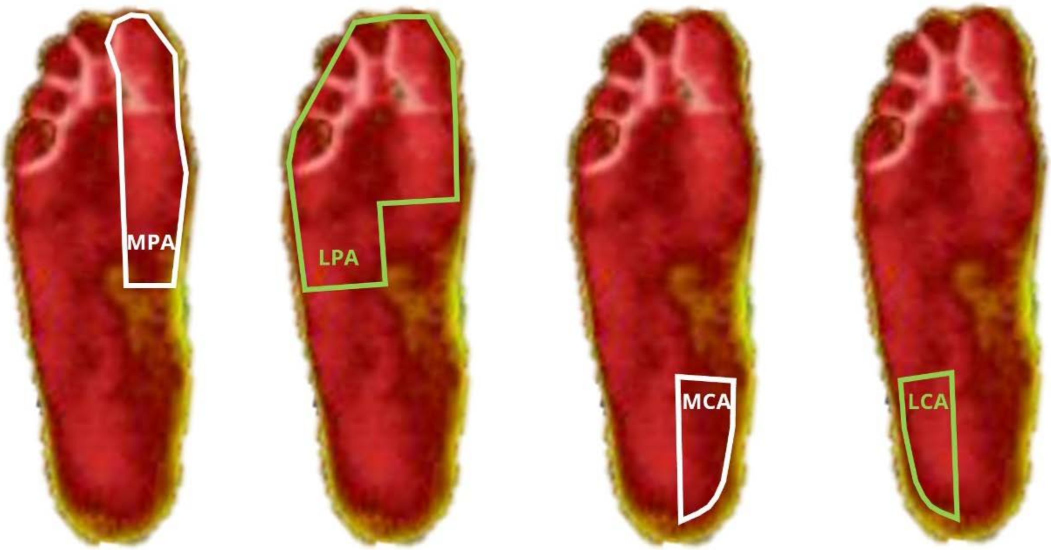

Figure 60. ROIs selection according to the four angiosomes MPA (medial plantar artery), LPA (lateral plantar artery), MCA (medial calcaneal artery), LCA (lateral calcaneal artery) [989].

Moreover, divisions based according to anatomical reasons have also been described (Figure 61). Although in some cases, the lesser toes are considered as one ROI [880,990,991], the analysis of toes separately, may also have relevance in the determination of thermal asymmetries on the sole, especially in some disorders [626].

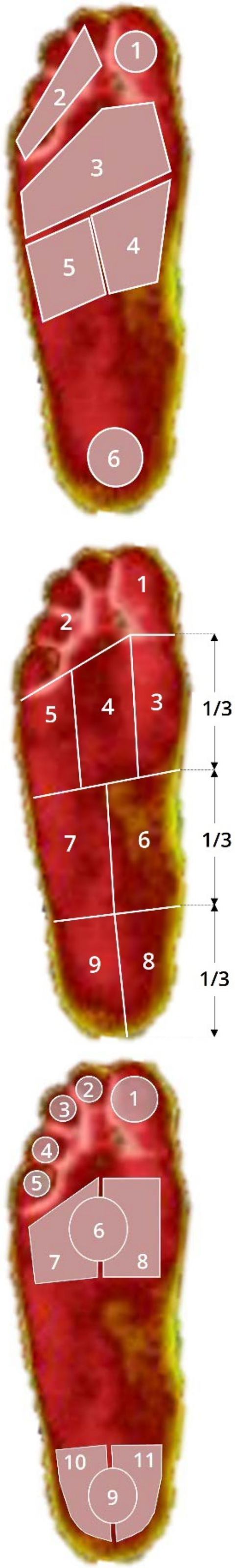

6 ROIs

1	Hallux
2	Lesser toes
3	Forefoot
4	Arch
5	Lateral sole
6	Heel

9 ROIs

1	Hallux
2	Lesser toes
3	Medial metatarsal
4	Central metatarsal
5	Lateral metatarsal
6	Medial midfoot
7	Lateral midfoot
8	Medial heel
9	Lateral heel

11 ROIs

1	Hallux
2-5	Lesser toes
6	Central metatarsal
7	Lateral metatarsal
8	Medial metatarsal
9	Central heel
10	Lateral heel
11	Medial heel

Figure 61. Feet anatomical ROIs according to different authors a) 6 ROIs [990], b) 9 [880,991], and c) 11 ROIs [981,992].

4.2.2 Feature selection and assessment

Feature extraction is performed to obtain the variables of interest from the thermal data and, as it has been described in previous sections, this process can be automatic, semi-automatic or manual depending on the degree of the human involvement on the process. Additionally, depending on the aim of the study, the variables to be evaluated would differ. In any case, the most evaluated variables generally include the mean, maximum and, or minimum temperatures as well as the standard deviation [993].

The mean temperature gives out the average temperature considering all the pixels within the ROI evaluated. Given its utility, this parameter is commonly used in medical and sports applications although in some cases it may not provide significant information [972]. On the other hand, the **maximum temperature** value depends on the method used to its extraction. In most commercial software, a selection of the five hottest pixels within the ROI, and then the temperature average of the 5x5 pixels areas around them is provided [982]. In other cases, this indicator refers to the pixel with the maximum temperature value within the ROI [973,994]. Although this parameter is commonly used [975,995], there is controversy about its eventual higher sensitivity to noise [996]. Likewise occurs with **minimum temperature,** which is used to detect areas with lower temperatures within a ROI [997].

Thermal symmetry describes the behaviour difference between, for instance, the ipsilateral and contralateral measurements. Vardasca et al. define the term thermal symmetries as “the degree of similarity between two areas of interest, mirrored across the human body’s longitudinal main axes which are identical in shape, identical in size and as near identical in position as possible” [998]. This method may be used to assess the presence of possible abnormalities because asymmetries higher than 0.5-0.7ºC are usually associated with a dysfunction in the musculoskeletal system [999].

The temperature variation may be used to evaluate the temperature differences between several moments, for instance the temperature variation between the baseline instant and after moments such as after running, after cold exposure, or after lidocaine injection, as in this work [995,1000].

4.3 Machine learning analysis

4.3.1 Definition and purpose

Machine learning (ML) can be considered as an artificial intelligent branch that deals with the design of systems capable of learning from data samples through mathematical and statistical techniques [1001-1003]. While artificial intelligence refers to any method that mimics human intelligence, machine learning, also known as data mining or predictive analytics, refers to providing the machines "the ability to learn without being explicitly programmed", that is, to generalize beyond the examples provided apart from the training set [1004]. Because of the computational power growth along with a huge amount of data, the use of ML algorithms has continuously evolved and currently, it is used in countless applications including medicine, psychology, marketing, etc [1005]. In medical imaging, ML helps in the detection and classification of lesions, in the automated image segmentation, diagnosis, data analysis, triage, etc [1006,1007].

Depending on the types of input and output data, or the kind of problems to be solved, ML algorithms can be classified into supervised and unsupervised methods (Figure 62) [1008,1009]. In the **supervised learning methods**, the relationship between input (features) and output (labels or classes) variables is intended to be deduced. Hence, once the output is provided, the algorithm is trained to learn the relationship between both variables and once the model is obtained, it can be extrapolated to predict the response in other similar cases. Among the supervised methods, classification (where the target is a qualitative variable, such as a class or tag) and regression (where the target is a continuous numeric value) problems are common [1009,1010]. Conversely, in **the unsupervised learning methods** only input dataset is available, and no output observation or labels are provided. In this case, the aim is to identify hidden patterns between samples, which is typically used in clustering or in data reduction [1011,1012].

Although there are different types of machine learning problems, this work is focus on the supervised classification algorithms. In these cases, a classifier is a system that inputs a vector of feature values, and outputs a single discrete value, the class. An example of a classification problem would be the spam filter used in the mail inbox system, which classifies email messages into "spam" or "not spam".

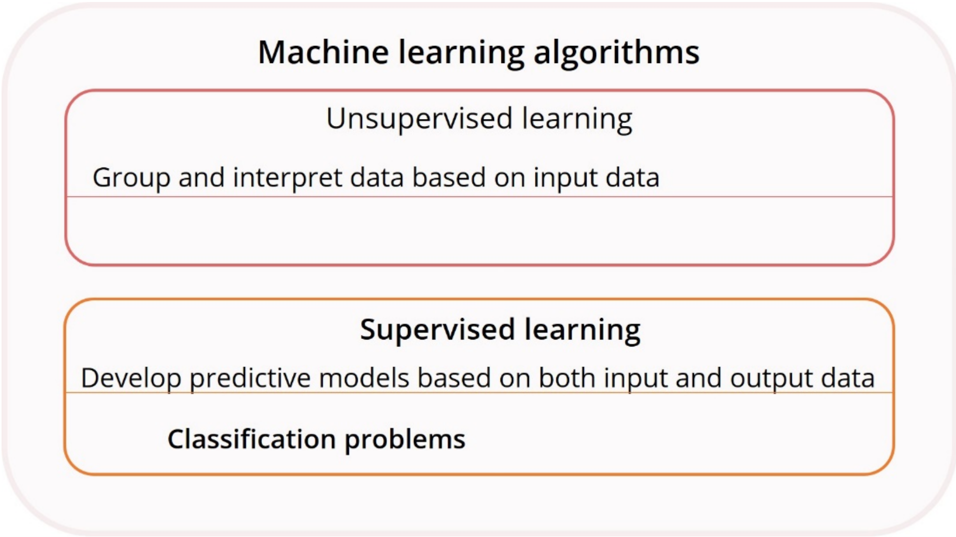

Figure 62. Classification of different machine learning algorithms (in bold the ones used in this work).

4.3.2 ML algorithms for classification

Among the different algorithms available for classification problems, hereafter the ones selected in this work are described.

K-Nearest Neighbours (KNN) is a non-parametric method which is commonly used with multi-modal problems because of its simplicity, flexibility, and good performance [1013,1014]. KNN is based on the similarity concept and its aim is to classify an unknown example to a class by using its k nearby neighbours. In order to classify new samples, a distance metric to the k nearest neighbours and their associated classes are utilized, as it is depicted in Figure 63. Therefore, the accuracy of KNN is influenced by the number of neighbours and by the distance or similarity metric used to determine which samples are nearby [1002]. In this sense, small *k* values may generate many small regions of each class, thus representing the patterns existing mainly in the training set (overfitting), whereas high *k* values may generate fewer and larger regions which would not really represent the local structure of the data. On the other hand and concerning the distance to assess the closeness of the training samples, several metrics can be considered, such as the Euclidean, Manhattan or the Minkowksi distance [1002].

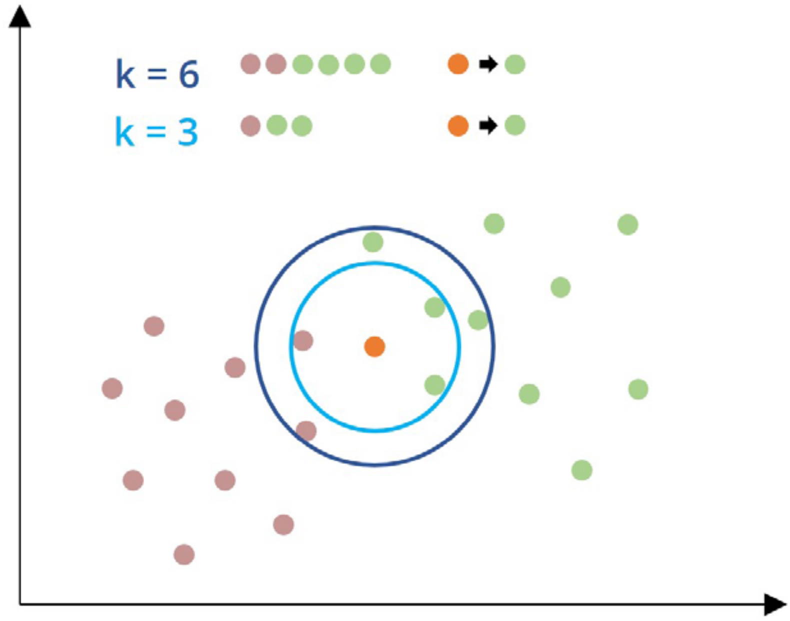

Figure 63. Example of the K-Nearest Neighbours classification for a binary problem with two classes (green and purple dots) in which a new sample (orange point) must be classed. The new sample will be classed as green in with k=3 and k=6 because in both cases the number of green samples is greater.

Decision Trees (DT) are predictive models based on the split of the initial data set into smaller and more homogeneous partitions. Hence, a decision tree consists of sequential partitions made up of nodes interconnected through branches, which represent the decisions to be made. When a new sample is introduced into the decision tree through the root node, it is sorted sequentially through the internal nodes, where the conditions based on the feature values are stored, until the prediction of the target outcome is reached (Figure 64) [1015].

Figure 64. An example of a Decision Tree.

Although decision trees have been popular due to its intuitive algorithm and its simplicity to use and to interpret, they are sensitive to small changes in the data, they may overlook important variables (when a small sample size and a large number of features are involved), and they are also commonly prone to overfitting [1016-1018]. To overcome these drawbacks, "**Random Forests" (RF)** were introduced with the aim to achieve better generalization accuracy than with a single tree [1019,1020]. Hence, random forests are based on the ensemble of various decision trees through random feature selection (Figure 65). Each decision tree can be regarded as a classifier that makes an independent decision and then, a combination of such decisions leads to the final prediction. The construction of random forests involves the selection of the number of trees and the selection of random features to be used in the split taking place in the nodes [1019,1020]. In some cases, large number of trees may be beneficial for generalization and deeper trees may have the risk of overfitting, however the effect of these different parameters would differ depending on the specific application.

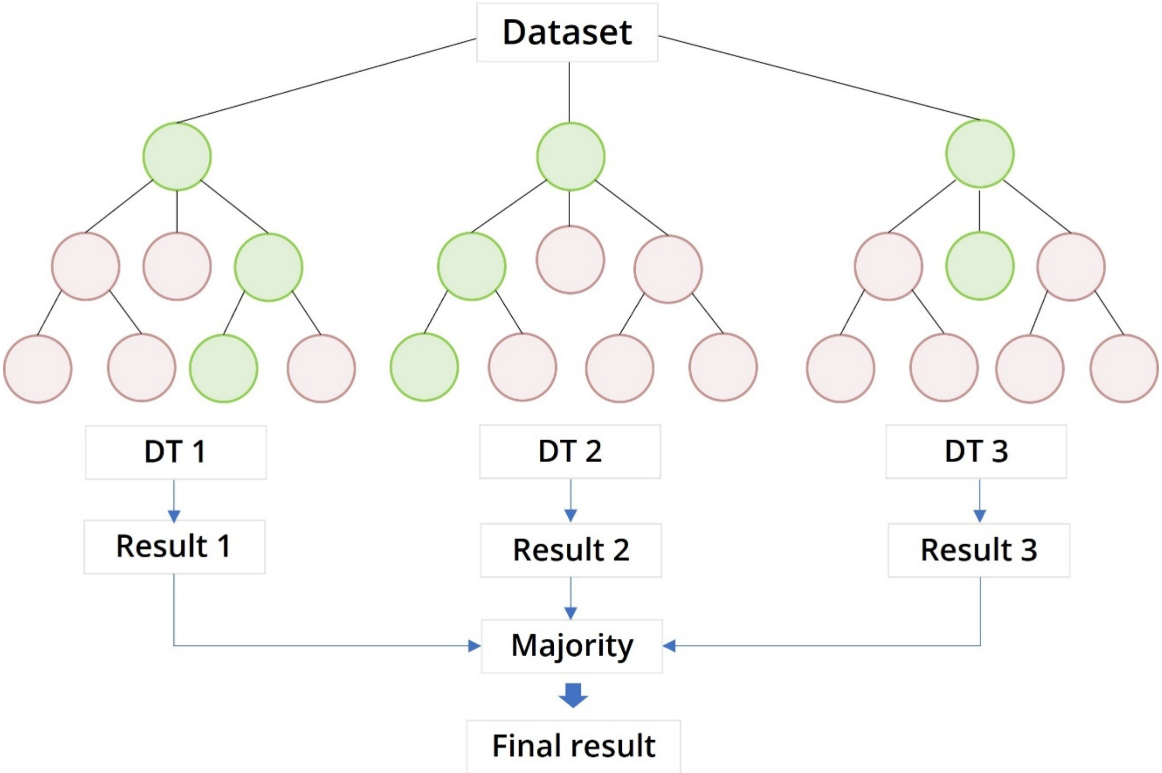

Figure 65. In Random Forests, Decision Trees are combined, and each individual tree in the forest provides a class prediction and the class with the most votes becomes the final model's prediction.

Support Vector Machines (SVM) are used to solve classification problems by finding an optimal hyperplane in an N-dimensional space which would distinguish between elements of the classes [1021,1022]. In a linearly separable dataset, a hyperplane passing through the middle of two classes is determined, but since the number of hyperplanes can be considerable, the SVM algorithm is aimed to maximize the margin (the gap) between the two classes, that is, to select the hyperplane that allows the maximum space from the boundary to the closes training set samples from both classes. Therefore, SVM is based on an optimal distance calculation between samples and the hyperplane (Figure 66). By doing so, not only the accuracy is improved, but the correct classification of the future data is also accomplished. Conversely, when non-linearly divisible data are to be used, a kernel function is applied, although there is risk of overfitting. The complexity of SVM mainly depends on the number of features and the number of examples [1023,1024].

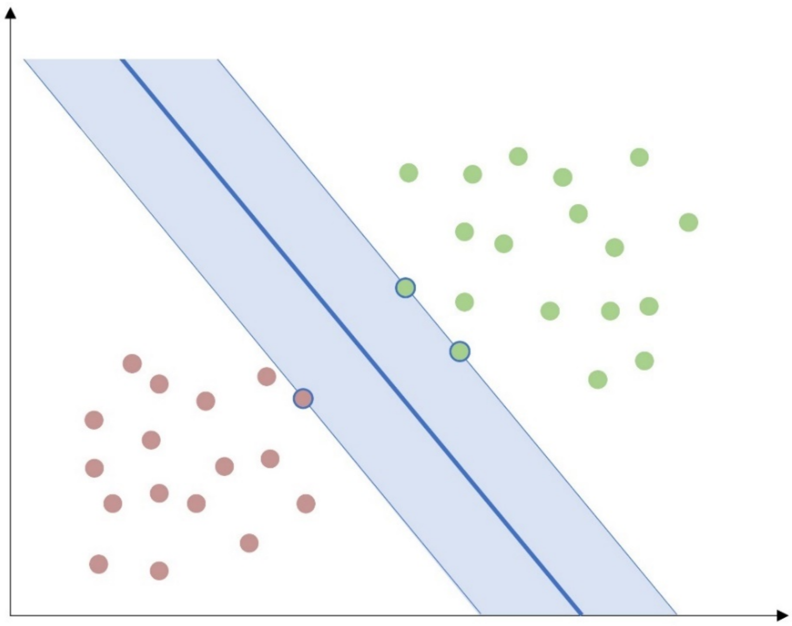

Figure 66. An example of Support Vector Machine algorithm in which the separating line is placed in the middle of the margin (widest gap), which is the distance from the solid line to either of the dashed lines (in light orange). The points circled in blue lie on the outer lines (examples being part of the boundaries) that are the support vectors.

Artificial neural networks (ANN) are systems with a structure and operation inspired by the neuronal architecture of the brain [1025]. They consist of a collection of neurons (units or nodes) responsible for processing the information and transmitting then signals to other neurons through established connections with associated weights. Hence, when the input data is received, it moves through the nodes, where the activation functions are applied to the total inputs weighted according to the connection weights. Once the activation functions are applied, an output value is obtained, which, in turn, is transmitted to the remaining nodes of the network. As it can be observed in Figure 67, the nodes are organized in layers: in the input layers the information to be process is collected, the output layers provide the outcome, and the hidden layers are the ones situated in the middle.

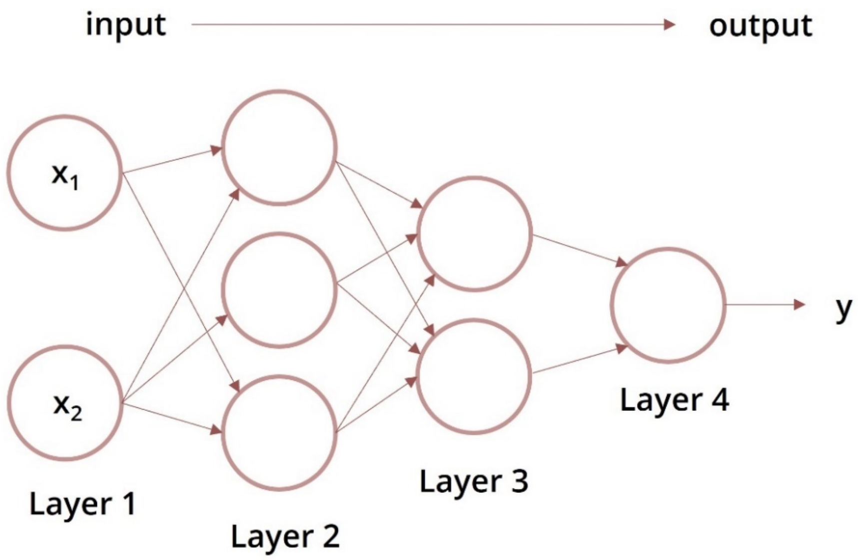

Figure 67. A simple neural architecture.

The aim of artificial neural networks is to maximize the correct predictions by establishing the proper weightings on each connection and, unlike other algorithms that have a fixed pipeline to process the data, in these learning systems, the way the information flows, depends on the layers, the neurons, and the connections established. Unfortunately to find the best structure, different options should be tested. In the biomedical field, ANN have been commonly used in clinical diagnosis and medical imaging analysis [1026-1028] and the most used method in applications of ANN is the multilayer perceptron (MLP) [1029]. In this specific system, the information is always transmitted from the input layer in which each node corresponds to a feature, towards the output layer, whose associated nodes correspond to classification. Between the input and the output layers, a number of hidden layers (at least one) are encountered. The capacity of MLPs to learn any kind of relationship between a set of input and output variables make them flexible and adaptative.

If the activation function chosen is a binary step function, each node will behave like a switch and activates only under certain thresholds just as neurons are activated only when sufficient neurotransmitter is accumulated. By doing so, the ANN behaves like a linear classifier. However, non-linear activation functions are usually preferred because this way the combination of nodes and activation functions will be able to represent non-linear relationships.

The data feeds one way forward into the network. Connections link the neurons (units) exclusively in one layer with the units in the following layer (from left to right). No connections exist between units in the same layer or with units outside the next layer. Moreover, the data never returns to previous neuron layers. Many neurons arranged in an interconnected structure make up a neural network, with each neuron linking to the inputs and outputs of other neurons. Hence, the data flows from the input to the output layer. The connections are weighted connections that scale the data flow while transfer functions in each neuron map inputs with outputs.

4.3.3 Feature selection

The choice of features (also known as predictors, parameters, or variables) is of paramount importance for building the appropriate models because they can interact in various ways, thus having different effects on the classification results [1009,1030,1031]. Therefore, the aim of this process is to achieve the best classification accuracy by selecting the proper subset of features. To do so, techniques commonly based on statistical metrics or search algorithms are implemented to generate a ranking indicating both the most meaningful and redundant features. Among them, the recursive feature selection algorithm (RFE) ranks the features by importance and discards the irrelevant ones until a specified number of features is reached [1009,1032].

4.3.4 Model optimization

Some machine learning models can be susceptible to overfitting, that is, to learn too much from the data, which can occur when small training dataset are implemented to train a complex algorithm [1016,1033]. Under these circumstances, the generalization of the model is not good since it does not perform well with sets of unknown data. In other cases, the model may result in less flexible and sensitive classification. For this reason, some techniques are used to maximize the classification accuracy [1034,1035]. To find the optimal model complexity**, cross-validation** is considered. Hence, given a dataset, it is divided into training and validation subsets. If the sample is large enough, it is divided into k parts and each part is, then divided into 2, so one half is used for training and the other half for validation (knowns as k-fold cross validation). Unfortunately, datasets are usually not large enough and the cross-validation is done by repeated use of the same data split in different ways.

Additionally, bootstrapping is an alternative technique that generates new samples from the original data set with replacement.

4.3.5 The model performance

The estimated performance of a model describes how well it works when new data is used and for this purpose, different metrics can be used. First, some common terms which would be used are described.

True positives (TP) are the predicted as positive which are actually positive.

False positives (FP) are the predicted as positive which are actually negative.

True negatives (TN) are the predicted as negative which are actually negative.

False negatives (FN) are the predicted as negative which are actually positive.

A way to represent the above parameters for a binary classification problem is through **the confusion matrix** (Figure 68).

		Actual values	
		Positive	Negative
Predicted values	Positive	True positives (TP)	False positives (FP)
	Negative	False negatives (FN)	True negatives (TN)

Figure 68. Confusion matrix for a binary classification problem.

Additionally, some metrics to evaluate the performance of a model are also used [1036,1037].

Sensitivity, also known as the true positive rate (TPR) or recall, describes the percentage of the correctly predicted as positive out of the total actually positive. In our case, the sensitivity would indicate the proportion of the total successful interventions that would be classified as successful.

$$\text{Sensitivity (TPR)} = \frac{\text{TP}}{\text{TP} + \text{FN}} \qquad \text{Equation [20]}$$

Specificity, also known as true negative rate (TNR), represents the proportion of the correctly predicted as negative out of the total actually negative. In our case, the specificity would indicate the proportion of the total failed interventions that would be classified as failed.

$$\text{Specificity (TNR)} = \frac{\text{TN}}{\text{TN} + \text{FP}} \qquad \text{Equation [21]}$$

The false positive rate (FPR) is calculated performing one minus the specificity, resulting in

$$\text{FPR} = \frac{\text{FP}}{\text{TN} + \text{FP}} \qquad \text{Equation [22]}$$

The accuracy or error rate, represents the proportion of the correctly predicted (both true positives and negatives) among the total number of cases evaluated. Hence, in our case, the accuracy would indicate the proportion of interventions that would be correctly classified.

$$\text{Accuracy} = \frac{\text{TP} + \text{TN}}{\text{TP} + \text{TN} + \text{FP} + \text{FN}} \qquad \text{Equation [23]}$$

Since the accuracy does not take into account the class imbalance, that is, the disparities in the class proportions, **the Cohen's Kappa** is used to measure the agreement between two samples caused by chance.

$$\kappa = \frac{p_0 - p_e}{1 - p_e} \qquad \text{Equation [24]}$$

Where p_o is the observed agreement and p_e is the expected agreement. Kappa values lower or equal to 0 would indicate no agreement whereas when values equal to 1 are obtained a perfect agreement would be reached. Although there is no standardized way for its interpretation, and the close to one, the better, values ranging from 0.3 to 0.5 may indicate reasonable agreement.

The Receiver Operating Characteristic curve (**ROC curve**) is one of the most common methods used to evaluate in a graphic way the performance of the classification model. To obtain the ROC curve, the sensitivity (TPR) against the false positive rate (FPR) are plot (Figure 69).

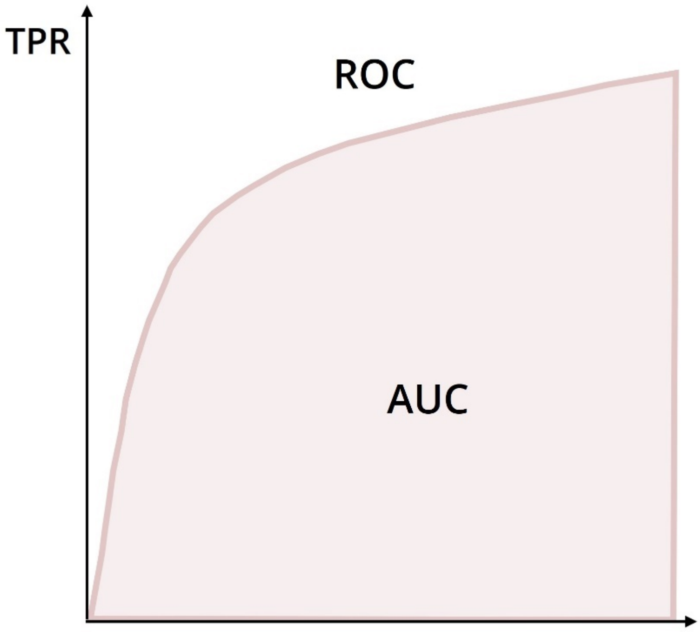

Figure 69. Representation of a ROC curve and the AUC.

On the other hand, **the area under the ROC curve (AUC)** is a numerical value that represents the classifier overall expected performance. A perfect classifier would present an AUC value equal to 1 whereas when the AUC value is lower than 0.5, indicates that a random selection performs better than the test. Hence, the higher the AUC, the better the model would be at classifying.

Finally, **the SHAP value** (shortcut from Shapley Additive exPlanations) is an approach based on the cooperative games' theory, which indicates the contribution of the model's features, that is, if they have a positive or negative contribution [1038,1039]. Figure 70 shows an example of the contribution of different predictors (age, gender, where they embarked, etc) for two Titanic passengers.

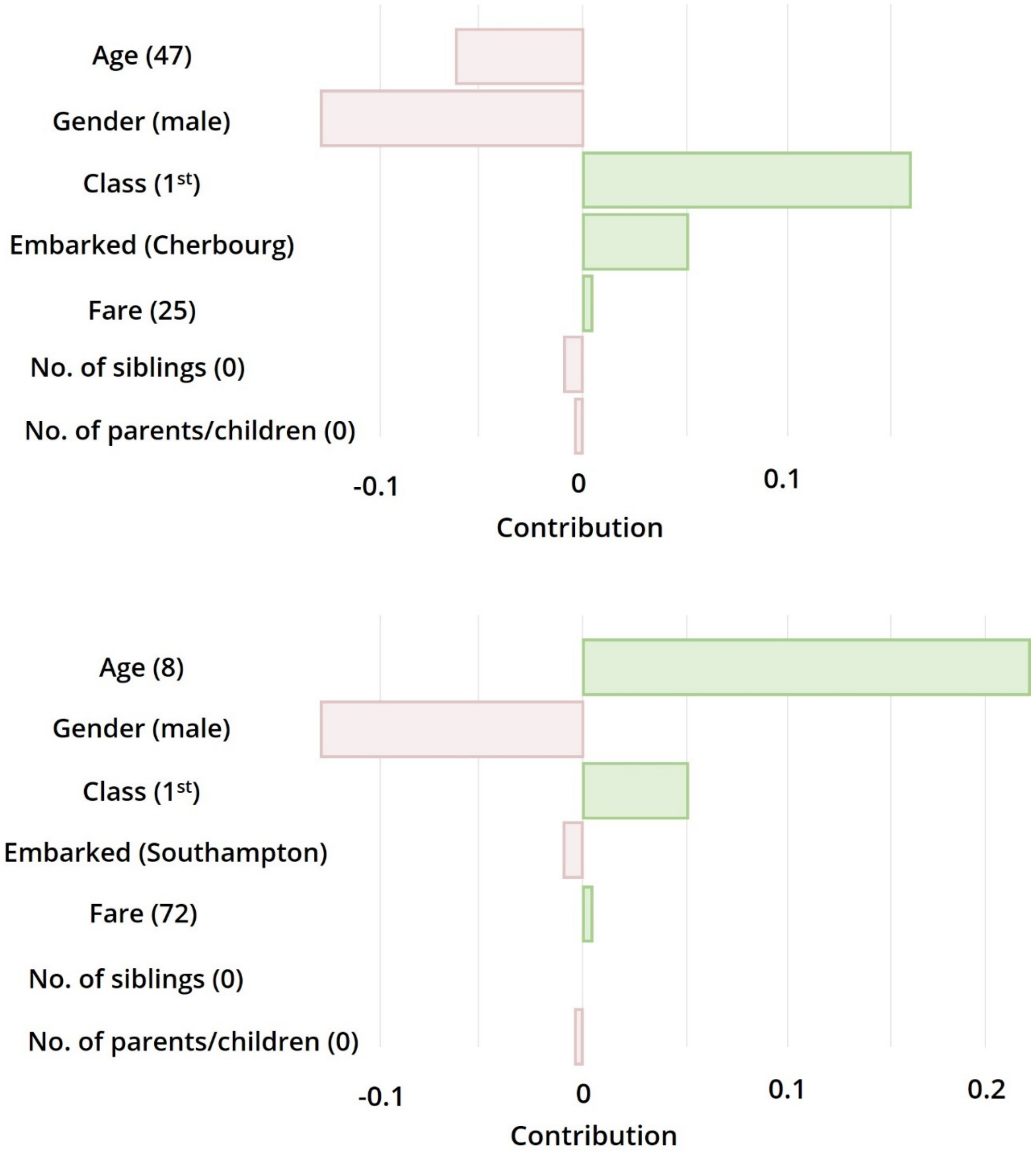

Figure 70. Example of the predictors' contribution of two Titanic passengers. Green and purple bars represent SHAP values. In this example, the young age of 8 increases the chances of survival, contrary to the negative contribution of the age of 47.

MATERIALS AND
METHODS

05

Infrared thermography for the assessment of lumbar sympathetic blocks in patients with Complex Regional Pain Syndrome

5 MATERIALS AND METHODS

5.1 Patients and protocol

This single-centre study was approved by the ethics committee of the Universitat de València (Reference: 1250779) and all patients signed the informed consent. All interventions were performed at Hospital Intermutual de Levante (Valencia, Spain), and they were in accordance with the ethical standards and with the Helsinki Declaration.

Patients previously diagnosed with lower limbs CRPS according to their clinical history along with the Budapest criteria were considered. Among them, patients who met the inclusion criteria (Table 10) were selected for the study.

Table 10. Patients' inclusion and exclusion criteria.

Inclusion criteria

Patients meeting the Budapest clinical criteria
Patients presenting signs and symptoms in only one lower limb
The clinical presentation is less than a year from the initial injury
Patients do not present almost reduction of pain and/or dysfunction of the affected limb*
Pain rate is > 5 in a pain rate scale from 0 to 10 *
(*) both evaluated one month after the beginning of the standard therapy

Exclusion criteria

Pregnant women	
Patients presenting	coagulopathies
	systemic or local infections in the puncture location
	amputations in lower limbs
	diabetic neuropathy or any other disease similar to CRPS
Patients	taking vasoactive drugs
	holding neurostimulators
	with lumbar instrumentation
	allergic to local anesthetics or contrast dye

To determine whether the patients previously diagnosed with CRPS satisfied the inclusion criteria, they should have started the standard therapy, consisting of both physical rehabilitation and pharmacological treatment. In physical rehabilitation, patients were instructed to carry out massages, mobility exercises, and contrast baths. Moreover, they undergone both physical (active mobilization) and mirror therapy. Additionally, patients in the acute phase (clinical presentation less than 3 months from the onset) would have initiated the pharmacological treatment as depicted in Table 11.

Table 11. Pharmacologic treatment.

Pharmacologic agents		**Regimen**
Oral corticosteroids	*Prednisone*	every 8 h in descendent regimen: 20 mg 1st week 15 mg 2nd week, ..., 5 mg 6th week
Bisphosphonates	*Alendronic acid*	70 mg weekly in 1 single dose
Calcium or vitamin D supplements		500 mg /400 UI
Dimethil sulfoxide		in 50% topical
Analgesics	*Tramadol*	37.5 mg
	Paracetamol	325 mg
	*Baclofen**	10 to 30 mg / day
** in case patients present tremor*		
If the pain cannot be controlled		
	Tapentadol	in escalating doses from 100 mg to 300 mg /day
When the rate scale evaluation did not change even administering the previous pharmacologic drugs for 4 weeks and patients present sleep disturbances:		
Antidepressants	*Amitriptyline*	25 mg every 24 h
	And/or pregabalin	75 mg every 12 h
	Or gabapentin	300 mg every 8 h

Thus, the patients finally included in the study were scheduled to undergo a set of 3 lumbar sympathetic blocks (LSBs) procedures, each of them, roughly two weeks apart. Each procedure was performed by the clinician team consisted of 1 or 2 pain medicine physicians, 1 or 2 nurses and 1 X-ray technician. For the block, levobupivacaine 0.25% 10 ml with triamcinolone 80 mg were used.

The collection of data was performed in two different series, the first one between November 2019 and March 2020, and the second one between February 2021 and May 2021. Table 12 shows a summary of these two series of data collection regarding the number of patients, their age, and their affected limb.

Table 12. Summary of patients' information included in the study.

		Total	Men	Women
Patients	1st series	12	8	4
	2nd series	12	10	2
	Total	24	18	6
Age ± SD	1st series	41± 7	41± 8	42 ± 6
	2nd series	40 ± 10	41 ± 10	37 ± 15
	Total	41 ± 9	41 ± 9	40 ± 9
Ipsilateral Left	1st series	10	7	3
	2nd series	8	8	0
	Total	18	15	3
Ipsilateral Right	1st series	2	1	1
	2nd series	4	2	2
	Total	6	3	3

In order to perform the clinical assessment by the physicians, some clinical data was collected before each LSB procedure (Table 13). In this sense, the demographic data and the data related to the descriptive aspects of CRPS was collected by the pain physicians when patients were included in the study. On the other hand, the part related to signs and symptoms was filled in before each LSB procedure and, also before each medical visit. Finally, the motion and pain assessment were completed before the first LSB procedure and then, before each clinical visit (on the first, third and sixth month after the third LSB procedure).

Table 13. Clinical data collected for each patient included in the study.

Demographic data	
Age	
Sex	
Weight	
Height	
CRPS descriptive aspects	
Affected limb	Left/ Right
Injury location	Knee/ Ankle/ Foot
Type of trauma	With fracture/ No fracture
Type of treatment	Conservative /Surgery
Immobilization time	
CRPS type	I/ II
CRPS	Warm/ Cold
Evolution time (from injury to 1st LSB)	
Visual analogue scale (VAS)	0 - 10
Symptoms	
Allodynia	Yes / No
Tingle	Yes/ No
Myoclonus	Yes / No
Sweating	Yes / No
Signs	
Edema	1 / 2 / 3
Colour asymmetry	1 / 2 / 3
Temperature asymmetry	No / Cold/ Warm
Visual analogue scale (VAS)	0 - 10
Motion assessment	
Active range of motion	1/ 2/ 3
Passive range of motion	1/ 2/ 3
Muscular balance	1/ 2/ 3/ 4/ 5
Use of crutches	0/ 1/ 2
Pain assessment	
Neuropathic pain questionnaire (NP4)	0-10
Quality of life scale (QOLs)	0 - 10
Likert scale	1 – 7

5.2 Experimental procedure in the clinical setting

5.2.1 Lumbar Sympathetic Block procedure

Although a more detailed description of the procedure is provided in the following paragraphs, for clarification purposes a short description of several terms is presented beforehand.

A lumbar sympathetic block (LSB) procedure carried out in the present study refers to the process performed on a patient which involves the subsequent main steps:

1. The needle placement.
2. The needle placement assessment by means of FL (based on the correct spread agent confirmation) and by means of IRT (based on the temperature increase confirmation on the ipsilateral sole after the lidocaine test).
3. The medication injection either when the temperature increase on the ipsilateral through IRT is observed or after 3 needle reposition manoeuvres.

Therefore, a LSB procedure may involve several interventions if no temperature increase on the ipsilateral sole is observed by means of IRT and, consequently, a needle reposition manoeuvre is required.

Each patient was scheduled for a set consisting of 3 LSB procedures, roughly two weeks apart each of them. Moreover, and after these 3 LSB procedures, a follow-up in the medical office, one, three, and six months after the third LSB procedure were carried out. Figure 71 shows this whole process. Before undergoing a LSB procedure, patients were asked to fast for 6 hours and to avoid smoking during the previous hour.

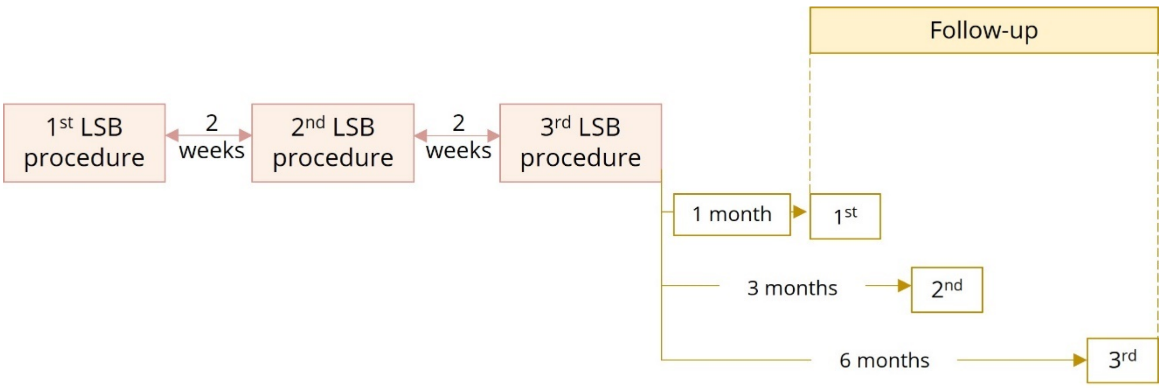

Figure 71. The schedule of a patient included in the study.

Following this clarification, the detailed description of a LSB procedure is presented. The technique was performed under FL guidance using the C-arm (Flexiview, General Electrical Medical System) shown in Figure 72, and the steps previously introduced in section 3.5 are to be described in detail. The procedures were performed using a needle 15 cm, 22-gauge, and the 4th lumbar was aimed.

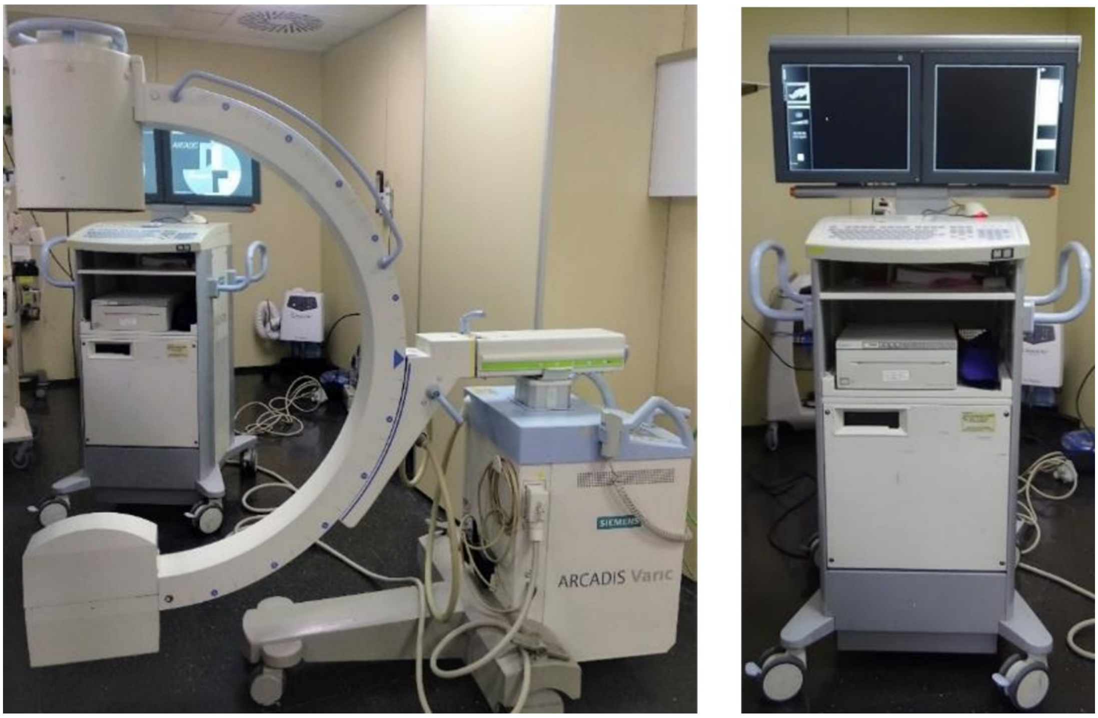

Figure 72. C-arm used for the fluoroscopic guidance.

The patient is positioned in prone position on the table with a pillow under the abdomen, a mid-sedation is performed, and vital signs are monitored. Then the skin area of needle entry is prepared (step 1). Fluoroscopic beam is adjusted in a posteroanterior position first until L4 level is identified. From there, the C-arm is rotated obliquely towards the affected limb until the transverse process is not observed behind the lateral side of the vertebral body (step 2) (Figure 73).

a) b)

Figure 73. C-arm in a) posteroanterior and b) oblique position.

The target point (at the inferior border of the transverse process) is marked on the lateral margin of the vertebra and then the needle is introduced in tunnelled vision until it contacts the paravertebral edge of the vertebral body (Figure 74a (step 3)). To confirm the position of the needle, the C-arm is rotated laterally so the needle tip is located at the anterior border of the vertebral body (Figure 74b). In posteroanterior view, the needle should be located within the external third of the vertebra (Figure 74c).

Then the contrast solution (1.5 ml Omnipaque®) is injected, and its proper distribution is checked. When the contrast shows appropriate spread (step 4) on the FL images (Figure 16), and before injecting the medication, the lidocaine test (2 ml lidocaine 2%) is injected to assess this step by infrared thermography. Once the infrared images confirm a temperature increase on the ipsilateral, the medication (levopuvicaine 0.25% 10 ml with 80 mg of triamicolone) is administered. Finally, the patient remains in prone position on the table monitored for 20 minutes.

Figure 74. Confirmation of the needle position in a) tunnel view, b) lateral view, and c) posteroanterior view.

5.2.2 Thermal data acquisition

Prior entering the operation room, participants were asked to take off their pants and shoes and they were placed surgical booties on their feet. For a period of 15 minutes, they were pre-acclimatized lying on a stretcher in which they were transferred to the operating room. When the participants arrived at the operating room, they were positioned in prone position with bare feet, and they held that position for about 10 minutes. IRT acquisitions were performed in the same operating room with a controlled ambient temperature of 22.0 ± 0.5°C and relative humidity 47 ± 5%. These ambient conditions were checked with a digital weather station Testo 623 (Testo SE&Co, Lenzkirch, Germany) situated in the operating room.

During the acclimatization period of the patient, the thermal acquisition set up was prepared. Infrared data were acquired using the thermal camera FLIR E60 (FLIR Systems, Inc., Wilsonville, OR) shown in Figure 75, with the technical data described in Table 14. The camera used in this work was checked before the experimental phase using a blackbody (BX-500 IR Infrared Calibrator, CEM, Shenzen, China) with target emissivity of 0.95, resolution of 0.1°C and measurement uncertainty of ± 0.8°C.

Figure 75. Infrared camera used (FLIR E60).

Table 14. Technical data of the infrared camera used.

	FLIR E60
Detector type	Uncooled microbolometer
FPA size	320 x 240
FOV (º)	25º x 19º
Minimum focus distance	0.4 m
IFOV	1.36 mrad
NETD	< 50 mK (at 30ºC)
Accuracy	± 2ºC or ± 2% of reading
Temperature range	-20ºC to +120ºC

The camera was mounted on a tripod at distance of 1.5 m from the participants' feet and perpendicular to them as shown in Figure 75 to ensure that both plantar feet were included in the IR image (Figure 77).

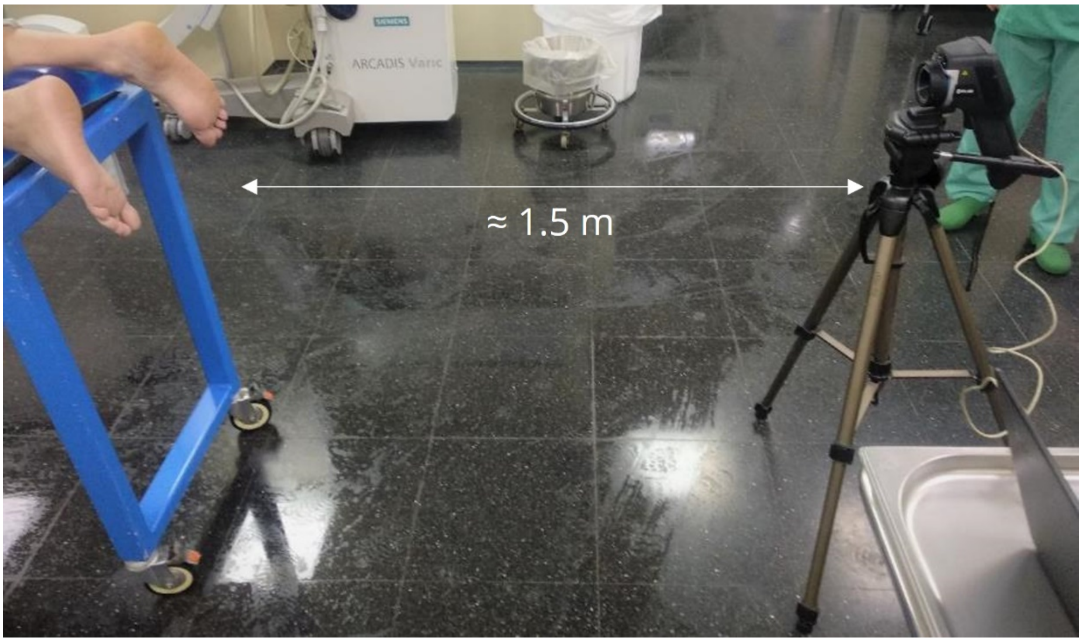

Figure 76. Infrared camera position with respect to the plantar feet.

Then, the IR camera was switched on with the aim of avoiding thermal drifts and achieving the thermal equilibrium at the time after the patient's acclimatization period. The thermal camera was connected via USB to a laptop through the software FLIR Tools+ (version 6.4, FLIR Systems, Inc., Wilsonville, OR) as shown in Figure 77. Via FlirTools+ software, the time interval between images was adjusted at 10 seconds. Hence, the acquisition was manually started right after the lidocaine test, and from that moment, the IR images were automatically recorded every 10 seconds. The recording finishing time was established after 4 or 10 minutes of the lidocaine test for failed or successful interventions respectively.

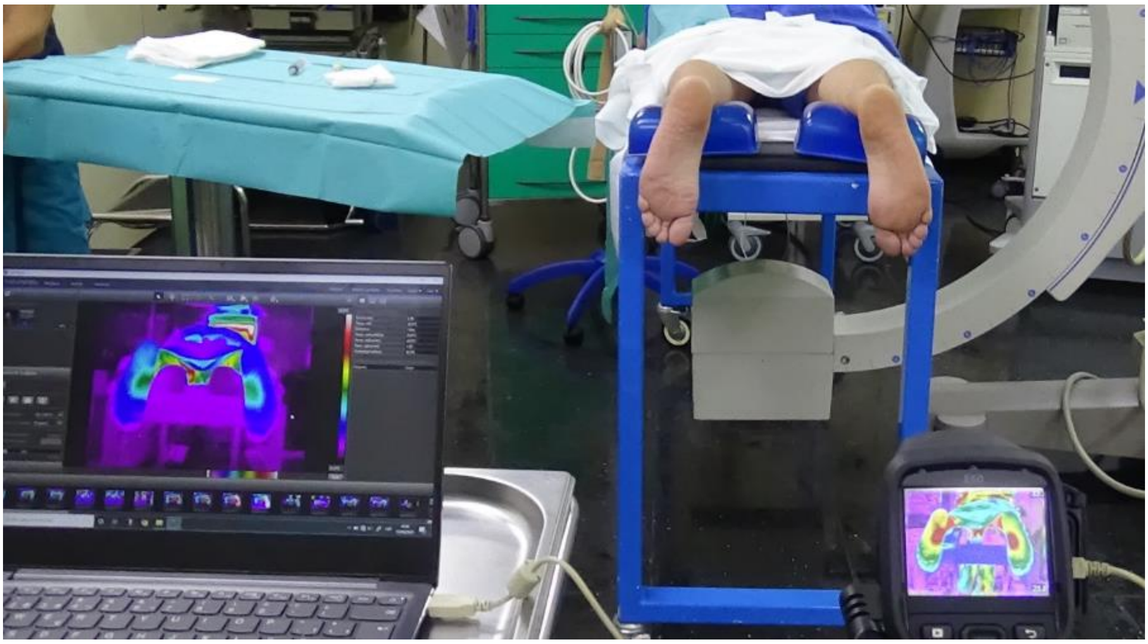

Figure 77. Infrared thermography camera setup in the operating room.

Additionally, and as general rule, the adjustments depicted in Table 15 were made in the IR acquisitions, notwithstanding this adjustment was not of paramount importance since all of them could be modified afterward through the analysis software.

Table 15. Parameters adjusted adopted in the thermography acquisitions.

Parameter	Adjustment
Temperature scale	20ºC to 35ºC
Colour palette	Rain
Emissivity	0.98
Reflected temperature	24 ºC
Distance	1.5 m

The several lockdowns and restrictions due to the COVID-19 took place while the IR acquisitions associated with this work were taking place. Since the LSB procedures were performed in a medical setting, the access to the operational room was restricted to exclusively the medical personnel. As a result, the thermal data acquisition associated with the second collection of data has to be performed by the medical team. Since they have never used the IR equipment before, some basic directions and guidelines of its use were provided. Moreover, to obtain the IR images meeting some minimum requirements, different indications were suggested. An example of some of the recommendations provided are shown in Figure 78.

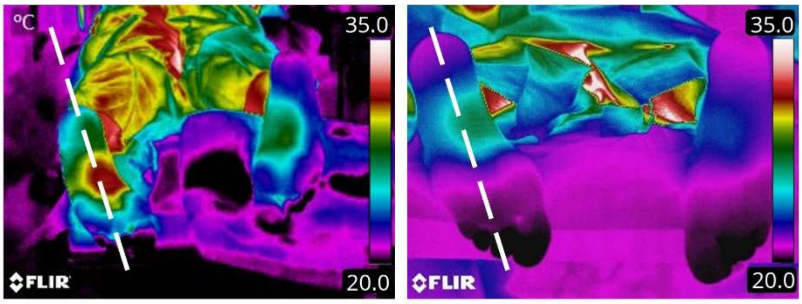

The plantar feet occupy most of the image	✗	✓
Feet placement	✗ skewed	✗ skewed
Image focus	✗ blurred	✗ blurred

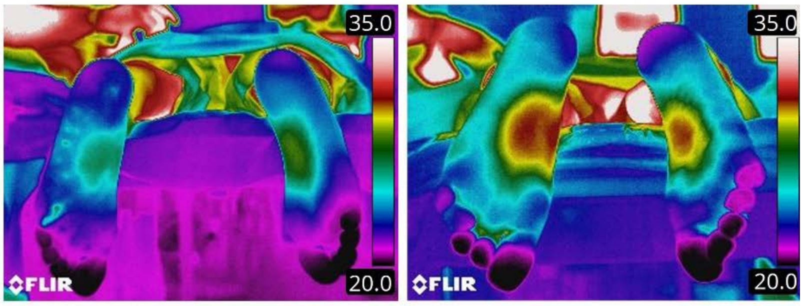

The plantar feet occupy most of the image	✓	✓
Feet placement	✓	could be improved
Image focus	✓	✓

Figure 78. Some indications about the thermal image appearance.

5.3 Medical classification based on real time infrared images

As previously described, the LSB procedure assessment in the clinical setting is usually performed under FL, but in this work the additional use of the infrared thermography has been evaluated. In this section, the medical classification of the LSBs using the infrared images is described. Figure 79 shows a general outline of the process.

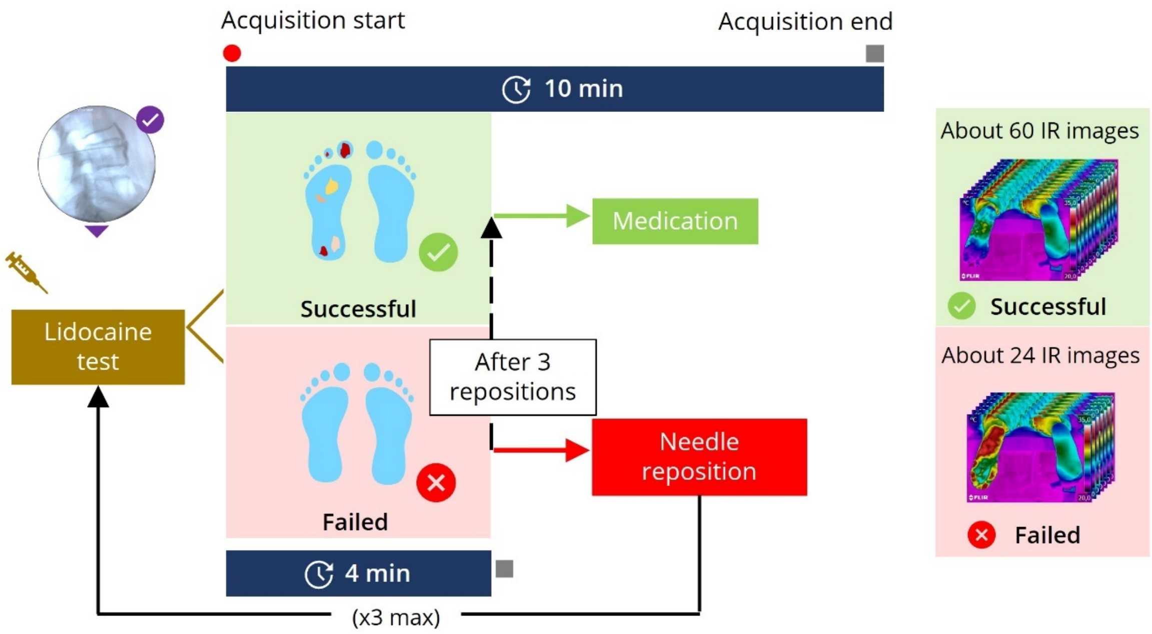

Figure 79. Thermography assessment of the lumbar sympathetic block procedure.

After the confirmation of correct spread agent on the radioscopic images, a local anaesthetic (2 ml lidocaine 2%) was injected. In this sense, since the lidocaine induces vasodilation, the thermal changes taking place in the affected plantar foot would be related to a proper needle placement and therefore, to a correct successful block. Just after the lidocaine test, the acquisition of the infrared images started. For the first four minutes after the lidocaine test, the thermal images were evaluated by the medical team. When skin temperature changes in the ipsilateral sole were observed within this period of time, the intervention was considered responsive (**successful**), and the medication was injected. In those cases, the thermal images acquisition kept on after 10 minutes from the start (lidocaine test). Conversely, when no thermal changes on the affected sole were detected, the procedure was determined as unresponsive (**failed**), and a repositioning manoeuvre of the needle was required. In those cases, the IR images acquisition was stopped after the first four minutes and the process from the lidocaine test was repeated. Considering the anatomy of the lumbar ganglia where the procedures were performed, only 3 consecutive repositioning manoeuvres were carried out at most in order to avoid complications in the patient. Therefore, once the patient had undergone 3 consecutive repositioning manoeuvres without observing thermal changes on the ipsilateral, and though considering the procedure unresponsive, the medication was injected anyway. In short, as is depicted in Figure 79, the LSBs interventions considered as successful, lasted about 10 minutes and 60 infrared images approximately were obtained. On the other hand, the LSB interventions considered as failed, lasted about 4 minutes and 24 images approximately were obtained. Therefore, the LSB procedures involving several interventions, contained a set of images associated with each failed intervention (in case several failed interventions occur) along with a set of images associated with either the successful or the last intervention (in those cases in which 3 reposition manoeuvres were carried out). In Table 16 these different possibilities are described.

Table 16. Different possibilities related to the number of interventions performed on a lumbar sympathetic block procedure and number of thermal images obtained.

No. of interventions	Intervention classification	No. of images in the intervention	No. total of images in the procedure
1 intervention	Successful	60	60
2 interventions	Failed	24	84
	Successful	60	
3 interventions	Failed	24	108
	Failed	24	
	Either successful or not	60	

Additionally, it should be mentioned that thermal patterns observed within the first minutes in the plantar feet were distinctive. As it can be observed in Figures 80 and 81, in successful procedures, during the first minutes it was observed that, isolated warm small spots appeared in different parts of the sole. Over the time, these spots became enlarged, and their temperature also progressively increased. Otherwise, when the procedure was unresponsive, no thermal changes were observed and neither these thermal patterns (Figure 82). Likewise, another thermal behavior was observed, when apart from the ipsilateral, the contralateral plantar foot also presented thermal alterations, as can be observed in Figure 81. In these situations, the intervention was classified as “successful with temperature increase on the contralateral”.

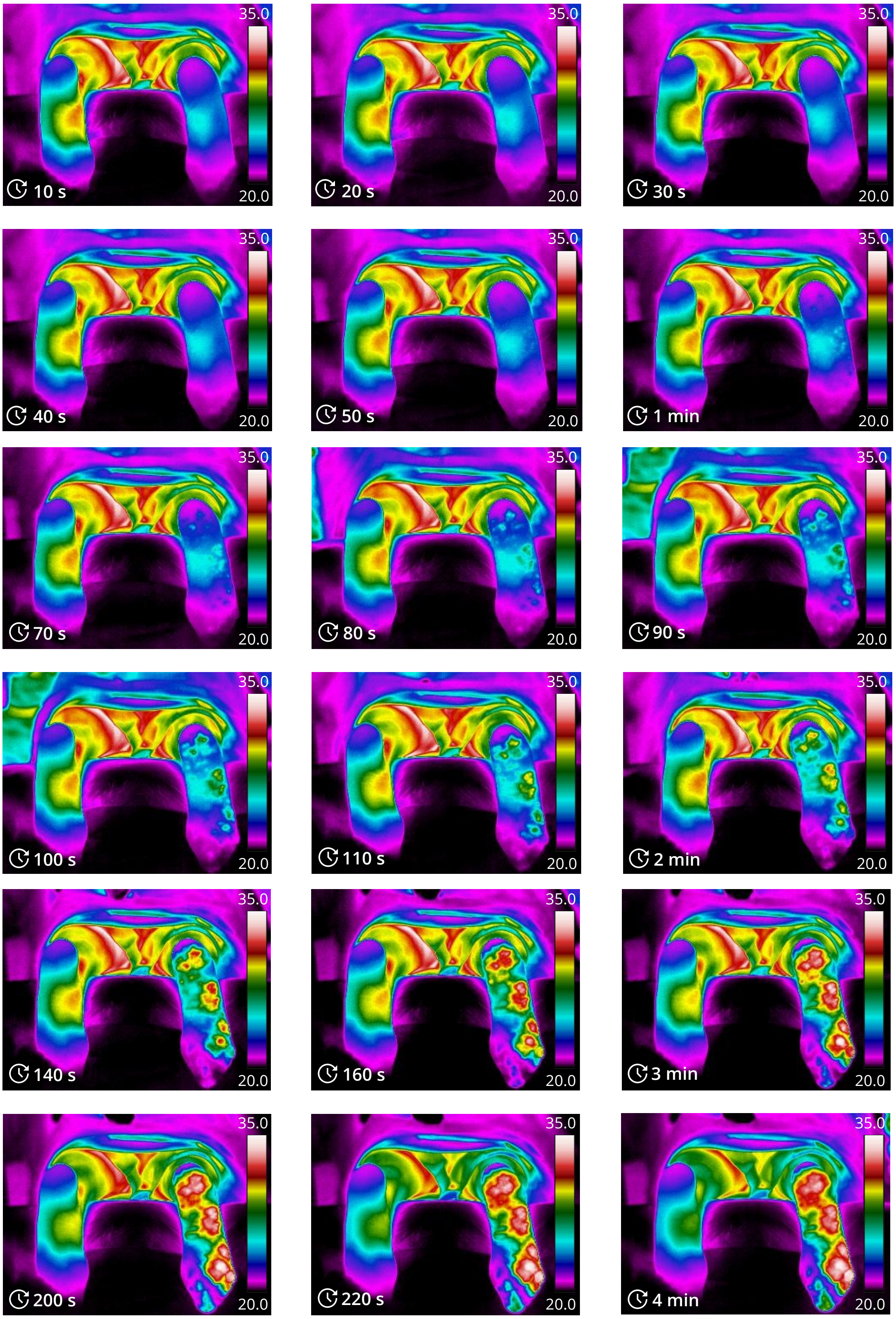

Figure 80. First 4 minutes after the lidocaine test thermal evolution of both plantar feet. This case corresponds to a procedure classified by the medical physician as successful.

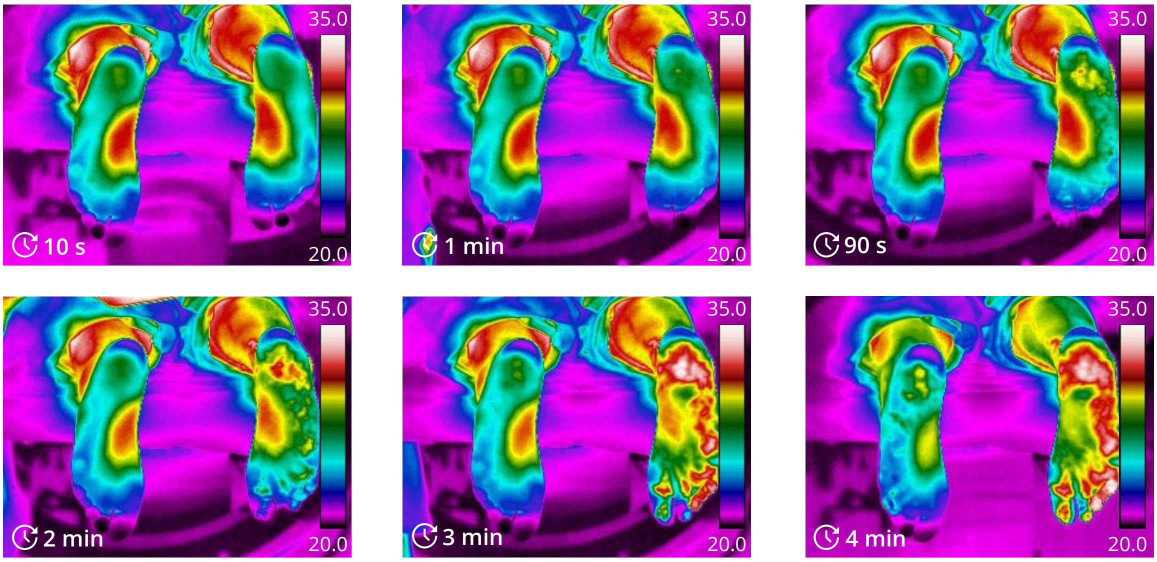

Figure 81. First 4 minutes after the lidocaine test thermal evolution of both plantar feet. This case corresponds to a procedure classified by the medical physician as successful with increase on the contralateral.

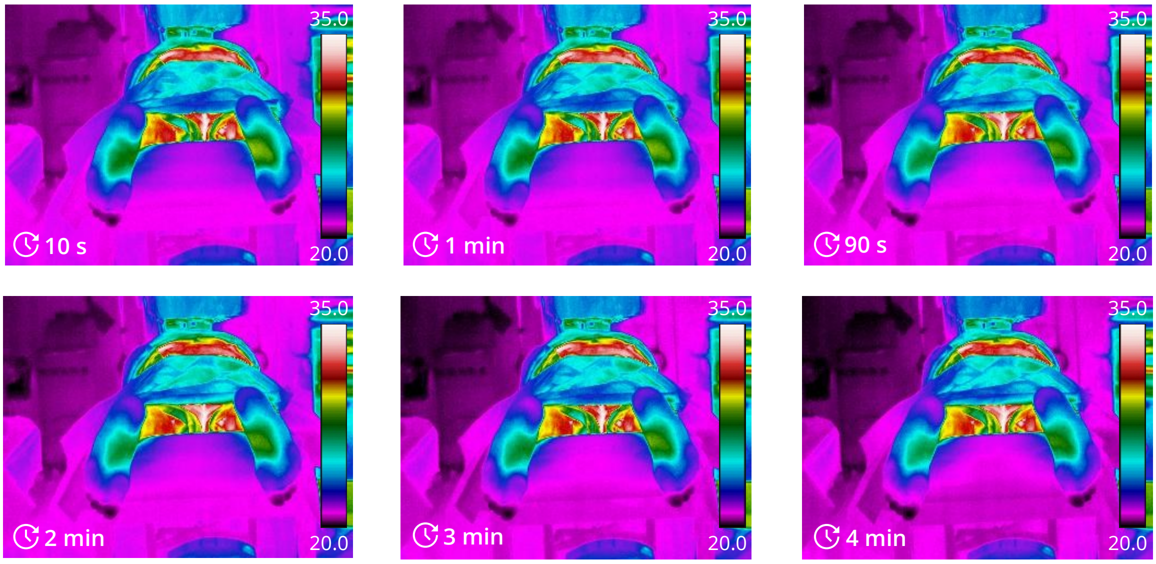

Figure 82. First 4 minutes after the lidocaine test thermal evolution of both plantar feet. This case corresponds to a procedure classified by the medical physician as failed.

5.4 Quantitative classification with statistical analysis

Once infrared data was collected in the clinical setting during the procedures, the statistical analysis was performed using the software RStudio (version 1.2.5033, RStudio, Boston, MA). A non-normal distribution of most of the thermal data was confirmed using the Shapiro-Wilk test ($p<0.05$). Then, to assess the evolution of skin temperature over time, Kruskal-Wallis with Wilcoxon the post-hoc and Bonferroni correction was performed for each parameter (mean, maximum and SD skin temperature), each foot (ipsilateral and contralateral), and for each medical classification (failed, successful, successful with increase in the contralateral foot). Since the aim of our study was to detect an alteration in the thermal parameters over the recording time, the baseline time (0 s: just after the lidocaine injection) was compared with the following times. In order to analyse which ROI were more sensitive to the temperature increase, differences between two times (baseline and 240 s) were assessed in each ROI using Kruskal-Wallis with Wilcoxon test post-hoc and Bonferroni correction for each parameter (mean, maximum and SD skin temperature) for the ipsilateral foot and for the successful group. Cohen effect size (ES) was calculated for the significant differences found in the pairwise comparisons and they were classified as small (0.2-0.5), moderate (0.5-0.8) or large (>0.8). Therefore, to detect a significant was established at $\alpha = 0.05$ and ES being moderate or large. Results are reported as mean with 95% confidence intervals (CI95%), presenting also the CI95% of the differences between conditions.

5.4.1 Regions of interest selection

Each plantar foot was divided into 11 ROIs shown in Figure 83: ROIs 1 to 5 are the toes, ROIs 6 to 8 are the metatarsal areas of the foot and finally, the ROIs 9 to 11 are the ones situated on the heel of the foot. Among all, the smallest ROIs (corresponding to the toes) presenting about 60 pixels, there were considered enough according to the requirements stablished for fever human screening (a minimum of 25 pixels are recommended) [901]. On the other hand, the camera used in this work was placed at a distance of 1.5 m from the participants' feet and presented an IFOV of 1.36 milliradian. Since this thermal resolution value should be multiplied by a factor 3 or 4 because of the diffraction of the optics, a minimum object size of about 6 millimetres would be required to obtain an accurate temperature measurement. In this sense, the little toe (corresponding to ROI 5) which entailed the most critical ROI, exceeded in most cases these requirements [896].

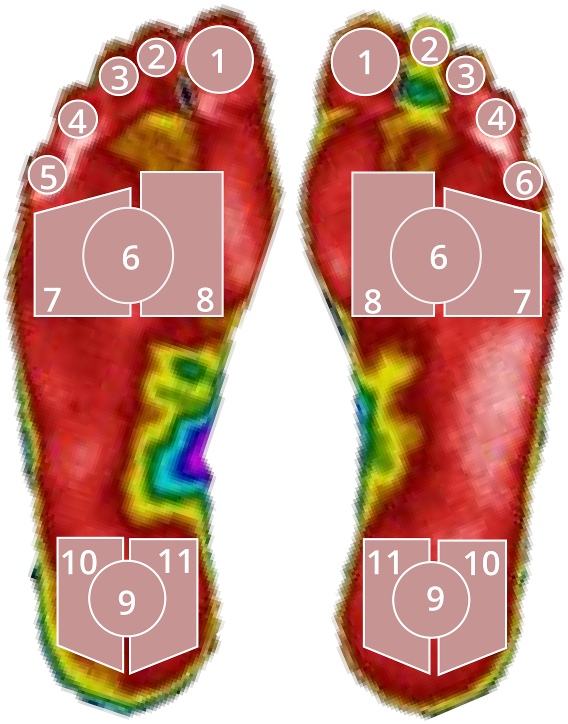

11 ROIs	
1	Hallux
2-5	Lesser toes
6	Central metatarsal
7	Lateral metatarsal
8	Medial metatarsal
9	Central heel
10	Lateral heel
11	Medial heel

Figure 83. Regions of interest selected indicated in an infrared image.

For each one of these regions, the mean temperature, the standard deviation, and the maximum temperature were extracted for each frame using in-house software developed under MATLAB (version R2020b, The MathWorks, Inc., Natick, MA) [1040].

5.4.2 Thermal data extraction

In most of the infrared images evaluated, either the toes or the medial part of the foot, were mixed up with the background and/ or with the patient's leg because of their radiation intensity similarity (Figure 58). Hence, with the goal of avoiding these mix-up issues, the adaption of the binary mask to the feet edges in the most accurate way was intended. For this reason, the feet segmentation was carried out using a semi-automatic tool through which the user had the chance to resize and reposition the binary mask, achieving a better adaptation to the aimed edges. Moreover, since in the first procedures it was observed that the thermal warming pattern differed among patients, it was considered appropriate that different areas of the foot could be evaluated independently. Therefore, the algorithm from Gauci et al. was selected through which 11 ROIs around the foot were extracted [1040].

In Figure 84, the whole process performed starting from the thermal data acquisition (step 1) and ending with the extraction of the variables of interest (step 4) is depicted. This process also includes the steps regarding the preliminary treatment (step 2), the feet segmentation, and ROIs extraction (step 3).

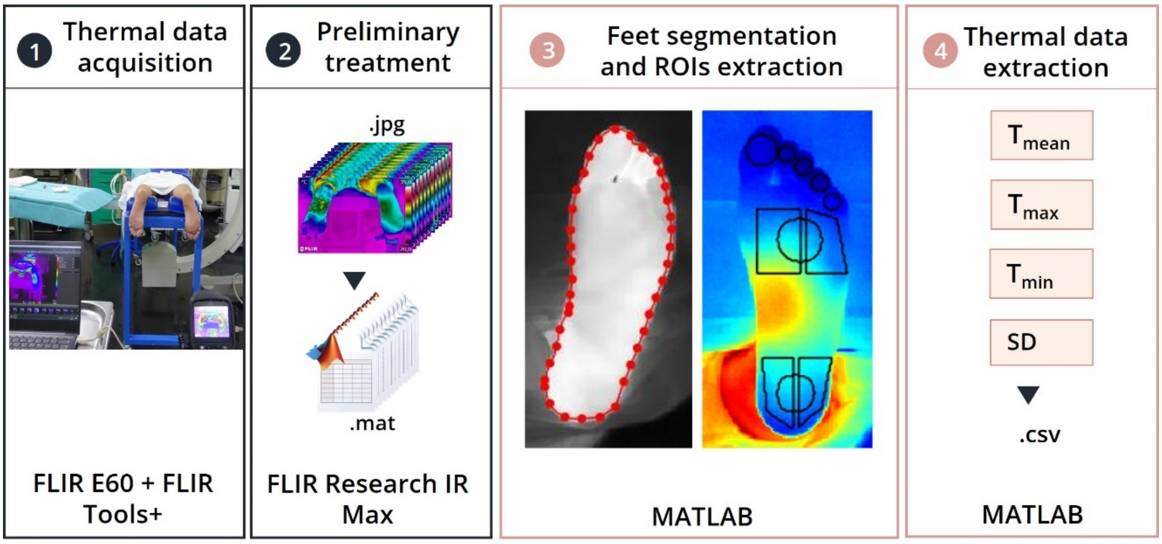

Figure 84. The process performed from the infrared images acquisition to the extraction of the variables.

Both steps 3 and 4 were performed using a semi-automatic algorithm specifically developed for this study in MATLAB, with a GUI to facilitate its use. Hence, once the infrared images were acquired in the clinical setting through the IR camera along with FLIR Tools+ version 6.4 (FLIR Systems, Inc., Wilsonville, OR), the IR data sets were converted into the appropriate format file (.mat) through FLIR ResearchIR Max version 4.40 (FLIR Systems, Inc., Wilsonville, OR). Then, the segmentation of both plantar feet using thresholding along with the ROIs obtention was conducted. Moreover, this step was complemented with additional methods allowing the user the ROIs modification (resize and replace them in the proper position). Finally, the ROIs extraction was performed using the MATLAB code implemented by Gauci et al. through which the variables of interest (the mean and maximum temperatures along with the standard deviation) for each ROI and frame were obtained.

5.5 Automatic classification with machine learning algorithms

Machine learning algorithms were used to assess LSBs classification performed by pain physicians using the infrared data collected. In this case, thermal data extracted from the IR images constituted input data, and the performance classification of the LSB procedure, constituted the output data. Thus, once the LSB classification outcome was provided (successful or failed), the supervised learning algorithm was applied to learn the relationship between the thermal data and the LSB performance.

The extraction of relevant features was carried out from the mean and maximum temperatures along with the standard deviation, all of them retrieved from the 11 ROIs previously defined. From these parameters, 66 features were obtained (Table 17): the variation for ipsilateral foot difference in ROI n (for n = 1 to 11) between the minute measured (4, 5 and 6) and at starting time in mean temperature (ΔMean), maximum temperature (ΔMax) and standard deviation (ΔSD). Additionally, the asymmetry variation between ipsilateral and contralateral foot at minute measured (4, 5 and 6) and the starting time for the 11 ROIs in mean temperature (ΔAsymMean), maximum temperature (ΔAsymMax) and standard deviation (ΔAsymSD) were obtained.

Table 17. The 66 features extracted from the 11 ROIs.

Feature	ROIs evaluated	Extremity evaluated	Description
ΔMean	11	Ipsilateral	$Tmean_t$-$Tmean_0$
ΔMax	11		$Tmax_t$ -$Tmax_0$
ΔSD	11		SD_t -SD_0
ΔAsymMean	11	Ipsilateral and contralateral	$\Delta Mean_{ipsi}$- $\Delta Mean_{contra}$
ΔAsymMax	11		ΔMax_{ipsi}- ΔMax_{contra}
ΔAsymSD	11		ΔSD_{ipsi}- ΔSD_{contra}

NOTE: “t” being the moment assessed: minute 4, minute or minute 6

The evaluation of the classification methods was performed using the Caret (Classification and REgression Training) package in RStudio (Version 1.2.5033) [1041]. The performance of four different machine learning classifiers was compared: Artificial Neuronal Network (ANN), K-Nearest Neighbours (KNN), Random Forest (RF), and Support Vector Machine (SVM) in three different moments: minute 4, minute 5 and minute 6 along with the baseline time. The data of successful and failed LSBs were randomly split preserving relative class sizes in each training and testing sample, using 60% for training and 40% for testing. This percentage of testing cases was determined to ensure a minimum number of failed cases (6 cases) in the testing dataset. Random splits were the same for the four supervised classification algorithms. Pre-process was performed to the features consisting of centering (subtracts the mean) and scaling (divides by the standard deviation). Before applying the classification algorithms, for each classification algorithm and minute assessed, a recursive feature selection (RFE) algorithm was used to determine the most important predictors [1049,1059].

Classification process was performed using a cross-validation structure with 10 repetitions for the split training data. Moreover, hyperparameters for ANN, KNN, RF and SVM were optimized. For KNN, the preset number of considered neighbours K values were K ∈ {1, 3,..., 15}. For RF the hyperparameters were mtry ∈ {2, 4,..., 14}. For SVM, the hyperparameters were C ∈ {2-2, 2-1,..., 22} and Σ ∈ {10-2, 10-1,..., 102}. Finally, for ANN, after a preliminary analysis, it was defined a size of 10 neurons and the decay was of 0.0001, 0.1 and 0.5. The ANN used a logistic classification method with a Multilayer Perceptron structure with 1 hidden layer composed by the 10 neurons.

Table 18. Hyperparameters set in the machine learning models.

Algorithm	Hyperparameters	Abr.	Set-up
ANN (MLP)	Number of hidden layers and neurons		1 hidden layer of 10 neurons
KNN	Number of neighbours	k	1, 3, 5…,15
RF	Number of random features and trees	mtry	2, 4,…, 14
SVM	Kernel	C	2-2, 2-1,…, 22
		Σ	10-2, 10-1,…, 102

For the feature evaluation, firstly, differences between failed and successful LSBs were assessed at each variable (ΔMean, ΔMax, ΔSD, ΔAsymMean, ΔAsymMax, and ΔAsymSD) and at each moment without considering the ROI. As non-normal distribution was observed (Shapiro-Wilk test, $p<0.05$), Mann-Whitney U tests were performed. For significant differences (p significance stablished at $\alpha = 0.05$), the Cohen effect size (ES) was calculated to determine the effects size and they were classified as small (0.2-0.5), moderate (0.5-0.8) or large (>0.8).

Classification performance of all methods and moments assessed was quantified by the accuracy, the sensitivity, the specificity, the Kappa coefficient, and the area under the curve (AUC). Finally, for the best models (based on AUC), the SHAP value (the contribution of each predictor) was quantified.

RESULTS

06

Infrared thermography for the assessment of lumbar sympathetic blocks in patients with Complex Regional Pain Syndrome

6 RESULTS

In this chapter, the results obtained regarding the three classification approaches for the assessment of LSB procedures are presented. In the first one, the medical classification was based exclusively on the thermal patterns within the feet observed in the infrared images in real time in the clinical setting. Then, the thermal features extracted from the 11 ROIs on each foot and each frame were used to carry out the quantitative analysis through statistical tools (second section) and then, through machine learning algorithms (third section).

6.1 Medical classification based on real time infrared images

In this section, the results concerning the feasibility of infrared thermography as a complementary technique in the clinical setting to assess in real time LSB procedures are presented. Hence, as described in section 2.9.2 and 5.2.1 (Figures 16 and 74), once the needle was considered to be placed in the correct position according to the FL images, a lidocaine test was performed. Then, the evaluation of the infrared images in real time confirmed whether the LSB procedure was technically performed (when thermal alterations within the first four minutes after the lidocaine test were observed on the ipsilateral) or not.

As described in section 5.2, the thermal data evaluation and acquisition in the clinical setting was performed in two different series, the first one between November 2019 and March 2020, and the second one between February 2021 and May 2021. The results concerning the medical classification based on the IR images of the first and second series are depicted in Table 19 and in Table 20, respectively. In each table, and for each patient, the number of procedures, interventions and the medical classification are shown. It should be noted that in patients undergoing a complete set of LSBs (3 LSB procedures), 3 interventions at least and 9 interventions at most were performed. Therefore, when each procedure required a single intervention, it was classified as successful in the first attempt resulting in successful rates of 100%. Conversely, when more than one intervention per procedure was carried out, it resulted in successful rates below 100% because in such cases, at least one repositioning manoeuvre of the needle was required.

Table 19. Summary of number of interventions and the medical classification performance based on the IR images for the first series of 12 patients.

Patient	No. of procedures	No. of interventions	No. of "successful" interventions	% "successful" interventions	Nº of "successful" interventions in the 1st attempt	% "successful" interventions in the 1st attempt
1	2	2	2	100	2	100
2	3	4	3	75	2	50
3	3	6	2	33.3	1	16.67
4	3	3	3	100	3	100
5	3	3	3	100	3	100
6	3	8	3	37.5	1	12.5
7	3	5	3	60	1	20
8	3	4	3	75	2	50
9	3	5	3	60	1	20
10	2	2	2	100	2	100
11	2	3	2	66.7	1	33.3
12	1	1	1	100	1	100
Total	31	46	30	65.2	20	43.5

Table 20. Summary of number of interventions and the medical classification performance based on the IR images for the second series of 12 patients.

Patient	No. of procedures	No. of interventions	No. of "successful" interventions	% "successful" interventions	Nº of "successful" interventions in the 1st attempt	% "successful" interventions in the 1st attempt
13	3	3	3	100	3	100
14	3	3	3	100	3	100
15	3	3	3	100	3	100
16	3	3	3	100	3	100
17	2	2	2	100	2	100
18	3	3	3	100	3	100
19	3	3	3	100	3	100
20	3	3	3	100	3	100
21	3	6	3	50	1	16.7
22	3	4	3	75	2	50
23	3	3	3	100	3	100
24	3	4	3	75	2	50
Total	35	40	35	87.5	31	77.5

In this study, 66 LSB procedures in 24 patients were performed in two rounds, 31 of them between November 2019 and March 2020, and 35 of them between February 2021 and May 2021. As shown in Tables 19 and 20, in most patients (19 out of 24), a complete LSBs set (3 procedures) evaluated with IRT was performed. However, in the remaining 5 patients, less than 3 procedures were available due to different reasons such as the lockdown (patients 10, 11 and 12), the patient's dropout (patient 17), or because the thermal data collection started once the first procedure had already been performed (patient 1).

Among the patients who underwent a complete LSBs set, and for the first and second series respectively, 3 interventions were performed in 8 and 2 patients, 4 interventions in 2 patients each series, 5 interventions in one patient, 6 interventions in one patient each series, and 8 interventions in one patient.

According to the results obtained, the successful rates were 100% in the first attempt in five (patients 1, 4, 5, 10 and 12) and in nine (patients 13 to 20 and 23) patients of the first and second series, respectively, since the interventions conducted were the same as the procedures. That is, in such cases, the LSBs were successfully performed in the first attempt without any reposition manoeuvre requirement and consequently, those patients underwent the minimum possible interventions. In the remaining cases, the successful rates in the first attempt were lower because more than one intervention was required in at least one of the procedures carried out. In this sense, for the first series, in 31 procedures performed, 46 interventions were necessary, whereas for the second series, this proportion was reduced, and 40 interventions per 35 procedures were conducted. Indeed, the lowest successful rate in the first attempt (12.5%) corresponds to patient 6, who underwent the highest number of interventions (8 interventions). Thus, in this patient, the maximum advisable number of interventions was reached in two out of the three procedures (3 repositioning manoeuvres within a single procedure). Conversely, in only 3 patients from the second series, more than one intervention per procedure was required. In fact, patients 22 and 24 underwent four interventions and, just in patient 21, six interventions were performed.

On the other hand, 30 out of the 46 interventions were classified as successful in first series whereas in second series the difference between both amounts diminishes, resulting in 35 successful interventions out of the 45 performed. As a consequence, patients from second series underwent fewer needle's reposition manoeuvres, which is in line with the previous remarks. It should be noted that both the number of successful interventions and procedures is the same in all patients but for patient 3. In this particular case, only two interventions were classified as successful, although three procedures were carried out. The reason behind this is despite having reached the maximum advisable number of interventions in one of the procedures, no thermal alterations in the ipsilateral were observed at all and consequently it could not be classified as successful. Overall, 65.2% and 87.5% of the interventions performed in patients from the first and second series, respectively, were classified by the medical staff as successful and among them, 43.5% and 77.5% were achieved in the first attempt.

6.2 Quantitative classification with statistical analysis

This study was aimed to establish specific cut-off time and temperature values to predict successful LSBs through the infrared images collected in the clinical setting. Hence, this section shows the results obtained from the statistical analysis performed on the thermal data retrieved from the first series of 12 patients. The minimum, maximum, and mean temperatures, along with the standard deviation were extracted using the in-house software developed under MATLAB for each ROI, foot (ipsilateral and contralateral), and frame. However, it should be noted that in this work, the minimum temperatures were excluded since they did not provide relevant information regarding the procedure performance, and therefore the evaluated thermal parameters include the mean and maximum temperatures and the standard deviation. Hence, the following 6 analysis are presented: for each medical classification, the mean and maximum temperatures, and the standard deviation for both feet (Figures 85, 87 and 89), additionally, just for the successful procedures according to the medical classification, the mean and maximum temperatures, and the standard deviation for both feet and each of the 11 ROIs (Figure 86, 88 and 90). Regarding the medical classification of the LSB procedures, it should be noted that in this study, 3 medical classifications were evaluated: successful, failed, and successful with increase in the contralateral foot. As one could notice, the “successful with increase in the contralateral foot” classification was not considered in the medical classification study. Although this new group would fundamentally belong to the successful group, and so was in the first study, it was considered relevant to independently evaluate this singular thermal pattern.

In this study, 44 interventions from 30 procedures were quantitatively analysed. It should be remarked that 2 out of the total interventions performed at first (46 interventions in the first series) were excluded because of problems with the IR data collected.

Figure 85 shows the mean skin temperature evolution for each medical classification group and for both feet. Regarding the failed group (Figure 85a), similar mean temperatures were observed in both feet at all evaluated moments ($p>0.05$ and $ES<0.5$). For the successful group (Figure 85b), it was at 240s (4 min) when the ipsilateral skin temperature presented greater values than at the baseline moment (0 s) (CI95% of the difference [1.4, 2.1°C], $p<0.001$ and $ES=0.5$). For this group, the contralateral foot presented similar temperatures between the baseline moment (0 s) and the following moments ($p>0.05$ and $ES<0.5$). When the successful with contralateral increase group (Figure 85c) is evaluated, the first moment when the ipsilateral presented higher skin temperatures than at the baseline moment was at 180 s (3 min) (CI95% [1.9, 3.3°C], $p<0.001$ and $ES=0.5$), with even higher increases at 300 s (5 min) (CI95% [3.4, 5.2°C], $p<0.001$ and $ES=0.8$). For this group, the contralateral foot presented higher skin temperatures at moment 540 s (9 min) than at the baseline moment (CI95% [1.6, 4.8°C], $p<0.001$ and $ES=0.5$).

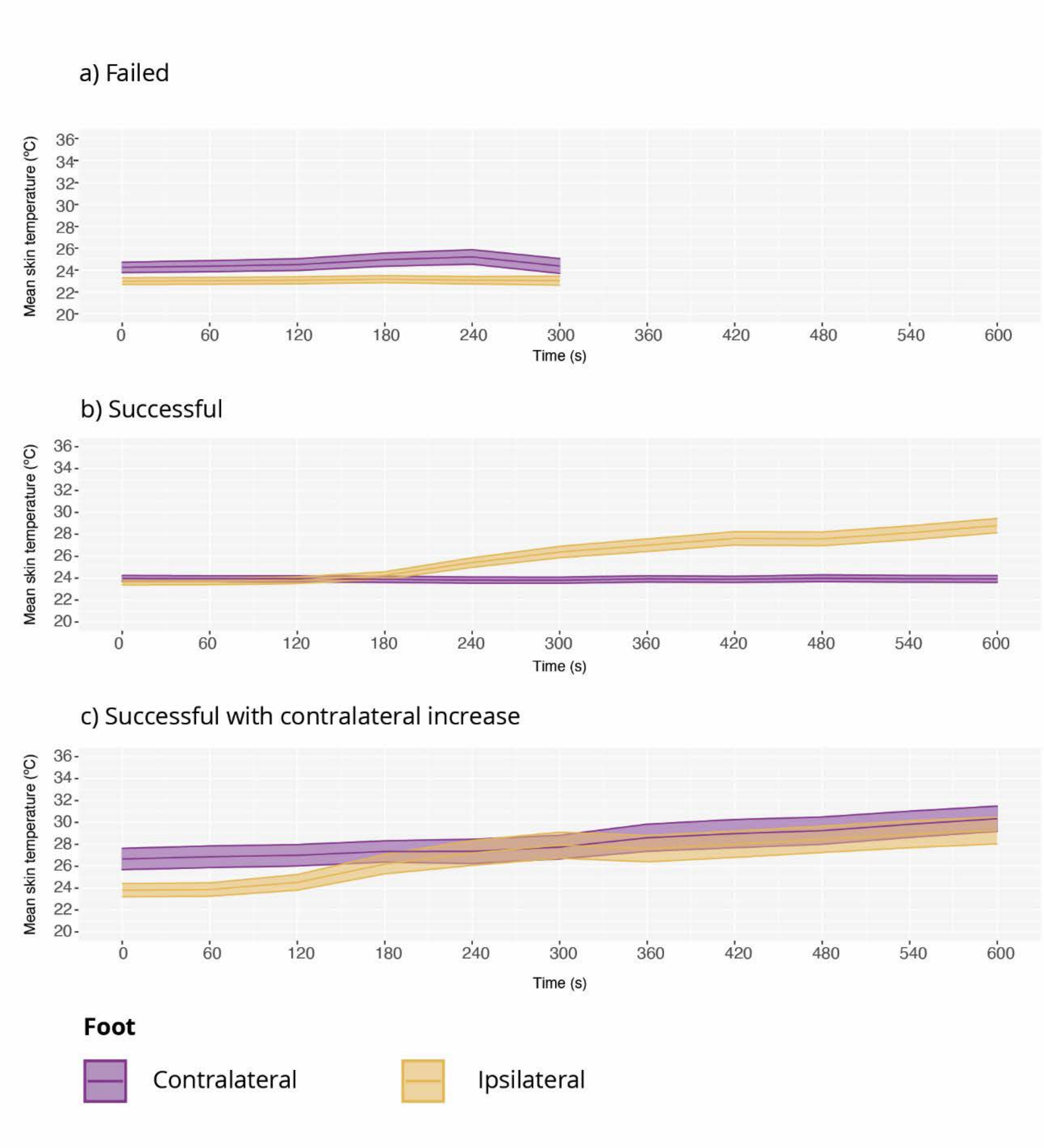

Figure 85. Evolution of mean skin temperature with shaded 95%CI area shown in the three classified groups using IRT in real time.

Figure 86 presents the mean skin temperature data for the successful group for each ROI and both feet. Ipsilateral mean skin temperature at 240 s (4 min) was higher in all ROIs than at the baseline moment: toe 1 (CI95% [0.5, 3.5°C], $p=0.01$ and ES=0.7); toe 2 (CI95% [0.6, 3.3°C], $p<0.001$ and ES=0.6); toe 3 (CI95% [0.6, 3.6°C], $p<0.01$ and ES=0.7); toe 4 (CI95% [0.7, 3.5°C], $p<0.01$ and ES=0.7); toe 5 (CI95% [0.7, 3.8°C], $p<0.001$ and ES=0.8); central metatarsal (CI95% [0.1, 2.1°C], $p=0.01$ and ES=0.5); lateral metatarsal (CI95% [0.3, 2.5°C], $p<0.01$ and ES=0.7); medial metatarsal (CI95% [0.0, 2.1°C], $p=0.04$ and ES=0.5); central heel (CI95% [0.9, 3.2°C], $p<0.001$ and ES=0.9); lateral heel (CI95% [0.8, 2.8°C], $p<0.001$ and ES=0.9); and medial heel (CI95% [0.6, 2.9°C], $p<0.01$ and ES=0.8).

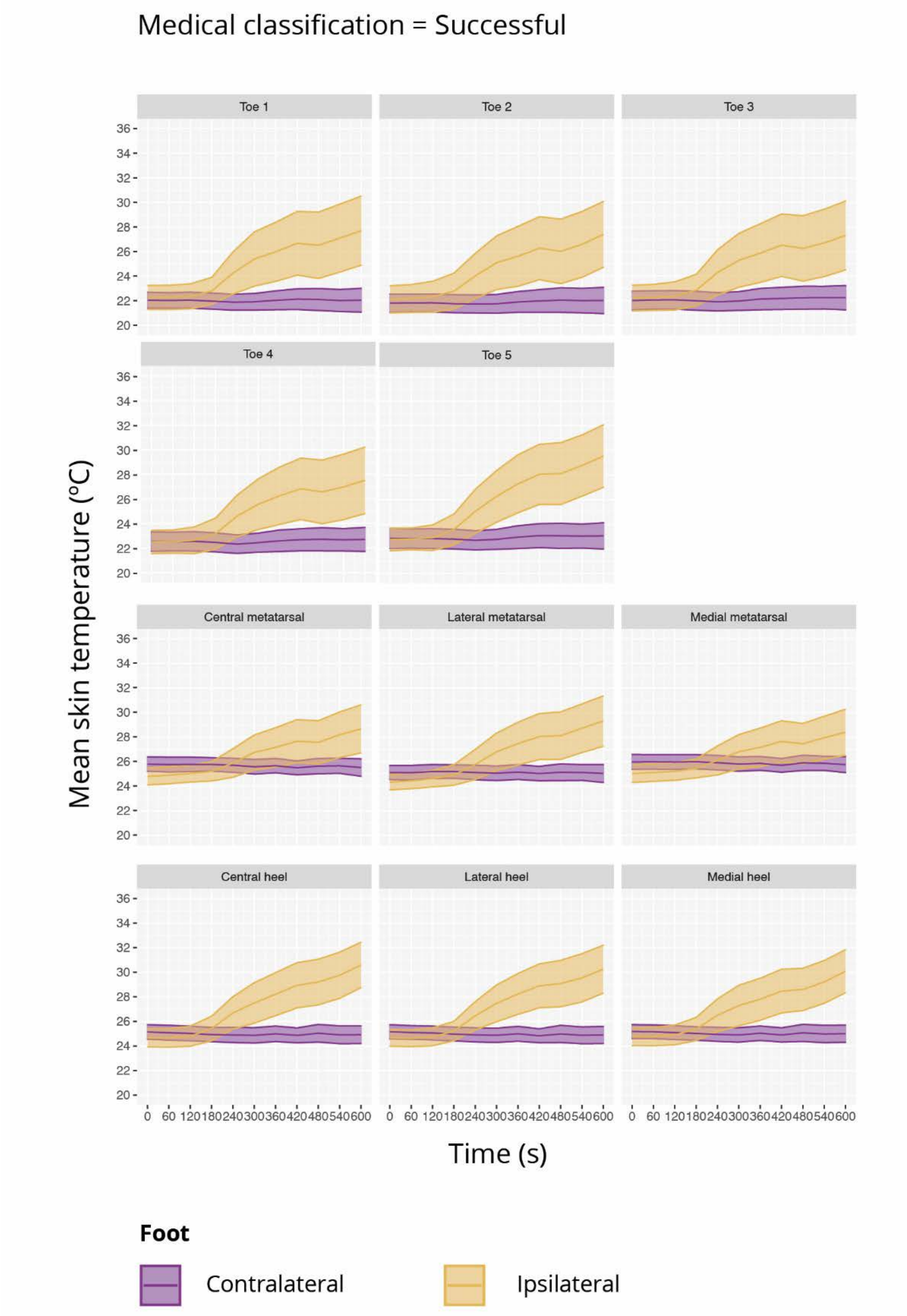

Figure 86. Evolution of mean skin temperature with shaded 95%CI area shown in the different regions of interest in the group classified as successful using IRT in real time.

Figure 87 shows the maximum skin temperature evolution for each medical classification group and for both feet. In the failed group, no increase of maximum skin temperature was observed (Figure 87a; $p>0.05$ and $ES<0.5$). For the successful group (Figure 87b), 300 s (5 min) was the first moment when maximum skin temperatures of the ipsilateral foot were higher than at the baseline moment (CI95% [2.3, 3.3°C], $p<0.001$ and $ES=0.6$), with no increases on the contralateral foot ($p>0.05$ and $ES<0.5$). In a similar way as in the case of the mean temperature, in the successful with contralateral increase group (Figure 87c), the first moment was at 240 s (4 min) (CI95% [3.0, 4.6°C], $p<0.001$ and $ES=0.6$). For this group, contralateral foot presented higher maximum skin temperatures at moment 540 s (9 min) than at the baseline moment (CI95% [1.5, 4.7°C], $p<0.001$ and $ES=0.5$).

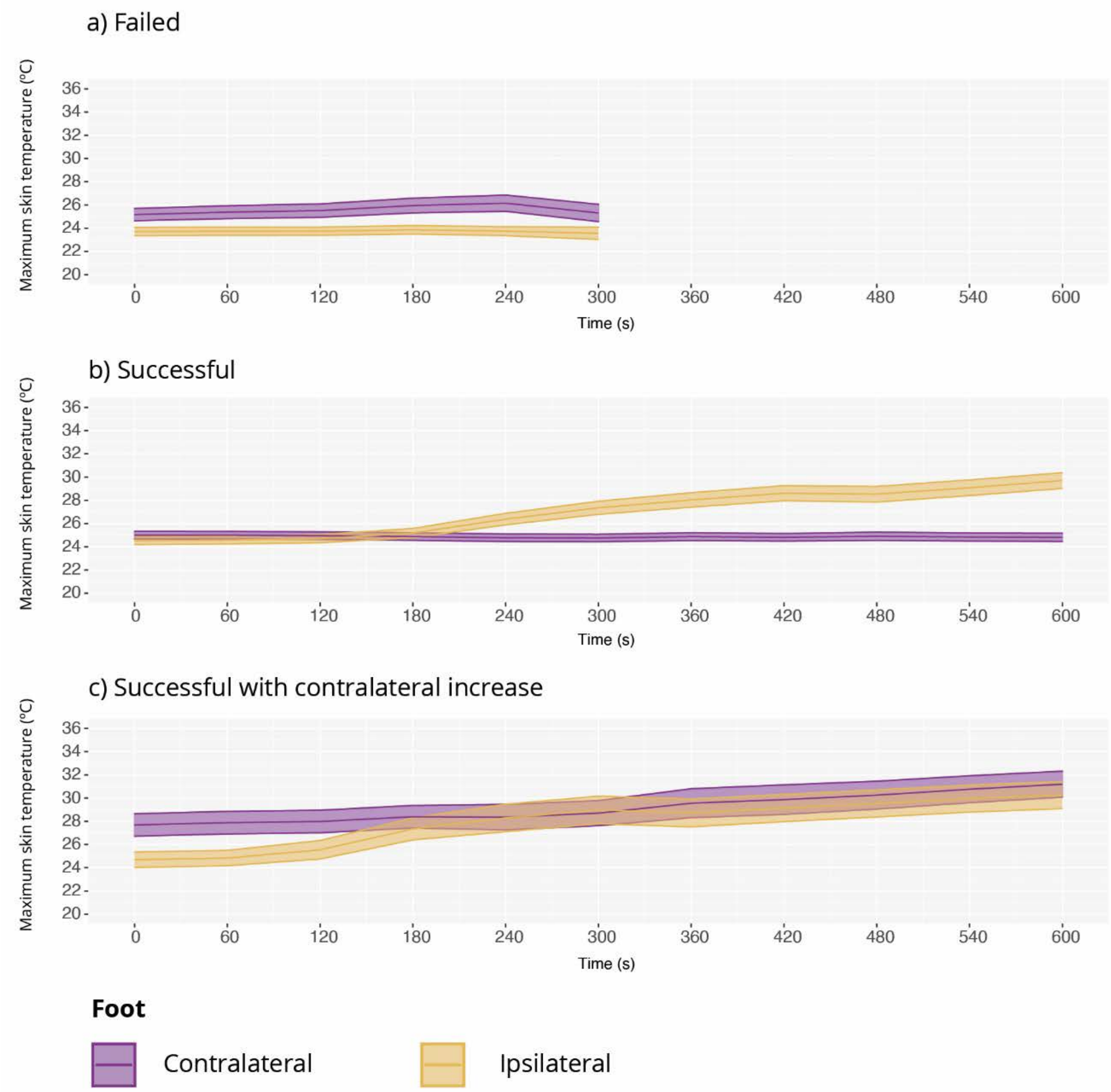

Figure 87. Evolution of maximum skin temperature with shaded 95%CI area shown in the three classified groups using IRT in real time.

Figure 88 presents the maximum skin temperature for the successful group for each ROI and both feet. Maximum skin temperature at 240 s (4min) was higher than at the baseline moment in the ROIs corresponding to the toes and heel, but not in the metatarsal ones ($p>0.05$ and $ES<0.5$): toe 1 (CI95% [0.4, 4.1°C], $p=0.03$ and $ES=0.7$); toe 2 (CI95% [0.6, 3.8°C], $p<0.001$ and $ES=0.6$); toe 3 (CI95% [0.4, 3.6°C], $p<0.01$ and $ES=0.6$); toe 4 (CI95% [0.5, 3.4°C], $p=0.01$ and $ES=0.7$); toe 5 (CI95% [0.5, 3.4°C], $p<0.01$ and $ES=0.7$); central heel (CI95% [1.2, 3.8°C], $p<0.001$ and $ES=1.0$); lateral heel (CI95% [0.8, 3.3°C], $p<0.01$ and $ES=0.9$); and medial heel (CI95% [0.4, 3.0°C], $p=0.01$ and $ES=0.8$).

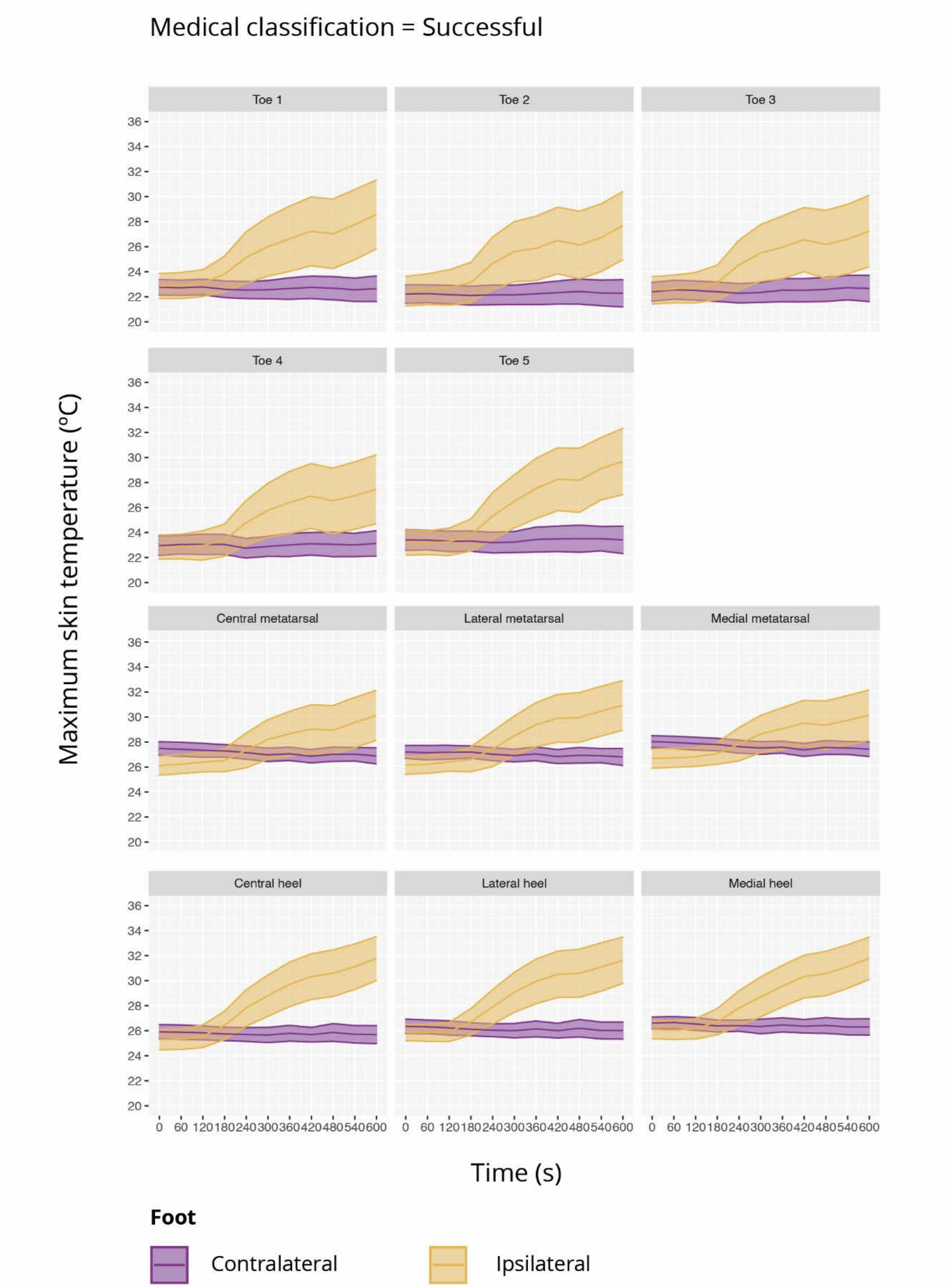

Figure 88. Evolution of maximum skin temperature with shaded 95%CI area shown in the different regions of interest in the group classified as successful using IRT in real time.

The standard deviation skin temperature depicted in Figure 89 was no different at the baseline moment compared with the following moments in any of the feet for both the failed and the successful with contralateral increase groups (Figure 88a; $p>0.05$ and $ES<0.5$). For the successful group (Figure 89b), at 360 s (6min) the SD skin temperature was higher than the baseline for the ipsilateral foot (CI95% [0.2, 0.3°C], $p<0.001$ and $ES=0.5$). The contralateral foot (Figure 89c) did not present any difference between the baseline and the following moments ($p>0.05$ and $ES<0.5$).

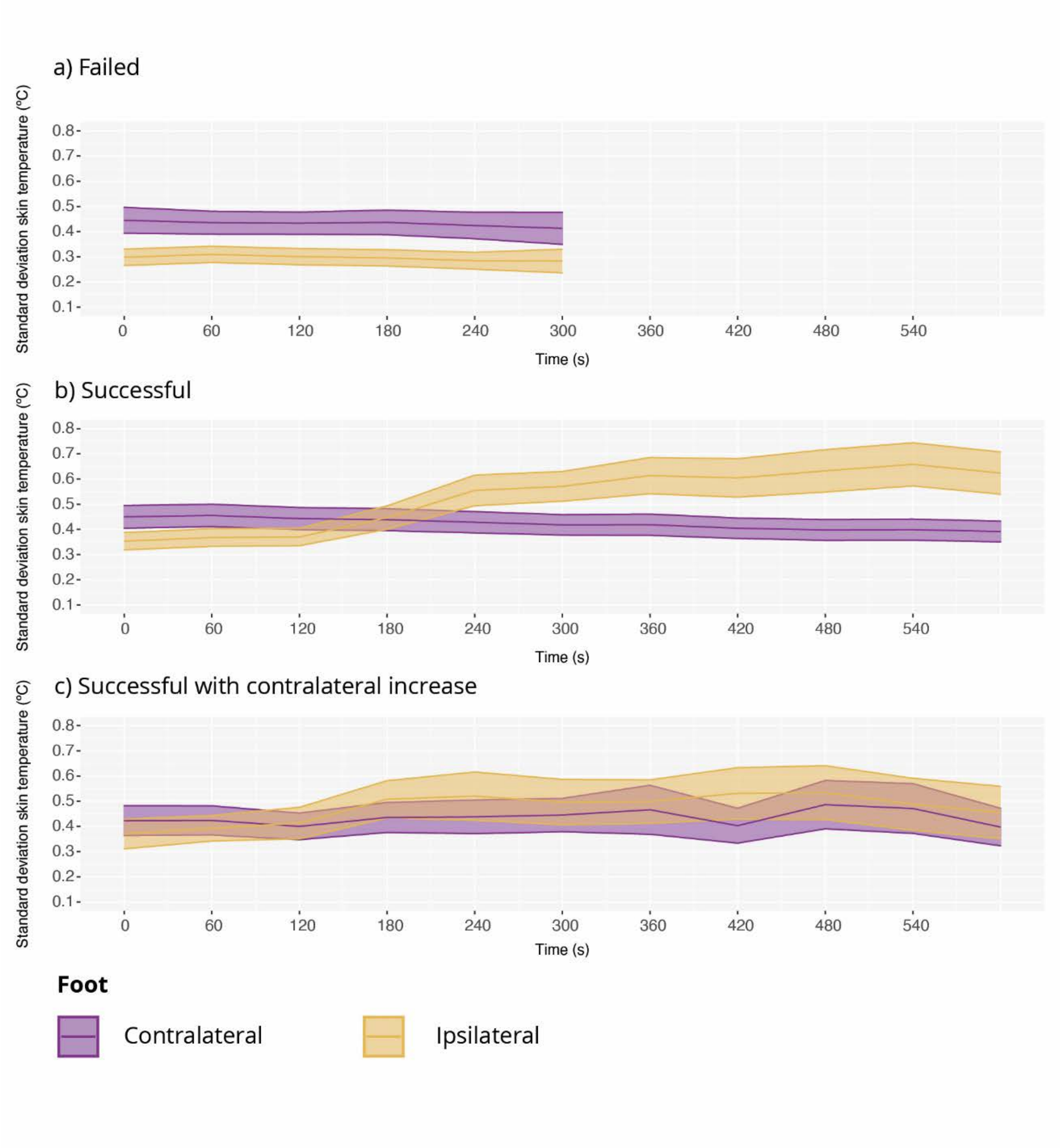

Figure 89. Evolution of standard deviation temperature with shaded 95%CI area shown in the three classified groups using IRT in real time.

Figure 90 shows the SD skin temperature for the successful group for each ROI and both feet. SD skin temperature at 240 s (4min) was higher than at the baseline moment in the ROIs corresponding to the first two toes and the heel: toe 1 (CI95% [0.1, 0.5°C], $p<0.01$ and ES=0.9); toe 2 (CI95% [0.0, 0.4°C], $p=0.04$ and ES=0.8); central heel (CI95% [0.2, 0.5°C], $p<0.001$ and ES=1.2); lateral heel (CI95% [0.3, 0.8°C], $p<0.001$ and ES=1.3); and medial heel (CI95% [0.0, 0.4°C], $p<0.01$ and ES=0.7).

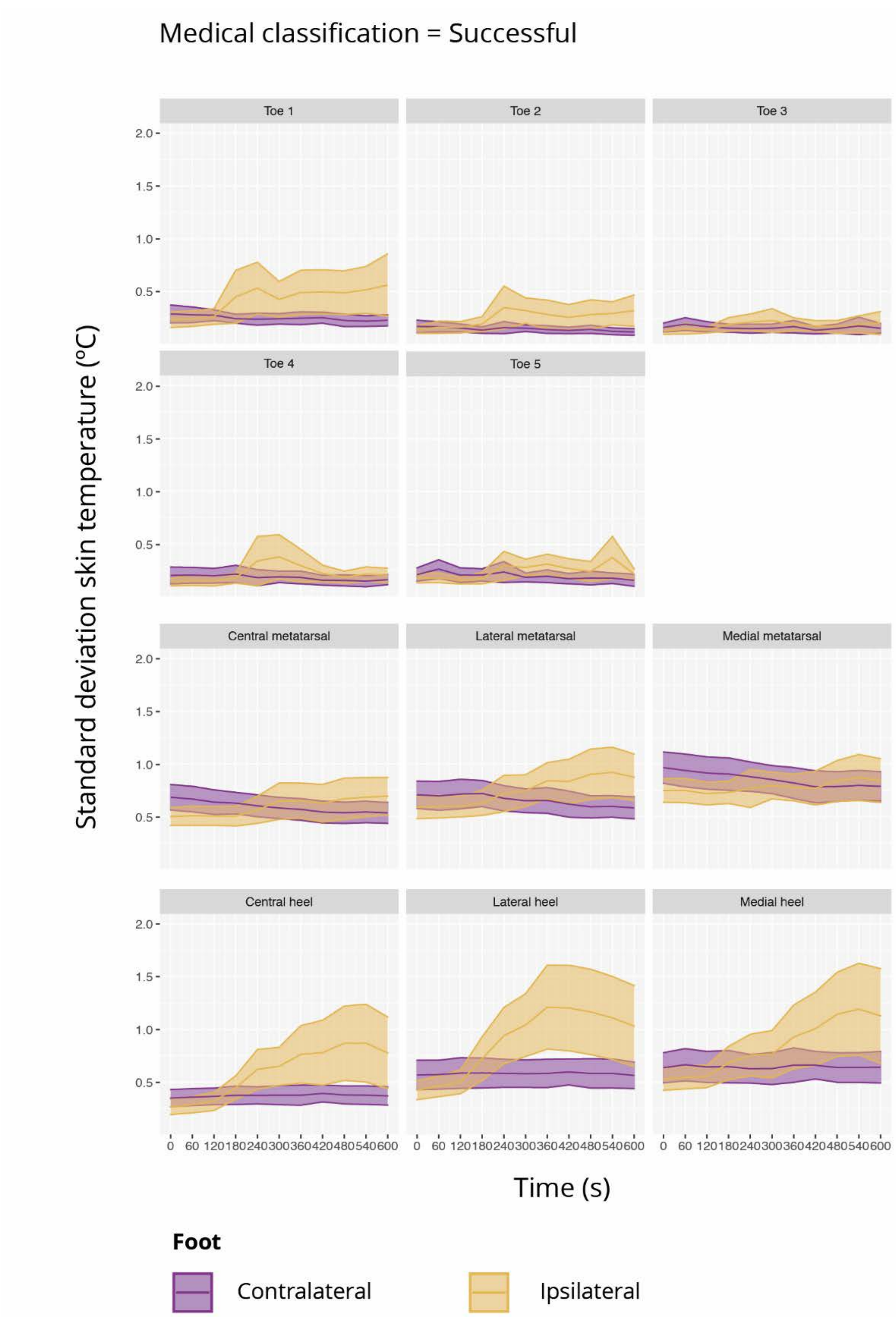

Figure 90. Evolution of standard deviation temperature with shaded 95%CI area shown in the different regions of interest in the group classified as successful using IRT in real time.

In Table 21, the most relevant results described previously are presented for both the successful and the successful with contralateral increase groups. The failed group has not been considered since it did not show significant neither mean nor maximum skin temperature increases within the evaluated moments. Hence, for both classification groups, the mean and maximum temperature increases considering the first moment at which they presented a moderate Cohen effect size (ES = 0.5-0.8).

Table 21. Ipsilateral mean and maximum temperature increases, and time elapsed since the base line moment for successful and successful with increase groups with CI95% and moderate ES.

	ΔTmean (t)	**ΔTmax (t)**	**SD (t)**
Successful	[1.4ºC, 2.1ºC] (4 min)	[2.3ºC, 3.3ºC] (5 min)	[0.2ºC, 0.3ºC] (6min)
Successful with temperature increase on the contralateral	[1.9ºC, 3.3ºC] (3 min)	[3ºC, 4.6ºC] (4 min)	-
	[1.6ºC, 4.8ºC] * (9 min)	[1.5ºC, 4.7ºC] * (9 min)	-

NOTE: * are referred to the contralateral feet

In Table 22, the most relevant results are presented for the ipsilateral foot only considering the successful group. Hence, this group presents the following mean and maximum temperatures at minute 4 for each ROI with moderate (ES = 0.5-0.8). or large Cohen effect size (ES > 0.8).

Table 22. Ipsilateral mean and maximum temperatures for each ROI at minute 4 for successful group with CI95% and moderate to large (*) ES.

ROI	Tmean	Tmax	SD
Toe 1	[0.5ºC, 3.5ºC]	[0.4ºC, 4.1ºC]	[0.1ºC, 0.5 ºC] *
Toe 2	[0.6ºC, 3.3ºC]	[0.6ºC, 3.8ºC]	[0ºC, 0.4 ºC]
Toe 3	[0.6ºC, 3.6ºC]	[0.4ºC, 3.6ºC]	
Toe 4	[0.7ºC, 3.5ºC]	[0.5ºC, 3.4ºC]	
Toe 5	[0.7ºC, 3.8ºC]	[0.5ºC, 3.4ºC]	
Central metatarsal	[0.1ºC, 2.1ºC]	-	
Lateral metatarsal	[0.3ºC, 2.5ºC]	-	
Medial metatarsal	[0ºC, 2.1ºC]	-	
Central heel	[0.9ºC, 3.2ºC] *	[1.2ºC, 3.8ºC] *	[0.2ºC, 0.5 ºC] *
Lateral heel	[0.8ºC, 2.8ºC] *	[0.8ºC, 3.3ºC] *	[0.3ºC, 0.8 ºC] *
Medial heel	[0.6ºC, 2.9ºC]	[0.4ºC, 3ºC]	[0ºC, 0.4 ºC]

6.3 Automatic classification with machine learning algorithms

The aim of this third study was to evaluate the capability of machine learning methods to automatically classify the performance of LSBs through the thermal data acquired in the clinical setting. Hence, four algorithms (ANN: Artificial Neuronal Network, KNN: K-Nearest Neighbours, RF: Random Forest, SVM: Support Vector Machine) were evaluated using the mean and maximum temperatures along with the standard deviation extracted for each ROI and frame for both the first and second series of patients. Specifically, for the three selected moments (minutes 4, 5 and 6) and for each ROI, the differences between successful and failed LSBs were assessed for the following features (Table 17): the ipsilateral temperature variation between the minute assessed and the starting time for the mean (ΔMean), the maximum (ΔMax) and the standard deviation (ΔSD) along with the asymmetry variation between ipsilateral and contralateral foot at the minute assessed and the starting time in mean temperature (ΔAsymMean), maximum temperature (ΔAsymMax) and standard deviation (ΔAsymSD).

According to Figure 91, all the variables assessed presented higher values at successful cases ($p<0.05$), a growing tendency over time. Specifically, for minutes 4 and 6, the differences obtained between successful and failed LSBs in all variables assessed were moderate to large. In minute 5, in turn, the magnitude of the effect size was moderate to large in five out of the six variables. In fact, the SD variables (ΔSD and ΔAsymSD) presented the lower effect size of the differences between failed and successful LSBs in all moments assessed. Therefore, the features related with the mean and maximum temperatures differences may be suggested for the LSBs classification in the three selected moments.

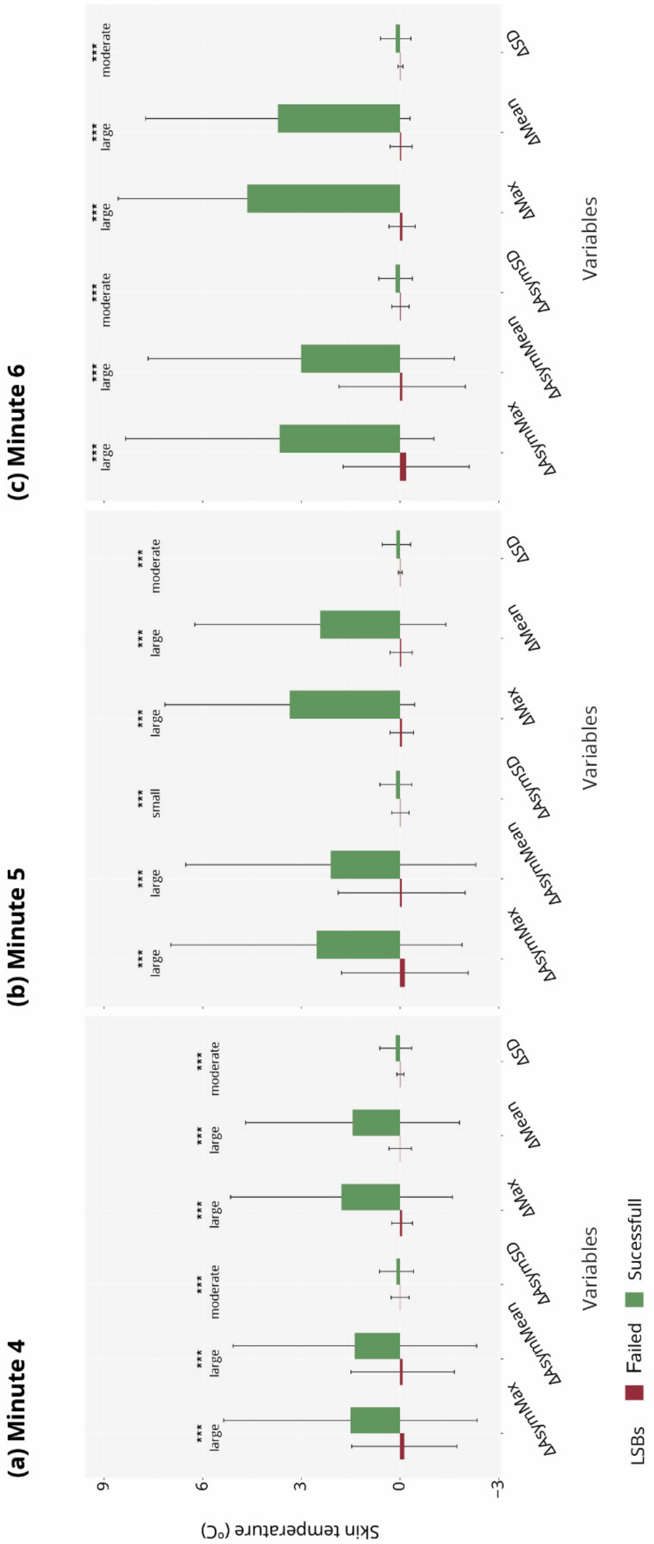

Figure 91. Median and standard deviation of the variables assessed for minutes 4 (a), 5 (b), and 6 (c) after the lidocaine injection. Differences between successful and failed Lumbar Sympathetic Blocks (LSBs) are shown by symbols (* p<0.001) and the magnitude of the effect size (large, moderate, and small).**

On the other hand, the performance metrics for the four classification algorithms assessed (ANN, KNN, RF, SVM) at the three different moments assessed (minutes 4, 5 and 6) are depicted in Table 23.

Table 23. Performance metrics for the classification methods assessed (ANN: Artificial Neuronal Network, KNN: K-Nearest Neighbors, RF: Random Forest, SVM: Support Vector Machine) at the three variations moments between baseline and minutes 4, 5, and 6.

	ANN	KNN	RF	SVM
t = 4 min				
No. of predictors	8	25	21	15
Accuracy	0.84	0.84	0.84	0.80
Kappa value	0.64	0.61	0.64	0.48
Sensitivity	1.00	0.83	1.00	0.67
Specificity	0.79	0.84	0.79	0.84
AUC	<u>0.89</u>	0.84	<u>0.89</u>	0.75
t = 5 min				
No. of predictors	3	11	6	13
Accuracy	0.88	0.84	0.80	0.76
Kappa	0.72	0.61	0.57	0.41
Sensitivity	1.00	0.83	1.00	0.67
Specificity	0.84	0.84	0.74	0.79
AUC	<u>0.92</u>	0.84	0.87	0.73
t = 6 min				
No. of predictors	4	5	7	17
Accuracy	0.88	0.80	0.80	0.80
Kappa	0.72	0.57	0.53	0.53
Sensitivity	1.00	1.00	0.83	0.83
Specificity	0.84	0.74	0.79	0.79
AUC	<u>0.92</u>	0.87	0.81	0.81

The RFE (recursive feature selection) determined the different number of predictors for each classification method and moment assessed, resulting, that at minute 4, the number of predictors necessary was higher in comparison with minute 5 and 6 in all methods assessed but SVM (Table 23). According to the performance metrics, ANN performed the best for both minutes 5 and 6 achieving a maximum accuracy of 88%, sensitivity of 100%, specificity of 84%, and AUC of 0.92. When AUC is specifically considered, the best classification model were ANN and RF at minute 4 (both with an AUC = 0.89) and ANN at every evaluated time (AUC = 0.89 at minute 4, and AUC = 0.92 at minute 5 and 6). Therefore, these results suggest that among the four ML algorithms evaluated, SVM and RF may be discarded for the LSBs classification based on the features previously selected. However, it should be note that in case more interventions were to be included in the evaluation, this consideration would be reconsidered since the starting conditions may have changed.

Considering the results based on the methods' performance metrics, in Table 24, the detailed descriptors for the best models (RF for minute 4 and ANN for both minute 4 and 5) are depicted. As it can be observed, the predictors corresponding to ΔAsymMean and ΔAsymMax of the central heel were obtained in the three models. Likewise, ΔMax of both central and medial heel ipsilateral along with ΔAsymMax of toe 2 are common at minute 4 for RF and ANN models.

Table 24. Predictors obtained for the best models.

Predictors	ANN Minute 4	RF Minute 4	ANN Minute 5
ΔMean toe 1 ipsilateral	X		
ΔMean toe 3 ipsilateral		X	
ΔMean toe 5 ipsilateral		X	
ΔMean lateral heel ipsilateral		X	
ΔMax toe 2 ipsilateral		X	
ΔMax toe 5 ipsilateral		X	
ΔMax central metatarsal ipsilateral		X (-)	
ΔMax lateral metatarsal ipsilateral		X (-)	X
ΔMax central heel ipsilateral	X (-)	X	
ΔMax lateral heel ipsilateral		X	
ΔMax medial heel ipsilateral	X (-)	X	
ΔSD central heel ipsilateral		X	
ΔSD lateral heel ipsilateral		X	
ΔAsymMean toe 2		X (-)	
ΔAsymMean toe 3		X	
ΔAsymMean toe 4		X	
ΔAsymMean central heel	X	X	X
ΔAsymMean lateral heel		X	
ΔAsymMax toe 2	X (-)	X	
AAsymMax toe 5	X		
ΔAsymMax central heel	X	X	X
ΔAsymMax lateral heel		X	
ΔAsymMax medial heel	X (-)		
ΔAsymSD medial heel		X	

NOTE: (-) describes a negative predictor's contribution.

In Figure 92, the SHAP values (the contribution of each predictor) obtained at minute 4 for both RF (Figure 92a) and ANN (Figure 92b) along with the ones obtained for ANN at minute 5 (Figure 92c) are shown. In the light of the results, the ΔAsymMean and ΔAsymMax of the central heel were the predictors with the highest contribution, and furthermore they are present in the best three models. Additionally, some of the predictors described in Table 23 presented negative contribution according to Figure 92. Among them, ΔMax corresponding to the ipsilateral central and medial heel present a negative contribution when ANN for minute 4 was evaluated whereas their contribution was positive for RF at the same evaluated moment. Therefore, the predictors presenting this uneven behaviour should be taken with caution.

(a) RF at minute 4

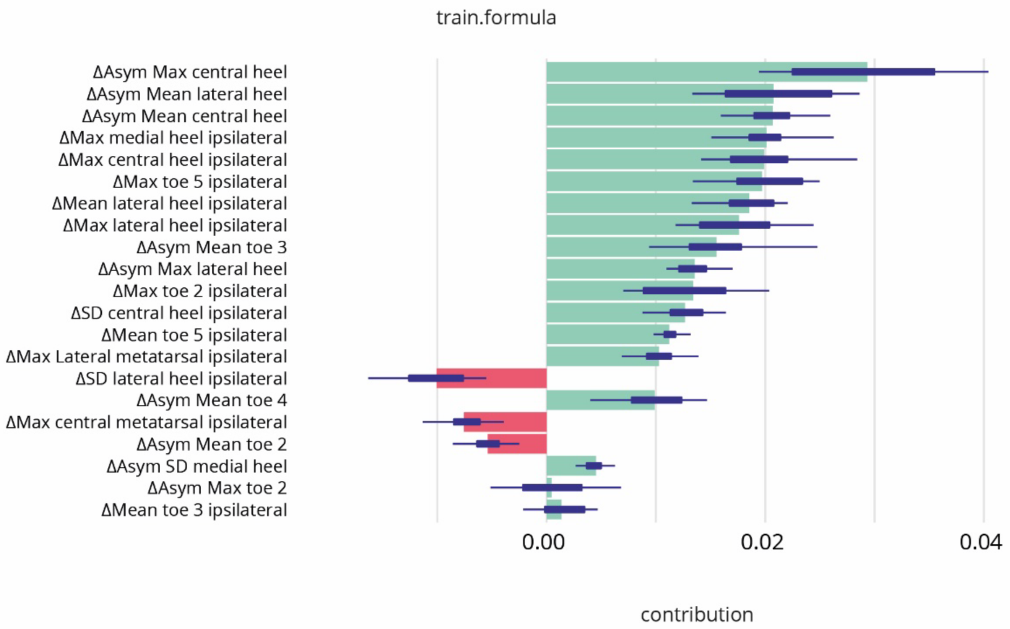

(b) ANN at minute 4

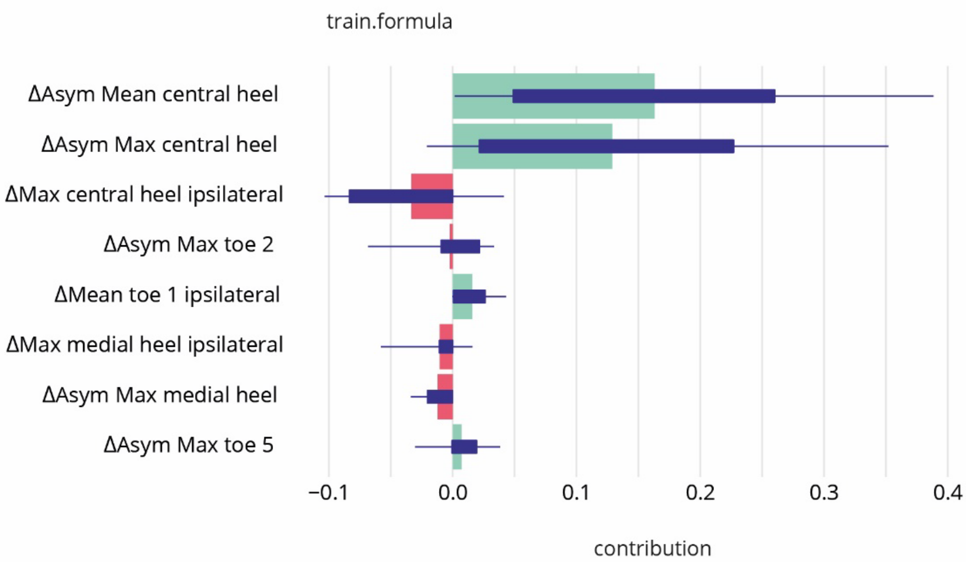

(c) ANN at minute 5

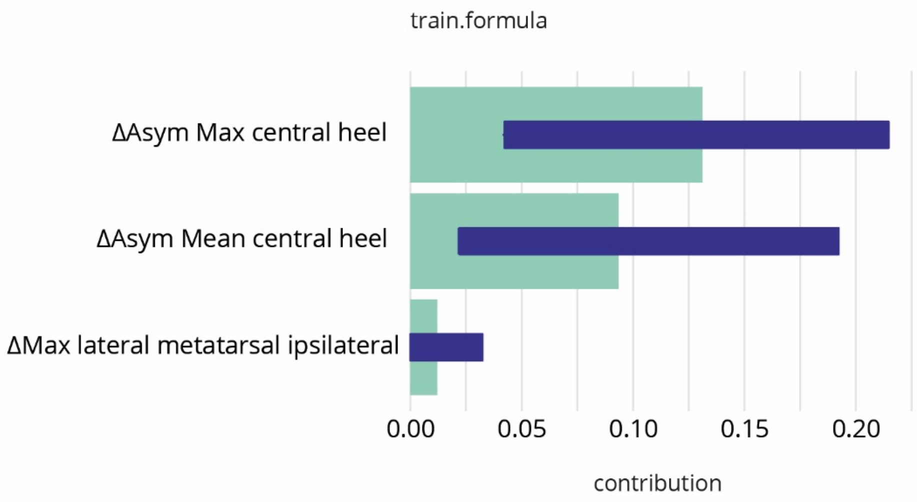

Figure 92. The predictor's contribution (SHAP values) in the best models: Random Forest (RF) at minute 4 (a), and Artificial Neuronal Network (ANN) at minute 4 (b) and at minute 5 (c).

DISCUSSION

07

Infrared thermography for the assessment of lumbar sympathetic blocks in patients with Complex Regional Pain Syndrome

7 DISCUSSION

Apart from actuating as analgesic, local anaesthetics such as lidocaine, behave also as vasodilator resulting in a blood flow increase in peripheral tissues [1060,1061]. Consequently, a raise in skin temperature at the distal part of an extremity is expected when sympathetic blocks are performed, and for this reason, temperature alterations within the plantar feet can be used as an indicator of sympathetic blocks success.

The aim of the first classification approach was to evaluate the capability of IRT to qualitatively assess in real time the LSBs performance in order to enable the physicians to carry out their classification. From this point, the thermal data collected in the clinical setting was then quantitative analysed through statistical and ML methods in the second and third classification approaches. Nevertheless, to obtain the thermal variables to be quantitative evaluated, a previous step consisting of the ROIs definition was required. Hence, in the second classification approach, it was intended to obtain temperature and time thresholds which could be used as indicators of successful LSBs, and, in the third classification approach, the evaluation of different ML algorithms to automatically classify a LSB procedure performance was aimed.

7.1 Medical classification based on real time infrared images

The main finding of this study was that the use of infrared thermography in the clinical setting to qualitative evaluate the performance of LSB procedures was demonstrated totally feasible. Likewise, IRT enabled physicians to check in real time the thermal patterns taking place on the plantar feet and, consequently, it helped them to assess their interventions. In fact, IRT allowed the medical staff to determine in the first attempt that 56.5% and 22.5% of the cases for the first and second series, respectively, did not show temperature variations after the lidocaine test, which forced them to relocate the needle. Additionally, the increase of the successful intervention rates from 65.2% to 87.5% for the second series in comparison with the first series, may indicate a significant improvement in the technique performance. However, it should be mentioned that the assessment of the LSB procedures in real time corresponding to the second series was carried out exclusively by the medical staff. Conversely, in the first series, both the infrared data collection and the evaluation of the blocks performance in real time was performed in conjunction. In this sense, the proportion of successful LSB procedures obtained in both series may not be straightforward, which presents a limitation.

Although IRT has proved to be a powerful technique for classifying the LSB performance in patients diagnosed with CRPS, there is a lack of literature about this topic and no previous studies addressing the impact of qualitative IRT on the improvement of the LSB technique performance have been found. In spite of this, different works have evaluated some common aspects. In a study performed by Park et al. [599], 185 LSBs were performed, and 124 (67%) of the total were reported as successful, results which are in agreement with the successful rates obtained in our work for the first series (65.2%). However, they used thermoprobes to obtain skin temperature measurements and, moreover, only 39 blocks out of the total (185) were performed on patients suspicious of presenting CRPS.

On the other hand, IRT has been implemented in the assessment of other nerve blocks regarding the upper and lower extremities [607]. In agreement with our findings, several authors have demonstrated that a successful block was related to skin temperature increases after the injection of the local anaesthetic [609,1045,1046]. In this sense, the skin temperature increase appears to be more or less significant depending on the innervated areas of the sympathetic nerve fibres blocked. Consequently, the choice of the skin temperature measurement sites may have great influence on the proper block success prediction [1047]. According to previous works, the effects of the skin temperature increase are most pronounced when distal parts of the extremities are involved, especially palms and soles (glabrous skin) but they are much less significant at more proximal parts [609,1048,1049]. When the nerve blocks are associated to upper extremities, the largest skin temperature increase has been reported to be located distally on the fingertips [609,1050].

On the other hand, concerning the assessment of nerve bocks of lower extremities, Stevens et al. observed that sciatic nerve blocks led to significant increase in skin temperatures within the foot [1051]. Van Haren et al. reported that after subgluteal sciatic nerve block, skin temperature changes within the plantar foot and the toes were noticeable, whereas at the dorsal foot they were less significant [1048]. In another study performed by Kim et al. the highest net increases in skin temperature following LSB were obtained at the plantar surface [1052]. The other regions within the low extremities presented less pronounced skin temperature increases. Specifically, and ordered from the highest to the lowest were plantar and dorsal surface, shin, anterior surface of the knee, calf, posterior surface of the knee, anterior surface of the thigh and posterior surface of the thigh [1052]. Therefore, according to these findings, the skin temperature measurements would be performed on the plantar feet, which is where our skin temperature measurements were performed. Despite the skin thermal changes in the plantar feet are proved to be more pronounced, it should be considered that distal parts of the body are subjected to major thermal fluctuations due to environmental factors, the sympathetic nervous activity, or the disease itself [617,624]. In this sense, since the thermal images allow the assessment in real time of multiple areas simultaneously (i.e., the comparison of skin temperature progression in both feet), the effect of the temperature fluctuations within the sole may be counteracted.

In some of the works previously considered, instead of using IRT for the temperature measurements, thermoprobes or IR thermometers were used [599,1051]. Considering that thermal changes are not always straightforward, the inadequate contact with the skin when thermocouples are used, or the insufficient thermal data when isolated points in time are assessed with IR thermometers may lead to inaccurate predictions of the block success. In fact, temperature measurements obtained with both contact and infrared devices have been compared in several studies [640,1053]. In the sports field, a study demonstrated that temperature discrepancies obtained between IRT and thermal contact sensors for measuring skin temperature were contained within the accuracy of the thermal camera (±2 Cº) [1054]. Moreover, another study stated that skin temperatures were higher when using thermocouples in comparison with the measurements obtained using infrared thermography [1055]. Therefore, the assessment of LSBs by means of IRT (complying with the minimum specifications as described in section 3.6.5), should be suggested.

The limitations of the study included the reduced number of patients evaluated, among others. In this sense, it is important to mention that the number of patients diagnosed with lower limbs CRPS and undergoing LSBs in everyday clinical practice is scarce [15,1056]. Thus, the number of LSB procedures performed in this work within a nine month-period (66 procedures) can be considered as substantial. Additionally, it should be remarked that the lockdown due to the COVID-19 took place within the collection period, which resulted in the hospital workload reduction, and consequently, in the number of patients diagnosed and treated. The sample size of several studies focused on the performance of LSBs in patients presenting CRSP are in line with our work. In the study performed by Kim et al., 26 lumbar sympathetic ganglion blocks were performed in patients with various sympathetic nerve system disorders (among them, 11 with CRPS) [1052]. Similarly, in the study of Park et al., 185 LSBs were performed on 82 patients, of which, only 39 were associated with CRPS [599]. Only in the retrospectives studies involving extended periods of time, a greater number of patients undergoing SBs are included [504,572]. Specifically, in the study of Cheng et al., although at first 647 procedures were performed (in the same number of patients), only 318 were finally analysed due to the exclusion criteria considered (i.e., the temperatures were not recorded, pre-procedure temperatures were missing, or pain evaluation was missing) [504]. Among the 318 procedures performed, 265 corresponded to LSBs, of which, 255 were addressed to patients' CRPS diagnosis. On the other hand, in the study of An et al. performed between 2012 and 2015, 74 LSB procedures in 62 patients were evaluated, of which 9 were with CRPS [572]. Therefore, and considering the significantly extended collection times (roughly 7 and 3 years), the sample size issue appears to be a common issue among studies aimed at either CRPS management or blocks assessment.

Another concern of this work was associated with the pain specialists performing the LSB procedure. While in the second series, every LSB was performed by the same pain physician, in the first series, different anaesthesiologists were involved. On one hand, the fact that the very same physician performed all LSBs may lead to maintain the uniformity and hence the intra-rater reliability. In fact, this option is selected in some previous works [503,600]. However, the outcomes regarding the procedures' performance when a single pain physician is involved, may not be generalised to different pain specialists, especially when untrained physicians with lack of experience in this technique would be involved. In fact, there are certain situations, for instance, when a great number of procedures in extended periods of time are involved, that the same anaesthesiologists would not perform all the operations [504,597].

Finally, although the absence of a control group may reduce the validity of this study, including one may lead to ethical concerns. In this sense, the inclusion of a control group was considered at first, in which the infrared images would not assist the medical staff to assess the LSBs performance. However, this initial approach was dismissed, and as an alternative, it was considered relevant to evaluate the contribution of the IRT in the improvement of the LSB procedure performance over time. Other studies have also raised the concern regarding the inclusion of a control group due to ethical reasons. Indeed, in the study of Kim et al., the volunteer control was dismissed, justifying their decision on grounds of the invasive nature of these procedures [1052].

7.2 Quantitative classification with statistical analysis

To present, no gold standard for determining a block success is available, and therefore, one of the purposes of this study was to establish a cut-off temperature value from which pain physicians could make a decision regarding the classification of the lumbar sympathetic block procedures.

In this study, the evolution of the mean and maximum temperatures along with the standard deviation for the medical classification groups was analysed for the first series. Likewise, the evolution of the mean and maximum temperatures along with the standard deviation for the successful group and each of the 11 ROIs was evaluated. In the light of the results, 4 or 5 minutes starting from the lidocaine test should be necessary to correctly classified a LSB as successful. At this point, the skin temperature alterations in the ipsilateral would present moderate effect and therefore they could be used as a successful predictor. Although the pain physicians considered at most the first 4 minutes after the lidocaine test based on both their experience and previous examinations, the results observed suggested that the observing times in the clinical setting to classify the interventions should be slightly extended. On the other hand, in patients with temperature increase on the contralateral foot, the classification could be performed shortly before (at 3 or 4 minutes after the anaesthetic injection). However, in these patients, the skin temperature alterations in the contralateral with moderate effect would not be observed until 9 minutes after the baseline time.

Although no recent studies addressing thoroughly the LSBs assessment with IRT have been found, several authors have addressed the issue of establishing the temperature and time threshold as indicators of a successful sympathetic block intervention. Kim et al. reported that the net changes in skin temperature at the plantar surfaces of the feet following a LSB were 6.2 ± 2.68ºC [1052]. Although the temperature measurements were performed using thermographic images, temperature increase within the feet were only checked 30 minutes after the block. In this sense, the time elapsed to validate the success of the procedure is excessive and shorter times are desirable, especially in failed blocks when further intervention attempts are required. Schürman et al. established an increase in the mean temperature difference after the blockade to represent a clinically successful sympathetic block of at least 1.5ºC [1057]. Park et al. considered a successful LSB procedure when the rate of temperature change reached 0.4°C/min within approximately 5 minutes, or when an increase in skin temperature of ≥ 2ºC was achieved after the local anaesthetic injection [599]. On the other hand, Ryu et al. showed that the onset time for obtaining a temperature increase of 2°C or more in successful LSBs was 476.2 ± 112.6 seconds (about 8 minutes) [600].

Although our results are in line with these previous studies, several remarks should be stated. In the last two studies, temperature probes instead of IRT were used to evaluate the changes in plantar feet skin temperatures. In this sense, only specific skin temperatures values associated with the specific points at which probes were attached could be obtained. Moreover, when thermocouples are used, a greater lag in the acquisition occurs, which lead to less accurate temperature measurements. On the other hand, Schürman et al. did not evaluated the skin temperatures of plantar feet, but they measured instead the thermal changes on the hands using IRT after performing stellate ganglion blocks [1057]. In our study, skin temperature of both plantar feet were obtained with IRT, which enable us not only to precisely locate the thermal changes within the foot, but also to specify the moment at which these thermal changes occurred.

This study also provides new information regarding the thermal behaviour of the eleven areas within the foot. Accordingly, in successful LSBs, the ipsilateral medial, lateral, and central heel presented skin temperature alterations 4 minutes after the lidocaine injection of moderate (medial heel) and large (lateral and central heel) effect. Therefore, the ipsilateral patients' heel could act as an indicator for successful blocks. However, the higher CI95% observed in these results (around 2ºC and 2.5ºC for mean and maximum temperature respectively, Table 22) compared with ones observed in successful LSBs without considering the ROIs separately (0.7ºC and 1ºC for mean and maximum temperatures respectively, Table 21), may suggest an inter-participant variability in which ROI starts to heat up first.

Therefore, the mean skin temperature differences at minute four (after the lidocaine test) could serve as indicative cut-off values for determining the intervention performance.

One of the limitations of this study may be the possible inaccuracies in the thermal parameters' extraction. As it would be described in section 7.4, the imprecisions during the feet segmentation along with the ROIs position may lead to the inclusion of non-relevant areas which may affect the final results. In this sense, it should be noted that, since a large number of images were available and processed for each intervention, these inaccuracies would be attenuated.

7.3 Automatic classification with machine learning algorithms

The main purpose of this study was to evaluate the capability of different ML algorithms (ANN, KNN, RF and SVM) for automatically classifying the performance of LSB procedures. In this respect, the results obtained are promising. The method may be considered as an effective tool to automatically classify LSBs into successful and failed since the differences obtained between them were large in four out of the six variables assessed (ΔMean, ΔMax, ΔAsymMean, and ΔAsymMax) for the three different moments (minute 4, 5 and 6) (Figure 91). The SD variables (ΔSD and ΔAsymSD), in turn, presented the lower effect size of the differences between failed and successful LSBs in all moments assessed. Among the metrics commonly used to assess the models' performance, ANN performed the best for both minutes 5 and 6 achieving a maximum accuracy of 88%, sensitivity of 100%, specificity of 84%, and AUC of 0.92 (Table 23). On the other hand, in all models except for SVM, a greater number of predictors at minute 4 would be necessary compared to both minutes 5 and 6. The reason behind this result may be due to both isolated and slight intensity of thermal alterations on the ipsilateral during the first few minutes. Conversely, in the successive minutes, these thermal changes become more extensive and significant and, as a result, a smaller number of predictors may be enough for a proper classification. Therefore, considering the performance metrics and the number of predictors, the best desirable model would be ANN for minute 5. Nevertheless, the model's performance may be affected by several factors such as the selected features, predictors, hyperparameters and so forth [1058,1059].

To our knowledge, there are no previous studies addressing automatic classification of LSBs into successful or failed using ML algorithms based on IRT features extracted from the plantar feet. However, works focused on the combined use of IRT and ML methods to classify different conditions have been recently published. According to a recent systematic review on this matter [1060], the most applied classifier in terms of performance is ANN followed by SVM, both of them mainly implemented in breast diagnosis. Other conditions such as diabetes have implemented ML methods through the use of plantar temperatures [948,954]. In a study focused on prediabetes identification from plantar thermograms, different classifiers (SVM, NB, MLP, k-NN and RF) were implemented in 60 subjects [1061]. The SVM outperformed the other classifiers with an accuracy rate of 81.60%, although RF presented the best value of AUC reaching 0.87. In another research, ANN and SVM along with other deep learning methods were compared to classify diabetic foot thermograms, achieving for ANN an accuracy of 83.33%, sensitivity of 66.60% and AUC of 0.83 [1062]. ANN has also been integrated successfully for the support of early diagnosis and follow-up of diabetic patients using plantar foot thermograms, with a classification rate of 94.33% [997]. Therefore, the results obtained in our study showed that, as a general rule, all algorithms worked well, which is in agreement with previous studies [997,1063].

This study also deals with the evaluation of the predictor's contribution (SHAP value), a topic that has received little attention so far due to its recent development [1064,1065]. When the predictors' contribution is evaluated, it can be observed (Figure 91) that ΔAsymMean and ΔAsymMax (the asymmetry variations between the ipsilateral and the contralateral foot between the moment assessed and the instant just after the lidocaine test in mean and maximum temperature, respectively), corresponding to the central heel in RF for minute 4 and ANN for both minutes 4 and 5, had the highest contribution. In this sense, the fact that the central heel presented the highest contribution may be attributed to the feet arterial vascularization, since the plantar blood suppliance has its origin primarily on the posterior tibial artery [632,1066]. On the other hand, the contribution of the predictors corresponding to the toes was hardly relevant, which could be related to the small size of the associated ROIs along with their thermal changes' variability.

Although no previous studies implementing SHAP values have been found concerning the application of ML models in IR features, its implementation in other topics shows promising outcomes, which is in agreement with our findings. In a very recent study [1067], the SHAP approach was used to determine the risk of amputation according to different clinical features (i.e., gangrene, diabetes duration, foot infection). In other recent work [1068], the SHAP value provided the risk factors in the prognosis of patients with COVID-19 in an intensive care unit. Accordingly, the SHAP approach facilitates interpreting the importance of the predictors selected by the ML model, that is, it improves the transparency of the ML algorithm, regarded so far as a kind of "black box" [1064,1069]. This yields, therefore, more transparent, and interpretable data, which in medicine are critical for the optimal diagnostic or treatment strategy. Taken all together, a definite conclusion about the best predictor for the LSB classification cannot be clearly stated, although predictors related to bigger ROI may perform better, which is in line with the considerations stated in the previous analysis.

The fact that machine learning is a constating evolving field along with the scarce literature concerning some ML performance parameters (i.e., SHAP values), makes this analysis approach a challenging task. Additionally, the small sample size gives rise to whether the models were trained with a sufficient number of images or not, which in turn may lead to bias in the results. Despite these limitations, it should be pointed out that this study has been the first to implement machine learning models with sufficient accuracy to predict the classification of LSBs interventions.

7.4 ROIs definition and thermal data extraction

As it has been described, both the quantitative classification performed through either statistical analysis or ML algorithms were based on the variables extracted from the 11 ROIs selected using the in-house software developed under MATLAB [1040]. On this basis, the ROIs definition along with the variables' selection constitute one of the cornerstones of these studies, and for this reason, the discussion about this matter is presented in this section.

Certainly, the ROIs selection is one of the most controversial steps regarding the analysis of infrared data since their shape, size, and position along with how they are chosen, differ between authors, even when the same area of the body is to be evaluated [974]. In this work, a semi-automatic algorithm was used for foot segmentation and ROIS extraction. According to a recent review, the proportion of works concerning ROIs in feet are significant in comparison with other regions of the body, and from them, nearly all cover ulcerations or diabetes [979]. In “the Glamorgan protocol” one ROI following the outline of the foot is suggested [895]. However, in our study, due to the peculiar thermal patterns observed within the feet during the first LSB procedures, it was considered advisable to analyse different areas independently.

When disorders in diabetic feet are evaluated, most authors divide the plantar foot into several ROIs, usually associated with common ulceration sites (876). Although in some previous works few ROIs were defined, some authors considered 9 [754,940] and even 12 ROIs [627,936]. However, since the aimed warming regions in the foot ulcerations detection with respect to the assessment of LSB procedures differ significantly, some areas, such as the metatarsal, may remained undefined using the first approach. Other authors have divided the sole into the four angiosomes [938,988,989] resulting in excellent inter and intra-rater reliability skin temperature measurements according to Seixas et al. [938]. Nevertheless, the angiosomes’ division was dismissed in our study because it does not consider the toes separately. On the other hand, some authors placed the ROIs according to different regions of the foot, such as the rearfoot, the midfoot, and the toes, however it resulted in lower inter-examiner intraclass correlation coefficients when defining the smallest ROIs corresponding to the toes and hallux [873]. Finally, 6 [990], 9 [880,991], and 11 [981,992] free anatomical ROIs to evaluate different conditions have been described by different authors (Figure 60). On this occasion, the Gauci et al. approach with 11 ROIs was the most appropriate since in the remaining approaches, the lesser toes were evaluated in conjunction.

Given that the toes size have a potential influence on the final temperature measurements, their evaluation was challenging [973,1054]. Certainly, a reduction in the number of pixels may derive in uncertain results, and for this reason, it is recommended a minimum of 25 pixel-size within the ROI [617,895]. In this work, the smallest ROIs (corresponding to the toes) presented about 60 pixels, which exceeded the minimum requirements. On the other hand, taking into account the camera performance parameters (section 3.6.3), a minimum object size of about 6 millimetres was required to conduct temperature measurements accurately. In this sense, the little toe (ROI 5) which entailed the most critical ROI, exceeded these requirements in most cases [896]. In a recent study, Seixas et al. observed that when mistakes were made in the ROIs positioning, the variations of temperature measurements had less influence in larger ROIs rather than in the smaller ones [939]. Despite of this, it should be noted that, in contrast with foot ulcers detections or similar conditions in which these small ROIs are of paramount importance, in the LSBs assessment, may be not so critical because temperature alterations take place primarily in many other areas of the foot, such as in the heel regions. Moreover, these issues in the small ROIs become more significant when IR cameras with low performance parameters (small FPA array sizes and big values of IFOV or NETD) are employed. Indeed, since they usually exhibit poorly defined contours, greater variation in the results has been reported when small inaccuracies in the ROIs positioning are made in comparison to the results obtained with better performance IR cameras [873,1070].

Apart from the ROIs' number and size, the way they are selected also plays a fundamental role in the final measurements. In a recent review focused on the ROIs selection in sport studies, it was reported that, out of 87 papers, 16 employed automatic methods, whereas in 53 studies, the ROIs were manually selected (the remaining 18 did not specified the method) [876]. Nevertheless, it has been suggested that the manual ROIs definition presents poor reproducibility, which may further lead to high variability of the subsequent analysis, especially in the small ROIs definition [873,1054]. In some situations, when the predefined shapes available in some analysis tools are used [944,947,975], the difficulty to adjust them to certain edges may result either in the inclusion or the exclusion of irrelevant data, which entails an important limitation [976,977]. Although some commercial software provide bendable shapes to define regions of interest within the infrared image, they also present some limitations. Hence, when an infrared sequence is to be evaluated, the ROIs are placed in the desired positions of the initial image. However, if the evaluated object undergoes a displacement in any time within the interval, the ROIs previously positioned would remain in the same place and therefore, the measurements provided would not correspond to the areas of interest designated at first. To avoid this, the repositioning of each ROI is required, but when a huge number of images and/or ROIs are to be evaluated, a significant time-consuming task is required. Additionally, every ROI reposition would lead to different areas evaluation, resulting in low reproducibility [873].

Considering the limitations usually encountered in the manual approaches, it should be recommended moving towards more automatic approaches. In fact, the implementation of machine learning algorithms for segmentation and ROIs selection have gained interest in the past years [979]. Maldonado et al. reported good levels of detection accuracy for ulcers in foot soles using a deep learning algorithm for the feet segmentation [954]. However, they observed the inclusion of background regions due to segmentation mask errors, which resulted in inaccuracies of the temperature measurements. In a recent study, an automatic software package for automatically define ROIs on the feet soles was evaluated [880]. The authors reported a correct definition in 88.4% of the images and, moreover, the reliability between the automatic and the manual procedures was reported excellent [880]. Other authors have also observed promising results using automatic methods for ROIs selection, but visual images were required for the segmentation [992,1071]. For this reason, the use of semi-automatic tools enabling the user intervention has been considered in some situations.

In a recent study, semi-automatic tools for the foot segmentation based on both IR and RGB images (also provided from the IR camera itself) were used [984,1071]. Although the RGB images provided additional and relevant information (i.e., defined edges that would be mixed-up in IR), the main issue emerged with the misaligning of both IR and RGB images, due to the different lenses position [981,1072]. Gauci et al. proposed a set of algorithms aimed to extract thermal parameters from different ROIs in different parts of the body (hands, feet, and shin) [992]. Although the interrater reliability tests demonstrated good tolerance between the ROIs retrieved both by the algorithm and the users, the foot ROIs were found the most demanding. Still, the success rates of the foot ROIs' extraction achieved values around 75%.

Since the algorithm used in this work was based on the Gauci's, most of the limitations encountered correspond to the ones they reported. Apart from the need of visual images, on several occasions, the binary masks did not fit with the feet edges, and their reposition were required. In other occasions, the desired ROI was not detected or was wrongly placed. On the other hand, an additional limitation was observed in this study since a larger number of images were evaluated. In the work fulfilled by Gauci et al. 171 feet images were evaluated whereas in our study at least 60 images per procedure were processed (roughly 4000 images) [992]. Moreover, during the whole IR sequence either one or both feet commonly presented shifts, resulting in the ROIs misplacing. Therefore, when the reposition of the ROIs was required, the extraction process not only became very lengthy, but it also presented nonrepeatable conditions.

In summary, when it comes to the ROIs selection, a fully automatic unsupervised process may constitute a great challenge, mainly when distal parts of the body are evaluated in which overlapping temperature ranges with other different areas can occur. For this reason, although automatic approaches would entail better reliability results, a minimum user interaction was considered appropriate in order to avoid sources of failures.

Finally, when it comes to decide among the most recommendable variable to use in the clinical research assessment, no consensus has been reached yet. According to a recent review performed in 87 studies in the sports science field, more than a half studies used the mean value of the temperature pixels within the ROI, whereas the maximum and the minimum pixel temperature of the ROI was reported in 15% of studies [876]. In this work, the mean and maximum temperatures along with the standard deviation of the temperature pixels within the ROIs have been evaluated. Although in some situations such as for the detection of necrotic zones in foot soles, the minimum temperature has been reported, it was discarded in this work since it was considered not relevant for our purpose [997]. Conversely, the maximum temperature evaluation was considered of notable importance since it could provide meaningful information about the procedures' success. However, its obtention usually entails measurement errors to a certain extent. Most commercial software tools obtain the maximum temperature value within a ROI by calculating the average temperature of an area of 5 x 5 pixels situated around the 5 hottest pixels (having a minimum distance of five pixels from each other). On the other hand, the maximum temperature value can also be referred to a single pixel with the maximum temperature within the ROI. In this sense, Formenti et al. demonstrated that the results obtained with one single pixel indicator presented higher noise although the median standard deviation of the noise affecting the results retrieved by one pixel was only 15% higher, which was suggested as a fairly usable indicator [996].

Therefore, the results obtained in this work related to maximum temperatures should be read with caution since each maximum temperature value was referred to a single pixel.

7.5 Future studies

The main concern of this work is the reduced sample size, that is, the number of patients evaluated, thus with a view to performing additional studies on the matter and to confirm the results obtained so far, more LSBs interventions should be performed and evaluated with IRT.

As it has been mentioned previously, to include a control group should be of interest and accordingly, two different approaches could be conducted. On the one hand, the learning process of a pain physician starting to perform LSB procedures could provide useful information about the contribution of including the IRT in the clinical setting as a supplementary assessment technique. On the other hand, the performance of LSB procedures carried out by skilled physicians could offer the possibility of evaluating the IRT operation in the assessment of LSBs thoroughly. In any case, an IRT protocol should be developed to ensure that all the required steps would be followed by the medical team, who may be unfamiliar with the thermal equipment and its operation.

On the other hand, in the light of the results obtained in previously published works on the matter so far, no significant association between temperature alterations of the affected extremity and the pain reduction after sympathetic blocks have been found [504,1073,1074]. Although it may suggest that thermal changes in the ipsilateral would not be predictive of successful clinical outcomes, an in-depth analysis of the thermal data collected should be performed. The relationship between both the ipsilateral temperature increases and their patterns and the clinical outcomes (the concerning signs and symptoms along with the motion and pain assessment; Table 13) after the LSBs should also be evaluated. Accordingly, a comprehensive evaluation of the clinical outcomes from the patients presenting temperature increase on the contralateral should be fulfilled. In these situations, the particular thermal patterns on the patient’s contralateral foot didn’t represent isolated cases but they were usually observed in several interventions instead. Although anatomic reasons are suggested to be behind these thermal behaviours, this assumption should be tackled in detail in order to establish whether these patients undergo comparable clinical improvements or not. On the other hand, the existence of significant differences between the classification groups in terms of gender distribution or the extremity affected should also be analysed.

Furthermore, since several difficulties regarding the ROIs selection and the subsequent temperature variables extraction have been encountered, additional studies on this matter should be developed. In this sense, broader analysis based on machine learning models without the previous feature selection could provide relevant information about the thermal patterns' spatial distribution. Hence, this approach would yield more tailored results, that is, the features along with the anatomical areas which would better obtain the most appropriate predictors could be automatically selected. Accordingly, the issues regarding the ROIs selection could be overcome and consequently, the implementation of ML algorithms in the quantitative analysis of the infrared data in the assessment of LSB procedures could entail a great progress. Nevertheless, research on this matter should be extended.

CONCLUSIONS

08

Infrared thermography for the assessment of lumbar sympathetic blocks in patients with Complex Regional Pain Syndrome

8 CONCLUSIONS

These results provided further evidence that infrared thermography would entail a valuable supplementary tool in the daily clinical practice for assessing lumbar sympathetic blocks procedures in real time. Specifically, the conclusions related to the specific objectives and the hypotheses initially raised are the following:

1. Infrared thermography allowed the pain physicians to objectively distinguish whether a block was correctly performed or not through the thermal variations observed within the ipsilateral plantar foot after the lidocaine injection. Hence, when infrared images did not show temperature increases within the ipsilateral, the needle was relocated, thus preventing failed LSBs.

2. The temperature-based parameters extracted from the infrared images of each plantar foot, allowed establishing potential indicators of successful LSBs. Hence, the temperature and time thresholds obtained may be predictive of successful outcomes and consequently, may assist anaesthesiologists in their interventions' classification in real time.

3. The four machine learning models evaluated through the thermal features retrieved from the infrared data at three different moments after the lidocaine injection presented good performance metrics. Therefore, the combination of infrared features with machine learning algorithms is effective for automatically classifying the performance of LSBs.

PUBLICATIONS

Derived from the doctoral thesis:

Papers

Cañada-Soriano M, Priego-Quesada JI, Bovaira M, García-Vitoria C, Salvador Palmer R, Cibrián Ortiz de Anda R, Moratal D. Quantitative Analysis of Real-Time Infrared Thermography for the Assessment of Lumbar Sympathetic Blocks: A Preliminary Study. Sensors (Basel). 2021 May 21;21(11):3573. doi: 10.3390/s21113573. PMID: 34063768; PMCID: PMC8196638. Impact factor: 3.576. First quartile in Instruments & Instrumentation.

Cañada-Soriano M, Bovaira M, García-Vitoria C, Salvador Palmer R, Cibrián Ortiz de Anda R, Priego-Quesada JI, Moratal D. Automatic classification of lumbar sympathetic blocks performance based on machine learning and thermal images. European Radiology (under review).

Conference proceedings

Jose IgnacioPriego-Quesada, **Mar Cañada**, Maite Bovaira, Carles García-Vitoria, David Moratal, Rosario Salvador Palmer, Rosa Cibrián Ortiz de Anda. Using infrared thermography to confirm the correct placement of the needle in the performance of lumbar sympathetic blocks for complex regional pain syndrome. XV Congress Thermology international, Online 2021. Awarded “The Francis Ring prize for the best presentation”.

Cañada-Soriano M, Priego-Quesada JI, Rubio, P, Bovaira M, García-Vitoria C, Salvador Palmer R, Cibrián Ortiz de Anda R, Moratal D. Skin Temperature Assessment During Lumbar Sympathetic Blocks by Infrared Thermography. Oral presentation in 43rd Annual International Conference of the IEEE Engineering in Medicina & Biology Society (EMBC), Online 2021.

Obtained during the PhD but not directly related to the doctoral thesis:

Papers

Alvaro S. Machado; **Mar Cañada-Soriano**; Irene Jimenez-Perez; Marina Gil-Calvo; Felipe Pivetta Carpes; Pedro Pérez-Soriano; Jose Ignacio Priego Quesada. Distance and camera features measurements affect detection of temperature asymmetries using infrared thermography. Journal of Thermal Analysis and Calorimetry (submitted).

Conference proceedings

Álvaro Sosa Machado; **Mar Cañada**; Irene Jimenez-Perez; Marina Gil-Calvo; Felipe Pivetta Carpes; Pedro Perez-Soriano; Jose Ignacio Priego-Quesada. Os recursos de desempenho justo com a distancia afetam a detecçao de assimetrias de temperatura com câmeras termográficas?. XIX Congresso Brasileiro de Biomecânica, Online CBB 2021.

Cañada Soriano, Mar; Vilar-Abad, Alejandro; Aparicio Fernandez, Carolina Sabina; Ferrer-Gisbert, Pablo-S.; Vivancos, José-Luis (2021). Application Of Infrared Thermography for The Assessment Of The Overall Heat Transfer Coefficient In a Building Envelope Situated In Valencia. EN XXV International Congress on Project Management and Engineering. (1574 - 1586). Alcoi, España: AEIPRO.

Ferrer-Gisbert, Pablo-S.; Vivancos, José-Luis; **Cañada Soriano, Mar**; Val Fiel, Mónica; Vilar-Abad, Alejandro (2021). State Of the Art Of Thermal Modelling Of Buildings From Point Clouds And Infrared Thermography. EN XXV International Congress on Project Management and Engineering. (1611 - 1622). Alcoi, España: AEIPRO.

Royo, Rafael; Tormo-Esteve, Santiago; **Cañada Soriano, Mar** (2019). Inspección Termográfica del Claustro de la Catedral de Vic. Oral presentation in 14º Congreso Nacional de Ensayos No Destructivos (END 2019). Vitoria-Gasteiz, España: Asociación Española de Ensayos no Destructivos.

REFERENCES

[1] Treede R-D, Rief W, Barke A, Aziz Q, Bennett MI, Benoliel R, et al. Chronic pain as a symptom or a disease: the IASP Classification of Chronic Pain for the International Classification of Diseases (ICD-11). PAIN 2019; 160:19–27.

[2] So A, Gritsenko K. The Disease-Based Treatment of Pain. In: Deer TR, Pope JE, Lamer TJ, Provenzano D, editors. Deer's Treatment of Pain: An Illustrated Guide for Practitioners, Cham: Springer International Publishing; 2019, p. 3–12.

[3] Raja SN, Carr DB, Cohen M, Finnerup NB, Flor H, Gibson S, et al. The revised International Association for the Study of Pain definition of pain: concepts, challenges, and compromises. Pain 2020; 161:1976–82.

[4] International association for the study of pain. IASP's Proposed New Definition of Pain Released for Comment 2019.

[5] Breivik H, Collett B, Ventafridda V, Cohen R, Gallacher D. Survey of chronic pain in Europe: prevalence, impact on daily life, and treatment. European Journal of Pain (London, England) 2006;10:287–333.

[6] Mailis A, Tepperman PS, Hapidou EG. Chronic Pain: Evolution of Clinical Definitions and Implications for Practice. Psychological Injury and Law 2020; 13:412–26.

[7] Raffaeli W, Tenti M, Corraro A, Malafoglia V, Ilari S, Balzani E, et al. Chronic Pain: What Does It Mean? A Review on the Use of the Term Chronic Pain in Clinical Practice. Journal of Pain Research 2021; 14:827–35.

[8] Bonica JJ, Hoffman JF. The Management of Pain. Anesthesia & Analgesia 1954;34.

[9] Sternbach RA. Psychophysiology of Pain. The International Journal of Psychiatry in Medicine 1975; 6:63–73.

[10] Sternbach RA. Chronic pain as a disease entity. Triangle; the Sandoz Journal of Medical Science 1981; 20:27–32.

[11] Cousins MJ. Pain: the past, present, and future of anesthesiology? Anesthesiology 1999; 91:538–51.

[12] Siddall PJ, Cousins MJ. Persistent pain as a disease entity: implications for clinical management. Anesthesia and Analgesia 2004; 99:510–20, table of contents.

[13] Raffaeli W, Arnaudo E. Pain as a disease: an overview. Journal of Pain Research 2017; 10:2003–8.

[14] Harden RN, Oaklander AL, Burton AW, Perez RSGM, Richardson K, Swan M, et al. Complex regional pain syndrome: practical diagnostic and treatment guidelines, 4th edition. Pain Medicine (Malden, Mass) 2013;14:180–229.

[15] Shim H, Rose J, Halle S, Shekane P. Complex regional pain syndrome: a narrative review for the practising clinician. British Journal of Anaesthesia 2019;123:e424–33.

[16] Pare A. The collected works of Ambroise Pare. N.Y: Milford House; 1968.

[17] Denmark A. An example of symptoms resembling Tic Douloureux produced by a wound in the radial nerve. Medico-Chirurgical Transactions 1813; 4:48–52.

[18] Mitchell SW, Morehouse GR, Keen WW. Gunshot wounds and other injuries of nerves. Philadelphia: J.B. Lippincott & Co.; 1864.

[19] Sudeck P. Über die akute Knochenatrophie nach Entzündungen und Traumen der Extremitäten. Dtsch Med Wochenschr 1902; 28:336–8.

[20] Iolascon G, de Sire A, Moretti A, Gimigliano F. Complex regional pain syndrome (CRPS) type I: Historical perspective and critical issues. Clinical Cases in Mineral and Bone Metabolism 2015; 12:4–10.

[21] Todorova J, Dantchev N, Petrova G. Complex Regional Pain Syndrome Acceptance and the Alternative Denominations in the Medical Literature. Medical Principles and Practice 2013; 22:295–300.

[22] Evans JA. Reflex sympathetic dystrophy. Surg Gynecol Obstet 1946;82.

[23] Merskey H, Bogduk N. Classification of Chronic Pain: Descriptions of Chronic Pain Syndromes and Definitions of Pain Terms. vol. 11. IASP Press; 1994.

[24] Harden RN, Bruehl S, Stanton-Hicks M, Wilson PR. Proposed new diagnostic criteria for complex regional pain syndrome. Pain Medicine 2007;8:326–31.

[25] Mesaroli G, Hundert A, Birnie KA, Campbell F, Stinson J. Screening and diagnostic tools for complex regional pain syndrome: a systematic review. Pain 2021; 162:1295–304.

[26] Harden RN, Bruehl S, Perez RSGM, Birklein F, Marinus J, Maihofner C, et al. Validation of proposed diagnostic criteria (the "budapest Criteria") for Complex Regional Pain Syndrome. Pain 2010; 150:268–74.

[27] Veldman Peter HJM, Reynen Han M, Arntz Ivo E GJA. Signs and symptoms of reflex sympathetic dystrophy: prospective study of 829 patients. The Lancet 1993; 342:1012–6.

[28] Bruehl S, Harden RN, Galer BS, Saltz S, Bertram M, Backonja M, et al. External validation of IASP diagnostic criteria for Complex Regional Pain Syndrome and proposed research diagnostic criteria. Pain 1999; 81:147–54.

[29] Bruehl S, Harden RN, Galer BS, Saltz S, Backonja M, Stanton-Hicks M. Complex regional pain syndrome: Are there distinct subtypes and sequential stages of the syndrome? Pain 2002; 95:119–24.

[30] Eldufani J, Elahmer N, Blaise G. A medical mystery of complex regional pain syndrome. Heliyon 2020;6: e03329.

[31] Bruehl S, Maihöfner C, Stanton-Hicks M, Perez RSGM, Vatine JJ, Brunner F, et al. Complex regional pain syndrome: Evidence for warm and cold subtypes in a large prospective clinical sample. Pain 2016; 157:1674–81.

[32] Vaneker M, Wilder-Smith OHG, Schrombges P, de Man-Hermsen I, Oerlemans HM. Patients initially diagnosed as "warm" or "cold" CRPS 1 show differences in central sensory processing some eight years after diagnosis: A quantitative sensory testing study. Pain 2005; 115:204–11.

[33] Lawson EF, Castellanos JP. Complex regional pain syndrome: A clinical guide. Springer International Publishin; 2021.

[34] Howard BA, Roy L, Kaye AD, Pyati S. Utility of Radionuclide Bone Scintigraphy in Complex Regional Pain Syndrome. Current Pain and Headache Reports 2018; 22:261–7.

[35] Wertli MM, Brunner F, Steurer J, Held U. Usefulness of bone scintigraphy for the diagnosis of Complex Regional Pain Syndrome 1: A systematic review and Bayesian meta-analysis. PLOS ONE 2017; 12:1–18.

[36] Munts AG, van Rootselaar A-F, van der Meer JN, Koelman JHTM, van Hilten JJ, Tijssen MAJ. Clinical and neurophysiological characterization of myoclonus in complex regional pain syndrome. Movement Disorders: Official Journal of the Movement Disorder Society 2008; 23:581–7.

[37] Dietz C, Müller M, Reinhold A-K, Karch L, Schwab B, Forer L, et al. What is normal trauma healing and what is complex regional pain syndrome I? An analysis of clinical and experimental biomarkers. PAIN 2019;160.

[38] Gierthmühlen J, Maier C, Baron R, Tölle T, Treede RD, Birbaumer N, et al. Sensory signs in complex regional pain syndrome and peripheral nerve injury. Pain 2012; 153:765–74.

[39] Harden RN, Bruehl S, Perez RSGM, Birklein F, Marinus J, Maihofner C, et al. Development of a severity score for CRPS. Pain 2010; 151:870–6.

[40] Krumova EK, Frettlöh J, Klauenberg S, Richter H, Wasner G, Maier C. Long-term skin temperature measurements - A practical diagnostic tool in complex regional pain syndrome. Pain 2008; 140:8–22.

[41] Harden RN, Maihofner C, Abousaad E, Vatine JJ, Kirsling A, Perez RSGM, et al. A prospective, multisite, international validation of the Complex Regional Pain Syndrome Severity Score. Pain 2017; 158:1430–6.

[42] Russo M, Georgius P, Santarelli DM. A new hypothesis for the pathophysiology of complex regional pain syndrome. Medical Hypotheses 2018; 119:41–53.

[43] Money S. Pathophysiology of Complex Regional Pain Syndrome and Treatment: Recent Advancements. Current Emergency and Hospital Medicine Reports 2019;7:203–7.

[44] Chakraborty R, Burns B. Systemic Inflammatory Response Syndrome. StatPearls [Internet] 2021. https://www.ncbi.nlm.nih.gov/books/NBK547669/#_NBK547669_pubdet_.

[45] Lord JM, Midwinter MJ, Chen Y-F, Belli A, Brohi K, Kovacs EJ, et al. The systemic immune response to trauma: an overview of pathophysiology and treatment. Lancet (London, England) 2014;384:1455–65.

[46] Kortekaas MC, Niehof SP, Stolker RJ, Huygen FJPM. Pathophysiological Mechanisms Involved in Vasomotor Disturbances in Complex Regional Pain Syndrome and Implications for Therapy: A Review. Pain Practice 2016; 16:905–14.

[47] Birklen F, Dimova V. Complex regional pain syndrome up-to-date. Pain Reports 2017; 624:1–8.

[48] Marinus J, Moseley GL, Birklein F, Baron R, Maihöfner C, Kingery WS, et al. Clinical features and pathophysiology of complex regional pain syndrome. The Lancet Neurology 2011; 10:637–48.

[49] Gallagher JJ, Tajerian M, Guo T, Shi X, Li W, Zheng M, et al. Acute and chronic phases of complex regional pain syndrome in mice are accompanied by distinct transcriptional changes in the spinal cord. Molecular Pain 2013; 9:40.

[50] Bharwani KD, Dik WA, Dirckx M, Huygen FJPM. Highlighting the Role of Biomarkers of Inflammation in the Diagnosis and Management of Complex Regional Pain Syndrome. Molecular Diagnosis & Therapy 2019; 23:615–26.

[51] Parkitny L, McAuley JH, di Pietro F, Stanton TR, O'Connell NE, Marinus J, et al. Inflammation in complex regional pain syndrome: a systematic review and meta-analysis. Neurology 2013; 80:106–17.

[52] Knudsen LF, Terkelsen AJ, Drummond PD, Birklein F. Complex regional pain syndrome: a focus on the autonomic nervous system. Clinical Autonomic Research 2019; 29:457–67.

[53] Loeser JD, Treede R-D. The Kyoto protocol of IASP Basic Pain Terminology. PAIN® 2008;137:473–7.

[54] Viana F. Nociceptors: thermal allodynia and thermal pain. In: Romanovsky AABT-H of CN, editor. Thermoregulation: From Basic Neuroscience to Clinical Neurology Part I, vol. 156, Elsevier; 2018, p. 103–19.

[55] Cervero F, Laird JMA. Mechanisms of touch-evoked pain (allodynia): a new model. PAIN 1996;68.

[56] Birklein F, Schmelz M. Neuropeptides, neurogenic inflammation and complex regional pain syndrome (CRPS). Neuroscience Letters 2008;437:199–202.

[57] Stanton-Hicks M. Complex Regional Pain Syndrome. In: Cheng J, Rosenquist RW, editors. Fundamentals of Pain Medicine, Cham: Springer International Publishing; 2018, p. 211–20.

[58] Maihöfner C, Baron R, DeCol R, Binder A, Birklen F, Deuschl G, et al. The motor system shows adaptive changes in complex regional pain syndrome. Brain 2007;130:2671–87.

[59] Krause P, Förderreuther S, Straube A. TMS motor cortical brain mapping in patients with complex regional pain syndrome type I. Clinical Neurophysiology : Official Journal of the International Federation of Clinical Neurophysiology 2006;117:169–76.

[60] Mancini F, Wang AP, Schira MM, Isherwood ZJ, McAuley JH, Iannetti GD, et al. Fine-Grained Mapping of Cortical Somatotopies in Chronic Complex Regional Pain Syndrome. The Journal of Neuroscience 2019;39:9185 LP – 9196.

[61] Lee B, Henderson LA, Rae CD, di Pietro F. CRPS Is Not Associated with Altered Sensorimotor Cortex GABA or Glutamate. ENeuro 2020;7:ENEURO.0389-19.2020.

[62] Lewis JS, Kersten P, McPherson KM, Taylor GJ, Harris N, McCabe CS, et al. Wherever is my arm? Impaired upper limb position accuracy in complex regional pain syndrome. Pain 2010;149:463–9.

[63] Brun C, Giorgi N, Pinard AM, Gagné M, McCabe CS, Mercier C. Exploring the Relationships Between Altered Body Perception, Limb Position Sense, and Limb Movement Sense in Complex Regional Pain Syndrome. Journal of Pain 2019;20:17–27.

[64] Lewis JS, Kersten P, McCabe CS, McPherson KM, Blake DR. Body perception disturbance: A contribution to pain in complex regional pain syndrome (CRPS). Pain 2007;133:111–9.

[65] Chang C, Mcdonnell P, Gershwin ME. Complex regional pain syndrome – Autoimmune or functional neurologic syndrome. Journal of Translational Autoimmunity 2021;4:100080.

[66] Clark JD, Tawfik VL, Tajerian M, Kingery WS. Autoinflammatory and autoimmune contributions to complex regional pain syndrome. Molecular Pain 2018;14:1–13.

[67] de Rooij AM, de Mos M, van Hilten JJ, Sturkenboom MCJM, Gosso MF, van den Maagdenberg AMJM, et al. Increased Risk of Complex Regional Pain Syndrome in Siblings of Patients? Journal of Pain 2009;10:1250–5.

[68] Jin E-H, Zhang E, Ko Y, Sim WS, Moon DE, Yoon KJ, et al. Genome-Wide Expression Profiling of Complex Regional Pain Syndrome. PLOS ONE 2013;8:e79435.

[69] Elramah S, Landry M, Favereaux A. MicroRNAs regulate neuronal plasticity and are involved in pain mechanisms. Frontiers in Cellular Neuroscience 2014;8:31.

[70] Dai Z, Chu H, Ma J, Yan Y, Zhang X, Liang Y. The Regulatory Mechanisms and Therapeutic Potential of MicroRNAs: From Chronic Pain to Morphine Tolerance. Frontiers in Molecular Neuroscience 2018;11:80.

[71] Xourgia E, Papazafiropoulou A, Melidonis A. Circulating microRNAs as biomarkers for diabetic neuropathy: A novel approach. World Journal of Experimental Medicine 2018;8:18–23.

[72] López-González MJ, Landry M, Favereaux A. MicroRNA and chronic pain: From mechanisms to therapeutic potential. Pharmacology & Therapeutics 2017;180:1–15.

[73] Dilek B, Yemez B, Kizil R, Kartal E, Gulbahar S, Sari O, et al. Anxious personality is a risk factor for developing complex regional pain syndrome type I. Rheumatology International 2012;32:915–20.

[74] Farzad M, Layeghi F, Hosseini A, Dianat A, Ahrari N, Rassafiani M, et al. Investigate the Effect of Psychological Factors in Development of Complex Regional Pain Syndrome Type I in Patients with Fracture of the Distal Radius: A Prospective Study. The Journal of Hand Surgery (Asian-Pacific Volume) 2018;23:554–61.

[75] Lee D-H, Noh EC, Kim YC, Hwang JY, Kim SN, Jang JH, et al. Risk Factors for Suicidal Ideation among Patients with Complex Regional Pain Syndrome. Psychiatry Investigation 2014;11:32–8.

[76] Goebel A, Barker C, Birklein | Frank, Brunner F, Casale R, Perez | R, et al. Standards for the diagnosis and management of complex regional pain syndrome: Results of a European Pain Federation task force. European Journal of Pain 2019;23:641–51.

[77] Ott S, Maihöfner C. Signs and Symptoms in 1,043 Patients with Complex Regional Pain Syndrome. Journal of Pain 2018;19:599–611.

[78] Kim H, Lee C-H, Kim S-H, Kim Y-D. Epidemiology of complex regional pain syndrome in Korea: An electronic population health data study. PLOS ONE 2018;13:e0198147.

[79] de Mos M, de Bruijn AGJ, Huygen FJPM, Dieleman JP, Stricker BHC, Sturkenboom MCJM. The incidence of complex regional pain syndrome: A population-based study. Pain 2007;129:12–20.

[80] Sandroni P, Benrud-Larson LM, McClelland RL, Low PA. Complex regional pain syndrome type I: incidence and prevalence in Olmsted county, a population-based study. Pain 2003;103:199–207.

[81] Groenveld TD, Boersma EZ, Blokhuis TJ, Bloemers FW, Frölke JPM. Decreasing incidence of complex regional pain syndrome in the Netherlands: a retrospective multicenter study. British Journal of Pain 2021:20494637211041936.

[82] Jo YH, Kim KW, Lee BG, Kim JH, Lee CH, Lee KH. Incidence of and Risk Factors for Complex Regional Pain Syndrome Type 1 after Surgery for Distal Radius Fractures: A Population-based Study. Scientific Reports 2019;9:1–7.

[83] Rolls C, McCabe C, Llewellyn A, Jones G. What is the incidence of complex regional pain syndrome (CRPS) Type I within four months of a wrist fracture in the adult population? A systematic review. Hand Therapy 2020;25:175899832091017.

[84] Malinowski MN. Mediators of Pain and Pain Processing. In: Deer TR, Pope JE, Lamer TJ, Provenzano D, editors. Deer's Treatment of Pain: An Illustrated Guide for Practitioners, Cham: Springer International Publishing; 2019, p. 61–73.

[85] Yam MF, Loh YC, Tan CS, Khadijah Adam S, Abdul Manan N, Basir R. General Pathways of Pain Sensation and the Major Neurotransmitters Involved in Pain Regulation. International Journal of Molecular Sciences 2018;19.

[86] Lee GI, Neumeister MW. Pain: Pathways and Physiology. Clinics in Plastic Surgery 2020; 47:173–80.

[87] Baron R, Schattschneider J, Binder A, Siebrecht D, Wasner G. Relation between sympathetic vasoconstrictor activity and pain and hyperalgesia in complex regional pain syndromes: A case-control study. Lancet 2002; 359:1655–60.

[88] Ringkamp M, Dougherty PM, Raja SN. Anatomy and Physiology of the Pain Signaling Process. Essentials of Pain Medicine, Elsevier; 2018, p. 3-10. e1.

[89] Frampton CL, Hughes-Webb P. The measurement of pain. Clinical Oncology (Royal College of Radiologists (Great Britain)) 2011; 23:381–6.

[90] Ferreira-Valente MA, Pais-Ribeiro JL, Jensen MP. Validity of four pain intensity rating scales. Pain 2011;152:2399–404.

[91] Scott J, Huskisson EC. Graphic representation of pain. Pain 1976;2:175–84.

[92] Carlsson AM. Assessment of chronic pain. I. Aspects of the reliability and validity of the visual analogue scale. Pain 1983;16:87–101.

[93] Flanagan JC. Measurement of quality of life: current state of the art. Archives of Physical Medicine and Rehabilitation 1982;63:56–9.

[94] Flanagan JC. A research approach to improving our quality of life. American Psychologist 1978;33:138–47.

[95] Perez C, Galvez R, Huelbes S, Insausti J, Bouhassira D, Diaz S, et al. Validity and reliability of the Spanish version of the DN4 (Douleur Neuropathique 4 questions) questionnaire for differential diagnosis of pain syndromes associated to a neuropathic or somatic component. Health and Quality of Life Outcomes 2007; 5:66.

[96] Likert R. A technique for the measurement of attitudes. Archives of Psychology 1932;22 140:55.

[97] Goebel A, Barker C, Turner-Stokes L, Al E. Complex regional pain syndrome in adults: UK guidelines for diagnosis, referral and management in primary and secondary care. London: RCP; 2018.

[98] Pons T, Shipton EA, Williman J, Mulder RT. A proposed clinical conceptual model for the physiotherapy management of Complex Regional Pain Syndrome (CRPS). Musculoskeletal Science and Practice 2018; 38:15–22.

[99] Perez RSGM, Zollinger PE, Dijkstra PU, Thomassen-Hilgersom IL, Zuurmond WWA, Rosenbrand CJGM, et al. Clinical practice guideline “Complex regional pain syndrome type I”. Nederlands tijdschrift voor geneeskunde 2007; 151:1674–9.

[100] Urits I, Shen AH, Jones MR, Viswanath O, Kaye AD. Complex Regional Pain Syndrome, Current Concepts and Treatment Options. Current Pain and Headache Reports 2018;22.

[101] Hudson J, Lake E, Spruit E, Terrell M, Cooper K, McFawn C, et al. Comprehensive Rehabilitation of Patients with Complex Regional Pain Syndrome. In: Lawson EF, Castellanos JP, editors. Complex Regional Pain Syndrome: A Clinical Guide, Cham: Springer International Publishing; 2021, p. 107–48.

[102] Smart K, O’Connel N. Physiotherapy for pain and disability in adults with complex regional pain syndrome (CRPS) types I and II. Cochrane Database of Systematic Reviews 2016;2.

[103] Moseley GL. Graded motor imagery for pathologic pain: a randomized controlled trial. Neurology 2006; 67:2129–34.

[104] Moseley GL. Graded motor imagery is effective for long-standing complex regional pain syndrome: a randomised controlled trial. Pain 2004; 108:192–8.

[105] Pervane Vural S, Nakipoglu Yuzer GF, Sezgin Ozcan D, Demir Ozbudak S, Ozgirgin N. Effects of Mirror Therapy in Stroke Patients With Complex Regional Pain Syndrome Type 1: A Randomized Controlled Study. Archives of Physical Medicine and Rehabilitation 2016; 97:575–81.

[106] Sayegh S al, Filén T, Johansson M, Sandström S, Stiewe G, Butler S. Mirror therapy for Complex Regional Pain Syndrome (CRPSI): A literature review and an illustrative case report. Scandinavian Journal of Pain 2013; 4:200–7.

[107] Cacchio A, de Blasis E, de Blasis V, Santilli V, Spacca G. Mirror therapy in complex regional pain syndrome type 1 of the upper limb in stroke patients. Neurorehabilitation and Neural Repair 2009;23:792–9..

[108] Yang Y, Zhao Q, Zhang Y, Wu Q, Jiang X, Cheng G. Effect of Mirror Therapy on Recovery of Stroke Survivors: A Systematic Review and Network Meta-analysis. Neuroscience 2018;390:318–36..

[109] Turk DC, Fillingim RB, Ohrbach R, Patel K v. Assessment of Psychosocial and Functional Impact of Chronic Pain. The Journal of Pain 2016;17:T21-49.

[110] Louw A, Zimney K, Cox T, O’Hotto C, Wassinger CA. The experiences and beliefs of patients with complex regional pain syndrome: An exploratory survey study. Chronic Illness 2018;14:104–18.

[111] Richardson PA, Poupore-King H, Griffin A, Cooley C, Bhandari RP. Behavioral Health Interventions for CRPS. In: Lawson EF, Castellanos JP, editors. Complex Regional Pain Syndrome: A Clinical Guide, Cham: Springer International Publishing; 2021, p. 79–105.

[112] Shin C, Cheng J. Interventional Treatment of Complex Regional Pain Syndrome. In: Lawson EF, Castellanos JP, editors. Complex Regional Pain Syndrome: A Clinical Guide, Cham: Springer International Publishing; 2021, p. 179–206.

[113] Patel T. Pharmacologic Treatments for CRPS. In: Lawson EF, Castellanos JP, editors. Complex Regional Pain Syndrome: A Clinical Guide, Cham: Springer International Publishing; 2021, p. 65–78.

[114] Chang C, McDonnell P, Gershwin ME. Complex regional pain syndrome – False hopes and miscommunications. Autoimmunity Reviews 2019; 18:270–8.

[115] Iolascon G, Moretti A. Pharmacotherapeutic options for complex regional pain syndrome. Expert Opinion on Pharmacotherapy 2019; 20:1377–86.

[116] Eun Young H, Hyeyun K, Sang Hee I. Pamidronate effect compared with a steroid on complex regional pain syndrome type I: Pilot randomised trial. The Netherlands Journal of Medicine 2016; 74:30–5.

[117] Kalita J, Misra U, Kumar A, Bhoi SK. Long-term Prednisolone in Post-stroke Complex Regional Pain Syndrome. Pain Physician 2016; 19:565–74.

[118] Breuer AJ, Mainka T, Hansel N, Maier C, Krumova EK. Short-term treatment with parecoxib for complex regional pain syndrome: a randomized, placebo-controlled double-blind trial. Pain Physician 2014; 17:127–37.

[119] Wiffen PJ, Derry S, Bell RF, Rice AS, Tölle TR, Phillips T, et al. Gabapentin for chronic neuropathic pain in adults. The Cochrane Database of Systematic Reviews 2017;6:CD007938.

[120] Derry S, Bell RF, Straube S, Wiffen PJ, Aldington D, Moore RA. Pregabalin for neuropathic pain in adults. The Cochrane Database of Systematic Reviews 2019;1:CD007076.

[121] Tan AK, Duman I, Taşkaynatan MA, Hazneci B, Kalyon TA. The effect of gabapentin in earlier stage of reflex sympathetic dystrophy. Clinical Rheumatology 2007; 26:561–5. https://doi.org/10.1007/s10067-006-0350-y.

[122] Brown S, Johnston B, Amaria K, Watkins J, Campbell F, Pehora C, et al. A randomized controlled trial of amitriptyline versus gabapentin for complex regional pain syndrome type I and neuropathic pain in children. Scandinavian Journal of Pain 2016; 13:156–63.

[123] Chevreau M, Romand X, Gaudin P, Juvin R, Baillet A. Bisphosphonates for treatment of Complex Regional Pain Syndrome type 1: A systematic literature review and meta-analysis of randomized controlled trials versus placebo. Joint Bone Spine 2017; 84:393–9.

[124] Varenna M, Crotti C. Bisphosphonates in the treatment of complex regional pain syndrome: is bone the main player at early stage of the disease? Rheumatology International 2018; 38:1959–62.

[125] O'Connell NE, Wand BM, Mcauley J, Marston L, Moseley GL. Interventions for treating pain and disability in adults with complex regional pain syndrome- an overview of systematic reviews. Cochrane Database of Systematic Reviews 2013;2013.

[126] Yang Y, Maher DP, Cohen SP. Emerging concepts on the use of ketamine for chronic pain. Expert Review of Clinical Pharmacology 2020; 13:135–46.

[127] Zhao J, Wang Y, Wang D. The Effect of Ketamine Infusion in the Treatment of Complex Regional Pain Syndrome: a Systemic Review and Meta-analysis. Current Pain and Headache Reports 2018; 22:12.

[128] Schwartzman RJ, Alexander GM, Grothusen JR. The use of ketamine in complex regional pain syndrome: possible mechanisms. Expert Review of Neurotherapeutics 2011; 11:719–34. https://doi.org/10.1586/ern.11.31.

[129] Connolly SB, Prager JP, Harden RN. A Systematic Review of Ketamine for Complex Regional Pain Syndrome. Pain Medicine 2015; 16:943–69.

[130] Jacques H, Jérôme V, Antoine C, Lucile S, Valérie D, Amandine L, et al. Prospective randomized study of the vitamin C effect on pain and complex pain regional syndrome after total knee arthroplasty. International Orthopaedics 2021; 45:1155–62.

[131] Laumonerie P, Martel M, Tibbo ME, Azoulay V, Mansat P, Bonnevialle N. Influence of vitamin C on the incidence of CRPS-I after subacromial shoulder surgery. European Journal of Orthopaedic Surgery & Traumatology : Orthopedie Traumatologie 2020;30:221–6.

[132] Aïm F, Klouche S, Frison A, Bauer T, Hardy P. Efficacy of vitamin C in preventing complex regional pain syndrome after wrist fracture: A systematic review and meta-analysis. Orthopaedics & Traumatology, Surgery & Research: OTSR 2017;103:465–70.

[133] Bellon G, Venturin A, Masiero S, del Felice A. Intra-articular botulinum toxin injection in complex regional pain syndrome: Case report and review of the literature. Toxicon: Official Journal of the International Society on Toxinology 2019;159:41–4.

[134] Siongco PRL, Rosales RL, Moore AP, Freynhagen R, Arimura K, Kanovsky P, et al. Botulinum neurotoxin injections for muscle-based (dystonia and spasticity) and non-muscle-based (neuropathic pain) pain disorders: a meta-analytic study. Journal of Neural Transmission 2020;127:935–51.

[135] Lessard L, Bartow MJ, Lee J, Diaz-Abel J, Tessler OES. Botulinum Toxin A: A Novel Therapeutic Modality for Upper Extremity Chronic Regional Pain Syndrome. Plastic and Reconstructive Surgery – Global Open 2018;6.

[136] Trofimovitch D, Baumrucker SJ. Pharmacology Update: Low-Dose Naltrexone as a Possible Nonopioid Modality for Some Chronic, Nonmalignant Pain Syndromes. The American Journal of Hospice & Palliative Care 2019;36:907–12.

[137] Younger J, Parkitny L, McLain D. The use of low-dose naltrexone (LDN) as a novel anti-inflammatory treatment for chronic pain. Clinical Rheumatology 2014;33:451–9.

[138] Aradillas E, Schwartzman RJ, Grothusen JR, Goebel A, Alexander GM. Plasma Exchange Therapy in Patients with Complex Regional Pain Syndrome. Pain Physician 2015;18:383–94.

[139] Benzon HT, Liu SS, Buvanendran A. Evolving Definitions and Pharmacologic Management of Complex Regional Pain Syndrome. Anesthesia and Analgesia 2016;122:601–4.

[140] Xu J, Yang J, Lin P, Rosenquist E, Cheng J. Intravenous Therapies for Complex Regional Pain Syndrome: A Systematic Review. Anesthesia and Analgesia 2016;122:843–56.

[141] Xu J, Herndon C, Anderson S, Getson P, Foorsov V, Harbut RE, et al. Intravenous Ketamine Infusion for Complex Regional Pain Syndrome: Survey, Consensus, and a Reference Protocol. Pain Medicine (Malden, Mass) 2019;20:323–34.

[142] Kim YH, Kim SY, Lee YJ, Kim ED. A Prospective, Randomized Cross-Over Trial of T2 Paravertebral Block as a Sympathetic Block in Complex Regional Pain Syndrome. Pain Physician 2019;22:E417–24.

[143] Nayak R, Banik RK. Current Innovations in Peripheral Nerve Stimulation. Pain Research and Treatment 2018;2018:9091216.

[144] Xu J, Liu A, Cheng J. New advancements in spinal cord stimulation for chronic pain management. Current Opinion in Anaesthesiology 2017;30:710–7.

[145] Ayyaswamy B, Shetty V. Quality of life after amputation in patients with advanced complex regional pain syndrome: a systematic review. General Orthopaedics 2019;4.

[146] Ackerman WE, Zhang JM. Efficacy of stellate ganglion blockade for the management of type 1 complex regional pain syndrome. Southern Medical Journal 2006;99:1084–8.

[147] Gunduz OH, Kenis-Coskun O. Ganglion blocks as a treatment of pain: Current perspectives. Journal of Pain Research 2017;10:2815–26.

[148] Imani F, Hemati K, Rahimzadeh P, Kazemi MR, Hejazian K. Effectiveness of Stellate Ganglion Block Under Fuoroscopy or Ultrasound Guidance in Upper Extremity CRPS. Journal of Clinical and Diagnostic Research : JCDR 2016;10:UC09-12.

[149] Qian S, Sengupta V, Urbiztondo N, Haider N. Lumbar Sympathetic Block. In: Deer TR, Pope JE, Lamer TJ, Provenzano D, editors. Deer's Treatment of Pain: An Illustrated Guide for Practitioners, Cham: Springer International Publishing; 2019, p. 467–75.

[150] Day M. Sympathetic Blocks: The Evidence. Pain Practice 2008;8:98–109.

[151] O'Connell NE, Wand BM, Gibson W, Carr DB, Birklein F, Stanton TR. Local anaesthetic sympathetic blockade for complex regional pain syndrome. The Cochrane Database of Systematic Reviews 2016;7:1–54.

[152] Zhu X, Kohan LR, Morris JD, Hamill-Ruth RJ. Sympathetic blocks for complex regional pain syndrome: A survey of pain physicians. Regional Anesthesia and Pain Medicine 2019;44:736–41.

[153] Stanton-Hicks M. Complex regional pain syndrome: manifestations and the role of neurostimulation in its management. Journal of Pain and Symptom Management 2006;31:S20-4.

[154] Yu K, Niu X, He B. Neuromodulation Management of Chronic Neuropathic Pain in the Central Nervous System. Advanced Functional Materials 2020;30:1908999.

[155] Chmiela MA, Hendrickson M, Hale J, Liang C, Telefus P, Sagir A, et al. Direct Peripheral Nerve Stimulation for the Treatment of Complex Regional Pain Syndrome: A 30-Year Review. Neuromodulation: Technology at the Neural Interface 2021;24:971–82.

[156] Herschkowitz D, Kubias J. Wireless peripheral nerve stimulation for complex regional pain syndrome type I of the upper extremity: a case illustration introducing a novel technology. Scandinavian Journal of Pain 2018;18:555–60.

[157] Herschkowitz D, Kubias J. A case report of wireless peripheral nerve stimulation for complex regional pain syndrome type-I of the upper extremity: 1 year follow up. Scandinavian Journal of Pain 2019;19:829–35.

[158] Piedade GS, Vesper J, Chatzikalfas A, Slotty PJ. Cervical and High-Thoracic Dorsal Root Ganglion Stimulation in Chronic Neuropathic Pain. Neuromodulation: Technology at the Neural Interface 2019;22:951–5.

[159] van Buyten J-P, Smet I, Liem L, Russo M, Huygen F. Stimulation of dorsal root ganglia for the management of complex regional pain syndrome: a prospective case series. Pain Practice: The Official Journal of World Institute of Pain 2015;15:208–16.

[160] Gill JS, Asgerally A, Simopoulos TT. High-Frequency Spinal Cord Stimulation at 10 kHz for the Treatment of Complex Regional Pain Syndrome: A Case Series of Patients With or Without Previous Spinal Cord Stimulator Implantation. Pain Practice: The Official Journal of World Institute of Pain 2019;19:289–94.

[161] Verrills P, Sinclair C, Barnard A. A review of spinal cord stimulation systems for chronic pain. Journal of Pain Research 2016;9:481–92.

[162] Visnjevac O, Costandi S, Patel BA, Azer G, Agarwal P, Bolash R, et al. A Comprehensive Outcome-Specific Review of the Use of Spinal Cord Stimulation for Complex Regional Pain Syndrome. Pain Practice 2017;17:533–45.

[163] van Bussel CM, Stronks DL, Huygen FJPM. Dorsal Column Stimulation vs. Dorsal Root Ganglion Stimulation for Complex Regional Pain Syndrome Confined to the Knee: Patients' Preference Following the Trial Period. Pain Practice 2018;18:87–93.

[164] Sivanesan E, Bicket MC, Cohen SP. Retrospective analysis of complications associated with dorsal root ganglion stimulation for pain relief in the FDA MAUDE database. Regional Anesthesia & Pain Medicine 2019;44:100–6.

[165] Deer TR, Levy RM, Kramer J, Poree L, Amirdelfan K, Grigsby E, et al. Dorsal root ganglion stimulation yielded higher treatment success rate for complex regional pain syndrome and causalgia at 3 and 12 months: a randomized comparative trial. Pain 2017;158:669–81.

[166] Levy RM, Mekhail N, Kramer J, Poree L, Amirdelfan K, Grigsby E, et al. Therapy Habituation at 12 Months: Spinal Cord Stimulation Versus Dorsal Root Ganglion Stimulation for Complex Regional Pain Syndrome Type I and II. The Journal of Pain 2020;21:399–408.

[167] Sdrulla AD, Guan Y, Raja SN. Spinal Cord Stimulation: Clinical Efficacy and Potential Mechanisms. Pain Practice: The Official Journal of World Institute of Pain 2018;18:1048–67.

[168] Russo M, Brooker C, Cousins MJ, Taylor N, Boesel T, Sullivan R, et al. Sustained Long-Term Outcomes With Closed-Loop Spinal Cord Stimulation: 12-Month Results of the Prospective, Multicenter, Open-Label Avalon Study. Neurosurgery 2020;87:E485–95.

[169] Farrell SM, Green A, Aziz T. The Current State of Deep Brain Stimulation for Chronic Pain and Its Context in Other Forms of Neuromodulation. Brain Sciences 2018;8.

[170] O'Connell NE, Marston L, Spencer S, DeSouza LH, Wand BM. Non-invasive brain stimulation techniques for chronic pain. The Cochrane Database of Systematic Reviews 2018.

[171] Su P-YP, Sharma S, Shirvalkar P, Poree L. Emerging Therapies for the Treatment of Complex Regional Pain Syndrome. In: Lawson EF, Castellanos JP, editors. Complex Regional Pain Syndrome: A Clinical Guide, Cham: Springer International Publishing; 2021, p. 213–27.

[172] Bodde MI, Dijkstra PU, den Dunnen WFA, Geertzen JHB, Pieter U, Dunnen D, et al. Therapy-Resistant Complex Regional Pain Syndrome Type I: To Amputate or Not? The Journal of Bone and Joint Surgery 2011;93:1799–805..

[173] Midbari A, Suzan E, Adler T, Melamed E, Norman D, Vulfsons S, et al. Amputation in patients with complex regional pain syndrome. The Bone & Joint Journal 2016;98-B:548–54.

[174] Wilson PR. Complex Regional Pain Syndrome: What Is the Evidence? Pain Medicine 2017;18:804–6.

[175] Borchers AT, Gershwin ME. The clinical relevance of complex regional pain syndrome type I: The Emperor's New Clothes. Autoimmunity Reviews 2017;16:22–33.

[176] Goebel A, Birklein F, Brunner F, Clark JD, Gierthmühlen J, Harden N, et al. The Valencia consensus-based adaptation of the IASP complex regional pain syndrome diagnostic criteria. Pain 2021;162:2346–8.

[177] Korwisi B, Barke A, Treede R-D. Evidence- and consensus-based adaption of the IASP complex regional pain syndrome diagnostic criteria to the ICD-11 category of chronic primary pain: a successful cooperation of the IASP with the World Health Organization. Pain 2021;162:2313–4.

[178] Henderson J. Updated guidelines on complex regional pain syndrome in adults. Journal of Plastic, Reconstructive & Aesthetic Surgery : JPRAS 2019;72:1–3.

[179] Oh S, Choi S, Park M, Shin J. Validity of the Budapest Criteria For Poststroke Complex Regional Pain Syndrome. Clinical Journal of Pain 2019;35:831–5.

[180] Zeiderman MR, Pereira CT. Reply to: "Updated guidelines on complex regional pain syndrome in adults". Journal of Plastic, Reconstructive & Aesthetic Surgery: JPRAS 2019;72:335–54.

[181] Kaur H, Muhleman M, Balon HR. Complex Regional Pain Syndrome Diagnosed with Triple-Phase Bone Scanning. Journal of Nuclear Medicine Technology 2017;45:243–4.

[182] Packham T, MacDermid J, Bain J, Buckley N. Identification of complex regional pain syndrome in the upper limb: Skin temperature asymmetry after cold pressor test. Canadian Journal of Pain 2018;2:248–57.

[183] Grieve S, Jones L, Walsh N, McCabe C. What outcome measures are commonly used for Complex Regional Pain Syndrome clinical trials? A systematic review of the literature. European Journal of Pain (London, England) 2016;20:331–40.

[184] Bijl EJ, Groeneweg JG, Wesselius DW, Stronks DL, Huygen FJPM. Diagnosing complex regional pain syndrome using an electronic nose, a pilot study. Journal of Breath Research 2019;13:36004.

[185] Agten CA, Kobe A, Barnaure I, Galley J, Pfirrmann CW, Brunner F. MRI of complex regional pain syndrome in the foot. European Journal of Radiology 2020;129:109044.

[186] Möller I, Szkudlarek M. Imaging of regional pain syndromes; from syndromes to conditions using imaging? Best Practice & Research Clinical Rheumatology 2016;30:707–19.

[187] Sivanesan E, Goebel A. Complex regional pain syndrome: developing diagnostic tools and treatments from sympathetic nervous system, neuroimmune and neuromodulation discoveries in neuropathic pain. Regional Anesthesia and Pain Medicine 2021;46:193–5.

[188] NCPD Tests: Complex Regional Pain Syndrome: The Importance of Early Diagnosis. Orthopaedic Nursing 2021;40.

[189] Cheon M, Kang HJ, Do KH, Yang HS, Han EJ, Yoo J. Diagnostic Performance of Three-Phase Bone Scintigraphy and Digital Infrared Thermography Imaging for Chronic Post-Traumatic Complex Regional Pain Syndrome. Diagnostics 2021;11.

[190] Dhatt S, Krauss EM, Winston P. The Role of FLIR ONE Thermography in Complex Regional Pain Syndrome: A Case Series. American Journal of Physical Medicine & Rehabilitation 2021;100.

[191] Pérez-Concha T, Tijero B, Acera M, Fernández T, Gabilondo I, Gómez-Esteban JC. Usefulness of thermography in the diagnosis and classification of complex regional pain syndrome. Neurología 2020:8.

[192] Jang SH, Kwon YH, Lee SJ. Central Pain Due to Injury of the Spinothalamic Tract Misdiagnosed as Complex Regional Pain Syndrome: A Case Report. Diagnostics 2019;9.

[193] Lunden LK, Kleggetveit IP, Jørum E. Delayed diagnosis and worsening of pain following orthopedic surgery in patients with complex regional pain syndrome (CRPS). Scandinavian Journal of Pain 2016;11:27–33.

[194] Varenna M, Crotti C, Ughi N, Zucchi F, Caporali R. Determinants of Diagnostic Delay in Complex Regional Pain Syndrome Type 1: An Observational Study of 180 Consecutive New Cases. Journal of Clinical Rheumatology: Practical Reports on Rheumatic & Musculoskeletal Diseases 2020.

[195] Michal M, Adler J, Reiner I, Wermke A, Ackermann T, Schlereth T, et al. Association of Neglect-Like Symptoms with Anxiety, Somatization, and Depersonalization in Complex Regional Pain Syndrome. Pain Medicine 2017;18:764–72.

[196] Choi J-W, Na S-Y. Image Gallery: Complex regional pain syndrome with changes in the nail unit. British Journal of Dermatology 2017;176:e121–e121.

[197] Lee WJ, Choi S-H, Jang JH, Moon JY, Kim YC, Noh E, et al. Different patterns in mental rotation of facial expressions in complex regional pain syndrome patients. Medicine 2017;96:e7990.

[198] Azqueta-Gavaldon M, Schulte-Göcking H, Storz C, Azad S, Reiners A, Borsook D, et al. Basal ganglia dysfunction in complex regional pain syndrome - A valid hypothesis? European Journal of Pain (London, England) 2017;21:415–24.

[199] Schuhfried O, Herceg M, Reichel-Vacariu G, Paternostro-Sluga T. Infrared Thermographic Pattern of Lower Limb Complex Regional Pain Syndrome (Type I) and its Correlation with Pain, Disease Duration and Clinical Signs TT - Das infrarot-thermografische Muster beim Komplexen Regionalen Schmerzsyndrom Typ I der unteren Ex. Physikalische Medizin, Rehabilitationsmedizin, Kurortmedizin 2016;26:288–92.

[200] Kuttikat A, Shaikh M, Oomatia A, Parker R, Shenker N. Novel Signs and Their Clinical Utility in Diagnosing Complex Regional Pain Syndrome (CRPS): A Prospective Observational Cohort Study. The Clinical Journal of Pain 2017;33:496–502.

[201] Woldeamanuel YW, Cooley C, Foley-Saldena K, Cowan RP. Migraine and Complex Regional Pain Syndrome: A Case-Referent Clinical Study. BioMed Research International 2017;2017:5714673.

[202] Christophe L, Delporte L, Revol P, DePaepe A, Rode G, Jacquin-Courtois S, et al. Complex regional pain syndrome associated with hyperattention rather than neglect for the healthy side: A comprehensive case study. Annals of Physical and Rehabilitation Medicine 2016;59:294–301.

[203] Wang R, Lefevre R. Management of Urinary and Fecal Incontinence in Patients With Complex Regional Pain Syndrome. Female Pelvic Medicine & Reconstructive Surgery 2016;22:e14-6.

[204] Reynolds M, Francis H. Vascular Changes of Complex Regional Pain Syndrome Unmask Buerger's Disease (Thromboangiitis Obliterans): A Letter to the Editor. Pain Medicine 2018;19:1880–1.

[205] Laroche M. Focus on the bone in complex regional pain syndrome type I. Joint Bone Spine 2016;83:731.

[206] Oehler N, Rolvien T, Schmidt T, Butscheidt S, Oheim R, Barvencik F, et al. Bone microstructure is significantly altered in CRPS-affected distal tibiae as detected by HR-pQCT: a retrospective cross-sectional study. Journal of Bone and Mineral Metabolism 2019;37:741–8.

[207] Bazika-Gerasch B, Maier C, Kumowski N, Fiege C, Kaisler M, Vollert J, et al. Compared to limb pain of other origin, ultrasonographic osteodensitometry reveals loss of bone density in complex regional pain syndrome. PAIN 2019;160.

[208] ten Brink AF, Goebel A, Berwick R, McCabe CS, Bultitude JH. Sensitivity to Ambient Temperature Increases in Fibromyalgia and CRPS. Pain Medicine (Malden, Mass) 2020;21:3726–9.

[209] Lee S-U, Na K-T, Lee Y-M, Park JH, Joo SY. Low vitamin D levels in post-menopausal women are associated with complex regional pain syndrome type I in surgically treated distal radius fractures. Journal of Orthopaedic Surgery and Research 2020;15:328.

[210] Verfaille C, Filbrich L, Rossetti Y, Berquin A, Mouraux D, Barbier O, et al. Visuomotor impairments in complex regional pain syndrome during pointing tasks. Pain 2021;162:811–22.

[211] Shiro Y, Nagai S, Hayashi K, Aono S, Nishihara M, Ushida T. Changes in visual attentional behavior in complex regional pain syndrome: A preliminary study. PLOS ONE 2021;16:e0247064.

[212] Pirri C, Stecco A, Stecco C, Özçakar L. Ultrasound imaging and Fascial Manipulation® for rigid retinacula in two cases of complex regional pain syndrome. Medical Ultrasonography 2021.

[213] Gorodkin R, Herrick AL, Murray AK. Microvascular Response in Patients with Complex Regional Pain Syndrome as Measured by Laser Doppler Imaging. Microcirculation (New York, NY : 1994) 2016;23:379–83.

[214] Rasmussen VF, Karlsson P, Drummond PD, Schaldemose EL, Terkelsen AJ, Jensen TS, et al. Bilaterally Reduced Intraepidermal Nerve Fiber Density in Unilateral CRPS-I. Pain Medicine (Malden, Mass) 2018;19:2021–30.

[215] Hegelmaier T, Kumowski N, Mainka T, Vollert J, Goertz O, Lehnhardt M, et al. Remote ischaemic conditioning decreases blood flow and improves oxygen extraction in patients with early complex regional pain syndrome. European Journal of Pain 2017;21:1346–54.

[216] Chu J, Bruyninckx F, Neuhauser D v. Autonomic components of Complex Regional Pain Syndrome (CRPS) are favourably affected by Electrical Twitch-Obtaining Intramuscular Stimulation (ETOIMS): effects on blood pressure and heart rate. BMJ Innovations 2017;3:176 LP – 187.

[217] Roh YH, Gong HS, Baek GH. Prognostic Value of Pain Sensitization During Early Recovery After Distal Radius Fracture in Complex Regional Pain Syndrome. Pain Medicine (Malden, Mass) 2019;20:1066–71.

[218] ten Brink AF, Bultitude JH. Predictors of Self-Reported Neglect-like Symptoms and Involuntary Movements in Complex Regional Pain Syndrome Compared to Other Chronic Limb Pain Conditions. Pain Medicine (Malden, Mass) 2021;22:2337–49.

[219] Lunden LK, Jorum E. The challenge of recognizing severe pain and autonomic abnormalities for early diagnosis of CRPS. Scandinavian Journal of Pain 2021.

[220] Cho CW, Nahm FS, Choi E, Lee PB, Jang IK, Lee CJ, et al. Multicenter study on the asymmetry of skin temperature in complex regional pain syndrome: An examination of temperature distribution and symptom duration. Medicine (United States) 2016;95:1–5.

[221] Breivik H. Complex Regional Pain Syndrome (CRPS): High risk of CRPS after trauma in another limb in patients who already have CRPS in one hand or foot: Lasting changes in neural pain modulating systems? Scandinavian Journal of Pain 2017;14:82–3.

[222] Chung BY, Choi YW, Jung MJ, Kim HO, Park CW. Complex Regional Pain Syndrome after Cryosurgery of Viral Warts. Ann Dermatol 2019;31:S3–4.

[223] Torres-Salguero I, Rubiano A. Complex regional pain syndrome secondary to sacrococcygeal dislocation following trauma to the lumbosacral region. Case report. Case Reports 2020;6:52–62.

[224] Parikh RP, Deshmukh P. Complex regional pain syndrome after transfemoral coronary balloon angioplasty. Turk Kardiyoloji Dernegi Arsivi: Turk Kardiyoloji Derneginin Yayin Organidir 2016;44:694–6.

[225] McCormack E, Mathkour MH, Kahn LW, Tolba R, Guirguis M, Chaiban G, et al. Central Neuropathic Pain and Complex Regional Pain Syndrome Following Brachial Plexus Injury Treated Successfully With Dorsal Root Entry Zone Lesioning. Neurosurgery 2019;66.

[226] Brunner F, Bachmann LM, Perez RSGM, Marinus J, Wertli MM. Painful swelling after a noxious event and the development of complex regional pain syndrome 1: A one-year prospective study. European Journal of Pain 2017;21:1611–7.

[227] Jang SH, Seo YS. Diagnosis of Complex Regional Pain Syndrome I Following Traumatic Axonal Injury of the Corticospinal Tract in a Patient with Mild Traumatic Brain Injury. Diagnostics 2020;10.

[228] Royeca JM, Cunningham CM, Pandit H, King SW. Complex regional pain syndrome as a result of total knee arthroplasty: A case report and review of literature. Case Reports in Women's Health 2019;23:e00136.

[229] Kim K-J, Choi SH, Jang J-S, Jang I-T. Complex regional pain syndrome following lumbar discectomy: A case report. Interdisciplinary Neurosurgery 2020;19:100587.

[230] Zanotti G, Slullitel PA, Comba FM, Buttaro MA, Piccaluga F. Three cases of type-1 complex regional pain syndrome after elective total hip replacement. SICOT-J 2017;3:52.

[231] Molina-Gil J, Fernández-Díaz Á, Caminal-Montero L. Complex regional pain syndrome following laparoscopic gynecological surgery. Medicina Clinica 2020;154:469–70.

[232] Satteson ES, Harbour PW, Koman LA, Smith BP, Li Z. The risk of pain syndrome affecting a previously non-painful limb following trauma or surgery in patients with a history of complex regional pain syndrome. Scandinavian Journal of Pain 2017;14:84–8.

[233] Ortiz-Romero J, Bermudez-Soto I, Torres-González R, Espinoza-Choque F, Zazueta-Hernandez JA, Perez-Atanasio JM. Factors associated with Complex Regional Pain Syndrome in surgically treated distal radius fracture. Acta Ortopedica Brasileira 2017;25:194–6.

[234] Tanesue R, Gotoh M, Mitsui Y, Nakamura H, Honda H, Ohzono H, et al. Hand lesion after arthroscopic rotator cuff repair: Association with complex regional pain syndrome. Journal of Orthopaedic Science: Official Journal of the Japanese Orthopaedic Association 2018;23:70–4.

[235] Tieppo Francio V, Barndt B, Towery C, Allen T, Davani S. Complex regional pain syndrome type II arising from a gunshot wound (GSW) associated with infective endocarditis and aortic valve replacement. BMJ Case Reports 2018;2018.

[236] Cowell F, Gillespie S, Cheung G, Brown D. Complex regional pain syndrome in distal radius fractures: How to implement changes to reduce incidence and facilitate early management. Journal of Hand Therapy: Official Journal of the American Society of Hand Therapists 2018;31:201–5.

[237] Walker M, Levitt MR. Complex regional pain syndrome after transradial cerebral intervention. BMJ Case Reports 2019;12.

[238] Patel P, Thadeshwar S, Maru M, Desai R, Fahey J. Reflex Sympathetic Dystrophy of the Right Hand following an Acute Traumatic Injury. Cureus 2019;11:e5363.

[239] Jogani A, Rathod T, Mohanty SS, Kamble P. Bimalleolar Fracture: A Unique Case of Complication of Complex Regional Pain Syndrome of Lower Extremity After Prolonged Undue Immobilisation. Journal of Orthopaedic Case Reports 2019;9:20–2.

[240] Martel M, Laumonerie P, Pecourneau V, Ancelin D, Mansat P, Bonnevialle N. Type 1 Complex Regional Pain Syndrome After Subacromial Shoulder Surgery: Incidence and Risk Factor Analysis. Indian Journal of Orthopaedics 2020;54:210–5.

[241] Duenes M, Schoof L, Schwarzkopf R, Meftah M. Complex Regional Pain Syndrome Following Total Knee Arthroplasty. Orthopedics 2020;43:e486–91.

[242] Howard D, Patel AJK. Complex regional pain syndrome following hand or forearm trauma at a regional plastic surgery service. Journal of Plastic, Reconstructive & Aesthetic Surgery: JPRAS 2021;74:1633–701.

[243] Chen A v, Evazyan T. Development of Upper Extremity Complex Regional Pain Syndrome After Prolonged surgery in Lithotomy Position: A Case Report. A&A Practice 2021;15:e01507.

[244] Dutton LK, Rhee PC. Complex Regional Pain Syndrome and Distal Radius Fracture: Etiology, Diagnosis, and Treatment. Hand Clinics 2021;37:315–22.

[245] Kim SH, Choi SS, Lee MK, Kin JE. Complex Regional Pain Syndrome Caused by Lumbar Herniated Intervertebral Disc Disease. Pain Physician 2016;19:E901-4.

[246] Mesa F, Diaz S, Restrepo S. Complex regional pain syndrome after breast implant exchange: a case report. European Journal of Plastic Surgery 2021;44:405–8.

[247] Wolter T, Knöller S, Rommel O. Complex regional pain syndrome in nerve root compression and after spinal surgery. Schmerz (Berlin, Germany) 2016;30:227–32.

[248] Harhaus L, Neubrech F, Hirche C, Schilling T, Kohler H, Mayr A, et al. Complex regional pain syndrome following distal fractures of the radius: Epidemiology, pathophysiological models, diagnostics and therapy. Der Unfallchirurg 2016;119:732–41.

[249] Erhard L. Complex pain regional syndrome after distal radius fractures. Hand surgery & rehabilitation 2016;35S:S144–9.

[250] Söylev GÖ, Boya H. A rare complication of total knee arthroplasty: Type I complex regional pain syndrome of the foot and ankle. Acta Orthopaedica et Traumatologica Turcica 2016;50:592–5.

[251] Crijns TJ, van der Gronde BATD, Ring D, Leung N. Complex Regional Pain Syndrome After Distal Radius Fracture Is Uncommon and Is Often Associated With Fibromyalgia. Clinical Orthopaedics and Related Research® 2018;476.

[252] Lee J-H, Park S, Kim JH. A Korean nationwide investigation of the national trend of complex regional pain syndrome vis-à-vis age-structural transformations. The Korean Journal of Pain 2021;34:322–31.

[253] Lee HJ, Lee CS, Yoo Y, Noh JM, Yu JH, Kim YC, et al. Complex regional pain syndrome in the young male population: A retrospective study of 200 Korean young male patients. Korean Journal of Pain 2019;32:292–300.

[254] Elsharydah A, Loo NH, Minhajuddin A, Kandil ES. Complex regional pain syndrome type 1 predictors — Epidemiological perspective from a national database analysis. Journal of Clinical Anesthesia 2017;39:34–7.

[255] Schulte-Goecking H, Azqueta-Gavaldon M, Storz C, Woiczinski M, Fraenkel P, Leukert J, et al. Psychological, social and biological correlates of body perception disturbance in complex regional pain syndrome. Current Psychology 2020.

[256] Brown CA, Scholtes I, Shenker N, Lee MC. Suboptimal learning of tactile-spatial predictions in patients with complex regional pain syndrome. Pain 2020;161:369–78.

[257] Trojan J, Speck V, Kleinböhl D, Benrath J, Flor H, Maihöfner C. Altered tactile localization and spatiotemporal integration in complex regional pain syndrome patients. European Journal of Pain (London, England) 2019;23:472–82.

[258] Verfaille C, Filbrich L, Cordova Bulens D, Lefèvre P, Berquin A, Barbier O, et al. Robot-assisted line bisection in patients with Complex Regional Pain Syndrome. PLOS ONE 2019;14:e0213732.

[259] Osumi M, Sumitani M, Otake Y, Imai R, Morioka S. Fear of movement disturbs inter-limb coupling in complex regional pain syndrome. Annals of Physical and Rehabilitation Medicine 2020;63:258–61.

[260] Tschopp M, Swanenburg J, Wertli MW, Langenfeld A, McCabe CS, Lewis J, et al. The German version of the Bath Body Perception Disturbance Scale (BBPDS-D) : Translation, cultural adaptation and linguistic validation on patients with complex regional pain syndrome. Schmerz (Berlin, Germany) 2018;32:195–200. 6.

[261] Reid EJ, Braithwaite FA, Wallwork SB, Harvie D, Chalmers KJ, Spence C, et al. Spatially-defined motor deficits in people with unilateral complex regional pain syndrome. Cortex; a Journal Devoted to the Study of the Nervous System and Behavior 2018;104:154–62.

[262] Filbrich L, Alamia A, Verfaille C, Berquin A, Barbier O, Libouton X, et al. Biased visuospatial perception in complex regional pain syndrome. Scientific Reports 2017;7:9712.

[263] Lee H-J, Lee KH, Moon JY, Kim Y-C. Prevalence of autonomic nervous system dysfunction in complex regional pain syndrome. Regional Anesthesia & Pain Medicine Pain Medicine 2021;46:193–5.

[264] Tajadura-Jiménez A, Cohen H, Bianchi-Berthouze N. Bodily Sensory Inputs and Anomalous Bodily Experiences in Complex Regional Pain Syndrome: Evaluation of the Potential Effects of Sound Feedback. Frontiers in Human Neuroscience 2017;11:379.

[265] Im JJ, Kim J, Jeong H, Oh JK, Lee S, Lyoo IK, et al. Prefrontal White Matter Abnormalities Associated With Pain Catastrophizing in Patients With Complex Regional Pain Syndrome. Archives of Physical Medicine and Rehabilitation 2021;102:216–24.

[266] König S, Steinebrey N, Herrnberger M, Escolano-Lozano F, Schlereth T, Rebhorn C, et al. Reduced serum protease activity in Complex Regional Pain Syndrome: The impact of angiotensin-converting enzyme and carboxypeptidases. Journal of Pharmaceutical and Biomedical Analysis 2021;205:114307.

[267] Lacagnina MJ, Heijnen CJ, Watkins LR, Grace PM. Autoimmune regulation of chronic pain. Pain Reports 2021;6:e905.

[268] Baerlecken NT, Gaulke R, Pursche N, Witte T, Karst M, Bernateck M. Autoantibodies against P29ING4 are associated with complex regional pain syndrome. Immunologic Research 2019;67:461–8.

[269] Tajerian M, Hung V, Khan H, Lahey LJ, Sun Y, Birklein F, et al. Identification of KRT16 as a target of an autoantibody response in complex regional pain syndrome. Experimental Neurology 2017;287:14–20.

[270] Bruehl S, Gamazon ER, van de Ven T, Buchheit T, Walsh CG, Mishra P, et al. DNA methylation profiles are associated with complex regional pain syndrome after traumatic injury. Pain 2019;160:2328–37.

[271] Golmirzaie G, Holland LS, Moser SE, Rastogi M, Hassett AL, Brummett CM. Time Since Inciting Event Is Associated With Higher Centralized Pain Symptoms in Patients Diagnosed With Complex Regional Pain Syndrome. Regional Anesthesia and Pain Medicine 2016;41:731–6.

[272] Duong HP, Konzelmann M, Vuistiner P, Burrus C, Léger B, Stiefel F, et al. Psychiatric Comorbidity and Complex Regional Pain Syndrome Through the Lens of the Biopsychosocial Model: A Comparative Study. Journal of Pain Research 2020;13:3235–45.

[273] Jung Y-H, Kim H, Jeon SY, Kwon JM, Lee WJ, Jang JH, et al. Peripheral and Central Metabolites Affecting Depression, Anxiety, Suicidal Ideation, and Anger in Complex Regional Pain Syndrome Patients Using a Magnetic Resonance Spectroscopy: A Pilot Study. Psychiatry Investigation 2018;15:891–9.

[274] Janicki PK, Alexander GM, Eckert J, Postula M, Schwartzman RJ. Analysis of Common Single Nucleotide Polymorphisms in Complex Regional Pain Syndrome: Genome Wide Association Study Approach and Pooled DNA Strategy. Pain Medicine (Malden, Mass) 2016;17:2344–52.

[275] Park HY, Jang YE, Oh S, Lee PB. Psychological Characteristics in Patients with Chronic Complex Regional Pain Syndrome: Comparisons with Patients with Major Depressive Disorder and Other Types of Chronic Pain. Journal of Pain Research 2020;13:389–98.

[276] Russo MA, Fiore NT, van Vreden C, Bailey D, Santarelli DM, McGuire HM, et al. Expansion and activation of distinct central memory T lymphocyte subsets in complex regional pain syndrome. Journal of Neuroinflammation 2019;16:63.

[277] Merchant SHI. Evidence already exists for motor system reorganization in CRPS. Canadian Journal of Pain 2018;2:27–9.

[278] Harvey M-P, Maher-Bussières S, Emery E, Martel M, Houde F, Tousignant-Laflamme Y, et al. Evidence of motor system reorganization in complex regional pain syndrome type 1: A case report. Canadian Journal of Pain 2018;2:21–6.

[279] Hu Q, Wang Q, Wang C, Tai Y, Liu B, Shao X, et al. TRPV1 Channel Contributes to the Behavioral Hypersensitivity in a Rat Model of Complex Regional Pain Syndrome Type 1. Frontiers in Pharmacology 2019;10:453.

[280] Alam OH, Zaidi B, Pierce J, Moser SE, Hilliard PE, Golmirzaie G, et al. Phenotypic features of patients with complex regional pain syndrome compared with those with neuropathic pain. Regional Anesthesia and Pain Medicine 2019.

[281] Shubayev VI, Strongin AY, Yaksh TL. Structural homology of myelin basic protein and muscarinic acetylcholine receptor: Significance in the pathogenesis of complex regional pain syndrome. Molecular Pain 2018;14:1744806918815005.

[282] König S, Bayer M, Dimova V, Herrnberger M, Escolano-Lozano F, Bednarik J, et al. The serum protease network-one key to understand complex regional pain syndrome pathophysiology. Pain 2019;160:1402–9.

[283] Jung Y-H, Kim H, Jeon SY, Kwon JM, Kim YC, Lee WJ, et al. Neurometabolite changes in patients with complex regional pain syndrome using magnetic resonance spectroscopy: a pilot study. Neuroreport 2019;30:108–12.

[284] Bar-Shalita T, Livshitz A, Levin-Meltz Y, Rand D, Deutsch L, Vatine J-J. Sensory modulation dysfunction is associated with Complex Regional Pain Syndrome. PloS One 2018;13:e0201354.

[285] Enax-Krumova EK, Baron R, Treede R-D, Vollert J. Contralateral sensitisation is not specific for complex regional pain syndrome. Comment on Br J Anaesth 2021; 127: e1-3. British Journal of Anaesthesia 2021;127:e173–6.

[286] Pande R, Parikh A, Shenoda B, Ramanathan S, Alexander GM, Schwartzman RJ, et al. Hsa-miR-605 regulates the proinflammatory chemokine CXCL5 in complex regional pain syndrome. Biomedicine & Pharmacotherapy 2021;140:111788.

[287] Schreiber U, Engl C, Bayer M, König S. Labeled substance P as a neuropeptide reporter substance for enzyme activity. Journal of Pharmaceutical and Biomedical Analysis 2020;178:112953.

[288] Dietz C, Reinhold A-K, Escolano-Lozano F, Mehling K, Forer L, Kress M, et al. Complex regional pain syndrome: role of contralateral sensitisation. British Journal of Anaesthesia 2021;127:e1–3.

[289] Drummond PD, Vo L, Finch PM. The Source of Hemisensory Disturbances in Complex Regional Pain Syndrome. The Clinical Journal of Pain 2021;37:79–85.

[290] Brun C, Mercier C, Grieve S, Palmer S, Bailey J, McCabe CS. Sensory disturbances induced by sensorimotor conflicts are higher in complex regional pain syndrome and fibromyalgia compared to arthritis and healthy people, and positively relate to pain intensity. European Journal of Pain (London, England) 2019;23:483–94.

[291] Li W-W, Guo T-Z, Shi X, Birklein F, Schlereth T, Kingery WS, et al. Neuropeptide regulation of adaptive immunity in the tibia fracture model of complex regional pain syndrome. Journal of Neuroinflammation 2018;15:105.

[292] ten Brink AF, Peters L, Kompouli P-I, Jordan A, McCabe CS, Goebel A, et al. Bodily changes and sensory sensitivity in complex regional pain syndrome and fibromyalgia. Pain 2020;161:1361–70.

[293] Cuhadar U, Gentry C, Vastani N, Sensi S, Bevan S, Goebel A, et al. Autoantibodies produce pain in complex regional pain syndrome by sensitizing nociceptors. Pain 2019;160:2855–65..

[294] Vas L. Commentary: Selective Fiber Degeneration in the Peripheral Nerve of a Patient With Severe Complex Regional Pain Syndrome. Frontiers in Neuroscience 2019;13:19.

[295] Reimer M, Rempe T, Diedrichs C, Baron R, Gierthmühlen J. Sensitization of the Nociceptive System in Complex Regional Pain Syndrome. PLOS ONE 2016;11:e0154553.

[296] Yvon A, Faroni A, Reid AJ, Lees VC. Selective Fiber Degeneration in the Peripheral Nerve of a Patient With Severe Complex Regional Pain Syndrome. Frontiers in Neuroscience 2018;12:207.

[297] Iwatsuki K, Hoshiyama M, Yoshida A, Uemura J-I, Hoshino A, Morikawa I, et al. Chronic pain-related cortical neural activity in patients with complex regional pain syndrome. IBRO Neuroscience Reports 2021;10:208–15..

[298] Wang AP, Butler AA, Valentine JD, Rae CD, McAuley JH, Gandevia SC, et al. A Novel Finger Illusion Reveals Reduced Weighting of Bimanual Hand Cortical Representations in People With Complex Regional Pain Syndrome. The Journal of Pain 2019;20:171–80.

[299] Pfannmöller J, Strauss S, Langner I, Usichenko T, Lotze M. Investigations on maladaptive plasticity in the sensorimotor cortex of unilateral upper limb CRPS I patients. Restorative Neurology and Neuroscience 2019;37:143–53.

[300] Butler S. Cortical reorganization of the healthy hand in upper-limb complex regional pain syndrome (CRPS): Is reorganizations of common beliefs about CRPS necessary? Scandinavian Journal of Pain 2016;13:136–7.

[301] di Pietro F, Moseley GL, Stanton TR. Functional and structural cortical reorganization in complex regional pain syndrome and implications for treatment. European Journal of Pain (London, England) 2016;20:1763–5.

[302] Enax-Krumova EK, Lenz M, Frettlöh J, Höffken O, Reinersmann A, Schwarzer A, et al. Changes of the Sensory Abnormalities and Cortical Excitability in Patients with Complex Regional Pain Syndrome of the Upper Extremity After 6 Months of Multimodal Treatment. Pain Medicine (Malden, Mass) 2017;18:95–106.

[303] Büntjen L, Hopf J-M, Merkel C, Voges J, Knape S, Heinze H-J, et al. Somatosensory Misrepresentation Associated with Chronic Pain: Spatiotemporal Correlates of Sensory Perception in a Patient following a Complex Regional Pain Syndrome Spread. Frontiers in Neurology 2017;8:142.

[304] Pietro F di, Stanton TR, Moseley GL, Lotze M, McAuley JH. An exploration into the cortical reorganisation of the healthy hand in upper-limb complex regional pain syndrome. Scandinavian Journal of Pain 2016;13:18–24.

[305] Lee D, Choi S-H, Noh E, Lee WJ, Jang JH, Moon JY, et al. Impaired Performance in Mental Rotation of Hands and Feet and Its Association with Social Cognition in Patients with Complex Regional Pain Syndrome. Pain Medicine 2021;22:1411–9.

[306] Bellan V, Braithwaite FA, Wilkinson EM, Stanton TR, Moseley GL. Where is my arm? Investigating the link between complex regional pain syndrome and poor localisation of the affected limb. PeerJ 2021;9:e11882.

[307] Echalier A, Borg C, Creac'h C, Laurent B, Michael GA. Spontaneous sensations reveal distorted body perception in complex regional pain syndrome (CRPS). Brain and Cognition 2020;142:105568.

[308] Halicka M, Vittersø AD, McCullough H, Goebel A, Heelas L, Proulx MJ, et al. Disputing space-based biases in unilateral complex regional pain syndrome. Cortex; a Journal Devoted to the Study of the Nervous System and Behavior 2020;127:248–68.

[309] Schulte-Göcking H. Das komplexe regionale Schmerzsyndrom (CRPS) und der Einfluss von psychosozialen Faktoren auf die KörperschemastörungPsychological and social correlates of body perception disturbance in complex regional pain syndrome. Deutsche Zeitschrift Für Akupunktur 2020;63.

[310] Vittersø AD, Buckingham G, Halicka M, Proulx MJ, Bultitude JH. Altered updating of bodily and spatial representations after tool-use in complex regional pain syndrome. Pain 2020;161:1609–28.

[311] Shenoda BB, Alexander GM, Ajit SK. Hsa-miR-34a mediated repression of corticotrophin releasing hormone receptor 1 regulates pro-opiomelanocortin expression in patients with complex regional pain syndrome. Journal of Translational Medicine 2016;14:64.

[312] Russo MA, Georgius P, Pires AS, Heng B, Allwright M, Guennewig B, et al. Novel immune biomarkers in complex regional pain syndrome. Journal of Neuroimmunology 2020;347:577330.

[313] Vasquez A. Neuroinflammation in fibromyalgia and CRPS is multifactorial. Nature Reviews Rheumatology 2016;12:242.

[314] Popkirov S, Hoeritzauer I, Colvin L, Carson AJ, Stone J. Complex regional pain syndrome and functional neurological disorders – time for reconciliation. Journal of Neurology, Neurosurgery &Amp; Psychiatry 2019;90:608 LP – 614.

[315] Heyn J, Azad SC, Luchting B. Altered regulation of the T-cell system in patients with CRPS. Inflammation Research : Official Journal of the European Histamine Research Society . [et Al] 2019;68:1–6.

[316] Dimova V, Herrnberger MS, Escolano-Lozano F, Rittner HL, Vlckova E, Sommer C, et al. Clinical phenotypes and classification algorithm for complex regional pain syndrome. Neurology 2020;94:e357–67.

[317] Gofiţă CE, Mușetescu AE, Ciurea PL, Boldeanu M v, Trăistaru MR, Bumbea AM, et al. Posttraumatic Complex Regional Pain Syndrome and Related Comorbidities. Current Health Sciences Journal 2019;45:321–8.

[318] Liu Q, Xu X, Xu L, Huang Y. Effects of N-methyl-D-aspartate Receptor in Keratinocyte on Type I Complex Regional Pain Syndrome. Zhongguo yi xue ke xue yuan xue bao Acta Academiae Medicinae Sinicae 2020;42:338–46.

[319] Baronio M, Sadia H, Paolacci S, Prestamburgo D, Miotti D, Guardamagna VA, et al. Molecular Aspects of Regional Pain Syndrome. Pain Research & Management 2020;2020:7697214.

[320] Jung Y-H, Kim H, Lee D, Lee J-Y, Lee WJ, Moon JY, et al. Disruption of Homeostasis Based on the Right and Left Hemisphere in Patients with Complex Regional Pain Syndrome. Neuroimmunomodulation 2019;26:276–84.

[321] Razaq S, Kara M, Kaymak B, Öner I, Ozkan Ö, Özçakar L. Dorsal Scapular Neuropathy as a Rare Cause 1 of Complex Regional Pain Syndrome: A Reappraisal on Ultrasound Imaging and Guidance for Recalcitrant Pain. American Journal of Physical Medicine & Rehabilitation 2019;98:e60–2.

[322] Crock LW, Baldridge MT. A role for the microbiota in complex regional pain syndrome? Neurobiology of Pain 2020;8:100054.

[323] Brunner F. Pathophysiology and Diagnosis of Chronic Regional Pain Syndrome: What is important for the General Practitioner and the Surgeon? Therapeutische Umschau Revue therapeutique 2020;77:258–62.

[324] Lee Y-H, Lee KM, Kim H-G, Kang S-K, Auh Q-S, Hong J-P, et al. Orofacial complex regional pain syndrome: pathophysiologic mechanisms and functional MRI. Oral Surgery, Oral Medicine, Oral Pathology and Oral Radiology 2017;124:e164–70.

[325] van Bussel CM, Stronks DL, Huygen FJPM. Phenotypic Variation in Complex Regional Pain Syndrome: Comparison Between Presentation in Knee Alone or in Ankle/Foot. Pain Medicine (Malden, Mass) 2016;17:2337–43.

[326] Loewenstein SN, Duquette SP, Adkinson JM. Combined Carpal Tunnel Release and Palmar Fasciectomy for Dupuytren's Contracture Does Not Increase the Risk for Complex Regional Pain Syndrome. Plastic and Reconstructive Surgery 2018;142:1251–7.

[327] Kuttikat A, Noreika V, Shenker N, Chennu S, Bekinschtein T, Brown CA. Neurocognitive and Neuroplastic Mechanisms of Novel Clinical Signs in CRPS. Frontiers in Human Neuroscience 2016;10:16.

[328] Kohler M, Strauss S, Horn U, Langner I, Usichenko T, Neumann N, et al. Differences in Neuronal Representation of Mental Rotation in Patients With Complex Regional Pain Syndrome and Healthy Controls. The Journal of Pain 2019;20:898–907.

[329] Bharwani KD, Dirckx M, Stronks DL, Dik WA, Huygen FJPM. Serum Soluble Interleukin-2 Receptor Does Not Differentiate Complex Regional Pain Syndrome from Other Pain Conditions in a Tertiary Referral Setting. Mediators of Inflammation 2020;2020:6259064.

[330] Pruthi P, Arora P, Bahrani K, Mittal M. Complex regional pain syndrome with an unusual aetiology. Indian Journal of Rheumatology 2018;13:277–9.

[331] Sumitani M, Osumi M. Two findings of CRPS-pain in deep tissues. PAIN RESEARCH 2017;32:7–12.

[332] Kuttikat A, Noreika V, Chennu S, Shenker N, Bekinschtein T, Brown CA. Altered Neurocognitive Processing of Tactile Stimuli in Patients with Complex Regional Pain Syndrome. The Journal of Pain 2018;19:395–409.

[333] Kim J, Kang I, Chung Y-A, Kim T-S, Namgung E, Lee S, et al. Altered attentional control over the salience network in complex regional pain syndrome. Scientific Reports 2018;8:7466.

[334] Shokouhi M, Clarke C, Morley-Forster P, Moulin DE, Davis KD, St Lawrence K. Structural and Functional Brain Changes at Early and Late Stages of Complex Regional Pain Syndrome. The Journal of Pain 2018;19:146–57.

[335] Kim J-H, Choi S-H, Jang JH, Lee D-H, Lee K-J, Lee WJ, et al. Impaired insula functional connectivity associated with persistent pain perception in patients with complex regional pain syndrome. PLOS ONE 2017;12:e0180479.

[336] Bultitude JH, Walker I, Spence C. Space-based bias of covert visual attention in complex regional pain syndrome. Brain: A Journal of Neurology 2017;140:2306–21.

[337] Hotta J, Zhou G, Harno H, Forss N, Hari R. Complex regional pain syndrome: The matter of white matter? Brain and Behavior 2017;7:e00647.

[338] Hotta J, Saari J, Koskinen M, Hlushchuk Y, Forss N, Hari R. Abnormal Brain Responses to Action Observation in Complex Regional Pain Syndrome. The Journal of Pain 2017;18:255–65.

[339] Halicka M, Vittersø AD, Proulx MJ, Bultitude JH. Neuropsychological Changes in Complex Regional Pain Syndrome (CRPS). Behavioural Neurology 2020;2020:4561831.

[340] Drummond PD, Morellini N, Visser E, Finch PM. Expression of Cutaneous Beta-2 Adrenoceptors Is Similar in Patients with Complex Regional Pain Syndrome and Pain-Free Controls. Pain Medicine (Malden, Mass) 2020;21:1199–207.

[341] Birklein F, Ajit SK, Goebel A, Perez RSGM, Sommer C. Complex regional pain syndrome - phenotypic characteristics and potential biomarkers. Nature Reviews Neurology 2018;14:272–84..

[342] König S, Schlereth T, Birklein F. Molecular signature of complex regional pain syndrome (CRPS) and its analysis. Expert Review of Proteomics 2017;14:857–67.

[343] van Velzen GAJ, Rombouts SARB, van Buchem MA, Marinus J, van Hilten JJ. Is the brain of complex regional pain syndrome patients truly different? European Journal of Pain 2016;20:1622–33.

[344] Packham TL, Bean D, Johnson MH, MacDermid JC, Grieve S, McCabe CS, et al. Measurement Properties of the SF-MPQ-2 Neuropathic Qualities Subscale in Persons with CRPS: Validity, Responsiveness, and Rasch Analysis. Pain Medicine 2019;20:799–809.

[345] Kammermann P, Tobler B, Vögelin E. Pain assessment of CRPS in Hand Therapy. Therapeutische Umschau Revue therapeutique 2020;77:263–9.

[346] ten Brink AF, Halicka M, Vittersø AD, Jones HG, Stanton TR, Bultitude JH. Validation of the Bath CRPS Body Perception Disturbance Scale. The Journal of Pain 2021.

[347] Christophe L, Chabanat E, Delporte L, Revol P, Volckmann P, Jacquin-Courtois S, et al. Prisms to Shift Pain Away: Pathophysiological and Therapeutic Exploration of CRPS with Prism Adaptation. Neural Plasticity 2016;2016:1694256.

[348] Rodham K, Gavin J, Coulson N, Watts L. Co-creation of information leaflets to meet the support needs of people living with complex regional pain syndrome (CRPS) through innovative use of wiki technology. Informatics for Health & Social Care 2016;41:325–39.

[349] Strauss S, Barby S, Härtner J, Neumann N, Moseley GL, Lotze M. Modifications in fMRI Representation of Mental Rotation Following a 6 Week Graded Motor Imagery Training in Chronic CRPS Patients. The Journal of Pain 2021;22:680–91.

[350] Bakshi P, Chang W-P, Fisher TF, Andreae B. Client buy-in: An essential consideration for graded motor imagery in hand therapy. Journal of Hand Therap : Official Journal of the American Society of Hand Therapists 2021;34:348–50.

[351] Fry K, Grieve S, Llewellyn A, McCabe C. Living with chronic pain: an investigation of online educational resources for people living with complex regional pain syndrome. Rheumatology 2019;58.

[352] Sethy D, Sahoo S. Kinesiophobia after complex regional pain syndrome type one in a case of stroke hemiplegia and effect of cognitive behavior therapy. Indian Journal of Psychiatry 2018;60:152–4.

[353] Shepherd M, Young J, McDevitt A. The clinical application of pain neuroscience, graded motor imagery, and graded activity with complex regional pain syndrome-A case report. Physiotherapy Theory and Practice 2020;36:1043–55.

[354] Storz C, Kraft E. Occupational therapy for complex regional pain syndrome. Schmerz (Berlin, Germany) 2021;35:285–93.

[355] McGee C, Skye J, van Heest A. Graded motor imagery for women at risk for developing type I CRPS following closed treatment of distal radius fractures: a randomized comparative effectiveness trial protocol. BMC Musculoskeletal Disorders 2018;19:202.

[356] Méndez-Rebolledo G, Gatica-Rojas V, Torres-Cueco R, Albornoz-Verdugo M, Guzmán-Muñoz E. Update on the effects of graded motor imagery and mirror therapy on complex regional pain syndrome type 1: A systematic review. Journal of Back and Musculoskeletal Rehabilitation 2017;30:441–9.

[357] Raucci U, Tomasello C, Marri M, Salzano M, Gasparini A, Conicella E. Scrambler Therapy® MC-5A for Complex Regional Pain Syndrome: Case Reports. Pain Practice 2016;16:E103–9.

[358] Rome L. The place of occupational therapy in rehabilitation strategies of complex regional pain syndrome: Comparative study of 60 cases. Hand Surgery & Rehabilitation 2016;35:355–62.

[359] Gutiérrez-Espinoza H, Tabach-Apraiz A, Oyanadel-Maldonado M. Physical therapy in patients with complex regional pain syndrome type I after distal radius fracture: a case series. Journal of Physical Therapy Science 2019;31:403–7.

[360] Barnhoorn K, Staal JB, van Dongen RT, Frölke JPM, Klomp FP, van de Meent H, et al. Pain Exposure Physical Therapy versus conventional treatment in complex regional pain syndrome type 1-a cost-effectiveness analysis alongside a randomized controlled trial. Clinical Rehabilitation 2018;32:790–8.

[361] Moretti A, Gimigliano F, Paoletta M, Liguori S, Toro G, Aulicino M, et al. Efficacy and Effectiveness of Physical Agent Modalities in Complex Regional Pain Syndrome Type I: A Scoping Review. Applied Sciences 2021;11.

[362] Oh H-M, Kim C-H, Kim A-R. Dramatic effect in passive ROM exercise under sedation in a patient with intractable complex regional pain syndrome (type I): A case report. Medicine 2019;98:e14990.

[363] Bravo D, Duong S, Todd KJ, Finlayson RJ, Tran DQ. In reply: Pain exposure physical therapy in complex regional pain syndrome: promising enough to warrant further investigation. Canadian Journal of Anaesthesia = Journal Canadien d'anesthesie 2019;66:117–8.

[364] Staal JB, Klomp FP, Nijhuis-van der Sanden MWG. Pain exposure physical therapy in complex regional pain syndrome: promising enough to warrant further investigation. Canadian Journal of Anaesthesia = Journal Canadien d'anesthesie 2019;66:115–6.

[365] den Hollander M, Heijnders N, de Jong JR, Vlaeyen JWS, Smeets RJEM, Goossens MEJB. Exposure in vivo versus pain-contingent physical in Complex Regional Pain Syndrome type I: a cost-effectiveness analysis. International Journal of Technology Assessment in Health Care 2018;34:400–9.

[366] Schmid A-C, Schwarz A, Gustin SM, Greenspan JD, Hummel FC, Birbaumer N. Pain reduction due to novel sensory-motor training in Complex Regional Pain Syndrome I - A pilot study. Scandinavian Journal of Pain 2017;15:30–7.

[367] Lebon J, Rongières M, Apredoaei C, Delclaux S, Mansat P. Physical therapy under hypnosis for the treatment of patients with type 1 complex regional pain syndrome of the hand and wrist: Retrospective study of 20 cases. Hand Surgery & Rehabilitation 2017;36:215–21. https://doi.org/10.1016/j.hansur.2016.12.008.

[368] Kraft E, Storz C, Ranker A. Physical therapy in the treatment of complex regional pain syndrome. Schmerz (Berlin, Germany) 2021;35:363–72.

[369] Kotiuk V, Burianov O, Kostrub O, Khimion L, Zasadnyuk I. The impact of mirror therapy on body schema perception in patients with complex regional pain syndrome after distal radius fractures. British Journal of Pain 2018;13:35–42.

[370] Wittkopf PG, Johnson MI. Mirror therapy: A potential intervention for pain management. Revista Da Associacao Medica Brasileira (1992) 2017;63:1000–5.

[371] Rowen RJ, Robins H. Ozone Therapy for Complex Regional Pain Syndrome: Review and Case Report. Current Pain and Headache Reports 2019;23:41.

[372] Sezgin Ozcan D, Tatli HU, Polat CS, Oken O, Koseoglu BF. The Effectiveness of Fluidotherapy in Poststroke Complex Regional Pain Syndrome: A Randomized Controlled Study. Journal of Stroke and Cerebrovascular Diseases: The Official Journal of National Stroke Association 2019;28:1578–85.

[373] Dunbar J, Wilson H. Emerging models for successful treatment of complex regional pain syndrome in children and young adults. Journal of Primary Health Care 2019;11:283–7.

[374] Kulbida R, Mathes A, Loeser J. Beneficial effects of hirudotherapy in a chronic case of complex regional pain syndrome. Journal of Integrative Medicine 2019;17:383–6.

[375] Gillespie S, Cowell F, McCabe C, Goebel A. Complex regional pain syndrome acute care pathways in England: Do they exist and what do they look like? Hand Therapy 2018;23:95–9.

[376] Quintal I, Poiré-Hamel L, Bourbonnais D, Dyer J-O. Management of long-term complex regional pain syndrome with allodynia: A case report. Journal of Hand Therapy: Official Journal of the American Society of Hand Therapists 2018;31:255–64.

[377] Żyluk A, Puchalski P. Effectiveness of complex regional pain syndrome treatment: A systematic review. Neurologia i Neurochirurgia Polska 2018;52:326–33.

[378] Kramer S. Das komplexe regionale Schmerzsyndrom (CRPS)The complex regional pain syndrome (CRPS): Psyche, Körper und Traditionelle Chinesische Therapie (TCM)Psyche, body, and traditional Chinese therapy (TCM). Deutsche Zeitschrift Für Akupunktur 2020;63:83–4.

[379] Hájek M, Chmelar D, Tlapák J, Novomeský F, Rybárová V, Klugar M. Hyperbaric oxygen treatment in recurrent development of complex regional pain syndrome: A case report. Diving and Hyperbaric Medicine 2021;51:107–10.

[380] Pons T, Shipton EA. Physiotherapy and the management of complex regional pain syndrome. Pain Management 2016;6:515–8.

[381] Schubert C. Treatment of complex regional pain syndrome in the hand region from the perspective of physiotherapy. Der Unfallchirurg 2021;124:456–64.

[382] Varenna M, Braga V, Gatti D, Iolascon G, Frediani B, Zucchi F, et al. Intramuscular neridronate for the treatment of complex regional pain syndrome type 1: a randomized, double-blind, placebo-controlled study. Therapeutic Advances in Musculoskeletal Disease 2021;13:1759720X211014020.

[383] Aminova LR, Lobashov VV, Akhtiamov IF. Treatment of complex regional pain syndrome after filling a single bone-cyst cavity with beta-tricalcium phosphate granules. Pediatric Traumatology, Orthopaedics and Reconstructive Surgery 2020;7:97–104.

[384] Varenna M, Manara M, Rovelli F, Zucchi F, Sinigaglia L. Predictors of Responsiveness to Bisphosphonate Treatment in Patients with Complex Regional Pain Syndrome Type I: A Retrospective Chart Analysis. Pain Medicine 2017;18:1131–8.

[385] Chang K-V, Chiu Y-H, Wu W-T, Hsu P-C, Özçakar L. Botulinum toxin injections for shoulder and upper limb pain: a narrative review. Pain Management 2020;10:411–20.

[386] Kapural L, Goebel A, Serpell M, Jones A, Kaye R, Tabuteau H. CREATE-1 study: a randomized, double-blind, placebo-controlled study to assess the efficacy and safety of AXS-02 (disodium zoledronate tetrahydrate) administered orally to subjects with Complex Regional Pain Syndrome Type 1 (CRPS-1). The Journal of Pain 2016;17:S81–2.

[387] Yazdani J, Khiavi RK, Ghavimi MA, Mortazavi A, Hagh EJ, Ahmadpour F. Calcitonin as an analgesic agent: review of mechanisms of action and clinical applications. Brazilian journal of anesthesiology (Elsevier) 2019;69:594–604.

[388] Javed S, Abdi S. Use of anticonvulsants and antidepressants for treatment of complex regional pain syndrome: a literature review. Pain Management 2021;11:189–99.

[389] Giray E, Şanal Toprak C, Saçaklidir R, Gündüz OH. Pregabalin-Associated Stuttering in a Patient With Complex Regional Pain Syndrome: A Case Report. Journal of Clinical Psychopharmacology 2016;36:740–2.

[390] Goebel A, Jacob A, Frank B, Sacco P, Alexander G, Philips C, et al. Mycophenolate for persistent complex regional pain syndrome, a parallel, open, randomised, proof of concept trial. Scandinavian Journal of Pain 2018;18:29–37.

[391] Rudd-Barnard G, Wallbom A, Pangarkar S, Baria A. A case study investigating opioid medication utilization in patients with complex regional pain syndrome before and after ketamine infusion therapy. The Journal of Pain 2016;17:S76.

[392] Kirkpatrick AF, Saghafi A, Yang K, Qiu P, Alexander J, Bavry E, et al. Optimizing the Treatment of CRPS With Ketamine. The Clinical Journal of Pain 2020;36:516–23.

[393] Park S, Kim H-J, Kim DK, Kim TH. Use of Oral Prednisolone and a 3-Phase Bone Scintigraphy in Patients with Complex Regional Pain Syndrome Type I. Healthcare 2020;8.

[394] Kumowski N, Hegelmaier T, Kolbenschlag J, Mainka T, Michel-Lauter B, Maier C. Short-Term Glucocorticoid Treatment Normalizes the Microcirculatory Response to Remote Ischemic Conditioning in Early Complex Regional Pain Syndrome. Pain Practice: The Official Journal of World Institute of Pain 2019;19:168–75.

[395] Jamroz A, Berger M, Winston P. Prednisone for Acute Complex Regional Pain Syndrome: A Retrospective Cohort Study. Pain Research and Management 2020;2020:8182569.

[396] Barbalinardo S, Loer SA, Goebel A, Perez RSGM. The Treatment of Longstanding Complex Regional Pain Syndrome with Oral Steroids. Pain Medicine (Malden, Mass) 2016;17:337–43.

[397] Eraghi AS, Khazanchin A, Hosseinzadeh N, Pahlevansabagh A. A randomized controlled trial on Aspirin and complex regional pain syndrome after radius fractures. European Journal of Translational Myology 2020;30:8643.

[398] Fulas OA, Laferriere A, Stein RS, Bohle DS, Coderre TJ. Topical combination of meldonium and N-acetyl cysteine relieves allodynia in rat models of CRPS-1 and peripheral neuropathic pain by enhancing NO-mediated tissue oxygenation. Journal of Neurochemistry 2020;152:e14943.

[399] Fusco R, Gugliandolo E, Campolo M, Evangelista M, di Paola R, Cuzzocrea S. Effect of a new formulation of micronized and ultramicronized N-palmitoylethanolamine in a tibia fracture mouse model of complex regional pain syndrome. PloS One 2017;12:e0178553.

[400] Mundluru T, Saraghi M. Anesthetic Management of a Complex Regional Pain Syndrome (CRPS) Patient With Ketamine. Anesthesia Progress 2020;67:219–25.

[401] Shenoda BB, Krevolin LE, Sherman M. Syndrome of Inappropriate Antidiuretic Hormone Release During Ketamine Infusion in Complex Regional Syndrome Patient Receiving Intrathecal Baclofen: A Case Report. A&A Practice 2019;13:386–8.

[402] Mandyam MC, Ahuja NK. Ketamine-Induced Mania During Treatment for Complex Regional Pain Syndrome. Pain Medicine (Malden, Mass) 2017;18:2040–1.

[403] Hewitt NA, Cox P. Recurrent Subanesthetic Ketamine Infusions for Complex Regional Pain Syndrome Leading to Biliary Dilation, Jaundice, and Cholangitis: A Case Report. A&A Practice 2018;10:168–70.

[404] Durham MJ, Mekhjian HS, Goad JA, Lou M, Ding M, Richeimer SH. Topical Ketamine in the Treatment of Complex Regional Pain Syndrome. International Journal of Pharmaceutical Compounding 2018;22:172–5.

[405] Sorel M, Beatrix J-C, Locko B, Armessen C, Domec A-M, Lecompte O, et al. Three-phase Bone Scintigraphy Can Predict the Analgesic Efficacy of Ketamine Therapy in CRPS. The Clinical Journal of Pain 2018;34:831–7.

[406] Sorel M, Zrek N, Locko B, Armessen C, Ayache SS, Lefaucheur J-P. A reappraisal of the mechanisms of action of ketamine to treat complex regional pain syndrome in the light of cortical excitability changes. Clinical Neurophysiology: Official Journal of the International Federation of Clinical Neurophysiology 2018;129:990–1000.

[407] Puchalski P, Zyluk A. Results of the Treatment of Chronic, Refractory CRPS with Ketamine Infusions: a Preliminary Report. Handchirurgie, Mikrochirurgie, Plastische Chirurgie : Organ Der Deutschsprachigen Arbeitsgemeinschaft Fur Handchirurgie : Organ Der Deutschsprachigen Arbeitsgemeinschaft Fur Mikrochirurgie Der Peripheren Nerven Und Gefasse : Organ Der V. 2016;48:143–7.

[408] Kim M, Cho S, Lee J-H. The Effects of Long-Term Ketamine Treatment on Cognitive Function in Complex Regional Pain Syndrome: A Preliminary Study. Pain Medicine (Malden, Mass) 2016;17:1447–51.

[409] Winston P. Early Treatment of Acute Complex Regional Pain Syndrome after Fracture or Injury with Prednisone: Why Is There a Failure to Treat? A Case Series. Pain Research and Management 2016;2016:7019196.

[410] Gatti D, Rossini M, Adami S. Management of patients with complex regional pain syndrome type I. Osteoporosis International: A Journal Established as Result of Cooperation between the European Foundation for Osteoporosis and the National Osteoporosis Foundation of the USA 2016;27:2423–31.

[411] Walfish L, Sbrocchi AM, Rivera G, Ricaurte Gracia YLN, Mohamed N, González Cárdenas VH, et al. Use of bisphosphonates in a retrospective case series of children and adolescents with complex regional pain syndrome. Paediatric Anaesthesia 2021;31:871–7.

[412] Tzschentke TM. Pharmacology of bisphosphonates in pain. British Journal of Pharmacology 2021;178:1973–94.

[413] Giustra F, Bosco F, Aprato A, Artiaco S, Bistolfi A, Masse A. Vitamin C Could Prevent Complex Regional Pain Syndrome Type I in Trauma and Orthopedic Care? A Systematic Review of the Literature and Current Findings. Sisli Etfal Hastanesi Tip Bulteni 2021;55:139–45.

[414] Hung K-C, Chiang M-H, Wu S-C, Chang Y-J, Ho C-N, Wang L-K, et al. A meta-analysis of randomized clinical trials on the impact of oral vitamin C supplementation on first-year outcomes in orthopedic patients. Scientific Reports 2021;11:9225.

[415] Hernigou J, Labadens A, Ghistelinck B, Bui Quoc E, Maes R, Bhogal H, et al. Vitamin C prevention of complex regional pain syndrome after foot and ankle surgery: a prospective randomized study of three hundred and twentynine patients. International Orthopaedics 2021;45:2453–9.

[416] Keef T, Keef S. The Efficacy of Vitamin C in the Prevention of Complex Regional Pain Syndrome After Distal Radius Fractures: A Synthesis. Journal of Pain & Palliative Care Pharmacotherapy 2018;32:208–11.

[417] Hernigou J, Valcarenghi J, Callewier A, Sohm L, Decottenier V, Ledoux A, et al. Correction to: prospective randomized study of the vitamin C effect on pain and complex pain regional syndrome after total knee arthroplasty. International Orthopaedics 2021;45:1385.

[418] Chen S, Roffey DM, Dion C-A, Arab A, Wai EK. Effect of Perioperative Vitamin C Supplementation on Postoperative Pain and the Incidence of Chronic Regional Pain Syndrome: A Systematic Review and Meta-Analysis. The Clinical Journal of Pain 2016;32:179–85.

[419] Onofrio S, Vartan CM, Nazario M, DiScala S, Cuevas-Trisan R, Melendez-Benabe J. The Use of Transdermal Buprenorphine in Complex Regional Pain Syndrome: A Report of Two Cases. Journal of Pain & Palliative Care Pharmacotherapy 2016;30:124–7.

[420] Drummond ES, Maker G, Birklein F, Finch PM, Drummond PD. Topical prazosin attenuates sensitivity to tactile stimuli in patients with complex regional pain syndrome. European Journal of Pain (London, England) 2016;20:926–35.

[421] Maihöfner C, Schneider S, Bialas P, Gockel H, Beer K-G, Bartels M, et al. Successful treatment of complex regional pain syndrome with topical ambroxol: a case series. Pain Management 2018;8:427–36.

[422] Russo MA, Santarelli DM. A Novel Compound Analgesic Cream (Ketamine, Pentoxifylline, Clonidine, DMSO) for Complex Regional Pain Syndrome Patients. Pain Practice 2016;16:E14–20.

[423] Faggiani M, Piccato A, Baroni C, Risitano S, Conforti LG. Intravenous treatment with biphosphates in Complex Regional Pain Syndrome. Acta Bio-Medica: Atenei Parmensis 2021;92:e2021190.

[424] Liu Y, Ke X, Wu X, Mei W. Ultrasound-guided Lumbar Plexus Block in Supine Position. Anesthesiology 2018;128:812.

[425] Pai RS, Vas L. Ultrasound-Guided Intra-articular Injection of the Radio-ulnar and Radio-humeral Joints and Ultrasound-Guided Dry Needling of the Affected Limb Muscles to Relieve Fixed Pronation Deformity and Myofascial Issues around the Shoulder, in a Case of Complex R. Pain Practice: The Official Journal of World Institute of Pain 2018;18:273–82.

[426] Mangnus TJP, Dirckx M, Bharwani KD, de Vos CC, Frankema SPG, Stronks DL, et al. Effect of intravenous low-dose S-ketamine on pain in patients with Complex Regional Pain Syndrome: A retrospective cohort study. Pain Practice 2021;n/a.

[427] Reilly JM, Dharmalingam B, Marsh SJ, Thompson V, Goebel A, Brown DA. Effects of serum immunoglobulins from patients with complex regional pain syndrome (CRPS) on depolarisation-induced calcium transients in isolated dorsal root ganglion (DRG) neurons. Experimental Neurology 2016;277:96–102.

[428] Roldan CJ, Lo TC, Huh B. Recurrence of complex regional pain syndrome after administration of adenosine. Pain Management 2019;9:233–7.

[429] Birklein F, Sommer C. Intravenous Immunoglobulin to Fight Complex Regional Pain Syndrome: Is Hope Gone? Annals of Internal Medicine 2017;167:515–6.

[430] Rickard JP, Kish T. Systemic Intravenous Lidocaine for the Treatment of Complex Regional Pain Syndrome: A Case Report and Literature Review. American Journal of Therapeutics 2016;23:e1266-9.

[431] Jang KS, Kim HS. Treatment for Acute Stage Complex Regional Pain Syndrome Type II with Polydeoxyribonucleotide Injection. Journal of Korean Neurosurgical Society 2016;59:529–32.

[432] Drummond PD, Morellini N, Finch PM, Birklein F, Knudsen LF. Complex regional pain syndrome: intradermal injection of phenylephrine evokes pain and hyperalgesia in a subgroup of patients with upregulated α1-adrenoceptors on dermal nerves. Pain 2018;159:2296–305.

[433] Hsiao H-T, Liu Y-Y, Wang JC-F, Lin Y-C, Liu Y-C. The analgesic effect of propofol associated with the inhibition of hypoxia inducible factor and inflammasome in complex regional pain syndrome. Journal of Biomedical Science 2019;26:74.

[434] Goebel A, Bisla J, Carganillo R, Frank B, Gupta R, Kelly J, et al. Low-Dose Intravenous Immunoglobulin Treatment for Long-Standing Complex Regional Pain Syndrome. Annals of Internal Medicine 2017;167:476–83.

[435] Hagedorn JM, McArdle I, D'Souza RS, Yadav A, Engle AM, Deer TR. Effect of Patient Characteristics on Clinical Outcomes More Than 12 Months Following Dorsal Root Ganglion Stimulation Implantation: A Retrospective Review. Neuromodulation: Journal of the International Neuromodulation Society 2021;24:695–9

[436] Mekhail N, Deer TR, Kramer J, Poree L, Amirdelfan K, Grigsby E, et al. Paresthesia-Free Dorsal Root Ganglion Stimulation: An ACCURATE Study Sub-Analysis. Neuromodulation: Journal of the International Neuromodulation Society 2020;23:185–95.

[437] Skaribas IM, Peccora C, Skaribas E. Single S1 Dorsal Root Ganglia Stimulation for Intractable Complex Regional Pain Syndrome Foot Pain After Lumbar Spine Surgery: A Case Series. Neuromodulation: Journal of the International Neuromodulation Society 2019;22:101–7.

[438] Martin SC, Macey AR, Raghu A, Edwards T, Watson C, Bojanić S, et al. Dorsal Root Ganglion Stimulation for the Treatment of Chronic Neuropathic Knee Pain. World Neurosurgery 2020;143:e303–8.

[439] Goebel A, Lewis S, Phillip R, Sharma M. Dorsal Root Ganglion Stimulation for Complex Regional Pain Syndrome (CRPS) Recurrence after Amputation for CRPS, and Failure of Conventional Spinal Cord Stimulation. Pain Practice 2018;18:104–8.

[440] Buwembo J, Munson R, Rizvi SA, Ijaz A, Gupta S. Direct Sciatic Nerve Electrical Stimulation for Complex Regional Pain Syndrome Type 1. Neuromodulation: Technology at the Neural Interface 2021;24:1075–82.

[441] Houde F, Harvey M-P, Tremblay Labrecque P-F, Lamarche F, Lefebvre A, Leonard G. Combining Transcranial Direct Current Stimulation and Transcutaneous Electrical Nerve Stimulation to Relieve Persistent Pain in a Patient Suffering from Complex Regional Pain Syndrome: A Case Report. Journal of Pain Research 2020;13:467–73.

[442] Yang A, Hunter CW. Dorsal Root Ganglion Stimulation as a Salvage Treatment for Complex Regional Pain Syndrome Refractory to Dorsal Column Spinal Cord Stimulation: A Case Series. Neuromodulation: Journal of the International Neuromodulation Society 2017;20:703–7.

[443] Hoikkanen T, Nissen M, Ikäheimo T-M, Jyrkkänen H-K, Huttunen J, von und zu Fraunberg M. Long-Term Outcome of Spinal Cord Stimulation in Complex Regional Pain Syndrome. Neurosurgery 2021;89:597–609.

[444] Ryan CG, King R, Robinson V, Punt TD, Dinse HR, Grunenberg C, et al. Transcutaneous electrical nerve stimulation using an LTP-like repetitive stimulation protocol for patients with upper limb complex regional pain syndrome: A feasibility study. Hand Therapy 2016;22:52–63.

[445] Zlatkovic-Svenda MI, Leitner C, Lazovic B, Petrovic DM. Complex Regional Pain Syndrome (Sudeck Atrophy) Prevention Possibility and Accelerated Recovery in Patients with Distal Radius at the Typical Site Fracture Using Polarized, Polychromatic Light Therapy. Photobiomodulation, Photomedicine, and Laser Surgery 2019;37:233–9.

[446] Narouze S, Souzdalnitski D. Ultrasound-Guided Percutaneous Cervical and Upper Thoracic Sympathetic Chain Neuromodulation for Upper Extremity Complex Regional Pain Syndrome. The Ochsner Journal 2017;17:199–203.

[447] Zhou L, Chou H, Holder E. Abdominal wall Type-I complex regional pain syndrome treated effectively with peripheral nerve field stimulation: a case report. Journal of Surgical Case Reports 2017;2017.

[448] Canós-Verdecho A, Abejón D, Robledo R, Izquierdo R, Bermejo A, Gallach E, et al. Randomized Prospective Study in Patients With Complex Regional Pain Syndrome of the Upper Limb With High-Frequency Spinal Cord Stimulation (10-kHz) and Low-Frequency Spinal Cord Stimulation. Neuromodulation: Journal of the International Neuromodulation Society 2021;24:448–58.

[449] Kasapovic A, Rommelspacher Y, Walter S, Gathen M, Pflugmacher R. Minimally invasive implantation technique of a system for spinal cord stimulation. Operative Orthopadie und Traumatologie 2021;33:364–73.

[450] Blackburn AZ, Chang HH, DiSilvestro K, Veeramani A, McDonald C, Zhang AS, et al. Spinal Cord Stimulation via Percutaneous and Open Implantation: Systematic Review and Meta-Analysis Examining Complication Rates. World Neurosurgery 2021;154:132-143.e1.

[451] Berger AA, Urits I, Hasoon J, Gill J, Aner M, Yazdi CA, et al. Improved Pain Control with Combination Spinal Cord Stimulator Therapy Utilizing Sub-perception and Traditional Paresthesia Based Waveforms: A Pilot Study. Anesthesiology and Pain Medicine 2021;11:e113089.

[452] Singla P, Kohan LR. Spinal Cord Stimulator Placement in Patient With von Willebrand Disease: A Case Report. A&A Practice 2020;14:149–51.

[453] Fontaine D. Spinal cord stimulation for neuropathic pain. Revue Neurologique 2021;177:838–42.

[454] Martini ML, Caridi JM, Zeldin L, Neifert SN, Nistal DA, Kim JD, et al. Perioperative Outcomes of Spinal Cord Stimulator Placement in Patients with Complex Regional Pain Syndrome Compared with Patients without Complex Regional Pain Syndrome. World Neurosurgery 2020;137:e106–17.

[455] Bakr SM, Knight J, Johnson SK, Williams AE, Tolley JA, Raskin JS. Spinal Cord Stimulation Improves Functional Outcomes in Children With Complex Regional Pain Syndrome: Case Presentation and Review of the Literature. Pain Practice 2020;20:647–55.

[456] Mekhail N, Costandi S, Mehanny DS, Armanyous S, Saied O, Taco-Vasquez E, et al. The Impact of Tobacco Smoking on Spinal Cord Stimulation Effectiveness in Complex Regional Pain Syndrome Patients. Neuromodulation: Journal of the International Neuromodulation Society 2020;23:133–9.

[457] Schwarm FP, Stein M, Uhl E, Maxeiner H, Kolodziej MA. Spinal cord stimulation for the treatment of complex regional pain syndrome leads to improvement of quality of life, reduction of pain and psychological distress: a retrospective case series with 24 months follow up. Scandinavian Journal of Pain 2020;20:253–9.

[458] Sokal P, Malukiewicz A, Kierońska S, Murawska J, Guzowski C, Rudaś M, et al. Sub-Perception and Supra-Perception Spinal Cord Stimulation in Chronic Pain Syndrome: A Randomized, Semi-Double-Blind, Crossover, Placebo-Controlled Trial. Journal of Clinical Medicine 2020;9.

[459] McCormack E, Mathkour MH, Kahn LW, Guirguis M, Chaiban G, Tolba R, et al. Complex Regional Pain Syndrome and Failed Back Surgery Syndrome With Failed High-Frequency Spinal Cord Stimulation Salvaged With Arthrodesis Revision Surgery and Burst Therapy. Neurosurgery 2019;66.

[460] Poe LM, Sobey CM. Spinal Cord Stimulation as Treatment for Truncal Chronic Regional Pain Syndrome After Cardiac Surgery: A Case Report. A&A Practice 2019;12:51–3.

[461] Garzón S JC, Poveda DS, Guardo LA, Garzón S A, Zaballos FH, Montero FJS, et al. Evaluation Through Transcutaneous Tissue Oximetry (Near Infrared Spectroscopy) of Spinal Cord Stimulation in Patients With Complex Regional Pain Syndrome Type I. Neuromodulation: Journal of the International Neuromodulation Society 2020;23:698–703.

[462] Urits I, Osman M, Orhurhu V, Viswanath O, Kaye AD, Simopoulos T, et al. A Case Study of Combined Perception-Based and Perception-Free Spinal Cord Stimulator Therapy for the Management of Persistent Pain after a Total Knee Arthroplasty. Pain and Therapy 2019;8:281–4.

[463] Lee SJ, Yoo YM, You JA, Shin SW, Kim TK, Abdi S, et al. Successful removal of permanent spinal cord stimulators in patients with complex regional pain syndrome after complete relief of pain. The Korean Journal of Pain 2019;32:47–50.

[464] Pinckard-Dover H, Palmer A, Petersen EA. A Review of Neuromodulation for Treatment of Complex Regional Pain Syndrome in Pediatric Patients and Novel Use of Dorsal Root Ganglion Stimulation in an Adolescent Patient With 30-Month Follow-Up. Neuromodulation: Journal of the International Neuromodulation Society 2021;24:634–8.

[465] Stolzenberg D, Ahn JJ, Lendner M, Kurd M. Thoracolumbar Spinal Cord Stimulator Trial: Procedural Technique. Clinical Spine Surgery 2021;34:51–5.

[466] Nardone R, Brigo F, Höller Y, Sebastianelli L, Versace V, Saltuari L, et al. Transcranial magnetic stimulation studies in complex regional pain syndrome type I: A review. Acta Neurologica Scandinavica 2018;137:158–64.

[467] Chauhan G, Roth BI, Mekhail N. Dorsal root ganglion stimulation lead fractures: potential mechanisms and ways to avoid. BMJ Case Reports 2021;14.

[468] Chang MC, Kwak SG, Park D. The effect of rTMS in the management of pain associated with CRPS. Translational Neuroscience 2020;11:363–70.

[469] Lagueux É, Bernier M, Bourgault P, Whittingstall K, Mercier C, Léonard G, et al. The Effectiveness of Transcranial Direct Current Stimulation as an Add-on Modality to Graded Motor Imagery for Treatment of Complex Regional Pain Syndrome: A Randomized Proof of Concept Study. The Clinical Journal of Pain 2018;34:145–54.

[470] Dombovy-Johnson ML, Hagedorn JM, Lamer TJ. Dorsal Root Ganglion Stimulation for Complex Regional Pain Syndrome in Spinal Cord Injury. Pain Medicine (Malden, Mass) 2021;22:1224–7.

[471] Smith GL, Petersen EA, Paul C, Goree JH. Transgrade Dorsal Root Ganglion Stimulation as a Salvage Technique for Three Different Anatomical Barriers: A Case Series. Neuromodulation: Journal of the International Neuromodulation Society 2021;24:763–8.

[472] Pendem K, Jassal N. Dorsal Root Ganglion Stimulation as Treatment for Complex Regional Pain Syndrome of the Foot Refractory to Spinal Cord Stimulation: A Case Report. Cureus 2021;13:e12753.

[473] Ghosh P, Gungor S. Utilization of Concurrent Dorsal Root Ganglion Stimulation and Dorsal Column Spinal Cord Stimulation in Complex Regional Pain Syndrome. Neuromodulation: Journal of the International Neuromodulation Society 2021;24:769–73.

[474] Kriek N, Groeneweg JG, Stronks DL, de Ridder D, Huygen FJPM. Preferred frequencies and waveforms for spinal cord stimulation in patients with complex regional pain syndrome: A multicentre, double-blind, randomized and placebo-controlled crossover trial. European Journal of Pain (London, England) 2017;21:507–19.

[475] Hoydonckx Y, Costanzi M, Bhatia A. A scoping review of novel spinal cord stimulation modes for complex regional pain syndrome. Canadian Journal of Pain 2019;3:33–48.

[476] Wolter T. Spinal Cord Stimulation with Percutaneous Type Lead in a Deaf Patient with Complex Regional Pain Syndrome Type II. Pain Practice: The Official Journal of World Institute of Pain 2018;18:815–6.

[477] Yang J, Choi Y, Park J, Jeong J, Lee B, Lee K, et al. Reversible Horner's syndrome after cervical spinal cord stimulator implantation in a patient with complex regional pain syndrome. Journal of Pain Research 2018;11:3019–23.

[478] Risson EG, Serpa AP, Berger JJ, Koerbel RFH, Koerbel A. Spinal cord stimulation in the treatment of complex regional pain syndrome type 1: Is trial truly required? Clinical Neurology and Neurosurgery 2018;171:156–62.

[479] Kriek N, Schreurs MWJ, Groeneweg JG, Dik WA, Tjiang GCH, Gültuna I, et al. Spinal Cord Stimulation in Patients With Complex Regional Pain Syndrome: A Possible Target for Immunomodulation? Neuromodulation: Technology at the Neural Interface 2018;21:77–86.

[480] Hao D, Kiss G, Grubb W, Cohen S, Levin D, Sakr A. Spinal Cord Neuromodulation Therapy for Levofloxacin-Reinduced Complex Regional Pain Syndrome and Neurotoxicity: A Case Report. A&A Practice 2018;11:158–9.

[481] Crapanzano JT, Harrison-Bernard LM, Jones MR, Kaye AD, Richter EO, Potash MN. High Frequency Spinal Cord Stimulation for Complex Regional Pain Syndrome: A Case Report. Pain Physician 2017;20:E177–82.

[482] Hylands-White N, Duarte R v, Beeson P, Mayhew SD, Raphael JH. Electroencephalographic evoked pain response is suppressed by spinal cord stimulation in complex regional pain syndrome: a case report. Journal of Clinical Monitoring and Computing 2016;30:845–8.

[483] Lopez WO, Barbosa DC, Teixera MJ, Paiz M, Moura L, Monaco BA, et al. Pain Relief in CRPS-II after Spinal Cord and Motor Cortex Simultaneous Dual Stimulation. Pain Physician 2016;19:E631-5.

[484] Jozwiak MJ, Wu H. Complex Regional Pain Syndrome Management: An Evaluation of the Risks and Benefits of Spinal Cord Stimulator Use in Pregnancy. Pain Practice 2020;20:88–94. https://doi.org/https://doi.org/10.1111/papr.12825.

[485] Bilgili A, Çakır T, Doğan ŞK, Erçalık T, Filiz MB, Toraman F. The effectiveness of transcutaneous electrical nerve stimulation in the management of patients with complex regional pain syndrome: A randomized, double-blinded, placebo-controlled prospective study. Journal of Back and Musculoskeletal Rehabilitation 2016;29:661–71.

[486] Alkosha HM, Elkiran YM. Predictors of Long-Term Outcome of Thoracic Sympathectomy in Patients with Complex Regional Pain Syndrome Type 2. World Neurosurgery 2016;92:74–82.

[487] Kim E, Roh M, Kim S, Jo D. Continuous Thoracic Sympathetic Ganglion Block in Complex Regional Pain Syndrome Patients with Spinal Cord Stimulation Implantation. Pain Research and Management 2016;2016:5461989.

[488] Gungor S, Aiyer R. Extrapyramidal signs occurring after sympathetic block for complex regional pain syndrome responding to diphenhydramine: Two case reports. Medicine 2018;97:e11301.

[489] Rajagopalan V, Chouhan RS, Pandia MP, Lamsal R, Bithal PK, Rath GP. Effect of Stellate Ganglion Block on Intraoperative Propofol and Fentanyl Consumption in Patients with Complex Regional Pain Syndrome Undergoing Surgical Repair of Brachial Plexus Injury: A Randomized, Double-blind, Placebo-controlled Trial. Neurology India 2020;68:617–23.

[490] Ferrillo MG. Treatment of complex regional pain syndrome with stellate ganglion local anesthetic blockade: a case report of one patient's experiences with traditional bupivacaine HCl and liposome bupivacaine. Clinical Case Reports 2016;4:861–5.

[491] Kim ED, Yoo WJ, Lee YJ, Park HJ. Perfusion index as a tool to evaluate the efficacy of stellate ganglion block for complex regional pain syndrome. Clinical Autonomic Research: Official Journal of the Clinical Autonomic Research Society 2019;29:257–9.

[492] Datta R, Agrawal J, Sharma A, Rathore VS, Datta S. A study of the efficacy of stellate ganglion blocks in complex regional pain syndromes of the upper body. Journal of Anaesthesiology, Clinical Pharmacology 2017;33:534–40.

[493] Kang SH, Sim WS, Park HJ, Moon JY, Seon HJ, Lee JY. Efficacy of adjuvant dexmedetomidine in supraclavicular brachial plexus block for intractable complex regional pain syndrome: A case report with a 3-year follow-up. Journal of Clinical Pharmacy and Therapeutics 2020;45:365–7.

[494] Gungor S, Brar J. Epidural approach to paravertebral thoracic sympathetic block as an alternative to stellate ganglion block: A case report. Medicine 2018;97:e11492.

[495] Zyluk A, Puchalski P. Pain control in chronic, refractory CRPS by continuous brachial plexus analgesia. Handchirurgie, Mikrochirurgie, Plastische Chirurgie: Organ Der Deutschsprachigen Arbeitsgemeinschaft Fur Handchirurgie : Organ Der Deutschsprachigen Arbeitsgemeinschaft Fur Mikrochirurgie Der Peripheren Nerven Und Gefasse : Organ Der V. 2018;50:190–5.

[496] Frederico TN, da Silva Freitas T. Peripheral Nerve Stimulation of the Brachial Plexus for Chronic Refractory CRPS Pain of the Upper Limb: Description of a New Technique and Case Series. Pain Medicine (Malden, Mass) 2020;21:S18–26.

[497] Elkoundi A, Eloukkal Z, Bensghir M, Belyamani L. Priapism following erector spinae plane block for the treatment of a complex regional pain syndrome. The American Journal of Emergency Medicine 2019;37:796.e3-796.e4.

[498] Emami SA, Majedi H, Espahbodi E, Sanatkar M. Bier block as a successful management of a patient with intractable complex regional pain syndrome (CRPS) type 1: A case report. Clinical Case Reports 2021;9:e04554.

[499] Dev S, Yoo Y, Lee H-J, Kim D-H, Kim Y-C, Moon JY. Does Temperature Increase by Sympathetic Neurolysis Improve Pain in Complex Regional Pain Syndrome? A Retrospective Cohort Study. World Neurosurgery 2018;109:e783–91.

[500] Hayashi K, Nishiwaki K, Kako M, Suzuki K, Hattori K, Sato K, et al. Combination of Continuous Epidural Block and Rehabilitation in a Case of Complex Regional Pain Syndrome. Journal of Nippon Medical School = Nippon Ika Daigaku Zasshi 2016;83:262–7.

[501] Henshaw DS, Kittner SL, Jaffe JD. Ultrasound-Guided Continuous Superficial Radial Nerve Block for Complex Regional Pain Syndrome. Journal of Pain & Palliative Care Pharmacotherapy 2016;30:118–23.

[502] Awal S, Madabushi R, Agarwal A, Singla V. CRPS: Early Lumbar Sympathetic Block is Better Compared to Other Interventions. Pain Physician 2016;19:E363.

[503] Gungor S, Rana B, Fields K, Bae JJ, Mount L, Buschiazzo V. Changes in the Skin Conductance Monitor as an End Point for Sympathetic Nerve Blocks. Pain Medicine 2017;18:2187–97.

[504] Cheng J, Salmasi V, You J, Grille M, Yang D, Mascha EJ, et al. Outcomes of Sympathetic Blocks in the Management of Complex Regional Pain Syndrome: A Retrospective Cohort Study. Anesthesiology 2019;131:883–93.

[505] Lee Y, Lee CJ, Choi E, Lee PB, Lee HJ, Nahm FS. Lumbar sympathetic block with botulinum toxin type A and type B for the complex regional pain syndrome. Toxins 2018;10:4–11.

[506] Dellon AL. Comments on "Targeted muscle reinnervation at the time of amputation in the management of complex regional pain syndrome of the leg: A case series". Microsurgery 2021;41:594.

[507] Russo M, Georgius P, Volschenk W, Santarelli D. Commentary on: Outcomes of amputation due to long-standing therapy-resistant complex regional pain syndrome type I. Journal of Rehabilitation Medicine 2020;52:jrm00117.

[508] Stoehr JR, Sood R, Jordan SW, Dumanian GA. Targeted muscle reinnervation at the time of amputation in the management of complex regional pain syndrome of the lower extremity. Microsurgery 2020;40:852–8.

[509] Geertzen JHB, Scheper J, Schrier E, Dijkstra PU. Outcomes of amputation due to long-standing therapy-resistant complex regional pain syndrome type I. Journal of Rehabilitation Medicine 2020;52:jrm00087.

[510] George JA, Brinton MR, Duncan CC, Hutchinson DT, Clark GA. Improved Training Paradigms and Motor-decode Algorithms: Results from Intact Individuals and a Recent Transradial Amputee with Prior Complex Regional Pain Syndrome. 40th Annual International Conference of the IEEE Engineering in Medicine and Biology Society (EMBC), IEEE; 2018, p. 3782–7.

[511] Schrier E, Geertzen JHB, Scheper J, Dijkstra PU. Psychosocial factors associated with poor outcomes after amputation for complex regional pain syndrome type-I. PLOS ONE 2019;14:e0213589.

[512] Midbari A, Eisenberg E. Is the Pain Medicine Community Reluctant to Discuss Limb Amputation in Patients with Intractable Complex Regional Pain Syndrome? Pain Medicine (Malden, Mass) 2017;18:1406–7.

[513] Schrier E, Dijkstra PU, Zeebregts CJ, Wolff AP, Geertzen JHB. Decision making process for amputation in case of therapy resistant complex regional pain syndrome type-I in a Dutch specialist centre. Medical Hypotheses 2018;121:15–20.

[514] Carpenter DP, Draeger RW. Neurogenic Edema from Complex Regional Pain Syndrome Resulting in Fulminant Infection Necessitating Below Elbow Amputation. Journal of Hand and Microsurgery 2017;9:159–62.

[515] Karatzios C, Luthi F, Muff G, Benaim C. Complex regional pain syndrome of the residual limb in a transtibial lower-limb amputee: diagnosis and treatment. BMJ Case Reports 2021;14.

[516] Hoellwarth JS, Al-Jawazneh SS, Tetsworth K, Lu W, Roberts C, al Muderis M. Amputation With Osseointegration for Patients With Intractable Complex Regional Pain Syndrome: A Report of 3 Cases. JBJS Case Connector 2021;11:e20.00267.

[517] Flor H. Home training in sensorimotor discrimination reduces pain in complex regional pain syndrome (CRPS). Scandinavian Journal of Pain 2017;15:113–4.

[518] Foncelle A, Christophe L, Revol P, Havé L, Jacquin-Courtois S, Rossetti Y, et al. Prism adaptation effects in complex regional pain syndrome: A therapo-physiological single case experimental design exploratory report. Neuropsychological Rehabilitation 2021:1–18.

[519] Duong S, Bravo D, Todd KJ, Finlayson RJ, Tran DQ. Treatment of complex regional pain syndrome: an updated systematic review and narrative synthesis. Canadian Journal of Anaesthesia = Journal Canadien d'anesthesie 2018;65:658–84.

[520] Thor JA, Mohamed Hanapi NH, Halil H, Suhaimi A. Perineural Injection Therapy in the Management of Complex Regional Pain Syndrome: A Sweet Solution to Pain. Pain Medicine (Malden, Mass) 2017;18:2041–5.

[521] Seo D-K, Lee H-S, Hong JP, Seo J-H, Shin JW. Treatment of complex regional pain syndrome using free-flap surgery: a case report. Journal of Pain Research 2017;10:2699–702.

[522] Cook D. Complex Regional Pain Syndrome: New and Emerging Therapies. Pain Management Nursing 2016;17:102.

[523] Wang J-H, Sun T. Comparison of effects of seven treatment methods for distal radius fracture on minimizing complex regional pain syndrome. Archives of Medical Science 2017;13:163–73.

[524] Conen H, Seelmann C, Ohmann T, Papenhoff M. Bilateral desensitization in CRPS with allodynia of the hand: An innovative treatment approach in ergotherapy. Schmerz (Berlin, Germany) 2020;34:79–83.

[525] Schneider B. Der Einsatz von Blutegeln bei der Behandlung eines komplexen regionalen Schmerzsyndroms (CRPS)The use of leeches in the treatment of complex regional pain syndrome (CRPS): Ein ErfahrungsberichtA field report. Deutsche Zeitschrift Für Akupunktur 2020;63.

[526] Binkley K, Katznelson R. Successful Treatment of Long Standing Complex Regional Pain Syndrome with Hyperbaric Oxygen Therapy. Journal of Neuroimmune Pharmacology 2020;15:1–6.

[527] Katznelson R, Segal SC, Clarke H. Successful Treatment of Lower Limb Complex Regional Pain Syndrome following Three Weeks of Hyperbaric Oxygen Therapy. Pain Research and Management 2016;2016:3458371.

[528] Halicka M, Vittersø AD, McCullough H, Goebel A, Heelas L, Proulx MJ, et al. Prism adaptation treatment for upper-limb complex regional pain syndrome: a double-blind randomized controlled trial. Pain 2021;162:471–89.

[529] Cha M, Lee KH, Kwon M, Lee BH. Possible Therapeutic Options for Complex Regional Pain Syndrome. Biomedicines 2021;9.

[530] Boichat C, Llewellyn A, Grieve S, McCabe C. The Role of Nonmedical Therapeutic Approaches in the Rehabilitation of Complex Regional Pain Syndrome. Current Treatment Options in Rheumatology 2020;6:299–311.

[531] Ramanathan S, Douglas SR, Alexander GM, Shenoda BB, Barrett JE, Aradillas E, et al. Exosome microRNA signatures in patients with complex regional pain syndrome undergoing plasma exchange. Journal of Translational Medicine 2019;17:81.

[532] Goebel A, Callaghan T, Jones S, Bridson J. Patient consultation about a trial of therapeutic plasma exchange for complex regional pain syndrome. Journal of Clinical Apheresis 2018;33:661–5.

[533] McRoberts WP, Apostol C, Haleem A. Intrathecal Bupivacaine Monotherapy with a Retrograde Catheter for the Management of Complex Regional Pain Syndrome of the Lower Extremity. Pain Physician 2016;19:E1087-92.

[534] Sweeting M-J, Llewellyn A, McCabe C. Living with complex regional pain syndrome: identifying the bio-psychosocial impacts. Rheumatology 2018;57.

[535] Speck V, Schlereth T, Birklein F, Maihöfner C. Increased prevalence of posttraumatic stress disorder in CRPS. European Journal of Pain (London, England) 2017;21:466–73.

[536] Brinkers M, Rumpelt P, Lux A, Kretzschmar M, Pfau G. Psychiatric Disorders in Complex Regional Pain Syndrome (CRPS): The Role of the Consultation-Liaison Psychiatrist. Pain Research and Management 2018;2018:2894360.

[537] Antunovich DR, Horne JC, Tuck NL, Bean DJ. Are Illness Perceptions Associated with Pain and Disability in Complex Regional Pain Syndrome? A Cross-Sectional Study. Pain Medicine (Malden, Mass) 2021;22:100–11.

[538] Lee J, Lim YH, Hong SJ, Jeong JH, Choi HR, Park SK, et al. Multicenter survey of symptoms, work life, economic status, and quality of life of complex regional pain syndrome patients. The Korean Journal of Pain 2021;34:288–303.

[539] Kwon SJ, Kim Y. Analysis of the Experiences of Adults with Complex Regional Pain Syndrome. Healthcare 2021;9.

[540] Johnston-Devin C, Oprescu F, Gray M, Wallis M. Patients Describe their Lived Experiences of Battling to Live with Complex Regional Pain Syndrome. The Journal of Pain 2021;22:1111–28.

[541] Yoo H, Jeong T, Cho S. Impact of Instability in Emotional Support Discrepancy from Significant Others on Daily Functioning in Patients with Complex Regional Pain Syndrome (CRPS) : A Diary Study. Stress 2020;28:276–84. https://doi.org/10.17547/kjsr.2020.28.4.276.

[542] Palmer S, Bailey J, Brown C, Jones A, McCabe CS. Sensory Function and Pain Experience in Arthritis, Complex Regional Pain Syndrome, Fibromyalgia Syndrome, and Pain-Free Volunteers: A Cross-Sectional Study. The Clinical Journal of Pain 2019;35:894–900.

[543] di Pietro F, Lee B, Henderson LA. Altered resting activity patterns and connectivity in individuals with complex regional pain syndrome. Human Brain Mapping 2020;41:3781–93.

[544] Beales D, Carolan D, Chuah-Choong J, Hammond S, O'Brien E, Boyle E, et al. Exploring peoples' lived experience of complex regional pain syndrome in Australia: a qualitative study. Scandinavian Journal of Pain 2021;21:393–405.

[545] Antunovich D, Tuck N, Reynolds LM, Bean D. I don’t identify with it": A qualitative analysis of people’s experiences of living with Complex Regional Pain Syndrome. Pain Medicine (Malden, Mass) 2021.

[546] Packham TL, Wainio K, Wong M-K. Persons with Complex Regional Pain Syndrome Renegotiate Social Roles and Intimacy: A Qualitative Study. Pain Medicine (Malden, Mass) 2020;21:239–46.

[547] Llewellyn A, McCabe CS, Hibberd Y, White P, Davies L, Marinus J, et al. Are you better? A multi-centre study of patient-defined recovery from Complex Regional Pain Syndrome. European Journal of Pain (London, England) 2018;22:551–64.

[548] Lewis J, Kellett S, McCullough R, Tapper A, Tyler C, Viner M. A clinical evaluation of rehabilitation outcomes in complex regional pain syndrome. Rheumatology 2018;57.

[549] Simmel S, Melf-Marzi A. Pain Rehabilitation in CRPS. Die Rehabilitation 2019;58:172–80.

[550] Miller C, Williams M, Heine P, Williamson E, O’connell N. Current practice in the rehabilitation of complex regional pain syndrome: a survey of practitioners. Disability and Rehabilitation 2019;41:847–53.

[551] Altas EU, Onat ŞŞ, Konak HE, Polat CS. Post-stroke complex regional pain syndrome and related factors: Experiences from a tertiary rehabilitation center. Journal of Stroke and Cerebrovascular Diseases 2020;29:104995.

[552] Kim IS, Hyun SE, Park J, Lim J-Y. Understanding the Rehabilitation Needs of Korean Patients With Complex Regional Pain Syndrome. Annals of Rehabilitation Medicine 2020;44:218–27.

[553] Simmel S, Melf-Marzi A. Schmerzrehabilitation beim CRPS. Physikalische Medizin, Rehabilitationsmedizin, Kurortmedizin 2021;31:136–50.

[554] Baygutalp F, Kul A. Effect of Early Orthopedic Rehabilitation on Development of Complex Regional Pain Syndrome Type 1. The Eurasian Journal of Medicine 2020;52:110–4.

[555] Mouraux D, Lenoir C, Tuna T, Brassinne E, Sobczak S. The long-term effect of complex regional pain syndrome type 1 on disability and quality of life after foot injury. Disability and Rehabilitation 2021;43:967–75.

[556] Packham TL, Spicher CJ, MacDermid JC, Michlovitz S, Buckley DN. Somatosensory rehabilitation for allodynia in complex regional pain syndrome of the upper limb: A retrospective cohort study. Journal of Hand Therapy: Official Journal of the American Society of Hand Therapists 2018;31:10–9.

[557] Packham T, Holly J. Mechanism-specific rehabilitation management of complex regional pain syndrome: Proposed recommendations from evidence synthesis. Journal of Hand Therapy: Official Journal of the American Society of Hand Therapists 2018;31:238–49.

[558] Taylor S-S, Noor N, Urits I, Paladini A, Sadhu MS, Gibb C, et al. Correction to: Complex Regional Pain Syndrome: A Comprehensive Review. Pain and Therapy 2021.

[559] Hernández-Porras BC, Plancarte-Sánchez R, Alarcón-Barrios S, Sámano-García M. Complex regional pain syndrome: A review. Cirugia y cirujanos 2017;85:366–74.

[560] Prasad Md A, Chakravarthy Md K. Review of complex regional pain syndrome and the role of the neuroimmune axis. Molecular Pain 2021;17:17448069211006616.

[561] Taylor S-S, Noor N, Urits I, Paladini A, Sadhu MS, Gibb C, et al. Complex Regional Pain Syndrome: A Comprehensive Review. Pain and Therapy 2021.

[562] Kessler A, Yoo M, Calisoff R. Complex regional pain syndrome: An updated comprehensive review. NeuroRehabilitation 2020;47:253–64.

[563] Capuco A, Urits I, Orhurhu V, Chun R, Shukla B, Burke M, et al. A Comprehensive Review of the Diagnosis, Treatment, and Management of Postmastectomy Pain Syndrome. Current Pain and Headache Reports 2020;24:41.

[564] Alkali NH, Al-Tahan AM, Al-Majed M, Al-Tahan H. Complex regional pain syndrome: A case report and review of the literature. Annals of African Medicine 2020;19:68–70.

[565] Bean DJ, Johnson MH, Heiss-Dunlop W, Kydd RR. Extent of recovery in the first 12 months of complex regional pain syndrome type-1: A prospective study. European Journal of Pain 2016;20:884–94.

[566] Bussa M, Mascaro A, Cuffaro L, Rinaldi S. Adult Complex Regional Pain Syndrome Type I: A Narrative Review. PM & R: The Journal of Injury, Function, and Rehabilitation 2017;9:707–19.

[567] Bean DJ, Johnson MH, Heiss-Dunlop W, Kydd RR. Factors Associated With Disability and Sick Leave in Early Complex Regional Pain Syndrome Type-1. The Clinical Journal of Pain 2016;32:130–8.

[568] Raut MS, Maheshwari A. Stellate Ganglion Block: Important Weapon in the Anesthesiologists' Armamentarium. Journal of Cardiothoracic and Vascular Anesthesia 2018;32:e36–7.

[569] Cornman-Homonoff J, Holzwanger DJ, Lee KS, Madoff DC, Li D. Celiac Plexus Block and Neurolysis in the Management of Chronic Upper Abdominal Pain. Seminars in Interventional Radiology 2017;34:376–86.

[570] John R, Dixon B, Shienbaum R. Celiac Plexus Block. StatPearls [Internet] 2021. https://www.ncbi.nlm.nih.gov/books/NBK531469/#_NBK531469_pubdet_.

[571] Mesa JMG, Granados EO, del Valle Hoyos M, Rivera M. Bloqueo simpático lumbar. Revista de La Sociedad Espanola Del Dolor 2013;20:324–31.

[572] An JW, Koh JC, Sun JM, Park JY, Choi JB, Shin MJ, et al. Clinical Identification of the Vertebral Level at Which the Lumbar Sympathetic Ganglia Aggregate. Korean Journal of Pain 2016;29:103–9.

[573] Mandl F. Die Paravertebrale Injektion: Anatomie und Technik, Begründung und Anwendung. Springer Vienna; 1926.

[574] Kappis M. Weitere erfahrungen mit der sympathektomie. Klinische Wochenschrift 1923;2:1441–6.

[575] Adson AW, Brown GE. The treatment of Raynaud's disease by resection of the upper thoracic and lumbar sympathetic ganglia and trunks. Surg Gynecol Obstet 1929;48:186.

[576] Adson AW, Brown GE. Treatment of Raynaud's disease: by lumbar ramisection and ganglionectomy and perivascular sympathetic neuroctomy of the common iliacs. Journal of the American Medical Association 1925;84:1908–10.

[577] Velzen GAJ van, Perez RSGM, Gestel MA van, Huygen FJPM, Kleef M van, Eijs F van, et al. Health-related quality of life in 975 patients with complex regional pain syndrome type 1. Pain 2014;155:629–34.

[578] Yoshida WB, Cataneo DC, Bomfim GAZ, Hasimoto E, Cataneo AJM. Chemical lumbar sympathectomy in plantar hyperhidrosis. Clinical Autonomic Research : Official Journal of the Clinical Autonomic Research Society 2010;20:113–5.

[579] Kim WO, Yoon KB, Kil HK, Yoon DM. Chemical lumbar sympathetic block in the treatment of plantar hyperhidrosis: a study of 69 patients. Dermatologic Surgery: Official Publication for American Society for Dermatologic Surgery [et Al] 2008;34:1340–5.

[580] Wu CL, Marsh A, Dworkin RH. The role of sympathetic nerve blocks in herpes zoster and postherpetic neuralgia. Pain 2000;87:121–9.

[581] Cheng J, Daftari A, Zhou L. Sympathetic blocks provided sustained pain relief in a patient with refractory painful diabetic neuropathy. Case Reports in Anesthesiology 2012;2012:285328.

[582] Sun H, He M, Pang J, Guo X. Continuous Lumbar Sympathetic Blockade Enhances the Effect of Lumbar Sympatholysis on Refractory Diabetic Neuropathy: A Randomized Controlled Trial. Diabetes Ther 2020;11:2647–55.

[583] Middleton WJ, Chan VWS. Lumbar sympathetic block: A review of complications. Techniques in Regional Anesthesia and Pain Management 1998;2:137–46.

[584] Kim WH, Kim SK, Lee CJ, Kim TH, Sim WS. Determination of adequate entry angle of lumbar sympathetic ganglion block in korean. The Korean Journal of Pain 2010;23:11–7.

[585] Stanton-Hicks M. Complications of sympathetic blocks for extremity pain. Techniques in Regional Anesthesia and Pain Management 2007;11:148–51.

[586] Brodal P. The Central Nervous System. Oxford University Press; 2016.

[587] Drake RL, Vogl W, Mitchell AWM, Gray H. Gray's anatomy for students, 4th edition. Philadelphia: Elsevier Inc.; 2020.

[588] Medium69, Jmarch. Nervous system diagram. Wikipedia n.d.

[589] Rothstein D, Demesmin D. Peripheral Nerve Anatomy. In: Deer TR, Pope JE, Lamer TJ, Provenzano D, editors. Deer's Treatment of Pain: An Illustrated Guide for Practitioners, Cham: Springer International Publishing; 2019, p. 35–42.

[590] Crossman AR, Neary D. Neuroanatomy E-Book: An Illustrated Colour Text. Elsevier Health Sciences; 2018.

[591] Cota AG. Spinal Cord Anatomy. In: Deer TR, Pope JE, Lamer TJ, Provenzano D, editors. Deer's Treatment of Pain: An Illustrated Guide for Practitioners, Cham: Springer International Publishing; 2019, p. 43–8.

[592] ScientificAnimation. n.d. https://www.scientificanimations.com.

[593] Rocco AG, Kaul AF, Reisman RM, Gallo JP, Lief PA. A comparison of regional intravenous guanethidine and reserpine in reflex sympathetic dystrophy a controlled, randomized, double-blind crossover study. Clinical Journal of Pain 1989;5:205–9.

[594] Gandhi KR, Verma VK, Chavan SK, Joshi SD, Joshi SS. The morphology of lumbar sympathetic trunk in humans: a cadaveric study. Folia Morphol 2013;72:217–22.

[595] Gofeld M, Shankar H, Benzon HT. Fluoroscopy and ultrasound-guided sympathetic blocks: stellate ganglion, lumbar sympathetic blocks, and visceral sympathetic blocks. In: Benzon HT, Raja SN, Liu SS, Fishman SM, Cohen SPBT-E of PM (Fourth E, editors. Essentials of Pain Medicine. Fourth Edi, Elsevier; 2018, p. 789–804.e2.

[596] Punj J, Marada S. Ultrasound lumbar sympathetic block: Out of plane approach with insulated stimulation needle - Case series of three patients. Indian Journal of Anaesthesia 2020;64.

[597] Schmid MR, Kissling RO, Curt A, Jaschko G. Sympathetic Skin Response: Monitoring of CT-guided Lumbar Sympathetic Blocks. Vascular and Interventional Radiology 2006;241:595–602.

[598] Sze DY, Mackey SC. MR Guidance of Sympathetic Nerve Blockade: Measurement of Vasomotor Response Initial Experience in Seven Patients. Radiology 2002;223:574–80.

[599] Park SY, Nahm FS, Kim YC, Lee SCJC, Sim SE, Lee SCJC. The cut-off rate of skin temperature change to confirm successful lumbar sympathetic block. Journal of International Medical Research 2010;38:266–75.

[600] Ryu J, Lee C, Kim Y, Lee S, Shankar H, Moon J. Ultrasound-Assisted Versus Fluoroscopic-Guided Lumbar Sympathetic Ganglion Block: A Prospective and Randomized Study. Chronic Pain Medicine 2018;126:1362–8.

[601] Marhofer D, Marhofer P, Kettner SC, Fleischmann E, Prayer D, Schernthaner M, et al. Magnetic resonance imaging analysis of the spread of local anesthetic solution after ultrasound-guided lateral thoracic paravertebral blockade: A volunteer study. Anesthesiology 2013;118:1106–12.

[602] Bang YJ, Sim WS, Lee DW, Lee JY. Correlation between paravertebral spread of injectate and clinical efficacy in lumbar transforaminal block. Scientific Reports 2020;10:1–7.

[603] Wasner G, Schattschneider J, Heckmann K, Maier C, Baron R. Vascular abnormalities in reflex sympathetic dystrophy (CRPS I): Mechanisms and diagnostic value. Brain 2001;124:587–99.

[604] Joo EY, Kong YG, Lee J, Cho HS, Kim SH, Suh JH. Change in pulse transit time in the lower extremity after lumbar sympathetic ganglion block: an early indicator of successful block. Journal of International Medical Research 2017;45:203–10.

[605] Park SY, Baek HJ, Park KS, Kim YC. Photoplethysmographic signals to predict the success of lumbar sympathetic blockade for lower extremity pain. Journal of International Medical Research 2014;42:938–48.

[606] Chung K, Kim KH, Kim ED. Perfusion index as a reliable parameter of vasomotor disturbance in complex regional pain syndrome. British Journal of Anaesthesia 2018;121:1133–7.

[607] Hermanns H, Werdehausen R, Hollmann MW, Stevens MF. Assessment of skin temperature during regional anaesthesia: What the anaesthesiologist should know. Acta Anaesthesiologica Scandinavica 2018;62:1280–9.

[608] Breivik H, Cousins MJ. Sympathetic neural blockade of upper and lower extremity. Anesthesia Key 2012.

[609] Lange KHW, Jansen T, Asghar S, Kristensen PL, Skjønnemand M, Nørgaard P. Skin temperature measured by infrared thermography after specific ultrasound-guided blocking of the musculocutaneous, radial, ulnar, and median nerves in the upper extremity. British Journal of Anaesthesia 2011;106:887–95.

[610] Schick CH, Fronek K, Held A, Birklein F, Hohenberger W, Schmelz M. Differential effects of surgical sympathetic block on sudomotor and vasoconstrictor function. Neurology 2003;60:1771–6.

[611] Galvin EM, Niehof S, Verbrugge SJ, Maissan I, Jahn A, Klein J, et al. Peripheral flow index is a reliable and early indicator of regional block success. Anesthesia and Analgesia 2006;103:239–43, table of contents.

[612] Ross JP. Some unsolved problems in the surgery of the sympathetic nervous system. Quarterly Bulletin Northwestern University (Evanston, Ill) Medical School 1954;28:1–9.

[613] Cracowski J-L, Roustit M. Human Skin Microcirculation. Comprehensive Physiology 2020;10:1105–54.

[614] Roddie IC. Circulation to Skin and Adipose Tissue. Comprehensive Physiology 2011:285–317.

[615] Incropera FP. Fundamentals of Heat and Mass Transfer. Hoboken, NJ, USA: John Wiley & Sons, Inc.; 2006.

[616] Blatteis CM. Physiology and Pathophysiology of Temperature Regulation. World Scientific; 1998.

[617] Ammer K, Ring F. The thermal human body: A practical guide to thermal imaging. Jenny Stanford Publishing Pte. Ltd.; 2019.

[618] Imeri L. Thermoregulation as a non-unified system: A difficult to teach concept. Temperature 2017;4:1–8.

[619] Childs C. Body temperature and clinical thermometry. In: Romanovsky AABT-H of CN, editor. Thermoregulation: From Basic Neuroscience to Clinical Neurology, Part II, vol. 157, Elsevier; 2018, p. 467–82.

[620] Romanovsky AA. The thermoregulation system and how it works. In: Romanovsky AABT-H of CN, editor. Thermoregulation: From Basic Neuroscience to Clinical Neurology Part I, vol. 156, Elsevier; 2018, p. 3–43.

[621] IUPS Thermal Commission. Glossary of terms for thermal physiology. Jpn J Physiol 2001;51:245–80.

[622] Kingma BR, Frijns AJ, Schellen L, van Marken Lichtenbelt WD. Beyond the classic thermoneutral zone: Including thermal comfort. Temperature (Austin, Tex) 2014;1:142–9.

[623] MitOpencourseWare. Human body temperature n.d. https://www.flickr.com/photos/mitopencourseware/3029642097/in/photostream/.

[624] Chudecka M, Lubkowska A. Thermal maps of young women and men. Infrared Physics & Technology 2015;69:81–7.

[625] Nardin RA, Fogerson PM, Nie R, Rutkove SB. Foot Temperature in Healthy Individuals: Effects of Ambient Temperature and Age. Journal of the American Podiatric Medical Association 2010;100:258–64.

[626] Zolet CMLS, Ulbricht L, Romaneli EFR, Neves EB. Thermal Asymmetries and Mean Foot Temperature. Annual International Conference of the IEEE Engineering in Medicine and Biology Society IEEE Engineering in Medicine and Biology Society Annual International Conference 2019;2019:2821–4.

[627] Macdonald A, Petrova N, Ainarkar S, Allen J, Plassmann P, Whittam A, et al. Thermal symmetry of healthy feet: a precursor to a thermal study of diabetic feet prior to skin breakdown. Physiological Measurement 2017;38:33–44.

[628] Carabott M, Formosa C, Mizzi A, Papanas N, Gatt A. Thermographic Characteristics of the Diabetic Foot With Peripheral Arterial Disease Using the Angiosome Concept. Experimental and Clinical Endocrinology & Diabetes: Official Journal, German Society of Endocrinology [and] German Diabetes Association 2021;129:93–8.

[629] Gatt A, Borg A, Mercieca C, Grech Scalpello A, Camilleri L, Gatt C, et al. Thermographic analysis of hands and wrists of rheumatoid arthritis patients. Annals of the Rheumatic Diseases 2018;77:803 LP – 804.

[630] Gatt A, Formosa C, Cassar K, Camilleri KP, de Raffaele C, Mizzi A, et al. Thermographic Patterns of the Upper and Lower Limbs: Baseline Data. International Journal of Vascular Medicine 2015;2015:831369.

[631] Walløe L. Arterio-venous anastomoses in the human skin and their role in temperature control. Temperature 2016;3:92–103.

[632] Xu X, Kim S, Clune JE, Narayan D. Upper and Lower Extremity Vascular Variations. In: Narayan D, Kapadia SE, Kodumudi G, Vadivelu N, editors. Surgical and Perioperative Management of Patients with Anatomic Anomalies, Cham: Springer International Publishing; 2021, p. 437–66.

[633] Varalakshmi K, Khzier Hussain Afroze M, Sangeeta M. Surgical Implications of Variations and Location of Plantar Arterial Arch: An Anatomical Study. Academia Anatomica International 2019;5:95–9

[634] Awari P, Vatsalaswamy P. Unusual anatomical variations in plantar metatarsal arteries and plantar arterial arch with surgical significance. Indian Journal of Vascular and Endovascular Surgery 2020;7:380–4.

[635] Imanishi N, Kish K, Chang H, Nakajima H, Aiso S. Anatomical Study of Cutaneous Venous Flow of the Sole. Plastic and Reconstructive Surgery 2007;120.

[636] Engelke C, Morgan RA, Quarmby JW, Taylor RS, Belli A-M. Distal Venous Arterialization for Lower Limb Salvage: Angiographic Appearances and Interventional Procedures. RadioGraphics 2001;21:1239–48.

[637] MacRae BA, Annaheim S, Spengler CM, Rossi RM. Skin Temperature Measurement Using Contact Thermometry: A systematic review of setup variables and their effects on measured values. Frontiers in Physiology 2018;9.

[638] MacRae BA, Spengler CM, Psikuta A, Rossi RM, Annaheim S. A Thermal Skin Model for Comparing Contact Skin Temperature Sensors and Assessing Measurement Errors. Sensors 2021;21.

[639] Childs PRN. Practical Temperature Measurement. Elsevier Science; 2001.

[640] Smith ADH, Crabtree DR, Bilzon JLJ, Walsh NP. The validity of wireless iButtons® and thermistors for human skin temperature measurement. Physiological Measurement 2009;31:95–114

[641] Serup J, Jemec GBE, Grove GL. Handbook of Non-Invasive Methods and the Skin. Taylor & Francis; 2006.

[642] Tyler CJ. The effect of skin thermistor fixation method on weighted mean skin temperature. Physiological Measurement 2011;32:1541–7.

[643] Psikuta A, Niedermann R, Rossi RM. Effect of ambient temperature and attachment method on surface temperature measurements. International Journal of Biometeorology 2014;58:877–85.

[644] Boetcher SKS, Sparrow EM, Dugay M v. Characteristics of direct-contact, skin-surface temperature sensors. International Journal of Heat and Mass Transfer 2009;52:3799–804.

[645] Arunachalam K, Maccarini P, Juang T, Gaeta C, Stauffer PR. Performance evaluation of a conformal thermal monitoring sheet sensor array for measurement of surface temperature distributions during superficial hyperthermia treatments. International Journal of Hyperthermia 2008;24:313–25.

[646] de Breteuil Du Châtelet GELT. Dissertation Sur La Nature Et La Propagation Du Feu. Prault; 1744.

[647] Herschel W. Experiments on the refrangibility of the invisible rays of the sun. Philosophical Transactions of the Royal Society of London 1800;90:284–92.

[648] Vollmer M MMK. Infrared thermal imaging : fundamentals, research and applications. Wiley-VCH; 2017.

[649] Villa E, Arteaga-Marrero N, Ruiz-Alzola J. Performance Assessment of Low-Cost Thermal Cameras for Medical Applications. Sensors n.d.;20.

[650] Ring E. The historical development of thermal imaging in medicine. Rheumatology (Oxford, England) 2004;43:800–2.

[651] Tyndall J. On calorescence. Phylosophical Magazine 1866:1–24.

[652] Holst G, de Boer J, Teves MC, Veenemans CF. An apparatus for the transformation of light of long wavelength into light of short wavelength. Physica D: Nonlinear Phenomena 1934;1:297–305.

[653] Montoro HP. Image intensification: The technology of night vision. The Photonics Handbook 2005.

[654] Vavilov V. Thermal NDT: Historical milestones, state-of-the-art and trends. Quantitative InfraRed Thermography Journal 2014;11.

[655] FLIR Systems. Photographs from our company archives 2011.

[656] Osornio-Rios RA, Antonino-Daviu JA, Romero-Troncoso R de J. Recent Industrial Applications of Infrared Thermography: A Review. IEEE Transactions on Industrial Informatics 2019;15:615–25.

[657] Garrido I, Lagüela S, Otero R, Arias P. Thermographic methodologies used in infrastructure inspection: A review—data acquisition procedures. Infrared Physics & Technology 2020;111:103481.

[658] Lucchi E. Applications of the infrared thermography in the energy audit of buildings: A review. Renewable and Sustainable Energy Reviews 2018;82:3077–90.

[659] Kirimtat A, Krejcar O. A review of infrared thermography for the investigation of building envelopes: Advances and prospects. Energy and Buildings 2018;176:390–406.

[660] Spagnolo GS, Vecchio P del, Makary G, Papalillo D, Martocchia A. A review of IR thermography applied to PV systems. 2012 11th International Conference on Environment and Electrical Engineering, 2012, p. 879–84.

[661] Muttillo M, Nardi I, Stornelli V, de Rubeis T, Pasqualoni G, Ambrosini D. On Field Infrared Thermography Sensing for PV System Efficiency Assessment: Results and Comparison with Electrical Models. Sensors 2020;20.

[662] Du Y, Zhou S, Jing X, Peng Y, Wu H, Kwok N. Damage detection techniques for wind turbine blades: A review. Mechanical Systems and Signal Processing 2020;141:106445.

[663] Worzewski T, Krankenhagen R, Doroshtnasir M, Röllig M, Maierhofer C, Steinfurth H. Thermographic inspection of a wind turbine rotor blade segment utilizing natural conditions as excitation source, Part I: Solar excitation for detecting deep structures in GFRP. Infrared Physics & Technology 2016;76:756–66.

[664] Doroshtnasir M, Worzewski T, Krankenhagen R, Röllig M. On-site inspection of potential defects in wind turbine rotor blades with thermography. Wind Energy 2016;19:1407–22.

[665] Meola C, Boccardi S, Carlomagno GM. Infrared thermography in the evaluation of aerospace composite materials: infrared thermography to composites. Woodhead Publishing; 2016.

[666] Cuevas E, García C, Hernández S, Pablo, Venegas, Gómez T, et al. Non destructive testing for non cured composites : Air coupled Ultrasounds and Thermography. 5th International Symposium on NDT in Aerospace, Singapore: 2013.

[667] Mercuri F, Orazi N, Paoloni S, Cicero C, Zammit U. Pulsed Thermography Applied to the Study of Cultural Heritage. Applied Sciences 2017;7.

[668] Williams J, Corvaro F, Vignola J, Turo D, Marchetti B, Vitali M. Application of non-invasive active infrared thermography for delamination detection in fresco. International Journal of Thermal Sciences 2022;171:107185.

[669] Yuan C, Liu Z, Zhang Y. Fire detection using infrared images for UAV-based forest fire surveillance. 2017 International Conference on Unmanned Aircraft Systems (ICUAS), 2017, p. 567–72.

[670] Pecho P, Hrúz M, Škvareková I, Ažaltovič V. Optimization of Persons Localization Using a Thermal Imaging Scanner Attached to UAV. 2020 New Trends in Aviation Development (NTAD), 2020, p. 192–6.

[671] Andrea CC, Byron JQ, Jorge PI, Inti TCH, Aguilar WG. Geolocation and Counting of People with Aerial Thermal Imaging for Rescue Purposes. In: de Paolis LT, Bourdot P, editors. Augmented Reality, Virtual Reality, and Computer Graphics, Cham: Springer International Publishing; 2018, p. 171–82.

[672] Lethbridge M, Stead M, Wells C. Estimating kangaroo density by aerial survey: a comparison of thermal cameras with human observers. Wildlife Research 2019;46:639–48.

[673] Hyun C-U, Park M, Lee WY. Remotely Piloted Aircraft System (RPAS)-Based Wildlife Detection: A Review and Case Studies in Maritime Antarctica. Animals 2020;10.

[674] Messina G, Modica G. Applications of UAV Thermal Imagery in Precision Agriculture: State of the Art and Future Research Outlook. Remote Sensing 2020;12.

[675] Wakeford ZE, Chmielewska M, Hole MJ, Howell JA, Jerram DA. Combining thermal imaging with photogrammetry of an active volcano using UAV: an example from Stromboli, Italy. The Photogrammetric Record 2019;34:445–66.

[676] Rakha T, Gorodetsky A. Review of Unmanned Aerial System (UAS) applications in the built environment: Towards automated building inspection procedures using drones. Automation in Construction 2018;93:252–64.

[677] Frodella W, Elashvili M, Spizzichino D, Gigli G, Adikashvili L, Vacheishvili N, et al. Combining infrared thermography and UAV digital photogrammetry for the protection and conservation of rupestrian cultural heritage sites in Georgia: A methodological application. Remote Sensing 2020;12.

[678] Thomas H. Some like it hot: The impact of next generation FLIR Systems thermal cameras on archaeological thermography. Archaeological Prospection 2018;25:81–7.

[679] Feroz S, Abu Dabous S. UAV-Based Remote Sensing Applications for Bridge Condition Assessment. Remote Sensing 2021;13.

[680] Jalil B, Pascali MA, Leone GR, Martinelli M, Moroni D, Salvetti O. To Identify Hot Spots in Power Lines Using Infrared and Visible Sensors. Advances in Intelligent Systems and Computing 2019;833:313–21.

[681] Rahaman SA, Urmee T, Parlevliet DA. PV system defects identification using Remotely Piloted Aircraft (RPA) based infrared (IR) imaging: A review. Solar Energy 2020;206:579–95.

[682] Lofstad-Lie V, Marstein ES, Simonsen A, Skauli T. Cost-effective flight strategy for aerial thermography inspection of photovoltaic power plants. 2021 IEEE 48th Photovoltaic Specialists Conference (PVSC), IEEE; 2021, p. 23–5.

[683] Kirsten Vidal de Oliveira A, Aghaei M, Rüther R. Aerial infrared thermography for low-cost and fast fault detection in utility-scale PV power plants. Solar Energy 2020;211:712–24.

[684] Huang Y, Chiang C-H, Hsu K-T, Cheng C-C. Employing unmanned aerial vehicle to monitor the health condition of wind turbines. AIP Conference Proceedings, vol. 1949, American Institute of Physics; 2018, p. 50003.

[685] Jasti N, Bista S, Bhargav H, Sinha S, Gupta S, Chaturvedi SK, et al. Medical Applications of Infrared Thermography: A Narrative Review. Journal of Stem Cells 2019;14:35–53.

[686] Williams KL, Williams FJ, Handley RS. Infrared thermometry in the diagnosis of breast disease. Lancet (London, England) 1961;2:1378–81.

[687] Melander O. Thermography as the primary step in mass screening for breast cancer. Bibliotheca Radiologica 1975:91–6.

[688] Ekici S, Jawzal H. Breast cancer diagnosis using thermography and convolutional neural networks. Medical Hypotheses 2020;137:109542.

[689] Stark AM. Malignant Diseases. Recent Advances in Medical Thermology, Springer; 1984, p. 549–50.

[690] Ilo A, Romsi P, Mäkelä J. Infrared Thermography as a Diagnostic Tool for Peripheral Artery Disease. Advances in Skin & Wound Care 2020;33.

[691] Padierna LC, Amador-Medina LF, Murillo-Ortiz BO, Villaseñor-Mora C. Classification method of peripheral arterial disease in patients with type 2 diabetes mellitus by infrared thermography and machine learning. Infrared Physics and Technology 2020;111:103531.

[692] Lindberg L, Kristensen B, Eldrup E, Thomsen JF, Jensen LT. Infrared Thermography as a Method of Verification in Raynaud's Phenomenon. Diagnostics 2021;11.

[693] Patil KD, Williams JR, Williams KL. Thermographic localization of incompetent perforating veins in the leg. British Medical Journal 1970;1:195–7.

[694] Priego-Quesada JI. Application of Infrared Thermography in Sports Science. Application of Infrared Thermography in Sports Science / 2017:1–327.

[695] Mekjavic IB, Tipton MJ. Myths and methodologies: Degrees of freedom – limitations of infrared thermographic screening for Covid-19 and other infections. Experimental Physiology 2020 Dec 28. Online ahead of print.

[696] Hoffer OA, Ben-David MA, Katz E, Kirshenbaum DZ, Alezra D, Zimmer Y, et al. Thermal imaging as a tool for evaluating tumor treatment efficacy. Journal of Biomedical Optics 2018;23:1–6.

[697] Zuluaga-Gomez J, Zerhouni N, al Masry Z, Devalland C, Varnier C. A survey of breast cancer screening techniques: thermography and electrical impedance tomography. Journal of Medical Engineering & Technology 2019;43:305–22.

[698] Feng H, Li X, Wang L, Xu L, Deng W, Kuang Y. A 4DCT Radiomics and Thermography-Based Radiothermomics Model for Early Prediction of Severe Radiation Dermatitis in Patients with Breast Cancer Receiving Radiation Treatment. International Journal of Radiation Oncology*Biology*Physics 2020;108:e65–6.

[699] Yadav SS, Jadhav SM. Thermal infrared imaging based breast cancer diagnosis using machine learning techniques. Multimedia Tools and Applications 2020.

[700] Fernández-Ovies FJ, Santiago Alférez-Baquero E, de Andrés-Galiana EJ, Cernea A, Fernández-Muñiz Z, Fernández-Martínez JL. Detection of Breast Cancer Using Infrared Thermography and Deep Neural Networks. In: Rojas I, Valenzuela O, Rojas F, Ortuño F, editors. Bioinformatics and Biomedical Engineering, Cham: Springer International Publishing; 2019, p. 514–23.

[701] Rastghalam R, Pourghassem H. Breast Cancer Detection Using MRF-Based Probable Texture Feature and Decision-Level Fusion-Based Classification Using HMM on Thermography Images. Pattern Recogn 2016;51:176–186.

[702] Gerasimova-Chechkina E, Toner B, Marin Z, Audit B, Roux SG, Argoul F, et al. Comparative Multifractal Analysis of Dynamic Infrared Thermograms and X-Ray Mammograms Enlightens Changes in the Environment of Malignant Tumors. Frontiers in Physiology 2016;7:336.

[703] Silva LF, Santos AASMD, Bravo RS, Silva AC, Muchaluat-Saade DC, Conci A. Hybrid analysis for indicating patients with breast cancer using temperature time series. Computer Methods and Programs in Biomedicine 2016;130:142–53.

[704] Lozano A, Hayes JC, Compton LM, Azarnoosh J, Hassanipour F. Determining the thermal characteristics of breast cancer based on high-resolution infrared imaging, 3D breast scans, and magnetic resonance imaging. Scientific Reports 2020;10:10105.

[705] Bhowmik MK, Gogoi UR, Majumdar G, Bhattacharjee D, Datta D, Ghosh AK, et al. Designing of Ground-Truth-Annotated DBT-TU-JU Breast Thermogram Database Toward Early Abnormality Prediction. IEEE Journal of Biomedical and Health Informatics 2018;22:1238–49.

[706] Wahab AA, Salim MIM, Ahamat MA, Manaf NA, Yunus J, Lai KW. Thermal distribution analysis of three-dimensional tumor-embedded breast models with different breast density compositions. Medical & Biological Engineering & Computing 2016;54:1363–73.

[707] Migowski A, Silva GAE, Dias MBK, Diz MDPE, Sant'Ana DR, Nadanovsky P. Guidelines for early detection of breast cancer in Brazil. II - New national recommendations, main evidence, and controversies. Cadernos de Saude Publica 2018;34:e00074817.

[708] Zade MA, Khodadadi H. Fuzzy controller design for breast cancer treatment based on fractal dimension using breast thermograms. IET Systems Biology 2019;13:1–7.

[709] Araújo MC, Souza RMCR, Lima RCF, Filho TMS. An interval prototype classifier based on a parameterized distance applied to breast thermographic images. Medical & Biological Engineering & Computing 2017;55:873–84.

[710] Amri A, Pulko SH, Wilkinson AJ. Potentialities of steady-state and transient thermography in breast tumour depth detection: A numerical study. Computer Methods and Programs in Biomedicine 2016;123:68–80.

[711] Saednia K, Tabbarah S, Lagree A, Wu T, Klein J, Garcia E, et al. Quantitative Thermal Imaging Biomarkers to Detect Acute Skin Toxicity From Breast Radiation Therapy Using Supervised Machine Learning. International Journal of Radiation Oncology, Biology, Physics 2020;106:1071–83.

[712] Figueiredo AAA, do Nascimento JG, Malheiros FC, da Silva Ignacio LH, Fernandes HC, Guimaraes G. Breast tumor localization using skin surface temperatures from a 2D anatomic model without knowledge of the thermophysical properties. Computer Methods and Programs in Biomedicine 2019;172:65–77.

[713] Singh D, Singh AK. Role of image thermography in early breast cancer detection- Past, present and future. Computer Methods and Programs in Biomedicine 2020;183:105074.

[714] Notter M, Thomsen AR, Nitsche M, Hermann RM, Wolff HA, Habl G, et al. Combined wIRA-Hyperthermia and Hypofractionated Re-Irradiation in the Treatment of Locally Recurrent

Breast Cancer: Evaluation of Therapeutic Outcome Based on a Novel Size Classification. Cancers 2020;12.

[715] Sánchez-Cauce R, Pérez-Martín J, Luque M. Multi-input convolutional neural network for breast cancer detection using thermal images and clinical data. Computer Methods and Programs in Biomedicine 2021;204:106045.

[716] Amri A, Wilkinson A, Pulko S. Potentialities of Dynamic Breast Thermography, 2017, p. 79–107.

[717] Damião CP, Montero JRG, Moran MBH, da Cruz Filho RA, Fontes CAP, Lima GAB, et al. On the possibility of using temperature to aid in thyroid nodule investigation. Scientific Reports 2020;10:21010.

[718] Dong F, Tao C, Wu J, Su Y, Wang Y, Wang Y, et al. Detection of cervical lymph node metastasis from oral cavity cancer using a non-radiating, noninvasive digital infrared thermal imaging system. Scientific Reports 2018;8:7219.

[719] Sohda M, Miyazaki T, Watanabe T, Nakazawa N, Ubukata Y, Kuriyama K, et al. Utility of Thermography of Reconstructed Gastric Conduit for Predicting Postoperative Anastomotic Leakage After Esophagectomy for Esophageal Cancer. Anticancer Research 2021;41:453–8.

[720] Ben-David MA, Hoffer O, Kirshenabum D, Katz E, Alezra D, Symon Z, et al. Thermal Monitoring of Tumor and Tissue State during Radiation Therapy - A Complex Case of Radiation Recall. Critical Reviews in Biomedical Engineering 2020;48:125–31.

[721] Benavent Casanova O, Benavente Gómez N, Priego Quesada JI, Galindo Gonzalez CM, Cibrián Ortiz de Anda RM, Salvador Palmero R, et al. Application of infrared thermography in diagnosing peripherally inserted central venous catheter infections in children with cancer. Physiological Measurement 2019;40:44002.

[722] Dębiec-Bąk A, Skrzek A, Woźniewski M, Malicka I. Using Thermography in the Diagnostics of Lymphedema: Pilot Study. Lymphatic Research and Biology 2019;18:247–53.

[723] Song CL, Ryu M, Morikawa J, Kothari A, Kazarian SG. Thermal effect on dispersive infrared spectroscopic imaging of prostate cancer tissue. Journal of Biophotonics 2018;11:e201800187.

[724] Damião CP, Montero JRG, Moran MBH, de Oliveira Marçal e Silva Carvalho ME, de Farias CG, Brito IB, et al. Application of thermography in the diagnostic investigation of thyroid nodules. Endocrine Journal 2021;68:573–81.

[725] Doughty A, Hasanjee A, Pettitt A, Silk K, Liu H, Chen WR, et al. Temperature distribution in target tumor tissue and photothermal tissue destruction during laser immunotherapy. Proc.SPIE, vol. 9709, 2016.

[726] Ghai S, Finelli A, Corr K, Chan R, Jokhu S, Li X, et al. MRI-guided Focused Ultrasound Ablation for Localized Intermediate-Risk Prostate Cancer: Early Results of a Phase II Trial. Radiology 2021;298:695–703.

[727] Kashyap U, Sarkar S, Saha SK. Study of hot stress dynamic IR thermography for detecting surface cancerous tissue. Journal of Medical Engineering & Technology 2020;44:284–98.

[728] Camargo VMB, Gamba H, Romaneli EFR, Ulbricht L. Using Thermography as Auxiliary Tool to Thyroid Cancer Diagnosis: a Case Study. 41st Annual International Conference of the IEEE Engineering in Medicine and Biology Society (EMBC), United States: IEEE; 2019, p. 5498–501.

[729] Zhao Y, Iyer RS, Reichley L, Oron AP, Gove NE, Kitsch AE, et al. A Pilot Study of Infrared Thermal Imaging to Detect Active Bone Lesions in Children With Chronic Nonbacterial Osteomyelitis. Arthritis Care & Research 2019;71:1430–5.

[730] Kacmaz S, Ercelebi E, Zengin S, Cindoruk S. The use of infrared thermal imaging in the diagnosis of deep vein thrombosis. Infrared Physics & Technology 2017;86:120–9.

[731] Najafi B, Reeves ND, Armstrong DG. Leveraging smart technologies to improve the management of diabetic foot ulcers and extend ulcer-free days in remission. Diabetes/Metabolism Research and Reviews 2020;36:e3239.

[732] Gooday C, Gray K, Game F, Woodburn J, Poland F, Hardeman W. Systematic review of techniques to monitor remission of acute Charcot neuroarthropathy in people with diabetes. Diabetes/Metabolism Research and Reviews 2020;36:e3328.

[733] Hazenberg CEVB, aan de Stegge WB, van Baal SG, Moll FL, Bus SA. Telehealth and telemedicine applications for the diabetic foot: A systematic review. Diabetes/Metabolism Research and Reviews 2020;36:e3247.

[734] Balasubramanian G, Vas P, Chockalingam N, Naemi R. A Synoptic Overview of Neurovascular Interactions in the Foot. Frontiers in Endocrinology 2020;11:308.

[735] Hayashi A, Shichiri M. Use of Noncontact Infrared Skin Thermometer for Peripheral Arterial Disease Screening in Patients With and Without Diabetes. Angiology 2020;71:650–7.

[736] Saxena A, Ng EYK, Lim ST. Active dynamic thermography to detect the presence of stenosis in the carotid artery. Computers in Biology and Medicine 2020;120:103718.

[737] Saxena A, Saha V, Ng EYK. Skin temperature maps as a measure of carotid artery stenosis. Computers in Biology and Medicine 2020;116:103548.

[738] Phillips CJ, Barron MR, Kuckelman J, Derickson M, Sohn VY, Paige KT, et al. Mobile Smartphone Thermal Imaging Characterization and Identification of Microvascular Flow Insufficiencies in Deep Inferior Epigastric Artery Perforator Free Flaps. The Journal of Surgical Research 2021;261:394–9.

[739] Chang W-C, Wang C-Y, Cheng Y, Hung Y-P, Lin T-H, Chen W-J, et al. Plantar thermography predicts freedom from major amputation after endovascular therapy in critical limb ischemic patients. Medicine 2020;99:e22391.

[740] Maley MJ, Hunt AP, Bach AJ, Eglin CM, Costello JT. Infrared cameras overestimate skin temperature during rewarming from cold exposure. Journal of Thermal Biology 2020;91:102614.

[741] Moon MH, Hyun K, Park JK, Lee J. Surgical treatment of compensatory hyperhidrosis: Retrospective observational study. Medicine 2020;99:e22466.

[742] Park JH, Kim R, Na SH, Kwon SY. Effect of botulinum toxin in stellate ganglion for craniofacial hyperhidrosis: a case report. The Journal of International Medical Research 2021;49:3000605211004213.

[743] Casal D, Pais D, Mota-Silva E, Pelliccia G, Iria I, Videira PA, et al. Reconstruction of a long defect of the ulnar artery and nerve with an arterialized neurovenous free flap in a teenager: A case report and literature review. Microsurgery 2018;38:209–17.

[744] Dahlmanns S, Reich-Schupke S, Schollemann F, Stücker M, Leonhardt S, Teichmann D. Classification of chronic venous diseases based on skin temperature patterns. Physiological Measurement 2021;42.

[745] Meyer A, Roof S, Gray ML, Fan CJ, Barber B, Miles BA, et al. Thermal imaging for microvascular free tissue transfer monitoring: Feasibility study using a low cost, commercially available mobile phone imaging system. Head & Neck 2020;42:2941–7.

[746] Chen R, Huang Z-Q, Chen W-L, Ou Z-P, Li S-H, Wang J-G. Value of a smartphone-compatible thermal imaging camera in the detection of peroneal artery perforators: Comparative study with computed tomography angiography. Head & Neck 2019;41:1450–6.

[747] Doesburg F, Smit JM, Paans W, Onrust M, Nijsten MW, Dieperink W. Use of infrared thermography in the detection of superficial phlebitis in adult intensive care unit patients: A prospective single-center observational study. PLOS ONE 2019;14:e0213754.

[748] Just M, Chalopin C, Unger M, Halama D, Neumuth T, Dietz A, et al. Monitoring of microvascular free flaps following oropharyngeal reconstruction using infrared thermography: first clinical experiences. European Archives of Oto-Rhino-Laryngology 2016;273:2659–67.

[749] Hummelink S, Kruit AS, van Vlaenderen ARW, Schreinemachers MJM, Steenbergen W, Ulrich DJO. Post-operative monitoring of free flaps using a low-cost thermal camera: a pilot study. European Journal of Plastic Surgery 2020;43:589–96.

[750] Machin G, Whittam A, Ainarkar S, Allen J, Bevans J, Edmonds M, et al. A medical thermal imaging device for the prevention of diabetic foot ulceration. Physiological Measurement 2017;38:420–30.

[751] Serantoni V, Jourdan F, Louche H, Sultan A. The Use of Thermography for Studying Diabetic Foot Complication through the Alteration of Thermoregulation Mechanism. Diabetes 2020;69:602-P.

[752] Thirunavukkarasu U, Umapathy S, Krishnan PT, Janardanan K. Human Tongue Thermography Could Be a Prognostic Tool for Prescreening the Type II Diabetes Mellitus. Evidence-Based Complementary and Alternative Medicine 2020;2020:3186208.

[753] Thiruvengadam J, Mariamichael A. A preliminary study for the assessment of hypertension using static and dynamic IR thermograms. Biomedical Engineering / Biomedizinische Technik 2018;63:197–206.

[754] van Doremalen RFM, van Netten JJ, van Baal JG, Vollenbroek-Hutten MMR, van der Heijden F. Validation of low-cost smartphone-based thermal camera for diabetic foot assessment. Diabetes Research and Clinical Practice 2019;149:132–9.

[755] Perng C-K, Ma H, Chiu Y-J, Lin P-H, Tsai C-H. Detection of free flap pedicle thrombosis by infrared surface temperature imaging. The Journal of Surgical Research 2018;229:169–76.

[756] Adam M, Ng EYK, Tan JH, Heng ML, Tong JWK, Acharya UR. Computer aided diagnosis of diabetic foot using infrared thermography: A review. Computers in Biology and Medicine 2017;91:326–36.

[757] Saxena A, Ng EYK, Lim ST. Infrared (IR) thermography as a potential screening modality for carotid artery stenosis. Computers in Biology and Medicine 2019;113:103419.

[758] Seixas A, Ammer K, Carvalho R, Vilas-Boas JP, Mendes J, Vardasca R. Relationship between skin temperature and soft tissue hardness in diabetic patients: an exploratory study. Physiological Measurement 2019;40:74007.

[759] Macdonald A, Petrova N, Ainarker S, Allen J, Lomas C, Tang W, et al. Between visit variability of thermal imaging of feet in people attending podiatric clinics with diabetic neuropathy at high risk of developing foot ulcers. Physiological Measurement 2019;40:84004.

[760] Tsuyuki S, Yamagami K, Yoshibayashi H, Sugie T, Mizuno Y, Tanaka S, et al. Effectiveness and safety of surgical glove compression therapy as a prophylactic method against nanoparticle albumin-bound-paclitaxel-induced peripheral neuropathy. Breast (Edinburgh, Scotland) 2019;47:22–7.

[761] Hughes M, Wilkinson J, Moore T, Manning J, New P, Dinsdale G, et al. Thermographic Abnormalities are Associated with Future Digital Ulcers and Death in Patients with Systemic Sclerosis. The Journal of Rheumatology 2016;43:1519–22.

[762] Ruaro B, Smith V, Sulli A, Pizzorni C, Tardito S, Patané M, et al. Innovations in the Assessment of Primary and Secondary Raynaud's Phenomenon. Frontiers in Pharmacology 2019;10:360.

[763] Nowicka D. Thermography Improves Clinical Assessment in Patients with Systemic Sclerosis Treated with Ozone Therapy. BioMed Research International 2017;2017:5842723.

[764] Umapathy S, Thulasi R, Gupta N, Sivanadhan S. Thermography and colour Doppler ultrasound: a potential complementary diagnostic tool in evaluation of rheumatoid arthritis in the knee region. Biomedical Engineering / Biomedizinische Technik 2020;65:289–99.

[765] von Schoen-Angerer T, Deckers B, Henes J, Helmert E, Vagedes J. Effect of topical rosemary essential oil on Raynaud phenomenon in systemic sclerosis. Complementary Therapies in Medicine 2018;40:191–4.

[766] Rausch Osthoff A-K, Niedermann K, Braun J, Adams J, Brodin N, Dagfinrud H, et al. Recommendations for physical activity in people with inflammatory arthritis and osteoarthritis. Annals of the Rheumatic Diseases 2018;77:1251–60.

[767] Wilkinson JD, Leggett SA, Marjanovic EJ, Moore TL, Allen J, Anderson ME, et al. A Multicenter Study of the Validity and Reliability of Responses to Hand Cold Challenge as Measured by Laser Speckle Contrast Imaging and Thermography: Outcome Measures for Systemic Sclerosis-Related Raynaud's Phenomenon. Arthritis & Rheumatology (Hoboken, NJ) 2018;70:903–11.

[768] Pauk J, Ihnatouski M, Wasilewska A. Detection of inflammation from finger temperature profile in rheumatoid arthritis. Medical & Biological Engineering & Computing 2019;57:2629–39.

[769] Gatt A, Mercieca C, Borg A, Grech A, Camilleri L, Gatt C, et al. A comparison of thermographic characteristics of the hands and wrists of rheumatoid arthritis patients and healthy controls. Scientific Reports 2019;9:17204.

[770] Lerkvaleekul B, Jaovisidha S, Sungkarat W, Chitrapazt N, Fuangfa P, Ruangchaijatuporn T, et al. The comparisons between thermography and ultrasonography with physical

examination for wrist joint assessment in juvenile idiopathic arthritis. Physiological Measurement 2017;38:691–700.

[771] Edelaar L, Nikiphorou E, Fragoulis GE, Iagnocco A, Haines C, Bakkers M, et al. Recommendations for the generic core competences of health professionals in rheumatology. Annals of the Rheumatic Diseases 2020;79:53–60.

[772] Fokam D, Lehmann C. Clinical assessment of arthritic knee pain by infrared thermography. Journal of Basic and Clinical Physiology and Pharmacology 2018;30.

[773] Manning JB, Marjanovic E, Moore TL, Dinsdale G, Wilkinson S, Dickinson MR, et al. A pilot study of cutaneous oxygenation and perfusion in systemic sclerosis-related digital calcinosis. Rheumatology (Oxford, England) 2020;59:3109–11.

[774] Sternbersky J, Tichy M, Zapletalova J. Infrared thermography and capillaroscopy in the diagnosis of Raynaud's phenomenon. Biomedical Papers of the Medical Faculty of the University Palacky, Olomouc, Czechoslovakia 2021;165:90–8.

[775] Ruaro B, Nallino MG, Casabella A, Salton F, Confalonieri P, de Tanti A, et al. Monitoring the microcirculation in the diagnosis and follow-up of systemic sclerosis patients: Focus on pulmonary and peripheral vascular manifestations. Microcirculation (New York, NY : 1994) 2020;27:e12647.

[776] Ritschl V, Stamm TA, Aletaha D, Bijlsma JWJ, Böhm P, Dragoi RG, et al. Points to consider for the prevention, screening, assessment and management of non-adherence to treatment in people with rheumatic and musculoskeletal diseases for use in clinical practice. Annals of the Rheumatic Diseases 2020.

[777] Nolan E, Manning J, Heal C, Moore T, Herrick AL. Impact and associates of digital pitting in patients with systemic sclerosis: a pilot study. Scandinavian Journal of Rheumatology 2020;49:239–43.

[778] Alfieri FM, Vargas E Silva NC de O, dos Santos ACA, Battistella LR. Cutaneous temperature and pressure pain threshold in individuals with knee osteoarthritis. Reumatologia 2020;58:272–6.

[779] Marjanovic E, Moore TL, Manning JB, Dinsdale G, Wilkinson S, Dickinson MR, et al. Systemic sclerosis-related digital calcinosis; a pilot study of cutaneous oxygenation and perfusion. Rheumatology (Oxford, England) 2020;59:3573–5.

[780] Laskari K, Pentazos G, Pitsilka D, Raftakis J, Konstantonis G, Toutouzas K, et al. Joint microwave radiometry for inflammatory arthritis assessment. Rheumatology 2020;59:839–44.

[781] Hillen B, Simon P. The Temperature Surface Radiation Pattern - A non-invasive Insight into Skin Blood Flow Response to Exercise. Medicine & Science in Sports & Exercise 2019;51:491–2.

[782] Vargas E Silva NC de O, dos Anjos RL, Santana MMC, Battistella LR, Marcon Alfieri F. Discordance between radiographic findings, pain, and superficial temperature in knee osteoarthritis. Reumatologia 2020;58:375–80.

[783] Loarce-Martos J, Bachiller-Corral J, Cuevas IF, Quintana MS, Díaz MV. Utilify of infrared thermography for the evaluation of rheumatoid arthritis. Annals of the Rheumatic Diseases 2019;78:313 LP – 314.

[784] Herrick AL, Murray A. The role of capillaroscopy and thermography in the assessment and management of Raynaud's phenomenon. Autoimmunity Reviews 2018;17:465–72.

[785] Horikoshi M, Inokuma S, Kijima Y, Kobuna M, Miura Y, Okada R, et al. Thermal Disparity between Fingers after Cold-water Immersion of Hands: A Useful Indicator of Disturbed Peripheral Circulation in Raynaud Phenomenon Patients. Internal Medicine 2016;55:461–6.

[786] Saygin D, Highland KB, Tonelli AR. Microvascular involvement in systemic sclerosis and systemic lupus erythematosus. Microcirculation 2019;26:e12440.

[787] Valladolid S, Chiwo F, Osornio Martinez C, Cabrera Alonso R, Moncada B, Gonzalez F. Thermal pattern determination in patients with rosacea using infrared thermography. Journal of Investigative Dermatology 2018;138:S83.

[788] Nowakowski A, Siondalski P, Moderhak M, Kaczmarek M. A new diagnostic method for evaluation of cardiosurgery wound healing. Quantitative InfraRed Thermography Journal 2016;13:19–34.

[789] Carrière ME, de Haas LEM, Pijpe A, Meij-de Vries A, Gardien KLM, van Zuijlen PPM, et al. Validity of thermography for measuring burn wound healing potential. Wound Repair and Regeneration : Official Publication of the Wound Healing Society [and] the European Tissue Repair Society 2020;28:347–54.

[790] Jaspers MEH, Maltha I, Klaessens JHGM, de Vet HCW, Verdaasdonk RM, van Zuijlen PPM. Insights into the use of thermography to assess burn wound healing potential: a reliable and valid technique when compared to laser Doppler imaging. Journal of Biomedical Optics 2016;21:96006.

[791] Singer AJ, Relan P, Beto L, Jones-Koliski L, Sandoval S, Clark RAF. Infrared Thermal Imaging Has the Potential to Reduce Unnecessary Surgery and Delays to Necessary Surgery in Burn Patients. Journal of Burn Care & Research: Official Publication of the American Burn Association 2016;37:350–5.

[792] Panasiti MS, Ponsi G, Monachesi B, Lorenzini L, Panasiti V, Aglioti SM. Cognitive load and emotional processing in psoriasis: a thermal imaging study. Experimental Brain Research 2019;237:211–22.

[793] Martínez-Jiménez MA, Ramirez-GarciaLuna JL, Kolosovas-Machuca ES, Drager J, González FJ. Development and validation of an algorithm to predict the treatment modality of burn wounds using thermographic scans: Prospective cohort study. PLOS ONE 2018;13:e0206477.

[794] Anzengruber F, Alotaibi F, Kaufmann LS, Ghosh A, Oswald MR, Maul J-T, et al. Thermography: High sensitivity and specificity diagnosing contact dermatitis in patch testing. Allergology International: Official Journal of the Japanese Society of Allergology 2019;68:254–8.

[795] Hoffmann A, Dumke C, Hanschmann K-MO, Wicker S. Local thermal reaction after influenza vaccination: Quantification by infrared imaging and biometric considerations. Vaccine 2018;36:2783–7.

[796] Szwedo M, Tomaka B, Targosz J, Targosz K, Jasiewicz-Honkisz B. Infrared thermography as an objective technique for evaluation of patch tests results. 2014.

[797] Jaspers ME, Maltha IM, Klaessens JH, Vet HC, Verdaasdonk RM, Zuijlen PP. Noninvasive measurement of burn wound depth applying infrared thermal imaging. Proc.SPIE, vol. 9689, IEEE; 2016.

[798] Belay RE, Huang GO, Shen JK-C, Ko EYK. Diagnosis of clinical and subclinical varicocele: how has it evolved? Asian Journal of Andrology 2016;18:182–5.

[799] Riquet D, Houel N, Bodnar J-L. Stimulated infrared thermography applied to differentiate scar tissue from peri-scar tissue: a preliminary study. Journal of Medical Engineering & Technology 2016;40:307–14.

[800] Keenan E, Gethin G, Flynn L, Watterson D, O'Connor GM. Enhanced thermal imaging of wound tissue for better clinical decision making. Physiological Measurement 2017;38:1104–15.

[801] Zouboulis CC, Nogueira da Costa A, Jemec GBE, Trebing D. Long-Wave Medical Infrared Thermography: A Clinical Biomarker of Inflammation in Hidradenitis Suppurativa/Acne Inversa. Dermatology (Basel, Switzerland) 2019;235:144–9.

[802] Maller JJ, George SS, Viswanathan RP, Fitzgerald PB, Junor P. Using thermographic cameras to investigate eye temperature and clinical severity in depression. Journal of Biomedical Optics 2016;21:26001.

[803] Yeo S, Tan JH, Acharya UR, Sudarshan VK, Tong L. Longitudinal Changes in Tear Evaporation Rates After Eyelid Warming Therapies in Meibomian Gland Dysfunction. Investigative Ophthalmology & Visual Science 2016;57:1974–81.

[804] Matteoli S, Favuzza E, Mazzantini L, Aragona P, Cappelli S, Corvi A, et al. Ocular surface temperature in patients with evaporative and aqueous-deficient dry eyes: a thermographic approach. Physiological Measurement 2017;38:1503–12.

[805] Su T-Y, Ho W-T, Chiang S-C, Lu C-Y, Chiang HK, Chang S-W. Infrared thermography in the evaluation of meibomian gland dysfunction. Journal of the Formosan Medical Association = Taiwan Yi Zhi 2017;116:554–9.

[806] Jędzierowska M, Koprowski R, Wilczyński S, Tarnawska D. The use of infrared thermal imaging in tonometry with a Scheimpflug camera. Journal of Thermal Biology 2021;96:102823.

[807] Matteoli S, Coppini D, Corvi A. A novel image processing procedure for thermographic image analysis. Medical & Biological Engineering & Computing 2018;56:1747–56.

[808] Sniegowski MC, Erlanger M, Olson J. Thermal imaging of corneal transplant rejection. International Ophthalmology 2018;38:2335–9.

[809] Tabuchi H, Masumoto H. Objective evaluation of allergic conjunctival disease (with a focus on the application of artificial intelligence technology). Allergology International 2020;69:505–9.

[810] Putrino A, Raso M, Caputo M, Calace2 V, Barbato E, Galluccio G. Thermographic Control of Pediatric Dental Patients During the SARS-CoV-2 Pandemics Using Smartphones. Pesquisa Brasileira Em Odontopediatria e Clínica Integrada 2021;21.

[811] Soori A, Kowsary F, Kasraei S. Experimental estimation of the emissivity of human enamel and dentin. Infrared Physics & Technology 2020:103234.

[812] Roointan S, Tavakolian P, Sivagurunathan KS, Mandelis A, Abrams SH. Detection and monitoring of early dental caries and erosion using three-dimensional enhanced truncated-correlation photothermal coherence tomography imaging. Journal of Biomedical Optics 2021;26.

[813] Yong ANC, Lu D, Sivaraja VK. Laser lock-in thermography on dental inspection. AIP Conference Proceedings 2019;2102:120008.

[814] Avdelidis NP, Kappatos V, Georgoulas G, Karvelis P, Deli CK, Theodorakeas P, et al. Detection and characterization of exercise induced muscle damage (EIMD) via thermography and image processing. Proc.SPIE, vol. 10171, 2017.

[815] Dimova M. Thermographic assessment of structural analysis in patients with temporomandibular disorders. Comptes Rendus de L'Academie Bulgare Des Sciences 2018;71:712–6.

[816] Maxel X, Girollet F, Stubbe L, Boudot E, Darraillans L, Bodnar JL. Aquatic Osteopathy Treatment Assessment by Infrared Thermography on Healthy Subjects After Thermoneutral Water Immersion. Journal of Chiropractic Medicine 2019;18:188–97.

[817] Vardasca R, Magalhaes C, Silva P, Abreu P, Mendes J, Restivo MT. Biomedical musculoskeletal applications of infrared thermal imaging on arm and forearm: A systematic review. Journal of Thermal Biology 2019;82:164–77.

[818] Skouroliakou A, Kalatzis I, Kalyvas N, Grivas TB. Infrared thermography quantitative image processing. Journal of Physics: Conference Series 2017;931:12033.

[819] Oliveira J, Vardasca R, Pimenta M, Gabriel J, Torres J. Use of infrared thermography for the diagnosis and grading of sprained ankle injuries. Infrared Physics & Technology 2016;76:530–41.

[820] Cabizosu A, Carboni N, Figus A, Vegara-Meseguer JM, Casu G, Hernández Jiménez P, et al. Is infrared thermography (IRT) a possible tool for the evaluation and follow up of Emery-Dreifuss muscular dystrophy? A preliminary study. Medical Hypotheses 2019;127:91–6.

[821] Baic A, Kasprzyk T, Rżany M, Stanek A, Sieroń K, Suszyński K, et al. Can we use thermal imaging to evaluate the effects of carpal tunnel syndrome surgical decompression? Medicine 2017;96:e7982.

[822] Kwok G, Yip J, Yick K-L, Cheung M-C, Tse C-Y, Ng S-P, et al. Postural Screening for Adolescent Idiopathic Scoliosis with Infrared Thermography. Scientific Reports 2017;7:14431.

[823] Riquet D, Houel N, Bodnar J-L. Effect of osteopathic treatment on a scar assessed by thermal infrared camera, pilot study. Complementary Therapies in Medicine 2019;45:130–5.

[824] Cabizosu A, Carboni N, Martinez-Almagro Andreo A, Vegara-Meseguer JM, Marziliano N, Gea Carrasco G, et al. Theoretical basis for a new approach of studying Emery-Dreifuss muscular dystrophy by means of thermography. Medical Hypotheses 2018;118:103–6.

[825] Albuquerque NF, Lopes BS. Musculoskeletal applications of infrared thermography on back and neck syndromes: a systematic review. European Journal of Physical and Rehabilitation Medicine 2021;57:386–96.

[826] Chetty T, Daniels BB, Ngandu NK, Goga A. A rapid review of the effectiveness of screening practices at airports, land borders and ports to reduce the transmission of

respiratory infectious diseases such as COVID-19. South African Medical Journal; Vol 110, No 11 (2020) 2020.

[827] Holm JK, Kellett JG, Jensen NH, Hansen SN, Jensen K, Brabrand M. Prognostic value of infrared thermography in an emergency department. European Journal of Emergency Medicine : Official Journal of the European Society for Emergency Medicine 2018;25:204–8.

[828] Ghassemi P, Pfefer TJ, Casamento JP, Simpson R, Wang Q. Best practices for standardized performance testing of infrared thermographs intended for fever screening. PloS One 2018;13:e0203302.

[829] Coats TJ, Morsy M, Naseer S, Keresztes K, Hussain S, Dexter K, et al. A pilot study of the Leicester ED medical infrared imaging protocol in fever and sepsis. PloS One 2018;13:e0201562.

[830] Zhou Y, Ghassemi P, Chen M, McBride D, Casamento JP, Pfefer TJ, et al. Clinical evaluation of fever-screening thermography: impact of consensus guidelines and facial measurement location. Journal of Biomedical Optics 2020;25.

[831] Buoite Stella A, Manganotti P, Furlanis G, Accardo A, Ajčević M. Return to school in the COVID-19 era: considerations for temperature measurement. Journal of Medical Engineering & Technology 2020;44:468–71.

[832] McConeghy KW, White E, Panagiotou OA, Santostefano C, Halladay C, Feifer RA, et al. Temperature Screening for SARS-CoV-2 in Nursing Homes: Evidence from Two National Cohorts. Journal of the American Geriatrics Society 2020;68:2716–20.

[833] Leach KC, Ellsworth MG, Ostrosky LZ, Bell CS, Masters K, Calhoun J, et al. Evaluation of a telethermographic system for temperature screening at a large tertiary-care referral hospital during the coronavirus disease 2019 (COVID-19) pandemic. Infection Control and Hospital Epidemiology 2021;42:103–5.

[834] Carpenè G, Henry BM, Mattiuzzi C, Lippi G. Comparison of forehead temperature screening with infra-red thermometer and thermal imaging scanner. The Journal of Hospital Infection 2021;111:208–9.

[835] Martinez-Jimenez MA, Loza-Gonzalez VM, Kolosovas-Machuca ES, Yanes-Lane ME, Ramirez-GarciaLuna AS, Ramirez-GarciaLuna JL. Diagnostic accuracy of infrared thermal imaging for detecting COVID-19 infection in minimally symptomatic patients. European Journal of Clinical Investigation 2021;51:e13474.

[836] Healy C, Segal Z, Hinnerichs C, Ace E, Ward D, Honovich J. Globally deployed COVID-19 fever screening devices using infrared thermographs consistently normalize high readings to afebrile range. Journal of Biomedical Optics 2021;26.

[837] Adams S, Bucknall T, Kouzani A. An initial study on the agreement of body temperatures measured by infrared cameras and oral thermometry. Scientific Reports 2021;11:11901.

[838] Pham Xuan R, Xiong Y, Brietzke A, Marker S. Thermal infrared imaging based facial temperature in comparison to ear temperature during a real-driving scenario. Journal of Thermal Biology 2021;96:102806.

[839] Alpar O, Krejcar O. Detection of Irregular Thermoregulation in Hand Thermography by Fuzzy C-Means. In: Rojas I, Ortuño F, editors. Bioinformatics and Biomedical Engineering, Cham: Springer International Publishing; 2018, p. 255–65.

[840] de Carvalho G, Girasol CE, Gonçalves LGC, Guirro ECO, Guirro RR de J. Correlation between skin temperature in the lower limbs and biochemical marker, performance data, and clinical recovery scales. PloS One 2021;16:e0248653.

[841] Priego Quesada JI, Salvador Palmer R, Cibrián Ortiz de Anda RM. Physics Principles of the Infrared Thermography and Human Thermoregulation. In: Priego Quesada JI, editor. Application of Infrared Thermography in Sports Science, Cham: Springer International Publishing; 2017, p. 25–48.

[842] Bauer J, Górecki I, Kohyt M, Migasiewicz A, Podbielska H. The influence of smartphones' operation modes on the superficial temperature distribution in the human auricle region. Journal of Thermal Analysis and Calorimetry 2018;133:559–69.

[843] Carroll MS, Reed DW, Kuntz NL, Weese-Mayer DE. Novel methods of imaging and analysis for the thermoregulatory sweat test. Journal of Applied Physiology (Bethesda, Md : 1985) 2018;125:755–62.

[844] Bauer J, O'Mahony C, Chovan D, Mulcahy J, Silien C, Tofail SAM. Thermal effects of mobile phones on human auricle region. Journal of Thermal Biology 2019;79:56–68.

[845] Tse J, Rand C, Carroll M, Charnay A, Gordon S, Morales B, et al. Determining peripheral skin temperature: subjective versus objective measurements. Acta Paediatrica (Oslo, Norway : 1992) 2016;105:e126-31

[846] Fernandes AA, Moreira DG, Brito CJ, da Silva CD, Sillero-Quintana M, Pimenta EM, et al. Validity of inner canthus temperature recorded by infrared thermography as a non-invasive surrogate measure for core temperature at rest, during exercise and recovery. Journal of Thermal Biology 2016;62:50–5.

[847] Raccuglia M, Heyde C, Lloyd A, Hodder S, Havenith G. The use of infrared thermal imaging to measure spatial and temporal sweat retention in clothing. International Journal of Biometeorology 2019;63:885–94.

[848] Charlton M, Stanley SA, Whitman Z, Wenn V, Coats TJ, Sims M, et al. The effect of constitutive pigmentation on the measured emissivity of human skin. PloS One 2020;15:e0241843.

[849] Kirimtat A, Krejcar O, Selamat A, Herrera-Viedma E. FLIR vs SEEK thermal cameras in biomedicine: comparative diagnosis through infrared thermography. BMC Bioinformatics 2020;21:88.

[850] Sánchez-Ureña B, Rojas-Valverde D, Gutierrez-Vargas R, Gutiérrez-Vargas J, Minson C. Effect Of Cold Water Immersion On Skin Temperature: A Thermography Study. Medicine & Science in Sports & Exercise 2018;50:802.

[851] Gomes Moreira D, Costello J, Brito C, Adamczyk J, Ammer K, Bach A, et al. Thermographic imaging in sports and exercise medicine: A Delphi study and consensus statement on the measurement of human skin temperature. Journal of Thermal Biology 2017;69:155–65.

[852] Fernandes T, Hernandez A, Albuquerque-Neto C, Mady C. Clinical application of thermography for energy balance in athletes – State of the art and new paradigms. Revista Brasileira de Medicina Do Esporte 2018;24:483–5.

[853] Viegas F, Mello M, Rodrigues S, Amaral Costa CM, Freitas L, Rodrigues E, et al. The use of thermography and its control variables: a systematic review. Revista Brasileira de Medicina Do Esporte 2020;26:82–6.

[854] Issaly N, Quintana M, Roller M. settings Open AccessArticle Analysis of Effectiveness of a Supplement Combining Harpagophytum procumbens, Zingiber officinale and Bixa orellana in Healthy Recreational Runners with Self-Reported Knee Pain: A Pilot, Randomized, Triple-Blind, Placebo-Contro. International Journal of Environmental Research and Public Health 2021;18(11), 55:18.

[855] Priego Quesada JI, Cibrián Ortiz de Anda RM, Pérez-Soriano P, Salvador Palmer R. Historical Perspective of Infrared Thermography and Its Application in Sport Science. In: Priego Quesada JI, editor. Application of Infrared Thermography in Sports Science, Cham: Springer International Publishing; 2017, p. 1–23.

[856] Priego Quesada JI, Carpes FP, Salvador Palmer R, Pérez-Soriano P, Cibrián Ortiz de Anda RM. Effect of saddle height on skin temperature measured in different days of cycling. SpringerPlus 2016;5:205.

[857] Ioannou S. Functional Infrared Thermal Imaging: A Contemporary Tool in Soft Tissue Screening. Scientific Reports 2020;10:9303.

[858] Cholewka A, Kasprzyk T, Stanek A, Sieroń-Stołtny K, Drzazga Z. May thermal imaging be useful in cyclist endurance tests? Journal of Thermal Analysis and Calorimetry 2016;123:1973–9.

[859] Formenti D, Ludwig N, Trecroci A, Gargano M, Michielon G, Caumo A, et al. Dynamics of thermographic skin temperature response during squat exercise at two different speeds. Journal of Thermal Biology 2016;59:58–63.

[860] Rodríguez-Sanz D, Losa-Iglesias ME, López-López D, Calvo-Lobo C, Palomo-López P, Becerro-de-Bengoa-Vallejo R. Infrared thermography applied to lower limb muscles in elite soccer players with functional ankle equinus and non-equinus condition. PeerJ 2017;5:e3388.

[861] Adamczyk JG, Krasowska I, Boguszewski D, Reaburn P. The use of thermal imaging to assess the effectiveness of ice massage and cold-water immersion as methods for supporting post-exercise recovery. Journal of Thermal Biology 2016;60:20–5.

[862] de Andrade Fernandes A, Pimenta EM, Moreira DG, Sillero-Quintana M, Marins JCB, Morandi RF, et al. Effect of a professional soccer match in skin temperature of the lower limbs: a case study. Journal of Exercise Rehabilitation 2017;13:330–4.

[863] Pérez-Guarner A, Priego-Quesada JI, Oficial-Casado F, Cibrián Ortiz de Anda RM, Carpes FP, Palmer RS. Association between physiological stress and skin temperature response after a half marathon. Physiological Measurement 2019;40:34009.

[864] Trecroci A, Formenti D, Ludwig N, Gargano M, Bosio A, Rampinini E, et al. Bilateral asymmetry of skin temperature is not related to bilateral asymmetry of crank torque during an incremental cycling exercise to exhaustion. PeerJ 2018;6:e4438.

[865] Weigert M, Nitzsche N, Kunert F, Lösch C, Schulz H. The influence of body composition on exercise-associated skin temperature changes after resistance training. Journal of Thermal Biology 2018;75:112–9.

[866] Priego-Quesada JI, Oficial-Casado F, Gandia-Soriano A, Carpes FP. A preliminary investigation about the observation of regional skin temperatures following cumulative training loads in triathletes during training camp. Journal of Thermal Biology 2019;84:431–8.

[867] de Carvalho G, Gobbi A, Gobbi RB, Alfredo DMN, do Carmo Furquim TH, Barbosa RI, et al. Photobiomodulation by light emitting diode applied sequentially does not alter performance in cycling athletes. Lasers in Medical Science 2020;35:1769–79.

[868] Priego-Quesada JI, Pérez-Guarner A, Gandia-Soriano A, Oficial-Casado F, Galindo C, Cibrián Ortiz de Anda RM, et al. Effect of a Marathon on Skin Temperature Response After a Cold-Stress Test and Its Relationship With Perceptive, Performance, and Oxidative-Stress Biomarkers. International Journal of Sports Physiology and Performance 2020;15:1467–75.

[869] Gómez-Carmona P, Fernández-Cuevas I, Sillero-Quintana M, Arnaiz-Lastras J, Navandar A. Infrared Thermography Protocol on Reducing the Incidence of Soccer Injuries. Journal of Sport Rehabilitation 2020;29:1222–7.

[870] Mendonça Teixeira R, Dellagrana RA, Priego-Quesada JI, Machado JCBP, Fernandes da Silva J, Pacheco Dos Reis TM, et al. Muscular Strength Imbalances Are not Associated with Skin Temperature Asymmetries in Soccer Players. Life (Basel, Switzerland) 2020;10.

[871] Ferreira-Júnior JB, Chaves SFN, Pinheiro MHA, Rezende VHS, Freitas EDS, Marins JCB, et al. Is skin temperature associated with muscle recovery status following a single bout of leg press? Physiological Measurement 2021;42.

[872] Priego-Quesada JI, de la Fuente C, Kunzler MR, Perez-Soriano P, Hervás-Marín D, Carpes FP. Relationship between Skin Temperature, Electrical Manifestations of Muscle Fatigue, and Exercise-Induced Delayed Onset Muscle Soreness for Dynamic Contractions: A Preliminary Study. International Journal of Environmental Research and Public Health 2020;17.

[873] Machado ÁS, Priego-Quesada JI, Jimenez-Perez I, Gil-Calvo M, Carpes FP, Perez-Soriano P. Influence of infrared camera model and evaluator reproducibility in the assessment of skin temperature responses to physical exercise. Journal of Thermal Biology 2021;98:102913.

[874] Sanchis-Sanchis R, Priego-Quesada JI, Ribas-Garcia V, Carpes FP, Encarnacion-Martinez A, Perez-Soriano P. Effects of asymmetrical exercise demands on the symmetry of skin temperature in archers. Physiological Measurement 2020;41:114002.

[875] del Estal A, Brito C-J, Galindo V-E, Lopez Diaz de Durana A, Franchini E, Sillero-Quintana M. Thermal asymmetries in striking combat sports athletes measured by infrared thermography. Science & Sports 2017;32:e61–7.

[876] Perpetuini D, Formenti D, Cardone D, Filippini C, Merla A. Regions of interest selection and thermal imaging data analysis in sports and exercise science: a narrative review. Physiological Measurement 2021;42.

[877] Fernández-Cuevas I, Arnáiz Lastras J, Escamilla Galindo V, Gómez Carmona P. Infrared Thermography for the Detection of Injury in Sports Medicine. In: Priego Quesada JI, editor. Application of Infrared Thermography in Sports Science, Cham: Springer International Publishing; 2017, p. 81–109.

[878] Gil-Calvo M, Herrero-Marco J, González-Peña R de J, Perez-Soriano P, Priego-Quesada JI. Acute effect of induced asymmetrical running technique on foot skin temperature. Journal of Thermal Biology 2020;91:102613.

[879] da Silva W, Machado ÁS, Souza MA, Kunzler MR, Priego-Quesada JI, Carpes FP. Can exercise-induced muscle damage be related to changes in skin temperature? Physiological Measurement 2018;39:104007.

[880] Requena-Bueno L, Priego-Quesada JI, Jimenez-Perez I, Gil-Calvo M, Pérez-Soriano P. Validation of ThermoHuman automatic thermographic software for assessing foot temperature before and after running. Journal of Thermal Biology 2020;92.

[881] Mazurkiewicz J, Bauer J, Mosion M, Migasiewicz A, Podbielska H. Severity of Cellulite Classification Based on Tissue Thermal Imagining. In: Rutkowski L, Scherer R, Korytkowski M, Pedrycz W, Tadeusiewicz R, Zurada JM, editors. Artificial Intelligence and Soft Computing, Cham: Springer International Publishing; 2018, p. 179–90.

[882] Gatidis S, Schmidt H, Pfannenberg CA, Nikolaou K, Schick F, Schwenzer NF. Is It Possible to Detect Activated Brown Adipose Tissue in Humans Using Single-Time-Point Infrared Thermography under Thermoneutral Conditions? Impact of BMI and Subcutaneous Adipose Tissue Thickness. PloS One 2016;11:e0151152.

[883] Ang QY, Goh HJ, Cao Y, Li Y, Chan S-P, Swain JL, et al. A new method of infrared thermography for quantification of brown adipose tissue activation in healthy adults (TACTICAL): a randomized trial. The Journal of Physiological Sciences: JPS 2017;67:395–406.

[884] Sun L, Yan J, Sun L, Velan SS, Leow MKS. A synopsis of brown adipose tissue imaging modalities for clinical research. Diabetes & Metabolism 2017;43:401–10.

[885] Neves EB, Salamunes ACC, de Oliveira RM, Stadnik AMW. Effect of body fat and gender on body temperature distribution. Journal of Thermal Biology 2017;70:1–8.

[886] Cholewka A, Stanek A, Wójcik M, Sieroń-Stołtny K, Drzazga Z. Does local cryotherapy improve thermal diagnosis similar to whole-body cryotherapy in spinal diseases? Journal of Thermal Analysis and Calorimetry 2016;127.

[887] Topalidou A, Downe S. Investigation of the use of thermography for research and clinical applications in pregnant women. Infrared Physics & Technology 2016;75.

[888] Al-Sadr H, Popescu M, Keller JM. Early Sepsis Recognition Based on Ear Localization using Infrared Thermography. 2018 IEEE International Conference on Bioinformatics and Biomedicine (BIBM), IEEE; 2018, p. 823–30.

[889] Malpique R, Gallego-Escuredo JM, Sebastiani G, Villarroya J, López-Bermejo A, de Zegher F, et al. Brown adipose tissue in prepubertal children: associations with sex, birthweight, and metabolic profile. International Journal of Obesity (2005) 2019;43:384–91.

[890] Owen R, Ramlakhan S. Infrared thermography in paediatrics: a narrative review of clinical use. BMJ Paediatrics Open 2017;1:e000080.

[891] Robinson LJ, Law J, Astle V, Gutiérrez-García M, Ojha S, Symonds ME, et al. Sexual Dimorphism of Brown Adipose Tissue Function. The Journal of Pediatrics 2019;210:166-172.e1.

[892] Martini G, Viale S, Sequi G, Ambrosio F. Infrared thermography in paediatric complex regional pain syndrome. Archives of Disease in Childhood 2021;106:841.

[893] Tieri G, Gioia A, Scandola M, Pavone EF, Aglioti SM. Visual appearance of a virtual upper limb modulates the temperature of the real hand: a thermal imaging study in Immersive Virtual Reality. European Journal of Neuroscience 2017;45:1141–51.

[894] Ali SS, Khan AY, Michael SG, Tankha P, Tokuno H. Use of Digital Infrared Thermal Imaging in the Electromyography Clinic: A Case Series. Cureus 2019;11.

[895] Ammer K. The Glamorgan Protocol for recording and evaluation of thermal images of the human body. Thermology Inernational 2008;18:125–9.

[896] Fernández-Cuevas I, Carlos J, Marins B, Arnáiz J, María P, Carmona G, et al. Classification of factors influencing the use of infrared thermography in humans : A review. Infrared Physics & Technology 2015;71:28–55.

[897] Tkáčová M, Foffová P, Živčák J, Hudák R. The methodics of medical thermography in the diagnostics of the human body musculoskeletal system. 2010 IEEE 8th International Symposium on Applied Machine Intelligence and Informatics (SAMI), 2010, p. 275–7.

[898] Ring EFJ, Ammer K. Infrared thermal imaging in medicine. Physiological Measurement 2012;33.

[899] Amalu W. International Academy of Clinical Thermology Medical Infrared Imaging Standards and Guidelines. 2018.

[900] ISO 9886: 2004. Ergonomics evaluation of thermal strain by physiological measurements. 2004.

[901] IEC 80601-2-59:2017, Particular requirements for the basic safety and essential performance of screening thermographs for human febrile temperature screening. 2017.

[902] Schwartz RG, O'Young B, Getson P, Govindan S, Uricchio J, Bernton T, et al. Guidelines for Neuromusculoskeletal Infrared Thermography Sympathetic Skin Response (SSR) Studies. Pan American Journal of Medical Thermology 2015;2:35–43.

[903] Ammer K. Do we need reference data of local skin temperatures? Thermology International 2015;25:45–7.

[904] Ammer K. Influence of Imaging and Object Conditions on Temperature Readings From Medical Infrared Images. Polish Journal of Environmental Studies 2006;15:117–9.

[905] Ammer K. Need for Standardisation of Measurements in Thermal Imaging. In: Wiecek B, editor. Thermography and Lasers in Medicine, 2003, p. 13–8.

[906] Quintana M, Fernández Cuevas I, Arnaiz-Lastras J, Marins J. TERMOINEF Group protocol for thermographic assessment in humans. 2015.

[907] Priego-Quesada JI, Kunzler MR, Carpes FP. Methodological Aspects of Infrared Thermography in Human Assessment. In: Priego Quesada JI, editor. Application of Infrared Thermography in Sports Science, Cham: Springer International Publishing; 2017, p. 49–79.

[908] Lahiri BB, Bagavathiappan S, Jayakumar T, Philip J. Medical applications of infrared thermography: A review. Infrared Physics and Technology 2012;55:221–35.

[909] Carmona P. Influencia de la información termográfica infrarroja en el protocolo de prevención de lesiones de un equipo de fútbol profesional español. 2012.

[910] Atmaca I, Yigit A. Predicting the effect of relative humidity on skin temperature and skin wettedness. Journal of Thermal Biology 2006;31:442–52.

[911] Ferreira JJA, Mendonça LCS, Nunes LAO, Andrade Filho ACC, Rebelatto JR, Salvini TF. Exercise-Associated Thermographic Changes in Young and Elderly Subjects. Annals of Biomedical Engineering 2008;36:1420–7.

[912] Holowatz LA, Kenney WL. Peripheral mechanisms of thermoregulatory control of skin blood flow in aged humans. Journal of Applied Physiology (Bethesda, Md : 1985) 2010;109:1538–44.

[913] Havenith G. Human surface to mass ratio and body core temperature in exercise heat stress - A concept revisited. Journal of Thermal Biology 2001;26:387–93.

[914] Savastano DM, Gorbach AM, Eden HS, Brady SM, Reynolds JC, Yanovski JA. Adiposity and human regional body temperature. The American Journal of Clinical Nutrition 2009;90:1124–31.

[915] Schmitt M, Guillot Y. Thermography and Muscular Injuries in Sports Medicine. In: Ring EFJ, Phillips B, editors. Recent Advances in Medical Thermology, Boston, MA: Springer New York; 1984, p. 439–45.

[916] Ismail E, Orlando G, Corradini ML, Amerio P, Romani GL, Merla A. Differential diagnosis of Raynaud's phenomenon based on modeling of finger thermoregulation. Physiological Measurement 2014;35:703–16.

[917] Bagavathiappan S, Saravanan T, Philip J, Jayakumar T, Raj B, Karunanithi R, et al. Infrared thermal imaging for detection of peripheral vascular disorders. Journal of Medical Physics 2009;34:43–7.

[918] Steketee J. Spectral emissivity of skin and pericardium. Phys Med Biol 1973;18:686–94.

[919] Togawa T. Non-contact skin emissivity: measurement from reflectance using step change in ambient radiation temperature. Clinical Physics and Physiological Measurement: An Official Journal of the Hospital Physicists' Association, Deutsche Gesellschaft Fur Medizinische Physik and the European Federation of Organisations for Medical Physics 1989;10:39–48.

[920] Sanchez-Marin FJ, Calixto-Carrera S, Villaseñor-Mora C. Novel approach to assess the emissivity of the human skin. Journal of Biomedical Optics 2009;14:24006.

[921] Koot P, Deurenberg P. Comparison of changes in energy expenditure and body temperatures after caffeine consumption. Annals of Nutrition & Metabolism 1995;39:135–42.

[922] Wolf R, Tüzün B, Tüzün Y. Alcohol ingestion and the cutaneous vasculature. Clinics in Dermatology 1999;17:395–403.

[923] Melnizky P, Ammer K. The influence of alcohol and smoking on the skin temperature of the face, hands and knees. Thermology International 2000;10:191–5.

[924] González-Alonso J. Human thermoregulation and the cardiovascular system. Experimental Physiology 2012;97:340–6.

[925] Tattersall GJ. Infrared thermography: A non-invasive window into thermal physiology. Comparative Biochemistry and Physiology Part A, Molecular & Integrative Physiology 2016;202:78–98.

[926] Dadashzadeh A, Garaje-Alamdari N, Ala A, Dehghannezhad J, Jabbarzadeh F, Babaei N. Triage guidelines for emergency department patients with COVID-19. Journal of Research in Clinical Medicine 2020;8:12.

[927] ASTM E1965-98:2016. Standard specification for infrared thermometers for intermitent determination of patient temperature. 2016.

[928] EN ISO 80601-2-56:2012. Medical Electrical Equipment. Particular requirements for basic safety and essential performance of clinical thermometers for body temperature measurement. 2012.

[929] Piccinini F, Martinelli G, Carbonaro A. Reliability of Body Temperature Measurements Obtained with Contactless Infrared Point Thermometers Commonly Used during the COVID-19 Pandemic. Sensors (Basel, Switzerland) 2021;21.

[930] Dell'Isola GB, Cosentini E, Canale L, Ficco G, Dell'Isola M. Noncontact Body Temperature Measurement: Uncertainty Evaluation and Screening Decision Rule to Prevent the Spread of COVID-19. Sensors 2021;21.

[931] Vardasca R, Magalhaes C, Silva P, Kluwe B, Mendes J. Are the IR cameras FLIR ONE suitable for clinical applications? Thermology International 2019;29:95–102.

[932] Kanazawa T, Nakagami G, Goto T, Noguchi H, Oe M, Miyagaki T, et al. Use of smartphone attached mobile thermography assessing subclinical inflammation: a pilot study. Journal of Wound Care 2016;25:177–82.

[933] Gizińska M, Rutkowski R, Szymczak-Bartz L, Romanowski W, Straburzyńska-Lupa A. Thermal imaging for detecting temperature changes within the rheumatoid foot. Journal of Thermal Analysis and Calorimetry 2021;145:77–85.

[934] Serantoni V, Jourdan F, Louche H, Sultan A. Proposal for a protocol using an infrared microbolometer camera and wavelet analysis to study foot thermoregulation. Quantitative InfraRed Thermography Journal 2021;18:73–91.

[935] Hernandez-Contreras D, Peregrina-Barreto H, Rangel-Magdaleno J, Gonzalez-Bernal JA, Altamirano-Robles L. A quantitative index for classification of plantar thermal changes in the diabetic foot. Infrared Physics and Technology 2017;81:242–9.

[936] Vardasca R, Magalhaes C, Seixas A, Carvalho R, Mendes J. Diabetic foot monitoring using dynamic thermography and AI classifiers. Proceedings of the 3rd Quantitative InfraRed Thermography Asia Conference (QIRT Asia 2019), Tokyo: QIRT Council; 2019, p. 1–5.

[937] Saminathan J, Sasikala M, Narayanamurthy VB, Rajesh K, Arvind R. Computer aided detection of diabetic foot ulcer using asymmetry analysis of texture and temperature features. Infrared Physics & Technology 2020;105:103219.

[938] Seixas A, Azevedo J, Pimenta I, Ammer K, Carvalho R, Vilas-Boas JP, et al. Skin temperature of the foot: Reliability of infrared image analysis based in the angiosome concept. Infrared Physics & Technology 2018;92:402–8.

[939] Seixas A, Pimenta I, Ammer K, Carvalho R, Vilas-Boas JP, Mendes J, et al. Reliability of infrared image analysis based on anatomical landmarks. Infrared Physics & Technology 2020;104:103149.

[940] Silva NCM, Castro HA, Carvalho LC, Chaves ÉCL, Ruela LO, Iunes DH. Reliability of Infrared Thermography Images in the Analysis of the Plantar Surface Temperature in Diabetes Mellitus. Journal of Chiropractic Medicine 2018;17:30–5.

[941] Astasio-Picado Á, Escamilla Martínez E, Gómez-Martín B. Comparative thermal map of the foot between patients with and without diabetes through the use of infrared thermography. Enfermería Clínica (English Edition) 2020;30:119–23.

[942] Wasilewska A, Pauk J, Ihnatouski M. Image Processing Techniques for ROI Identification in Rheumatoid Arthritis Patients from Thermal Images. Acta Mechanica et Automatica 2018;12:49–53.

[943] Priego Quesada JI, Gil-Calvo M, Jimenez-Perez I, Lucas-Cuevas ÁG, Pérez-Soriano P. Relationship between foot eversion and thermographic foot skin temperature after running. Applied Optics 2017;56:5559–65.

[944] Priego-Quesada JI, Machado AS, Gil-Calvo M, Jimenez-Perez I, Cibrian Ortiz de Anda RM, Salvador Palmer R, et al. A methodology to assess the effect of sweat on infrared thermography data after running: Preliminary study. Infrared Physics & Technology 2020;109:103382.

[945] Antônio de Carvalho Abreu J, de Oliveira RA, Martin AA. Correlation between ankle-brachial index and thermography measurements in patients with peripheral arterial disease. Vascular 2021:1708538121996573.

[946] Gatt A, Cassar K, Falzon O, Ellul C, Camilleri KP, Gauci J, et al. The identification of higher forefoot temperatures associated with peripheral arterial disease in type 2 diabetes mellitus as detected by thermography. Primary Care Diabetes 2018;12:312–8.

[947] Ilo A, Romsi P, Mäkelä J. Infrared Thermography and Vascular Disorders in Diabetic Feet. Journal of Diabetes Science and Technology 2019;14:28–36.

[948] Vardasca R, Vaz L, Magalhaes C, Seixas A, Mendes J. Towards the Diabetic Foot Ulcers Classification with Infrared Thermal Images. In: Organizing Committee of the Conference QIRT 2018 (Berlin G, editor. Proceedings Quantitative InfraRed Thermography Conference (QIRT 2018), QIRT Council; 2018, p. 293–6.

[949] Etehadtavakol M, Ng EYK, Kaabouch N. Automatic segmentation of thermal images of diabetic-at-risk feet using the snakes algorithm. Infrared Physics and Technology 2017;86:66–76. https://doi.org/10.1016/j.infrared.2017.08.022.

[950] Nandagopan GL, Bhargavi Haripriya A. Implementation and comparison of two image segmentation techniques on thermal foot images and detection of ulceration using asymmetry. International Conference on Communication and Signal Processing, ICCSP 2016, IEEE; 2016, p. 356–60.

[951] Hutting KH, aan de Stegge WB, Kruse RR, van Baal JG, Bus SA, van Netten JJ. Infrared thermography for monitoring severity and treatment of diabetic foot infections. Vascular Biology 2020;2:1–10.

[952] Kyle D, Allen J, Overbeck K, Stansby G. Exploratory Thermal Imaging Assessments of the Feet in Patients with Lower Limb Peripheral Arterial Disease. In: Ng EYK, Etehadtavakol M, editors. Application of Infrared to Biomedical Sciences, Singapore: Springer Singapore; 2017, p. 249–63.

[953] Sudha BG, Umadevi V, Shivaram JM. Thermal image acquisition and segmentation of human foot. 2017 4th International Conference on Signal Processing and Integrated Networks, SPIN 2017, 2017, p. 80–5.

[954] Maldonado H, Bayareh R, Torres IA, Vera A, Gutiérrez J, Leija L. Automatic detection of risk zones in diabetic foot soles by processing thermographic images taken in an uncontrolled environment. Infrared Physics and Technology 2020;105:103187.

[955] Renero-C F-J. The abrupt temperature changes in the plantar skin thermogram of the diabetic patient: looking in to prevent the insidious ulcers. Diabetic Foot & Ankle 2018;9:1430950.

[956] Madarasingha KCM, Perera WND, Rathnayaka A, Savindu HP, Jayasinghe S, Kahaduwa KTD, et al. Development of a system to profile foot temperatures of the plantar and the periphery. TENCON 2018 - 2018 IEEE Region 10 Conference, Jeju, Korea: IEE; 2018, p. 1928–32.

[957] Chatchawan U, Narkto P, Damri T, Yamauchi J. An exploration of the relationship between foot skin temperature and blood flow in type 2 diabetes mellitus patients: a cross-sectional study. Journal of Physical Therapy Science 2018;30:1359–63.

[958] Guzaitis J, Kadusauskiene A, Raisutis R. Algorithm for Automated Foot Detection in Thermal and Optical Images for Temperature Asymmetry Analysis. Electronics 2021;10.

[959] Sandi S, Yusuf S, Kaelan C, Mukhtar M. Evaluation risk of diabetic foot ulcers (DFUs) using infrared thermography based on mobile phone as advanced risk assessment tool in the community setting: A multisite cross-sectional study. Enfermería Clínica 2020;30:453–7.

[960] Wallace GA, Singh N, Quiroga E, Tran NT. The Use of Smart Phone Thermal Imaging for Assessment of Peripheral Perfusion in Vascular Patients. Annals of Vascular Surgery 2018;47:157–61.

[961] Peleki A, da Silva A. Novel Use of Smartphone-based Infrared Imaging in the Detection of Acute Limb Ischaemia. EJVES Short Reports 2016;32:1–3.

[962] Zenunaj G, Lamberti N, Manfredini F, Traina L, Acciarri P, Bisogno F, et al. Infrared Thermography as a Diagnostic Tool for the Assessment of Patients with Symptomatic Peripheral Arterial Disease Undergoing Infrafemoral Endovascular Revascularisations. Diagnostics 2021;11.

[963] Mancilla RB, Daul C, Martínez JG, Salas LL, Wolf D, Hernández A v. A Quantitative Method for the Detection of Temperature Differences on the Sole of the Foot in Diabetic Patients. 2021 Global Medical Engineering Physics Exchanges/Pan American Health Care Exchanges (GMEPE/PAHCE), 2021, p. 1–5.

[964] Maddah E, Beigzadeh B. Use of a smartphone thermometer to monitor thermal conductivity changes in diabetic foot ulcers: a pilot study. Journal of Wound Care 2020;29:61–6.

[965] Boguski R, Khan T, Woelfel S, Huyvetter K, Armstrong A, Armstrong D. Clinical utility of mobile phone-based thermography and low-cost infrared handheld thermometry in high-risk diabetic foot. Indian Journal of Vascular and Endovascular Surgery 2019;6:7–9.

[966] Fraiwan L, AlKhodari M, Ninan J, Mustafa B, Saleh A, Ghazal M. Diabetic foot ulcer mobile detection system using smart phone thermal camera: a feasibility study. BioMedical Engineering OnLine 2017;16:117.

[967] van Doremalen RFM, van Netten JJ, van Baal JG, Vollenbroek-Hutten MMR, van der Heijden F. Infrared 3D Thermography for Inflammation Detection in Diabetic Foot Disease: A Proof of Concept. Journal of Diabetes Science and Technology 2020;14:46–54.

[968] Usamentiaga R, Venegas P, Guerediaga J, Vega L, Molleda J, Bulnes FG. Infrared thermography for temperature measurement and non-destructive testing. Sensors (Switzerland) 2014;14:12305–48.

[969] Kakuta N, Yokoyama S, Mabuchi K. Human thermal models for evaluating infrared images. IEEE Engineering in Medicine and Biology Magazine: The Quarterly Magazine of the Engineering in Medicine & Biology Society 2002;21:65–72.

[970] Zaproudina N, Varmavuo V, Airaksinen O, Närhi M. Reproducibility of infrared thermography measurements in healthy individuals. Physiological Measurement 2008;29:515–24.

[971] Marins JCB, Moreira DG, Cano SP, Quintana MS, Soares DD, de Andrade Fernandes A, et al. Time required to stabilize thermographic images at rest. Infrared Physics and Technology 2014;65:30–5.

[972] Priego Quesada JI, Lucas-Cuevas A, Salvador-Palmer R, Perez-Soriano P, Cibrian R. Definition of the thermographic regions of interest in cycling by using a factor analysis. Infrared Physics & Technology 2016;75.

[973] Maniar N, Bach AJE, Stewart IB, Costello JT. The effect of using different regions of interest on local and mean skin temperature. Journal of Thermal Biology 2015;49–50:33–8.

[974] Kurt Ammer MD. Sources of uncertainty in the evaluation of thermal images in medicine. Proc.SPIE, vol. 11060, 2019.

[975] della Corte J, Pinheiro C, Lima B, Vignoli F, Oliveira J, Brandão Pinto de Castro J, et al. Thermographic analysis of thighs of trained men during the leg extension exercise. Journal of Physical Education and Sport 2019;19:2458–65.

[976] Duarte A, Carrão L, Espanha M, Viana T, Freitas D, Bártolo P, et al. Segmentation Algorithms for Thermal Images. Procedia Technology 2014;16:1560–9.

[977] Bagavathiappan S, Philip J, Jayakumar T, Raj B, Rao PNS, Varalakshmi M, et al. Correlation between plantar foot temperature and diabetic neuropathy: a case study by using an infrared thermal imaging technique. Journal of Diabetes Science and Technology 2010;4:1386–92..

[978] Vardasca R, Mendes J, Jones C, Plassmann P, Ring EFJ. A Template Based Method for Normalizing Thermal Images of the Human Body. The 12th International Conference on Quantitative infrared Thermography, Bordeaux: 2014.

[979] Singh J, Arora AS. Automated approaches for ROIs extraction in medical thermography: a review and future directions. Multimedia Tools and Applications 2020;79:15273–96.

[980] Barcelos EZ, Caminhas WM, Ribeiro E, Pimenta EM, Palhares RM. A Combined Method for Segmentation and Registration for an Advanced and Progressive Evaluation of Thermal Images. Sensors 2014;14.

[981] Gauci J, Falzon O, Camilleri K, Formosa C, Gatt A, Ellul C, et al. Automated Segmentation and Temperature Extraction from Thermal Images of Human Hands, Shins and Feet. XIV Mediterranean Conference on Medical and Biological Engineering and Computing 2016. IFMBE Proceedings, vol. 57, Springer, Cham; 2016, p. 275–80.

[982] Ludwig N, Formenti D, Gargano M, Alberti G. Skin temperature evaluation by infrared thermography : Comparison of image analysis methods. Infrared Physics & Technology 2014;62:1–6.

[983] Umapathy S, Vasu S, Gupta N. Computer Aided Diagnosis Based Hand Thermal Image Analysis: A Potential Tool for the Evaluation of Rheumatoid Arthritis. Journal of Medical and Biological Engineering 2018;38:666–77.

[984] Arteaga-Marrero N, Hernández A, Villa E, González-Pérez S, Luque C, Ruiz-Alzola J. Segmentation Approaches for Diabetic Foot Disorders. Sensors 2021;21.

[985] Mendes R, Sousa N, Almeida A, Vilaça-Alves J, Reis VM, Neves EB. Thermography: a technique for assessing the risk of developing diabetic foot disorders. Postgraduate Medical Journal 2015;91:538.

[986] Taylor GI, Palmer JH. The vascular territories (angiosomes) of the body: experimental study and clinical applications. British Journal of Plastic Surgery 1987;40:113–41.

[987] Attinger CE, Evans KK, Bulan E, Blume P, Cooper P. Angiosomes of the foot and ankle and clinical implications for limb salvage: reconstruction, incisions, and revascularization. Plastic and Reconstructive Surgery 2006;117:261S-293S.

[988] Peregrina-Barreto H, Morales-Hernandez LA, Rangel-Magdaleno JJ, Avina-Cervantes JG, Ramirez-Cortes JM, Morales-Caporal R. Quantitative Estimation of Temperature Variations in Plantar Angiosomes: A Study Case for Diabetic Foot. Computational and Mathematical Methods in Medicine 2014;2014:585306.

[989] Nagase T, Sanada H, Takehara K, Oe M, Iizaka S, Ohashi Y, et al. Variations of plantar thermographic patterns in normal controls and non-ulcer diabetic patients: Novel classification using angiosome concept. Journal of Plastic, Reconstructive & Aesthetic Surgery 2011;64:860–6.

[990] Sun PC, Jao S-HE, Cheng C-K. Assessing foot temperature using infrared thermography. Foot & Ankle International 2005;26.

[991] Wang MZ, Song Y, Fekete G, Gu YD. The Variation of Plantar Temperature and Plantar Pressure during Shod Running with Socks or not. Journal of Biomimetics, Biomaterials and Biomedical Engineering 2018;35:1–8.

[992] Gauci J, Falzon O, Formosa C, Gatt A, Ellul C, Mizzi S, et al. Automated Region Extraction from Thermal Images for Peripheral Vascular Disease Monitoring. Journal of Healthcare Engineering 2018;2018.

[993] Wiecek B, Danych R, Zwolenik Z, Jung A, Zuber J. Advanced thermal image processing for medical and biological applications. Annual Reports of the Research Reactor Institute, Kyoto University 2001;3:2805–7.

[994] Bouzas Marins JC, de Andrade Fernandes A, Gomes Moreira D, Souza Silva F, Costa CMA, Pimenta EM, et al. Thermographic profile of soccer players' lower limbs. Revista Andaluza de Medicina Del Deporte 2014;7:1–6.

[995] Formenti D, Ludwig N, Gargano M, Gondola M, Dellerma N, Caumo A, et al. Thermal imaging of exercise-associated skin temperature changes in trained and untrained female subjects. Annals of Biomedical Engineering 2013;41:863–71.

[996] Formenti D, Ludwig N, Rossi A, Trecroci A, Alberti G, Gargano M, et al. Is the maximum value in the region of interest a reliable indicator of skin temperature? Infrared Physics & Technology 2018;94:299–304.

[997] Hernandez-Contreras D, Peregrina-Barreto H, Rangel-Magdaleno J, Ramirez-Cortes J, Renero-Carrillo F. Automatic classification of thermal patterns in diabetic foot based on morphological pattern spectrum. Infrared Physics & Technology 2015;73:149–57.

[998] Vardasca R, Ring F, Plassmann P, Jones C. Thermal symmetry of the upper and lower extremities in healthy subjects. Thermology International 2012;22:53–60.

[999] Nowakowski A. Advances of QIRT in medical diagnostics. 9th International Conference on Quantitative Infrared Thermography (QIRT), 2008.

[1000] Priego Quesada JI, Kunzler M, da Rocha E, Machado Á, Carpes F. Plantar Pressure and Foot Temperature Responses to Acute Barefoot and Shod Running. Human Movement 2015;16:112

[1001] Mitchell TM. Machine Learning. 1997.

[1002] Witten I, Frank IH. Data Mining - Practical Machine Learning Tools and Techniques with JAVA Implementations. Morgan Kaufmann 2002;31.

[1003] Russell S, Norvig P. Artificial intelligence: a modern approach. Upper Saddle River, N.J.: Prentice Hall; 2010.

[1004] Samuel AL. Some Studies in Machine Learning Using the Game of Checkers. IBM Journal of Research and Development 1959;3:210–29.

[1005] Hau K. We analyzed 16,625 papers to figure out where AI is headed next. MIT Technology Review 2019.

[1006] Bi WL, Hosny A, Schabath MB, Giger ML, Birkbak NJ, Mehrtash A, et al. Artificial intelligence in cancer imaging: Clinical challenges and applications. CA: A Cancer Journal for Clinicians 2019;69:127–57.

[1007] Thrall JH, Li X, Li Q, Cruz C, Do S, Dreyer K, et al. Artificial Intelligence and Machine Learning in Radiology: Opportunities, Challenges, Pitfalls, and Criteria for Success. Journal of the American College of Radiology : JACR 2018;15:504–8.

[1008] Ng EYK, Etehadtavakol M. Application of Infrared to Biomedical Sciences. Springer; 2017.

[1009] Kuhn M, Johnson K. An Introduction to Feature Selection. In: Kuhn M, Johnson K, editors. Applied Predictive Modeling, New York, NY: Springer New York; 2013, p. 487–519.

[1010] Fernandez-Delgado M, Cernadas E, Barro S, Amorim D. Do we Need Hundreds of Classifiers to Solve Real World Classification Problems? Journal of Machine Learning Research 2014;15:3133–81.

[1011] Hartigan JA, Wong MA. A K-Means Clustering Algorithm. Journal of the Royal Statistical Society: Series C (Applied Statistics) 1979;28:100–8.

[1012] Abdi H, Williams LJ. Principal component analysis. WIREs Computational Statistics 2010;2:433–59.

[1013] Wang J. Encyclopedia of data warehousing and mining. iGi Global; 2005.

[1014] Wu X, Kumar V, Ross Quinlan J, Ghosh J, Yang Q, Motoda H, et al. Top 10 algorithms in data mining. Knowledge and Information Systems 2008;14:1–37.

[1015] Kuhn M, Johnson K. Classification Trees and Rule-Based Models. Applied Predictive Modeling, Springer, New York, NY; 2013, p. 369–413.

[1016] Kuhn M, Johnson K. Over-Fitting and Model Tuning. In: Kuhn M, Johnson K, editors. Applied Predictive Modeling, New York, NY: Springer New York; 2013, p. 61–92.

[1017] Palmer A, Jiménez R, Gervilla E. Data Mining: Machine Learning and Statistical Techniques. In: Funatsu K, editor. Knowledge-Oriented Applications in Data Mining, IntechOpen; 2011, p. 373–96.

[1018] Criminisi A, Shotton J, Konukoglu E. Decision Forests: A Unified Framework for Classification, Regression, Density Estimation, Manifold Learning and Semi-Supervised Learning. Now Foundations and Trends; 2012.

[1019] Breiman L. Random Forests. Machine Learning 2001;45:5–32.

[1020] Konukoglu E, Glocker B. Random forests in medical image computing. In: Zhou SK, Rueckert D, Fichtinger GBT-H of MIC and CAI, editors. The Elsevier and MICCAI Society Book Series, Academic Press; 2020, p. 457–80.

[1021] Vapnik VN. Statistical Learning Theory. New York : NJ, USA: Wiley; 1998.

[1022] Hearst MA, Dumais ST, Osuna E, Platt J, Scholkopf B. Support vector machines. IEEE Intelligent Systems and Their Applications 1998;13:18–28.

[1023] Fricke C, Alizadeh J, Zakhary N, Woost TB, Bogdan M, Classen J. Evaluation of Three Machine Learning Algorithms for the Automatic Classification of EMG Patterns in Gait Disorders. Frontiers in Neurology 2021;12:666458.

[1024] Kuhn M, Johnson K. Nonlinear Classification Models. In: Kuhn M, Johnson K, editors. Applied Predictive Modeling, New York, NY: Springer New York; 2013, p. 329–67.

[1025] Priddy KL, Keller PE. Artificial Neural Networks: An Introduction. SPIE Press; 2005.

[1026] Azimi P, Mohammadi HR, Benzel EC, Shahzadi S, Azhari S, Montazeri A. Artificial neural networks in neurosurgery. Journal of Neurology, Neurosurgery, and Psychiatry 2015;86:251–6.

[1027] Amato F, López A, Peña-Méndez EM, Vaňhara P, Hampl A, Havel J. Artificial neural networks in medical diagnosis. Journal of Applied Biomedicine 2013;11:47–58.

[1028] Wang S, Summers RM. Machine learning and radiology. Medical Image Analysis 2012;16:933–51.

[1029] Kotsiantis SB, Zaharakis ID, Pintelas PE. Machine learning: a review of classification and combining techniques. Artificial Intelligence Review 2006;26:159–90.

[1030] Guyon I, Elisseeff A. An introduction to variable and feature selection. Journal of Machine Learning Research 2003;3:1157–82.

[1031] Hira ZM, Gillies DF. A Review of Feature Selection and Feature Extraction Methods Applied on Microarray Data. Advances in Bioinformatics 2015;2015:198363.

[1032] Memon MH, Li JP, Haq AU, Memon MH, Zhou W. Breast Cancer Detection in the IOT Health Environment Using Modified Recursive Feature Selection. Wireless Communications and Mobile Computing 2019;2019:5176705.

[1033] Dietterich TG. Overfitting and undercomputing in machine learning. ACM Comput Surv 1995;27:326–7.

[1034] Molinaro AM, Simon R, Pfeiffer RM. Prediction error estimation: a comparison of resampling methods. Bioinformatics 2005;21:3301–7.

[1035] Refaeilzadeh P, Tang L, Liu H. Cross-validation. Encyclopedia of Database Systems 2009;5:532–8.

[1036] Erickson BJ, Korfiatis P, Akkus Z, Kline TL. Machine Learning for Medical Imaging. Radiographics : A Review Publication of the Radiological Society of North America, Inc 2017;37:505–15.

[1037] Kuhn M, Johnson K. Measuring Performance in Classification Models. In: Kuhn M, Johnson K, editors. Applied Predictive Modeling, New York, NY: Springer New York; 2013, p. 247–73.

[1038] Lundberg SM, Lee S-I. A unified approach to interpreting model predictions. Proceedings of the 31st international conference on neural information processing systems, 2017, p. 4768–77.

[1039] Shapley LS. A Value for N-Person Games. Santa Monica, CA: RAND Corporation PP - Santa Monica, CA; 1952.

[1040] Rubio Mayo P. Desarrollo de una herramienta software para la cuantificación de secuencias de vídeo e imágenes de termografía infrarroja en el diagnóstico y seguimiento del Síndrome de Dolor Regional Complejo. Universitat Politècnica de València; 2021.

[1041] Kuhn M. Building predictive models in R using the caret package. Journal of Statistical Software 2008;28:1–26.

[1042] Guyon I, Weston J, Barnhill S, Vapnik V. Gene Selection for Cancer Classification using Support Vector Machines. Machine Learning 2002;46:389–422.

[1043] Newton DJ, McLeod GA, Khan F, Belch JJF. Mechanisms influencing the vasoactive effects of lidocaine in human skin*. Anaesthesia 2007;62:146–50.

[1044] Cederholm I, Evers H, Löfström JB. Effect of intradermal injection of saline or a local anaesthetic agent on skin blood flow--a methodological study in man. Acta Anaesthesiologica Scandinavica 1991;35:208–15.

[1045] Galvin EM, Niehof S, Medina HJ, Zijlstra FJ, van Bommel J, Klein J, et al. Thermographic temperature measurement compared with pinprick and cold sensation in predicting the effectiveness of regional blocks. Anesthesia and Analgesia 2006;102:598–604.

[1046] Andreasen AM, Linnet KE, Asghar S, Rothe C, Rosenstock C v, Lange KHW, et al. "Eyeball test" of thermographic patterns for predicting a successful lateral infraclavicular block. Canadian Journal of Anesthesia/Journal Canadien d'anesthésie 2017;64:1111–8.

[1047] Asghar S, Bjerregaard LS, Lundstrøm LH, Lund J, Jenstrup MT, Lange KHW. Distal infrared thermography and skin temperature after ultrasound-guided interscalene brachial plexus block: A prospective observational study. European Journal of Anaesthesiology | EJA 2014;31.

[1048] van Haren FGAM, Kadic L, Driessen JJ. Skin temperature measured by infrared thermography after ultrasound-guided blockade of the sciatic nerve. Acta Anaesthesiologica Scandinavica 2013;57:1111–7.

[1049] Hermanns H, Braun S, Werdehausen R, Werner A, Lipfert P, Stevens MF. Skin temperature after interscalene brachial plexus blockade. Regional Anesthesia and Pain Medicine 2007;32:481–7.

[1050] Ashgar S, Lundstrøm LH, Bjerregaard LS, Lange KHW. Ultrasound-guided lateral infraclavicular block evaluated by infrared thermography and distal skin temperature. Acta Anaesthesiologica Scandinavica 2014;58:867–74.

[1051] Stevens MF, Werdehausen R, Hermanns H, Lipfert P. Skin Temperature During Regional Anesthesia of the Lower Extremity. Anesthesia and Analgesia 2006;102:1247–51.

[1052] Kim YC, Bahk JH, Lee SC, Lee YW. Infrared Thermographic Imaging in the assessment of successful block on lumbar sympathetic ganglion. Yonsei Medical Journal 2003;44:119–24.

[1053] James CA, Richardson AJ, Watt PW, Maxwell NS. Reliability and validity of skin temperature measurement by telemetry thermistors and a thermal camera during exercise in the heat. Journal of Thermal Biology 2014;45:141–9.

[1054] Priego-Quesada JI, Martínez Guillamón N, Cibrián Ortiz de Anda RM, Psikuta A, Annaheim S, Rossi RM, et al. Effect of perspiration on skin temperature measurements by infrared thermography and contact thermometry during aerobic cycling. Infrared Physics & Technology 2015;72:68–76.

[1055] Fernandes A de A, Amorim PR dos S, Brito CJ, de Moura AG, Moreira DG, Costa CMA, et al. Measuring skin temperature before, during and after exercise: a comparison of thermocouples and infrared thermography. Physiological Measurement 2014;35:189–203.

[1056] Cutts S, Gangoo S, Srinivasan SH, Pasapula C, Power D, Modi N. Complex regional pain syndrome: an evolving perspective. Postgrad Med J 2020;0:1–6.

[1057] Schurmann M, Gradl G, Wizgal I, Tutic M, Moser C, Azad S, et al. Clinical and physiologic evaluation of stellate ganglion blockade for complex regional pain syndrome type I. Clinical Journal of Pain 2001;17:94–100.

[1058] Sammut C, Webb GI. Encyclopedia of Machine Learning. New York, NY: Springer US; 2010.

[1059] Taha AA, Hanbury A. Metrics for evaluating 3D medical image segmentation: analysis, selection, and tool. BMC Medical Imaging 2015;15:29.

[1060] Magalhaes C, Mendes J, Vardasca R. Meta-Analysis and Systematic Review of the Application of Machine Learning Classifiers in Biomedical Applications of Infrared Thermography. Applied Sciences 2021;11.

[1061] Thirunavukkarasu U, Umapathy S. Classification of Prediabetes and Healthy Subjects in Plantar Infrared Thermal Imaging Using Various Machine Learning Algorithms. In: Sharma DK, Balas VE, Son LH, Sharma R, Cengiz K, editors. Micro-Electronics and Telecommunication Engineering, Singapore: Springer Singapore; 2020, p. 85–96.

[1062] Cruz-Vega I, Hernandez-Contreras D, Peregrina-Barreto H, Rangel-Magdaleno J de J, Ramirez-Cortes JM. Deep Learning Classification for Diabetic Foot Thermograms. Sensors (Basel, Switzerland) 2020;20.

[1063] Ibrahim I, Abdulazeez A. The role of machine learning algorithms for diagnosing diseases. Journal of Applied Science and Technology Trends 2021;2:10–9.

[1064] Rodríguez-Pérez R, Bajorath J. Interpretation of machine learning models using shapley values: application to compound potency and multi-target activity predictions. Journal of Computer-Aided Molecular Design 2020;34:1013–26.

[1065] Wang K, Tian J, Zheng C, Yang H, Ren J, Liu Y, et al. Interpretable prediction of 3-year all-cause mortality in patients with heart failure caused by coronary heart disease based on machine learning and SHAP. Computers in Biology and Medicine 2021;137:104813.

[1066] Anupama K, Saraswathi G, Shailaja S. A Study of Plantar Arterial Arch With Its Surgical Perspective. International Journal of Anatomy and Research 2016;4:2392–6.

[1067] Xie P, Li Y, Deng B, Du C, Rui S, Deng W, et al. An explainable machine learning model for predicting in-hospital amputation rate of patients with diabetic foot ulcer. International Wound Journal 2021;n/a.

[1068] Pan P, Li Y, Xiao Y, Han B, Su L, Su M, et al. Prognostic Assessment of COVID-19 in the Intensive Care Unit by Machine Learning Methods: Model Development and Validation. J Med Internet Res 2020;22:e23128.

[1069] Mangalathu S, Hwang S-H, Jeon J-S. Failure mode and effects analysis of RC members based on machine-learning-based SHapley Additive exPlanations (SHAP) approach. Engineering Structures 2020;219:110927.

[1070] Liu X, Feng J, Luan J, Dong C, Fu H, Wu Z. Intra- and Interrater Reliability of Infrared Image Analysis of Facial Acupoints in Individuals with Facial Paralysis. Evidence-Based Complementary and Alternative Medicine 2020;2020:9079037.

[1071] Liu C, van Netten JJ, van Baal JG, Bus SA, van der Heijden F. Automatic detection of diabetic foot complications with infrared thermography by asymmetric analysis. Journal of Biomedical Optics 2015;20:026003.

[1072] Jin X, Jiang Q, Yao S, Zhou D, Nie R, Hai J, et al. A survey of infrared and visual image fusion methods. Infrared Physics and Technology 2017;85:478–501.

[1073] Hartrick CT, Kovan JP, Naismith P. Outcome prediction following sympathetic block for complex regional pain syndrome. Pain Practice: The Official Journal of World Institute of Pain 2004;4:222–8.

[1074] van Eijs F, Geurts J, van Kleef M, Faber CG, Perez RS, Kessels AGH, et al. Predictors of pain relieving response to sympathetic blockade in complex regional pain syndrome type 1. Anesthesiology 2012;116:113–21.

UNIVERSITAT POLITÈCNICA DE VALÈNCIA